Entanglement in Quantum Lifshitz Theories

Juanfernando Angel-Ramelli

Faculty of Physical Sciences
University of Iceland
2020

Entanglement in Quantum Lifshitz Theories

Juanfernando Angel-Ramelli

Dissertation submitted in partial fulfillment of a
Philosophiae Doctor degree in Physics

Advisor

Prof. Valentina G.M. Puletti

PhD Committee

Prof. Valentina G.M. Puletti
Prof. Lárus Thorlacius
Assoc. Prof. Erik Tonni
Prof. Þórður Jónsson

Opponents

Prof. Stefan Vandoren
Assoc. Prof. Jens Bárðarson

Faculty of Physical Sciences
School of Engineering and Natural Sciences
University of Iceland
Reykjavík, November 2020

Entanglement in Quantum Lifshitz Theories
Dissertation submitted in partial fulfillment of a *Philosophiae Doctor* degree in Physics

Faculty of Physical Sciences
School of Engineering and Natural Sciences
University of Iceland
Dunhaga 5
107, Reykjavik
Iceland

Telephone: 525-4000

Bibliographic information:
Juanfernando Angel-Ramelli, 2020, *Entanglement in Quantum Lifshitz Theories*, PhD dissertation, Faculty of Physical Sciences, University of Iceland, 241 pp.

ISBN 978-9935-9564-1-5

Printing: Háskólaprent
Reykjavik, Iceland, November 2020

Abstract

In recent years, the study of entanglement properties of quantum field theories has led to deep insights in fields as diverse as quantum gravity and condensed matter physics. Originating as effective field theories for certain quantum dimer models, the Quantum Lifshitz Model (QLM) and its generalizations are bosonic quantum field theories with anisotropic scaling symmetry between space and time. Being closely related to conformal field theories, they provide a fruitful playground, where diverse entanglement calculations can be performed analytically.

In this thesis, we concentrate on two entanglement measures, the entanglement entropy and logarithmic negativity. Motivated to extract sub-leading universal behavior, we perform analytic calculations in two and higher even dimensions. In order to make the calculations tractable, we put the QLM on compact manifolds, such as spheres and tori, where the spectrum of a certain operator appearing in the ground state of the theory is explicitly known. Mostly by means of the replica method, we then find analytic expressions for the finite sub-leading terms of the entanglement entropy and logarithmic negativity of the ground state, as well as the entanglement entropy of the excited states of the QLM. In the case of the ground state entanglement entropy, we provide analytic expressions for the sub-leading terms as functions of the dimension and the dynamical critical exponent. For the excited states we provide analytic formulae of the sub-leading coefficients as functions of the excitation numbers.

To my mother, who is watching somewhere.
To Salome, always by my side.
And to Leon, who brought new life.

Table of Contents

List of Figures

List of Original Papers

I : Angel-Ramelli, J., Puletti, V.G.M. & Thorlacius, L. Entanglement entropy in generalised quantum Lifshitz models. *J. High Energ. Phys.* **2019**, 72 (2019).

II: Angel-Ramelli, J., Berthiere, C., Puletti, V.G.M. & Thorlacius, L. Logarithmic negativity in quantum Lifshitz theories. *J. High Energ. Phys.* **2020**, 11 (2020).

III: Angel-Ramelli, J., Entanglement Entopy of Excited States in the Quantum Lifshitz Model, *arXiv:2009.02283 [hep-th]*, under review at J.Stat.Mech.

1 Introduction

Soon after quantum mechanics had found its modern mathematical foundations in the 1930's, [Einstein et al., 1935] and [Schrödinger, 1935] discovered the phenomenon that lies at the heart of the differences between the quantum and the classical world: *Entanglement.*

In essence, entanglement implies the existence of systems that, even if they consist of multiple parts, can only be treated as a whole. Let us be more concrete. Say there is a system made up of several components such as, for example, a collection of particles – though other systems exhibiting entanglement are abundant – and separate these particles until they all are very far apart from each other. Our intuition would tell us that, if we perform experiments on one of those particles, the results should be independent of the other. After all, how could all these distant particles conspire to correlate? However, if the system is entangled this intuition is not true, and the result of our experiment will be connected to the results of the experiments by far-away labs on the other particles.

Perhaps the most famous example of an entangled system is that of an EPR-pair (named after the authors of the seminal paper by Einstein, Podolsky, Rosen [Einstein et al., 1935]). Such a pair consists of two particles, each of which can be either in a spin up or in a spin down state. The spins of an EPR-pair are entangled in such a way that they must *both* either point up or *both* down and nothing else is allowed[1]. Imagine creating such an EPR-pair and taking one of the particles to a hypothetical laboratory on Mars, while the other remains in a laboratory on Earth. Then, a measurement of the spin of the Earth particle immediately determines the spin of the Mars particle: If we measure spin up, the Mars particle must also have spin up.

This phenomenon seems to go against relativity, with information travelling faster than light, and its discovery triggered a discussion on the nature of physics, experiments, and reality that lasted for many decades, and, to some degree, still continues. Some physicists, such as Einstein, argued the incompleteness of quantum mechanics, stating that

[1] An analogous situation with opposite pointing spins not allowed to point in the same direction is also possible.

the strange behavior of entangled systems must be due to our ignorance of some unknown quantities, dubbed hidden variables. Other physicists, like Bohr, took a more pragmatic approach, accepting the new ideas as a fundamental, yet counter-intuitive part of reality. After all, why should reality cater to our intuition? It was not until some decades after the discovery of entanglement that the seminal work by [Bell, 1964] and its multiple experimental confirmations, see for example [Freedman and Clauser, 1972] and [Aspect et al., 1982], ruled out local hidden-variables and cemented entanglement as a real part of physics.

Interestingly, one of the first motivations to study entanglement outside of the realm of the foundations of quantum mechanics came from black hole physics. The work of [Bekenstein, 1973] and [Hawking, 1976] in the 1970's showed that black holes behave as thermodynamical objects with an entropy proportional to the area of their event horizon. Some years later, looking for a source for the entropy of a black hole, [Bombelli et al., 1986] and [Srednicki, 1993] independently showed the entanglement entropy – an entanglement measure that we will later analyze in detail – between two complementary regions of space to be proportional to the area between the two regions for a scalar field in its ground state. Imagining the two regions to be the inside and outside regions of a black hole, this result suggested a tantalizing explanation for the area law behavior of the black hole entropy. Later work by [Callan and Wilczek, 1994] and [Holzhey et al., 1994] confirmed this type of area law behavior in the context of conformal field theory, and introduced some of the modern techniques to calculate entanglement entropy in quantum field theory. Since then, a lot of work has been devoted to understand the entanglement properties of quantum field theory and to find ways to calculate them, see [Casini and Huerta, 2009] and [Calabrese and Cardy, 2009] for reviews.

The idea that information about a black hole is stored on its surface also inspired the concept of holography, see ['t Hooft, 1993] and [Susskind, 1995]. This is the notion that quantum gravity is highly redundant, only needing a surface of one dimension less than the dimension of the spacetime to describe all of its contents. In the late 1990's holography was first concretely realized in string theory as the AdS/CFT correspondence in the seminal papers [Maldacena, 1999], [Witten, 1998], and [Gubser et al., 1998]. In its original form, the AdS/CFT correspondence states that a string theory defined on $\mathrm{AdS}_5 \times S^5$, that is five dimensional anti de Sitter space times a five sphere, is dual to a conformal field theory that lives on the boundary of the anti de Sitter space. The Bekenstein-Hawking formula then seemed to suggest that in holography geometric

quantities, such as the area of the black hole horizon, should be related to quantum mechanical quantities, such the entanglement entropy. It didn't take long for this notion to be realized in the context of the AdS/CFT correspondence. The Ryu-Takayanagi formula [Ryu and Takayanagi, 2006a, Ryu and Takayanagi, 2006b] and its covariant generalization, the Hubeny-Rangamani-Takayanagi formula [Hubeny et al., 2007], state that the entanglement entropy of a region of a d-dimensional CFT is determined by the area of an extremal surface with the same boundary as the CFT region, but reaching into the $d+1$-dimensional bulk on whose boundary the CFT is considered to live. Taking these ideas even further, it has been suggested that in the context of quantum gravity spacetime itself should be considered an emergent quantity, determined by the entanglement properties of the corresponding boundary theory [Van Raamsdonk, 2009], see also [Rangamani and Takayanagi, 2017].

In another corner of physics the practical potential of entanglement was also recognized in the 1990's. Several famous results such as quantum cryptography by [Ekert, 1991] and quantum teleportation by [Bennett et al., 1993] paved the way for the vast and very active fields of quantum information and computing, both of which have entanglement at their core. The activity in these fields has pushed our understanding of entanglement and how to quantize it and work with it, although it mostly deals with discrete systems, see [Plenio and Virmani, 2007, Horodecki et al., 2009]. Not long after the first breakthroughs in quantum information, it was also realized that entanglement served as a great tool for condensed matter physics. In 2002, [Osterloh et al., 2002] and [Osborne and Nielsen, 2002] found that during a quantum phase transition of a certain spin-chain model the entanglement remained short-ranged, as opposed to the diverging classical correlation length, and that a specific measure of entanglement was maximal at the critical point. This observation revealed a deep connection between entanglement and critical phenomena. The relevance of entanglement to condensed matter physics was further underlined by the discovery that sub-leading corrections to the area law divergence of the entanglement entropy encoded universal features of critical theories [Vidal et al., 2003, Calabrese and Cardy, 2004], see [Amico et al., 2008, Eisert et al., 2010, Laflorencie, 2016] for reviews.

As can be seen from the last few paragraphs, entanglement is a rich and important subject, touching upon many branches of physics, and leading to deep insights where it does. However, quantifying and calculating entanglement is hard, especially in the context of quantum field theory, and analytic results are not as plentiful as one would like, and

are mostly concentrated to CFTs, where powerful machineries come to aid. Another fruitful source of analytic results for entanglement has been that of Lifshitz field theories, and in particular that of the quantum Lifshitz model (QLM). Lifshitz field theories are non-relativistic and exhibit a scale invariance that is anisotropic between space and time, and which is characterized by the so-called dynamical critical exponent z. Concretely, the space and times coordinates transform as

$$\vec{x} \mapsto \lambda \vec{x} \qquad\qquad t \mapsto \lambda^z t \tag{1}$$

under a scaling λ. The QLM is a $2+1$-dimensional QFT that realizes this symmetry for $z = 2$. It was first introduced in [Ardonne et al., 2004] as the continuum limit of the quantum dimer model [Kivelson et al., 1987], which was in turn originally used as a tool to understand certain properties of high temperature superconductivity. One of the striking features of the QLM is that its ground state wave function can be easily found and, even more, it turns out to be invariant under 2-dimensional (spatial) conformal transformations. It was quickly realized by [Fradkin and Moore, 2006] that this could be exploited to perform an analytic calculation of the ground state entanglement entropy of the theory. Since then, the QLM has served as an excellent toy model for performing analytic entanglement calculations, see for example [Hsu and Fradkin, 2010, Oshikawa, 2010, Zaletel et al., 2011, Zhou et al., 2016]. One can generalize the QLM to higher dimensions and arbitrary critical exponents. The $d+1$-dimensional form of the QLM, which goes by the name of generalized quantum Lifshitz model (GQLM), is deeply connected to d-dimensional CFT. As we have now reached the setting for this thesis, let us abandon our historical digressions and take a closer look at the subject at hand.

1.1 Background

The thesis is based on the three papers listed on page xiii. In order to emphasize these papers, we will cite them as [I], [II], and [III] instead of [Angel-Ramelli et al., 2019], [Angel-Ramelli et al., 2020], and [Angel-Ramelli, 2020]. The papers are attached and can be found in pages 78, 141, and 193 respectively. Let us inspect the core concepts on which we base this thesis a little closer.

Our main motivation is to expand our exact knowledge on entanglement in quantum field theory. We do this in the setting of the $2+1$-dimensional quantum Lifshitz model (QLM) [Ardonne et al., 2004] and

its generalizations to higher dimensions [Keränen et al., 2017] and curved higher dimensional manifolds [I]. We refer to the higher dimensional models as generalized quantum Lifshitz models (GQLM). One of the most important features of the QLM is that its ground state takes the following simple form

$$|\psi_0\rangle = \frac{1}{\sqrt{Z}} \int \mathcal{D}\phi \; e^{-\frac{1}{2}S[\phi]} |\phi\rangle, \tag{2}$$

with $S[\phi]$ the conformally invariant[2] action of a 2 dimensional free scalar

$$S[\phi] = g \int_M \mathrm{d}^2x \;\; (\nabla\phi)^2 \,. \tag{3}$$

We take the scalar ϕ to be compactified with compactification radius R, that is $\phi \sim \phi + 2\pi R$. This very simple ground state, provides us with a suitable playground on which many difficult calculations can be performed explicitly, turning the QLM into an excellent toy model for entanglement calculations.

We will consider bipartite entanglement of pure and mixed states, and for this we need suitable measures of entanglement. There are many ways to quantify entanglement, for reviews see for example [Plenio and Virmani, 2007, Amico et al., 2008, Horodecki et al., 2009]. An entanglement measure takes the density matrix of a system as an argument, and returns a positive real number that characterizes its entanglement. In order to do the latter, a good entanglement measure should satisfy at least two properties. First of all, unentangled states are described by separable density matrices, and thus a good entanglement measure vanishes for separable density matrices. Secondly, the entanglement measure should introduce an order into the space of density matrices, reflecting the fact that some systems are more entangled than others. In order to do this, the concept of "Local Operations and Classical Communication" is useful. Let us consider two particles in a maximally entangled EPR state. If we take each of the particles to a different lab, LOCC transformations capture the type of operations the labs can perform: They can inspect their respective particle by performing local quantum operations (LO), and they can communicate via classical means (CC) to compare results. The crucial observation is that entanglement can never be created, only conserved or destroyed, by these means. The two labs can by means of LOCC determine that their particles were entangled, but in the process they destroy the entangled state. Thus, if a state can be reached from another by LOCC transformations, then the former was more entangled than the

[2] Under conformal transformations involving only the spatial part of the QLM.

latter. A good entanglement measure must therefore never increase under LOCC transformations. A measure that satisfies the properties above is called an entanglement monotone.

Most good measures of entanglement come from the quantum information community and are ill-suited for analytic calculations in quantum field theory. We will concentrate on two entanglement measures that allow us to achieve the desired analytic results: the entanglement entropy and logarithmic negativity[3]. The entanglement entropy is a good measure for bipartite entanglement of pure quantum states [Bennett et al., 1996a]. In fact, many measures of entanglement, such as the distillable entanglement [Bennett et al., 1996a] and the entanglement of formation [Bennett et al., 1996b], reduce to the entanglement entropy for bipartite pure systems. For mixed states, however, the entanglement entropy fails to account for only quantum correlations between the subsystems and thus cannot identify entanglement reliably. In that case, we will consider the logarithmic negativity [Vidal and Werner, 2002], which is an entanglement monotone for mixed states. In contrast to most other entanglement measures, the logarithmic negativity distinguishes itself by being relatively easy to calculate, and can be used to provide upper bounds for other entanglement measures [Vidal and Werner, 2002]. Let us take a closer look the the entanglement entropy and logarithmic negativity.

Entanglement entropy

The entanglement entropy has is roots in statistical quantum mechanics and is related to the Shannon entropy in information theory. Let $\mathcal{H}$ be the Hilbert space of a quantum system defined on the manifold M, and let us assume that upon dividing the manifold into the submanifolds A and B, the Hilbert space can be expressed as the tensor product of the Hilbert spaces corresponding to the subsystems: $\mathcal{H} = \mathcal{H}_A \otimes \mathcal{H}_B$. For a state described by a density matrix ρ, the entanglement entropy of the subsystem A is then given as the von Neumann entropy of the reduced density matrix on A

$$S[A] = -\mathrm{Tr}(\rho_A \log \rho_A), \tag{4}$$

where the reduced density matrix was obtained by tracing out the degrees of freedom on B: $\rho_A = \mathrm{Tr}_B \rho$. The entanglement entropy has been studied in various contexts, as can be seen from our previous historical

[3] As a byproduct of the logarithmic negativity, we also get results for a third, the odd-entropy. As this goes beyond the scope of this thesis, we refer the interested reader to [II].

introduction. In this thesis we view it as a theoretical probe that encodes universal properties of critical field theories. This standpoint has been widely studied and there are several reviews on the matter, such as [Calabrese and Cardy, 2006, Amico et al., 2008, Eisert et al., 2010, Laflorencie, 2016]. Most work on the universal properties of entanglement entropy has been focused on CFTs, where powerful tools are available, and in particular 2-dimensional CFTs, where these tools are the most powerful. In general, one expects the ground state entanglement entropy of a D-dimensional CFT (see [Nishioka et al., 2009, Nishioka, 2018, Rangamani and Takayanagi, 2017] for reviews) to behave as

$$S[A] = \begin{cases} c_{D-2}\left(\frac{L_A}{\varepsilon}\right)^{D-2} + \cdots + c_0 \log\left(\frac{L_A}{\varepsilon}\right) + \cdots, & D \text{ even} \\ c_{D-2}\left(\frac{L_A}{\varepsilon}\right)^{D-2} + \cdots + c_0 + \cdots, & D \text{ odd} \end{cases} \tag{5}$$

where L_A is a characteristic length of A, such that $\text{Area}(A) \propto L_A^{D-2}$, and ε is a UV-cutoff. All coefficients apart from c_0 depend on the regularization scheme and are not physically meaningful. On the other hand, c_0 does not depend on the regularization scheme or the specific realization of the theory within the same universality class, and is thus said to be universal. In even dimensions c_0 is related to the conformal anomaly of the stress-energy tensor of the corresponding CFT [Ryu and Takayanagi, 2006a, Solodukhin, 2008, Fursaev et al., 2013]. We note that expression (5) is in agreement with the famous leading logarithmic divergence in 2-dimensional CFT [Callan and Wilczek, 1994, Holzhey et al., 1994, Calabrese and Cardy, 2004], with $c_0 = c/3$ and c the central charge of the theory. While most work on the entanglement entropy has focused on the ground state, there has also been some research on excited states. A central observation here is that the area law scaling of the ground state is quite special within the Hilbert space. In fact, the entanglement entropy of a pure state picked at random from the Hilbert space generically obeys a volume law [Page, 1993]. Notably, this implies that highly excited states are expected to obey volume laws. On the other hand, the low-lying excitations of various theories have been observed to obey area laws. In [Masanes, 2009], for example, a lattice argument valid for a wide range of theories limited the entanglement entropy of low-lying excited states to obey at most an area law with a logarithmic correction. Examples of this are low-energy excitations corresponding to primary fields in a $1+1$-dimensional CFT [Alcaraz et al., 2011, Berganza et al., 2012], and finite quasi particle excitations in a certain limit of a wide class of theories [Castro-Alvaredo et al., 2018]. In both these cases

the entanglement entropy of the excited states still respects an area law like (5), albeit with a universal correction with respect to the ground state. From a different perspective, numerical studies of spin-chains have shown that, depending on their local properties, one finds both excited states that obey area laws, as well as those that obey volume laws, see for example [Alba et al., 2009].

The entanglement entropy of the $2+1$-dimensional quantum Lifshitz model has also been widely studied, see for example [Fradkin and Moore, 2006, Hsu and Fradkin, 2010, Zaletel et al., 2011, Zhou et al., 2016]. Here, it has been found that the ground state of the model obeys an area law of the form

$$S[A] = c_1 \frac{L_A}{\varepsilon} + \frac{c}{6} \Delta\chi \log \frac{L_A}{\varepsilon} + \gamma_{\mathrm{QCP}} + \ldots, \tag{6}$$

where c is the central charge of CFT whose action describes the ground state of the QLM, $\Delta\chi$ is the change in Euler characteristic after surgery, and c_1 a non-universal constant. The scaling behavior and the logarithmic correction follow from the celebrated result by [Cardy and Peschel, 1988] on the free energies of 2-dimensional CFTs. The sub-leading constant term was shown to be universal whenever $\Delta\chi = 0$ in [Hsu et al., 2009]. There have, to our best knowledge, only been two works on the entanglement entropy of excited states of the QLM. In [Zhou, 2016] an excited state was constructed by acting with a vertex and time evolution operator on the QLM ground state. The excess entanglement entropy after some time was then analyzed and found to be expressed in terms of certain correlation functions of the theory. Our work on excited states [III] is largely based on [Parker et al., 2017]. Here, the entanglement entropy of states obtained by exciting the eigenmodes of the Laplace-Beltrami operator on the spatial manifold was analyzed by replica approach. While the complexity of the problem only allowed the authors to conjecture an expression for the entanglement entropy in some special cases, it was found that it generally depends on quantities that the authors dubbed "Entanglement propagator amplitudes". We will take a closer look at the results from [Parker et al., 2017] in section 2.1 and compare them to our own.

We note here, that a holographic formulation of the entanglement entropy for theories with Lifshitz scaling, see (1), à la Ryu-Takayanagi is not yet well understood. Taking a gravitational solutions that realize Lifshitz scaling, for example [Kachru et al., 2008, Taylor, 2008], one would be tempted to construct the entanglement entropy by the standard Ryu-Takayanagi prescription [Ryu and Takayanagi, 2006b, Ryu and

Takayanagi, 2006a]. However, it turns out that in static Lifshitz spacetimes the resulting entanglement entropy is independent of the critical exponent z, see [Keränen and Thorlacius, 2015]. This has prompted further studies of the entanglement entropy of non-relativistic field theories with general critical exponents such as [He et al., 2017, Mozaffar and Mollabashi, 2017, Gentle and Vandoren, 2018] and our own work [I].

Logarithmic negativity

Let us consider a state described by a density matrix ρ_A on the bipartite geometry $A_1 \cup A_2$, such that the Hilbert space of the total system factors as $\mathcal{H} = \mathcal{H}_1 \otimes \mathcal{H}_2$. Then the logarithmic negativity is defined as [Peres, 1996, Vidal and Werner, 2002]

$$\mathcal{E} = \log \|\rho_A^{T_2}\|, \tag{7}$$

where $(\ )^{T_2}$ represents the partial transposition over the A_2 part of the system, and $\|\mathcal{O}\| = \mathrm{Tr}\sqrt{\mathcal{O}^\dagger \mathcal{O}}$ is the trace norm. This definition relies on the fact that for separable systems the partially transposed density matrix $\rho_A^{T_2}$ is, again, a density matrix. Thus, $\mathcal{E}$ must vanish for non-entangled systems, and a non-vanishing $\mathcal{E}$ detects entanglement. While the literature on the logarithmic negativity is not as vast as that concerning the entanglement entropy, there has been much recent interest. For example, an equivalent definition of the logarithmic negativity that is well-suited for replica calculations [Calabrese et al., 2012, Calabrese et al., 2013a], has been used to analyze different systems in their ground states and at finite temperature, see for example [Calabrese et al., 2013b, Calabrese et al., 2014, Coser et al., 2016, Shapourian and Ryu, 2019]. Until our analytic work [II], the logarithmic negativity of Lifshitz models had only been analyzed numerically [Mozaffar and Mollabashi, 2018].

1.2 Overview of the thesis

This thesis is structured as follows. In section 2 we review the quantum Lifshitz model (QLM) and its generalization to higher dimensions, the generalized quantum Lifshitz model (GQLM), as well as the construction of the ground and excited states of the theory. The generalization of the model is part of [I]. In section 3 we first review the calculation of the ground state entanglement entropy of the QLM, and then show how to generalize those calculations to two situations. First, we apply them to the ground state of the higher dimensional GQLM, and then to the as

the excited states of the QLM. These generalizations are the content of [I]and [III]respectively. Finally, in section 4 we calculate the logarithmic negativity of certain mixed states of the QLM by two different approaches, summarizing the content of paper [II].

In the following we briefly describe of the main results of our papers. These results will be discussed in more detail in the main body of the thesis.

Paper I: Entanglement entropy in generalized quantum Lifshitz models

The QLM was originally defined in $2+1$-dimensions and with dynamical critical exponent $z = 2$, and while the generalization to flat $d+1$-dimensions and $z = d$ is relatively straight-forward, one has to be careful when putting the model on curved manifolds. In this paper we generalize the definition of the $d+1$-dimensional GQLM in flat space given in [Keränen et al., 2017] to encompass curved geometries. Here, two issues are important. First, for $z > 2$ the operator appearing in the action that characterizes the ground state of the model is a higher derivative operator. This means that further boundary conditions need to be specified in order to make the corresponding variational principle well-defined, as well as the operator self-adjoint. Second, one would like the generalized model to retain the connection to CFT that was present in the $2+1$-dimensional QLM. However, on curved manifolds this cannot be achieved if the operator in the ground state action is simply a power of the standard Laplacian (as is the case for flat manifolds). It thus becomes necessary to alter said operator in order to restore the spatial conformal invariance of the ground state. For even spatial dimensions we take the GQLM with critical exponent z to be defined by having the ground state (2) with a ground state action given by

$$S[\phi] = S_0[\phi] + S_{\partial M}[\phi] = g \int_M \mathrm{d}^d x \, \sqrt{G}\, \phi \mathcal{P}_{z,M} \phi + S_{\partial M}[\phi], \tag{8}$$

where G is the determinant of the Euclidean metric on M, the operator $\mathcal{P}_{z,M}$ is the conformal generalization of an integer power of the Laplacian $\Delta^{\frac{z}{2}}$ on M, and S_∂ is a boundary action that makes the variational problem well-defined. We consider two types of geometry, flat tori and spheres. On flat manifolds $\mathcal{P}_{z,M}$ reduces to $\Delta^{\frac{z}{2}}$, and for $d = z = 2$ the bulk action agrees with that of the QLM, that is (3). On spheres and hemispheres $\mathcal{P}_{z,M}$ is a so-called GJMS operator [Graham et al., 1992], which in essence is a polynomial of degree $z/2$ in the Laplace-Beltrami operator on the

manifold, constructed such that it transforms in a specific way under Weyl transformations. In even d dimensions this operator is well-defined for $z = 2, 4, \ldots, d$ [Gover and Hirachi, 2004, Juhl, 2009, Juhl, 2011]. Performing a replica calculation on the spherical geometry we find that the entanglement entropy at $z = d$ of a d-hemisphere H^d can be written as

$$S[H^d] = -\log\left(\frac{Z_{H^d_D} Z_{H^d_D}}{Z_{S^d}}\right) - \frac{1}{2}, \tag{9}$$

with Z the partition function corresponding to the action (8) on the respective manifolds with appropriate boundary conditions. Repeating the calculation on the flat torus $T^d_{L_1,\ldots,L_d} := \mathbb{R}^d/(L_1\mathbb{Z}\times\cdots\times L_d\mathbb{Z})$ cut into the two cylinders $Y_B := [-L_B, 0] \times T^{d-1}_{L_2,\ldots,L_d}$ and $Y_A := [0, L_A] \times T^{d-1}_{L_2,\ldots,L_d}$ we find the entanglement entropy of the cylinder Y_A to be

$$S[Y_A] = -\log\left(\frac{Z_{Y_{A,D}} Z_{Y_{B,D}}}{Z_{T^d}}\right) - \frac{1}{2} - \bar{W}'(1) \tag{10}$$

where $\bar{W}'(1)$ is the contribution from the so-called winding sector. We note that $F[A] = -\log Z_A = \frac{1}{2}\log \mathcal{P}_{d,A}$ is the free energy of the ground state CFT (8). In the paper we put considerable effort into evaluating the resulting determinants and bringing them into relatively simple forms.

Paper II: Logarithmic negativity of the quantum Lifshitz model

We analyze the logarithmic negativity of a certain type of bipartite mixed states of the QLM. These mixed are constructed by putting the ground state density matrix on a tripartite geometry and tracing over one of the parts, resulting in a bipartite mixed state, whose two parts we denote by A_1 and A_2.

We first apply the correlator method to the non-compact QLM in $1+1$-dimensions with spatial part given by a line with either open or periodic boundary conditions, and find that the logarithmic negativity depends on whether the submanifolds A_1 and A_2 are adjacent or not. In both cases the result can be summarized by the following formula in terms of the partition functions with Dirichlet boundary conditions of the subsystems

$$\mathcal{E} = -\log\left(\frac{Z_{A_1} Z_{A_2}}{Z_{A_1\cup A_2}}\right). \tag{11}$$

In the disjoint case the subsystems are not allowed to talk to each other and the partition function factors as $Z_{A_1\cup A_2} = Z_{A_1} Z_{A_2}$. There, we find

the surprising result that the logarithmic negativity vanishes exactly

$$\mathcal{E}_{A_1,A_2 \text{ disjoint}} = 0. \tag{12}$$

Then, we perform an analogous calculation by a replica approach in the $2+1$-dimensional QLM on either a sphere or a torus. In the non-compact case we confirm the result (11), and in the compact case we find the slight generalization

$$\mathcal{E} = -\log\left(\frac{Z_{A_1} Z_{A_2}}{Z_{A_1 \cup A_2}}\right) + \log W_{\mathcal{E}}(1). \tag{13}$$

In the disjoint case $W_{\mathcal{E}}(1) = 1$, so we, again, observe an exact vanishing of the logarithmic negativity. In the adjacent case the winding contribution is non-trivial and, for the sphere, can be related to the winding sector of the entanglement entropy of a tripartite system. As a by-product of our calculations we also find analytic expressions for the odd entanglement entropy of the system.

Paper III: Excited state entanglement entropy of the quantum Lifshitz model

In this third and final paper, we analyze the bipartite entanglement entropy of a certain class of states constructed by exciting the eigenmodes $\Delta L_\lambda(x) = -\lambda L_\lambda(x)$ of the Laplace-Beltrami operator – which is just the differential operator appearing in the ground state action of the QLM. In order to be able to do this, we assume the spatial manifold M of the model to be compact, such that the spectrum of the Laplacian on it is discrete. The general finitely excited state is then labelled by the number of excitations m_{λ_r} in the modes λ_r. We demand that the following integral vanishes (and show that this is justified in the geometries considered)

$$\int_X \mathrm{d}^2x \; L_\lambda(x)\phi^{\mathrm{cl}}(x) = 0, \tag{14}$$

with $X = M$ for the singly excited state. Here ϕ^{cl} is a solution of the equations of motion $\Delta\phi^{\mathrm{cl}} = 0$ on the submanifolds A and B of the bipartite geometry with a specific set of boundary conditions dictated by the replica approach in between. For general excitations, we make the stronger demand that the integrals with $X = A, B$ vanish separately. Whenever this assumption is fulfilled, the replica calculation can be performed analytically and, in particular, we find that the entanglement

entropy of the excited state labelled by $(m_{\lambda_1}, \ldots, m_{\lambda_\nu})$ can be expressed as

$$S_{m_{\lambda_1},\ldots,m_{\lambda_\nu}}[A] = S_{GS}[A]\mathrm{Tr}(\mathcal{M}) + \mathrm{Tr}(\log(\mathcal{A}\mathcal{B})\mathcal{M}). \tag{15}$$

Here, $S_{GS}[A]$ is the ground state entanglement entropy and $\mathcal{A}$, $\mathcal{B}$, and $\mathcal{M}$ are rank 2ν tensors with elements determined by the correlation functions on A, B, and M respectively. For example, the tensor on A is defined as

$$\mathcal{A}^{k'_1,\ldots,k'_\nu}_{k_1,\ldots,k_\nu} := \left(\prod_{r=1}^{\nu} \frac{1}{2^{m_r}} \sqrt{\frac{1}{m_r!}\binom{m_r}{k_r}\binom{m_r}{k'_r}}\right) \times \left\langle \prod_{r=1}^{\nu} H_{m_r-k_r}\left(\varphi_A^{\lambda_r}\right) H_{k'_r}\left(\varphi_A^{\lambda_r}\right) \right\rangle_{A_D}, \tag{16}$$

with each index k_r and k'_r running from 0 to m_{λ_r}, and where the fields are all free in A and with Dirichlet boundary conditions at ∂A. These correlation functions can be resolved by Wicks theorem into polynomials of certain integrals of the Green's functions that were, in a slightly different form, considered by [Parker et al., 2017], and under some numerical evidence conjectured to be universal. Our calculations add evidence to the universality of these quantities. Consequently, it seems that all quantities appearing equation (15) are universal. In the paper we consider two explicit geometries, the sphere and rectangle, and construct all quantities explicitly. In the particular case where all the excitations are put into a single mode, we observe a logarithmic behavior of the entanglement entropy with respect to the excitation number.

2 The Quantum Lifshitz Model

The $2+1$-dimensional quantum Lifshitz model with dynamical critical exponent $z=2$ on a spatial manifold M is defined by the Hamiltonian [Ardonne et al., 2004]

$$H = \frac{1}{2}\int_M \mathrm{d}^2x \ \left(\pi^2 + g^2\left(\Delta\phi\right)^2\right), \tag{17}$$

where Δ is the Laplace-Beltrami operator on M and $g>0$ a real parameter. We take ϕ to be a compactified scalar field with compactification radius R, that is $\phi \sim \phi + 2\pi R$, and $\pi = -i\frac{\delta}{\delta\phi}$ to be its canonical conjugate momentum, with equal time commutator

$$[\phi(x), \pi(x)] = i\delta(x-y). \tag{18}$$

We note that the compactification radius R and the parameter g are not independent of each other, and that physical quantities that are invariant under a rescaling of ϕ are expressed in terms of $R\sqrt{g}$. For different choices of g, the QLM describes the continuum limit of the quantum dimer model [Rokhsar and Kivelson, 1988] and some of its generalizations, e.g [Henley, 1997, Moessner et al., 2001, Castelnovo et al., 2005, Freedman et al., 2005, Fendley, 2008], at criticality. The critical point described by the QLM is an example of a conformal critical point, which is reflected in the fact that the ground state and equal time correlators of the QLM are described by a 2-dimensional euclidean CFT. Note, that this CFT in turn corresponds to a 2-dimensional classical statistical system at criticality.

In order to understand the connection between the QLM and 2-dimensional CFT, let us construct the ground state of the QLM. We first define the operators

$$Q(x) = \frac{1}{\sqrt{2}}\left[i\pi(x) + g(-\Delta)\phi(x)\right] \tag{19}$$

$$Q^\dagger(x) = \frac{1}{\sqrt{2}}\left[-i\pi(x) + g(-\Delta)\phi(x)\right]. \tag{20}$$

The Hamiltonian can then be recast in the form

$$H = \frac{1}{2}\int_M \mathrm{d}^dx \ Q^\dagger(x)Q(x) + E_0, \tag{21}$$

where E_0 is the constant (and UV-divergent) vacuum energy, and can be subtracted from the Hamiltonian without loss of generality. On that account we define $\tilde{H} = H - E_0$. The Hamiltonian $\tilde{H}$ is positive semi-definite, implying that if we can find a state $|\Psi_0\rangle$ that is annihilated by $Q(x)$ for all x, it must be the ground state of the theory. Setting $\Psi_0[\phi] = \langle\phi|\Psi_0\rangle$ we can write out the corresponding functional differential equation as

$$Q(x)\Psi_0[\phi] = \frac{1}{\sqrt{2}}\left(\frac{\delta}{\delta\phi} - g\Delta\phi\right)\Psi_0[\phi] = 0, \tag{22}$$

which has the solution

$$\Psi_0[\phi] = \frac{1}{\sqrt{Z}} e^{\frac{g}{2}\int_M \mathrm{d}^2x\phi(x)\Delta\phi(x)} \tag{23}$$

with normalization given by the partition function $Z = \int \mathcal{D}\phi\ e^{-S[\phi]}$ and where the action $S[\phi]$ is the negative exponent in (23). After integration by parts $S[\phi]$ can be written as

$$S[\phi] = g\int \mathrm{d}^2x\ \left(\nabla\phi(x)\right)^2. \tag{24}$$

which is simply the conformally invariant action of a free scalar in two dimensions.

2.1 Excited states

One can consider many different types of excited states for the quantum Lifshitz model. In [Zhou, 2016], for example, coherent excitations of the vacuum by vertex operators were considered, and the excess entanglement entropy after a time t was found. We will consider another situation that was first studied by [Parker et al., 2017]. Let M be a compact manifold, such that the spectrum of Δ is discrete on it and given by

$$-\Delta L_\lambda(x) = \lambda L_\lambda(x). \tag{25}$$

By projecting $Q(x)$ and $Q^\dagger(x)$ onto $L_\lambda(x)$ we can define creation and annihilation operators $A^\dagger_\lambda$ and A_λ for the eigenmode $L_\lambda(x)$[4]

$$A^\dagger_\lambda := \frac{1}{\sqrt{g\lambda}}\int_M \mathrm{d}^2x\ L_\lambda(x)Q^\dagger(x), \quad A_\lambda := \frac{1}{\sqrt{g\lambda}}\int_M \mathrm{d}^2x\ L_\lambda(x)Q(x). \tag{26}$$

[4]Note that there is an A_λ for each eigenmode, regardless of the degeneracy of the eigenvalue λ. When λ is used as an index, it is meant as a unique label for the mode. For example we mean $\lambda = \ell(\ell+1)$, but $A_\lambda = A_{(\ell,m)}$ on the spherical geometry where the eigenmodes are the spherical harmonics $L_\lambda(x) = Y^m_\ell(x)$.

From the commutation relation $[Q(x)^\dagger, Q(y)] = g(-\Delta)\delta(x-y)$ for the position space operators, which in turn follows from the canonical commutation relation between $\phi(x)$ and $\pi(x)$, see (18), we find that

$$[A_\lambda, A_\mu^\dagger] = \delta_{\lambda\mu}, \quad [A_\lambda^\dagger, A_\mu^\dagger] = [A_\lambda, A_\mu] = 0, \tag{27}$$

$$[H, A_\lambda^\dagger] = g\lambda\, A_\lambda^\dagger. \tag{28}$$

These correspond to the commutation relations of a harmonic oscillator for each mode, with $g\lambda$ the energy of a single excitation in the λ-mode. The Hamiltonian can then be recast as

$$H = \sum_\lambda g\lambda\, A_\lambda^\dagger A_\lambda. \tag{29}$$

It is now straight-forward to construct any such finitely excited state. We pick a set of modes $\{\lambda_1, \ldots, \lambda_\nu\}$ and act on the ground state m_{λ_r} times with each of the corresponding creation operators $A_{\lambda_r}^\dagger$. The general excited state is then labeled by the numbers m_{λ_r} and given by

$$|(m_{\lambda_1}, \ldots, m_{\lambda_\nu})\rangle = \frac{\left(A_{\lambda_1}^\dagger\right)^{m_{\lambda_1}}}{\sqrt{m_{\lambda_1}!}} \cdots \frac{\left(A_{\lambda_r}^\dagger\right)^{m_{\lambda_r}}}{\sqrt{m_{\lambda_r}!}} \cdots \frac{\left(A_{\lambda_\nu}^\dagger\right)^{m_{\lambda_\nu}}}{\sqrt{m_{\lambda_\nu}!}} |\Psi_0\rangle \tag{30}$$

$$= \frac{1}{\sqrt{Z}} \int \mathcal{D}\phi \left(\prod_{r=1}^{\nu} \frac{1}{\sqrt{2^{m_{\lambda_r}} m_{\lambda_r}!}} H_{m_{\lambda_r}} \left(\frac{\phi^{\lambda_r}}{\sqrt{2}} \right) \right) e^{-\frac{1}{2}S[\phi]} |\phi\rangle, \tag{31}$$

where $H_m(\phi)$ is a Hermite polynomial defined as

$$H_m(x) = m! \sum_{k=0}^{\lfloor \frac{m}{2} \rfloor} \frac{(-1)^k (2x)^{m-2k}}{k!(m-2k)!} \tag{32}$$

and where ϕ_r^λ is in essence the projection of $\phi(x)$ onto the eigenmode $L_\lambda(x)$

$$\phi^\lambda = \sqrt{2g\lambda} \int_M \mathrm{d}^2x\; L_\lambda(x)\phi(x) \tag{33}$$

with a factor $\sqrt{2g\lambda}$ chosen to simplify the coming entanglement calculations.

2.2 Generalization to higher dimensions

Our goal in this section is to find a generalization of the quantum Lifshitz model to geometries with a spatial part determined by a curved higher

dimensional manifold M. Our guiding principle is that we would like the resulting model to maintain the nice properties of the $d = z = 2$ QLM. More concretely, we want the generalized model to have a ground state that is defined through a CFT action, and thus still describes a classical critical system. Our starting point is the generalization of the quantum Lifshitz model to flat $d+1$-dimensional space by [Keränen et al., 2017] and dubbed generalized quantum Lifshitz models. Let us briefly review this models before continuing. It is defined by the Hamiltonian

$$H = \frac{1}{2}\int \mathrm{d}^d x \ \left(\pi^2 + g^2\left(\Delta^{\frac{z}{2}}\phi\right)^2\right), \tag{34}$$

where $\Delta = -\partial^a\partial_a$ is the Laplace-Beltrami operator and $g > 0$ a real parameter. As before, ϕ is a compact scalar field and π its conjugate momentum. At $d = z = 2$ this definition reduces the standard QLM (see equation (17)) as defined by [Ardonne et al., 2004]. The ground state of the model can be calculated in an analogous way to before, by defining

$$Q(x) = \frac{1}{\sqrt{2}}\left(i\pi(x) + g(-\Delta)^{\frac{z}{2}}\phi(x)\right) \tag{35}$$

such that $H = \int \mathrm{d}^d x Q^\dagger(x)Q(x) + E_0$, and then finding the state $\Psi_0[\phi]$ annihilated by $Q(x)$ for all x. The ground state takes the same form as before

$$\Psi_0[\phi] = \frac{1}{\sqrt{Z}}e^{-\frac{1}{2}S[\phi]} \tag{36}$$

with normalization given by the partition function $Z = \int \mathcal{D}\phi e^{-S[\phi]}$ and where the action $S[\phi]$ is now

$$S[\phi] = -g\int \mathrm{d}^d x \ \phi(x)(-\Delta)^{\frac{z}{2}}\phi(x). \tag{37}$$

It was observed in [Keränen et al., 2017] that for $z = d$ the action corresponds to that of the higher derivative CFT studied in [Brust and Hinterbichler, 2017]. As we will see, other values of z can also lead do higher derivative CFTs.

The naïve ansatz of simply putting the action (38) on a curved manifold does not necessarily work, as the operator $(-\Delta)^{\frac{z}{2}}$ is not a conformal differential operator in general. The first step in defining the generalized action is thus replacing the operator by a conformal counterpart. We denote the conformally invariant generalization of $(-\Delta)^{\frac{z}{2}}$ by $\mathcal{P}_{z,M}$. It is an operator of degree z that depends on the geometry of the manifold M. Furthermore, in order to have a well-defined variational

principle when M has a boundary we need to include boundary terms for the action, which we denote by $S_{\partial M}[\phi]$. This is of special importance to us, as the entanglement calculations demand a surgery that introduces a non-trivial boundary. With this considerations we can write down our ansatz for the generalized action as

$$S[\phi] = S_0[\phi] + S_{\partial M} = g \int_M \mathrm{d}^d x \sqrt{G}\ \phi \mathcal{P}_{z,M} \phi + S_{\partial M}[\phi]. \tag{38}$$

Both the generalized conformal Laplacian and the boundary terms depend on the manifold, so let us take a look a two concrete geometries: the flat torus and the sphere.

The flat torus

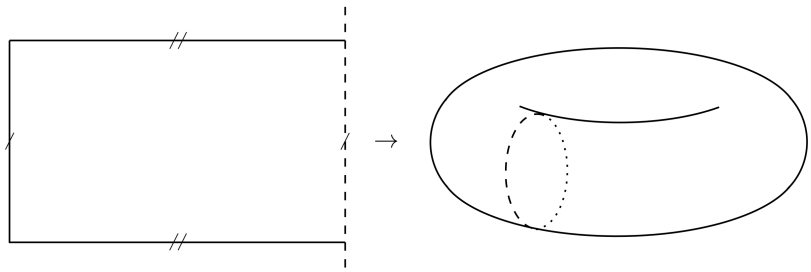

Figure 2.1. The flat torus as a rectangle with opposite sides periodically identified.

Let the d-dimensional flat torus with circumferences $L_1, \ldots, L_d$ be defined by

$$T^d_{L_1,\ldots,L_d} := \mathbb{R}^d / \left(L_1 \mathbb{Z} \ldots L_d \mathbb{Z}\right). \tag{39}$$

The situation in two dimensions is depicted in figure 2.1. The d-torus defined above is flat and thus $\mathcal{P}_{z,M}$ is the same operator that appears in (38), that is

$$\mathcal{P}_{z,T^d_{L_1,\ldots,L_d}} = (-1)^{\frac{z}{2}+1} \Delta^{\frac{z}{2}} \tag{40}$$

with $\Delta = -\partial^a \partial_a$. We want the variational principle associated to the action defined by inserting this operator into (38) to be well-defined. As the operator is a higher derivative operator, this forces us to impose a set of boundary conditions on the variations of the field ϕ. Such a consistent choice of boundary conditions for the variations is given by

$$\delta\phi|_{\partial M} = 0, \quad \Delta^k \delta\phi|_{\partial M} = 0, \quad k = 1, \ldots, \frac{z}{2} - 1. \tag{41}$$

Here, there is an implicit assumption about the surgery that we will perform on the torus. We will divide it into two cylinders, so the manifolds that we finally consider have two boundaries. With $z/2$ boundary conditions at each boundary we arrive at the z boundary conditions needed to have a well-defined fluctuation associated to a linear differential equation of degree z. The motivation for the choice (41) has two origins. On one hand, we will perform a replica calculation, for which it is important to demand that the fluctuations obey Dirichlet boundary conditions. On the other hand, we want the boundary conditions to be consistent with the self-adjointness of the operator (40). Both these requirements are satisfied by (41). Finally, we define the boundary action to be

$$S_{\partial M} := (-1)^{z/2+1} \int_{\partial M} \mathrm{d}^{d-1}x \sum_{k=0}^{\frac{z}{2}-1} (\partial_n^{2k}\phi)(\partial_n^{z-2k-1}\delta\phi). \tag{42}$$

With this choice and the boundary conditions for the fluctuations (41) the variation of the action (38) vanishes at the boundary and gives the equation of motion

$$\Delta^{\frac{z}{2}}\phi = 0 \tag{43}$$

inside the manifold. We will talk about the boundary conditions for the fields when we perform the replica calculation of the entanglement entropy. For now we note that again z boundary conditions are needed and that they need to be chosen carefully in order to be consistent with the previous discussion.

The sphere

On the sphere, the proper generalization of the $(-\Delta)^{\frac{z}{2}}$ is given by a so-called GJMS-operator $\mathcal{P}_{z,S^d}$ [Graham et al., 1992]. These operators are generalizations of the conformal Laplacian to higher derivatives defined to transform covariantly under Weyl transformations. Concretely, the GJMS-operator transforms as

$$\mathcal{P}_{z,S^d}(e^{2\omega}G) = e^{-\frac{d+z}{2}\omega}\mathcal{P}_{z,S^2}(G)e^{\frac{d-k}{2}\omega}, \tag{44}$$

under the Weyl transformation of the metric $G_{ab} \mapsto e^{2\omega}G_{ab}$. Let $z > 0$ be even, that is $z = 2k$ for a positive integer k. On the sphere the GJMS-operator can then be explicitly written as

$$\mathcal{P}_{2k,S^d} = \prod_{j=1}^{k} \left[\Delta_{S^d} + \left(\frac{d}{2} - j\right)\left(\frac{d}{2} + j - 1\right)\right], \tag{45}$$

where $\Delta_{S^d} = -\frac{1}{\sqrt{G}}\partial_a\left(\sqrt{G}G^{ab}\partial_b\right)$ is the corresponding Laplace-Beltrami operator. For even dimensions the GJMS-operator is well-defined for $k = 1, \ldots, d/2$, while for odd dimensions the GJMS operator is well-defined for any positive integer k [Gover and Hirachi, 2004, Juhl, 2009, Juhl, 2009]. The case $z = d$ is called the critical case and will be our focus of attention when we consider the entanglement entropy, as it is the most direct generalization of the flat $z = d$ quantum Lifshitz model from [Keränen et al., 2017].

As for the torus, we need to introduce boundary conditions for the fluctuations whenever the manifold has a boundary. This is, for example, the case when we consider a hemisphere instead of the full sphere. A consistent choice of boundary conditions in that case is

$$\delta\phi|_{\partial M} = 0, \quad \Delta^k_{S^d}\delta\phi|_{\partial M} = 0, \quad k = 1, \ldots, \frac{z}{2} - 1. \tag{46}$$

For $z = d$ we can define the boundary action

$$\begin{aligned} S_{\partial M}[\phi] := \\ \sum_{\ell=1}^{d/2}\int_M \mathrm{d}^d x\ \partial_a\Bigg[\sqrt{G}G^{ab}\left(\prod_{j=1}^{d/2-\ell}\left[\Delta_{S^d} + \left(\frac{d}{2}-j\right)\left(\frac{d}{2}+j-1\right)\right]\phi\right) \\ \times\partial_b\left(\prod_{j=d/2-\ell+2}^{d/2}\left[\Delta_{S^d} + \left(\frac{d}{2}-j\right)\left(\frac{d}{2}+j-1\right)\right]\phi\right)\Bigg]. \end{aligned} \tag{47}$$

This choice of boundary action together with the boundary conditions for the fluctuations (46) makes the variations of the action (38) with $\mathcal{P}_{z,M}$ given by the GJMS-operator (45) well-defined. In particular the variation leads to the desired equations of motion on the sphere

$$\mathcal{P}_{d,S^d}\phi = 0 \tag{48}$$

and vanishes at the boundary.

3 Entanglement entropy

Consider a bipartite geometry consisting of a manifold M that is cut into two parts A and B such that the Hilbert space $\mathcal{H}$ on M decomposes into the tensor product of the Hilbert spaces on the submanifolds[5]

$$\mathcal{H} = \mathcal{H}_A \otimes \mathcal{H}_B. \tag{49}$$

Let there be a quantum state on M described by the density matrix ρ. The entanglement entropy of the region A is then defined as the von Neumann entropy of the reduced density matrix $\rho_A = \mathrm{Tr}_B \rho$ on A

$$S[A] = -\mathrm{Tr}\rho_A \log \rho_A. \tag{50}$$

As mentioned in the introduction, the entanglement entropy has in general leading power-law UV-divergences that are non-universal. Depending on the dimension these are followed by a logarithmic divergence or a constant subleading term that are universal. For the types of smooth surgeries that we consider the logarithmic divergence will always vanish, and the universality will be captured in the constant subleading coefficient. Our goal is to calculate this universal subleading term. We thus not care about the exact coefficients of the power-law divergences. We will perform the entanglement entropy calculations by means of the replica method. This approach was first formulated by [Callan and Wilczek, 1994] and brought to the form most commonly used for entanglement entropy calculations in QFT by the work of Cardy and Calabrese, see [Calabrese and Cardy, 2004, Calabrese and Cardy, 2009]. In the context of the QLM, [Fradkin and Moore, 2006] were the first to perform a replica calculation of the entanglement entropy, although they missed the winding sector – a topological contribution due to the compactification of the scalar. This was later pointed out and corrected by [Oshikawa, 2010] and [Zaletel et al., 2011]. In [Zhou et al., 2016] analytic results for the entanglement entropy

[5] Generically in quantum field theory this assumption fails, leading to the famous UV-divergences in the entanglement entropy. However, some of the results calculated under this assumption, and in particular those concerning universal terms, can be made rigorous, see for example [Witten, 2018] for an introduction. As interesting as it is, this discussion is outside the scope of this thesis.

of the $z = d = 2$ QLM were found for various "circular" geometries such as spheres, cylinders, and annuli. Our approach to the replica calculation in the QLM follows [Zhou et al., 2016].

The essence of the replica approach lies in the observation that the entanglement entropy (50) can be rewritten as the limit

$$S[A] = -\lim_{n\to 1} \partial_n \mathrm{Tr}\left(\rho_A^n\right), \tag{51}$$

where each of the n copies of the density matrix is called a replica. The calculation of the entanglement entropy is then reduced to three steps. First, find an analytic expression for $\mathrm{Tr}\rho_A^n$. For us, this is done using path integral methods and it is much easier than calculating the matrix logarithm of the reduced density matrix. Second, find an analytic continuation in n. This step is the trickiest, as finding analytic continuations is not straight-forward at all and highly dependent on the explicit situation. The third and easiest step is then to calculate the derivative of the expression and find the limit.

Let us make few remarks on the analytic continuation before continuing. In principle, the path integral calculations only lead to expressions for positive integer n, and thus the analytic continuation to complex n need not be unique. This apparent problem is solved by Carlson's theorem [Carlson, 1914] regarding analytic continuations from the integers and its the extension by Rubel [Rubel, 1956] concerning analytic continuations from the positive integers. In our context, the essence of the theorems is that two analytic continuations from the positive integers can only differ, if their difference grows more than exponentially as the argument goes to complex infinity. In other words, if we find an analytic continuation in n that grows less then exponentially in n as $n \to i\infty$, then it is the only one with that asymptotic behavior. A simple example of this is the following. Let there be a function $f(n)$ that vanishes for all positive integers. The unique analytic continuation with sub-exponential asymptotics is simply the constant zero-function. If we however allow exponential asymptotic behavior, then $f(n) = \sin(\pi n)$ with $f(in) \sim e^{\pi n}$ for large n, is also an analytic continuation. The uniqueness in the analytic continuation needed to calculate the limit (51) should thus always be interpreted from the perspective of Carlson's theorem. Therefore whenever we say that an analytic continuation is unique we mean it to be unique in its asymptotic class. For most of our analytic continuations it will not be hard to see that they fall into the sub-exponential category, as their dependence on n is through a power $(\ )^n$ which oscillates as $in \to \infty$.

3.1 Warming up: $z = d = 2$

Let us review the replica calculation of the ground state entanglement entropy in the $z = d = 2$ QLM on the sphere and cylinder. The calculation will only change in some minor key points for the generalizations, so it is instructive to understand the simpler case first. In fact, one can say that these calculations lie precisely at the heart of all our replica calculations. The geometries are chosen to exhibit certain features: The sphere has a 0-mode which leads to some non-trivial effects, and the cylinder displays a non-trivial winding sector. The following calculations were first performed by [Zhou et al., 2016] building on the results by [Fradkin and Moore, 2006, Zaletel et al., 2011]. We follow the calculations by [Zhou et al., 2016] and our own [I] closely in this section. Our starting point is the density matrix corresponding to the ground state (23), which, using the assumption that the Hilbert space splits as $\mathcal{H} = \mathcal{H}_A \otimes \mathcal{H}_B$, we rewrite as

$$\rho = |\Psi_0\rangle\langle\Psi_0| \tag{52}$$

$$= \frac{1}{Z}\int \mathcal{D}\phi_A \mathcal{D}\phi'_A \mathcal{D}\phi_B \mathcal{D}\phi'_B \; e^{-\frac{1}{2}S[\phi]-\frac{1}{2}S[\phi']} |\phi_A\rangle \otimes |\phi_B\rangle\langle\phi'_A| \otimes \langle\phi'_B|, \tag{53}$$

with the action, see equation (24),

$$S[\phi] = g\int_M \mathrm{d}^2x \, (\nabla\phi)^2 \, . \tag{54}$$

The fields indexed by A have support on A and live in $\mathcal{H}_A$, while those indexed by B have support on B and belong to $\mathcal{H}_B$. It is clear that

$$S[\phi] = S[\phi_A] + S[\phi_B]. \tag{55}$$

The reduced density matrix is found by tracing out $\mathcal{H}_B$, that is

$$\rho_A = \mathrm{Tr}_B \rho \tag{56}$$

$$= \int \mathcal{D}\varphi_B \langle\varphi_B|\rho|\varphi_B\rangle. \tag{57}$$

We assume that the path integrals are all taken over orthonormal bases of the Hilbert spaces $\mathcal{H}_A$ and $\mathcal{H}_B$. After the partial tracing operation there are thus three path integrals over $\mathcal{H}_B$, namely over $\mathcal{D}\phi_B$, $\mathcal{D}\phi'_B$, and $\mathcal{D}\varphi_B$, and two δ-functions, $\langle\varphi_B|\phi_B\rangle = \delta(\varphi_B - \phi_B)$ and $\langle\phi'_B|\varphi_B\rangle = \delta(\phi'_B - \varphi_B)$. Resolving the delta functions with two of the path integrals leaves us with one integral and the gluing condition $\phi_B = \phi'_B$.

Next, we want to calculate $\mathrm{Tr}\rho_A^n$. In order to keep track of the different replicas it is helpful to introduce the replica index $i = 1, \ldots, n$ and rewrite it as $\mathrm{Tr}\prod_{i=1}^n \rho_{A,i}$, where $\rho_{A,i}$ is given by

$$\rho_{A,i} = \frac{1}{Z}\int \mathcal{D}\phi_{A,i}\mathcal{D}\phi'_{A,i}\mathcal{D}\phi_{B,i} e^{-\frac{1}{2}S[\phi_{A,i}]-\frac{1}{2}S[\phi'_{A,i}]-S[\phi_{B,i}]}|\phi_{A,i}\rangle\langle\phi'_{A,i}|. \quad (58)$$

Continuing our calculation, it isn't hard to see that each adjacent product of density matrices leads to a delta function that can be resolved by performing the path integral over the primed field

$$\rho_{A,i}\rho_{A,i+1} \propto \int \mathcal{D}\phi'_{A,i}\mathcal{D}\phi_{A,i+1}\langle\phi'_{A,i}|\phi_{A,i+1}\rangle \quad (59)$$

$$\propto \int \mathcal{D}\phi_{A,i+1} \quad \text{with} \quad \phi'_{A,i} = \phi_{A,i+1}. \quad (60)$$

Thus we get the gluing conditions that $\phi'_{A,i} = \phi_{A,i+1}$ for $i = 1, \ldots, n-1$. The final trace over A is

$$\mathrm{Tr}\rho_A^n = \int \mathcal{D}\varphi_A \langle\varphi_A|\mathrm{Tr}\rho_A^n|\varphi_A\rangle, \quad (61)$$

and leads, similarly to the partial trace over B, to the gluing conditions $\phi'_{A,n} = \phi_{A,1}$. Let us briefly look at the gluing conditions that we have. They can all be summarized by $\phi'_{A,i} = \phi_{A,i+1}$ and $\phi'_{B,i} = \phi_{B,i}$ for $i = 1, \ldots, n$ and $n+1 \sim 1$. They are depicted in figure 3.2 together with the continuity condition at the entangling cut Γ between A and B, which is given by $\phi_{A,i}|_\Gamma = \phi_{B,i}|_\Gamma$ for all i as well as for the primed fields. As can be seen in the image, the gluing and continuity conditions force all fields to collapse into a single value at the entangling cut Γ. We can thus finally write the following expression for $\mathrm{Tr}\rho_A^n$

$$\mathrm{Tr}\rho_A^n = \frac{1}{Z^n}\int_{\mathcal{B}} \prod_{i=1}^n \mathcal{D}\phi_{A,i} e^{-\sum_{i=1}^n S[\phi_{A,i}]} \int_{\mathcal{B}} \prod_{i=1}^n \mathcal{D}\phi_{B,i} e^{-\sum_{i=1}^n S[\phi_{B,i}]}, \quad (62)$$

where $\mathcal{B}$ represents the boundary conditions at the entangling cut

$$\mathcal{B}: \quad \phi_{A,i}|_\Gamma(x) = \phi_{B,j}|_\Gamma(x) =: \mathrm{cut}(x), \quad i,j = 1, \ldots, n, \quad (63)$$

and $\mathrm{cut}(x)$ is a function on the entangling cut Γ. Because the field is compactified, that is $\phi \sim \phi + 2\pi R$, this boundary conditions only have to be satisfied modulo $2\pi R$. The standard way of accounting for this, is by dividing the field into a classical part and a fluctuation, see for example [Di Francesco et al., 1997]. We therefore write each replicated field as

$$\phi_{X,i} = \phi^{\mathrm{cl}}_{X,i} + \varphi_{X,i}, \quad \text{for} \quad X = A, B \text{ and } i = 1, \ldots, n. \quad (64)$$

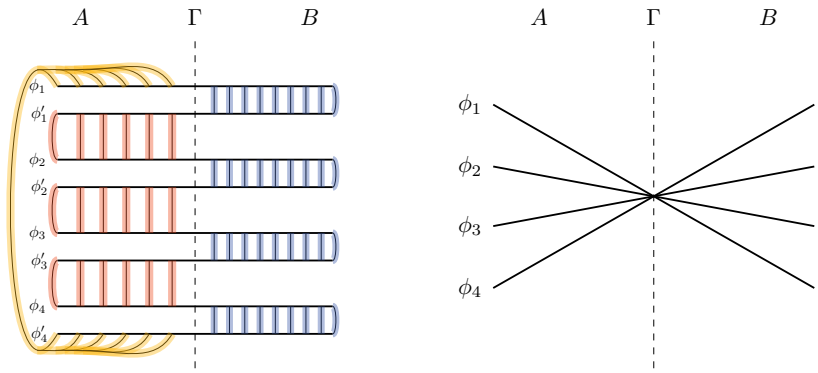

(a) Gluing conditions (b) Resulting configuration

Figure 3.2. The gluing conditions arising from the calculation of $\mathrm{Tr}\rho_A^n$ *and the geometry that results are depicted. The blue lines represent the gluing conditions due to the partial tracing on the B-side of each replica. The red lines represent the gluing conditions resulting from the multiplication of the replicated reduced density matrices. The yellow lines represent the gluing conditions from the final total trace. Figure taken from [III].*

We demand that the classical fields satisfy the equations of motion corresponding to $S[\phi]$, and that they take up the value of the total field at the entangling cut Γ, that is

$$\Delta\phi_{X,i}^{\mathrm{cl}} = 0 \quad \text{with} \quad \phi_{X,i}^{\mathrm{cl}}|_\Gamma(x) = \mathrm{cut}(x), \tag{65}$$

while we only demand from the fluctuations that they satisfy Dirichlet boundary conditions at Γ

$$\varphi_{X,i}|_\Gamma = 0. \tag{66}$$

Note that unless stated otherwise, the equations are satisfied for the complete index range $X = A, B$ and $i = 1, \ldots, n$. The above definitions make sure that the action factors as

$$S[\phi_{X,i}] = S[\phi_{X,i}^{\mathrm{cl}}] + S[\varphi_{X,i}]. \tag{67}$$

Let us examine the classical field a little closer. From the equations of motion, one can see that the classical field accounts for the compact behavior of the total field[6] and the fluctuation is allowed to be non-compact.

[6] Since $\Delta 2\pi R = 0$, it is part of the classical part of the field.

Concretely, this implies that the boundary condition for the classical field stated in (65) only has to be satisfied modulo $2\pi R$. Furthermore, the classical fields on A and B obey the same boundary conditions at the cut between the two submanifolds. They can thus be stitched together to form a continuous classical field on $A \cup B$[7] by

$$\phi_i^{\mathrm{cl}}(x) := \begin{cases} \phi_{A,i}^{\mathrm{cl}}(x), & x \in A \\ \phi_{B,i}^{\mathrm{cl}}(x), & x \in B. \end{cases} \tag{68}$$

In order to account for the compact nature of the classical field, we rewrite its boundary conditions (65) as

$$\phi_i^{\mathrm{cl}}|_\Gamma(x) = \mathrm{cut}(x) + 2\pi R\omega_i, \quad \text{for } i = 1, \ldots, n \tag{69}$$

where ω_i are integers referred to as winding numbers. Using the fact that $\mathrm{cut}(x)$ is an arbitrary function, we can can redefine it as $\mathrm{cut}(x) \mapsto \mathrm{cut}(x) - 2\pi R\omega_n$ while simultaneously redefining $\omega_i \mapsto \omega_i + \omega_n$ for $i = 1, \ldots, n-1$. This gets rid of the n-th winding number, and the boundary conditions for the classical field are finally

$$\begin{aligned} \phi_i^{\mathrm{cl}}|_\Gamma(x) &= \mathrm{cut}(x) + 2\pi R\omega_i \quad i = 1, \ldots, n-1, \\ \phi_n^{\mathrm{cl}}|_\Gamma(x) &= \mathrm{cut}(x). \end{aligned} \tag{70}$$

We can now finally return to equation (62) and recast it as

$$\mathrm{Tr}\rho_A^n = \frac{1}{Z^n} \prod_{i=1}^n \int_D \mathcal{D}\varphi_{A,i} e^{-S[\varphi_{A,i}]} \prod_{i=1}^n \int_D \mathcal{D}\varphi_{B,i} e^{-S[\varphi_{B,i}]} W(n). \tag{71}$$

The D below the path integrals over the fluctuations emphasizes that they obey Dirichlet boundary conditions, while $W(n)$ represents the sum over all classical fields obeying the boundary conditions (70)

$$W(n) = \sum_{\phi_i^{\mathrm{cl}}} e^{-\sum_{i=1}^n S[\phi_i^{\mathrm{cl}}]}. \tag{72}$$

We note that $W(n)$ as written above is just a formal expression. At this point it also includes a path integration over all possible functions at the cut. In the following we will separate that contribution from the other, and $W(n)$ will turn into an actual classical sum over winding modes. From this point on however, the discussion depends on the specific geometry. Let us thus consider the simple cases of a halved sphere and bipartite cylinder separately.

[7] This field should not be confused with the classical field on the complete manifold obtained by solving the equations of motion on M with boundary conditions on ∂M. In particular the stitched together field isn't necessarily differentiable at the cut, while the 0-mode on M is.

The cylinder

The calculation of the entanglement entropy of the quantum Lifshitz model on a bipartite cylinder has been considered by many authors, see for example [Chen et al., 2015, Stéphan et al., 2013, Hsu et al., 2009] apart from those already mentioned.

The cylinder is defined as the rectangle $(x, y) \in [0, L_x] \times [0, L_y]$ with the second coordinate identified $y \sim y + L_y$. We cut the cylinder at $x = \ell_x$ into the two smaller cylinders $A = [0, \ell_x] \times [0, L_y]$ and $B = [\ell_x, L_x] \times [0, L_y]$ with the same periodical identification along the y-direction. We choose Dirichlet boundary conditions at the ends of the cylinder $\phi(0, y) = \phi(L_x, y) = 0$ for all y.

Our starting point for the cylinder, is the observation that in the boundary conditions for the classical fields (70) all fields depend on the same $\mathrm{cut}(x)$ function, and since there is only one such function, there is a sort of redundancy in how the boundary values are distributed. In other words, apart from the winding numbers, there is only one degree of freedom, $\mathrm{cut}(x)$, at the entangling cut Γ, but, how things are, it is distributed among all replicas. In order to resolve this we follow [Zaletel et al., 2011, Zhou et al., 2016] and define the unitary rotation U_n as

$$U_n := \begin{bmatrix} \frac{1}{\sqrt{2}} & -\frac{1}{\sqrt{2}} & 0 & & \dots \\ \frac{1}{\sqrt{6}} & \frac{1}{\sqrt{6}} & -\frac{2}{\sqrt{6}} & 0 & \dots \\ \vdots & & & & \\ \frac{1}{\sqrt{n(n-1)}} & \frac{1}{\sqrt{n(n-1)}} & \dots & \dots & -\sqrt{1-\frac{1}{n}} \\ \frac{1}{\sqrt{n}} & \frac{1}{\sqrt{n}} & \dots & \dots & \frac{1}{\sqrt{n}} \end{bmatrix}, \tag{73}$$

as well as the minor matrix M_{n-1} found by deleting the n-th row and column of U_n. We then rotate the classical fields[8] as

$$\bar{\phi}^{\mathrm{cl}} = U_n \phi^{\mathrm{cl}}. \tag{74}$$

The rotated classical fields now obey the nicer set of boundary conditions

$$\bar{\phi}_i^{\mathrm{cl}}|_\Gamma(x) = 2\pi R \bar{\omega}_i, \quad i = 1, \dots, n-1 \tag{75}$$

$$\bar{\phi}_n^{\mathrm{cl}}|_\Gamma = \sqrt{n}\,\mathrm{cut}(x) + \frac{2\pi R}{\sqrt{n}} \sum_{i=1}^{n-1} \omega_i, \tag{76}$$

with $\bar{\omega} = M_{n-1}\omega$. The first $n-1$ classical fields now only depend on the rotated winding modes, and the dependence on the cut-function is shifted

[8] Note that the action is invariant under this transformation.

to only the n-th field. This allows us to rewrite the winding sector

$$\begin{aligned} W(n) &= \sum_{\phi_i^{\mathrm{cl}}} e^{-\sum_{i=1}^{n} S[\phi_i^{\mathrm{cl}}]} \\ &= \sum_{\omega \in \mathbb{Z}^{n-1}} e^{-\sum_{i=1}^{n-1} S[\bar{\phi}_i^{\mathrm{cl}}]} \int \mathcal{D}\,\mathrm{cut}\, e^{-S[\bar{\phi}_n^{\mathrm{cl}}]} \\ &= n^{-\frac{\mathrm{Area}(\Gamma)}{\varepsilon}} \bar{W}(n) \int \mathcal{D}\bar{\phi}_n^{\mathrm{cl}} e^{-S[\bar{\phi}_n^{\mathrm{cl}}]}. \end{aligned} \tag{77}$$

In the second line the path integral is taken over all possible boundary functions $\mathrm{cut}(x)$. To arrive at the last line we perform the following change of path integral measure (due to [Zaletel et al., 2011])

$$\mathcal{D}\,\mathrm{cut} = \mathcal{D}\left[\frac{1}{\sqrt{n}}\left(\bar{\phi}_n^{\mathrm{cl}} - \frac{2\pi R}{\sqrt{n}} \sum_{i=1}^{n-1} \omega_i\right)\right] = n^{-\frac{\mathrm{Area}(\Gamma)}{\varepsilon}} \mathcal{D}\bar{\phi}_n^{\mathrm{cl}}, \tag{78}$$

where ε is a UV-cutoff and $n^{-\frac{\mathrm{Area}(\Gamma)}{\varepsilon}}$ only contributes an area law term to the entanglement entropy and, as we are only interested in the sub-leading terms, can thus be ignored in the following. Furthermore, we defined the factor

$$\bar{W}(n) = \sum_{\omega \in \mathbb{Z}^{n-1}} e^{-\sum_{i=1}^{n-1} S[\bar{\phi}_i^{\mathrm{cl}}]}. \tag{79}$$

Now comes the final crucial observation. We can take the path integrals of the fluctuations of the n-th field on A and B in (71), and stitch them together with the path integral over the n-th rotated classical field[9] to form a path integral over a full rotated field

$$\int_D \mathcal{D}\varphi_{A,n} \mathcal{D}\varphi_{B,n} \int \mathcal{D}\bar{\phi}_n^{\mathrm{cl}} e^{-(S[\varphi_{A,n}] + S[\varphi_{B,n}] + S[\bar{\phi}_n^{\mathrm{cl}}])} = \int \mathcal{D}\bar{\phi}_n e^{-S[\bar{\phi}_n]}. \tag{80}$$

Noting that this is just the partition function Z on the complete cylinder and that the remaining path integrals over the fluctuations in (71) are simply Dirichlet partition functions on A and B, which we denote by Z_A and Z_B, we can write our final expression for the trace of the n-th power of the reduced density matrix

$$\mathrm{Tr}\rho_A^n = \left(\frac{Z_A Z_B}{Z}\right)^{n-1} \bar{W}(n). \tag{81}$$

[9] Note that by (78) the latter path integral is equivalent to a path integral over all possible values of the total field at the cut.

The analytic continuation in n for the powers of the partition functions is straight-forward. Since the partition functions are real, it is oscillating as $n \to i\infty$ and thus unique[10]. Finding an analytic continuation for the winding sector $\bar{W}(n)$ is far less trivial and was done by [Oshikawa, 2010, Zaletel et al., 2011, Zhou et al., 2016]. We refrain from writing it here as it is a complicated expression and doesn't contribute to the discussion, but point out that it obeys the right asymptotics and is thus also unique and in the same class as the rest. Taking the partial derivative with respect to n of (81), followed by the limit $n \to 1$, we find the entanglement entropy

$$\begin{aligned} S[A] &= -\lim_{n\to 1} \mathrm{Tr}\rho_A^n \\ &= -\log\left(\frac{Z_A Z_B}{Z}\right) - \bar{W}'(1) \\ &= \frac{1}{2}\log\left(\frac{\det\Delta_A \det\Delta_B}{\det\Delta_M}\right) - \bar{W}'(1), \end{aligned} \tag{82}$$

where $\det\Delta_X$ is the functional determinant of the Laplacian on $X = A, B, M$ with Dirichlet boundary conditions. Note that the functional determinants are related to the free energies of the underlying CFT by

$$F[A] = -\log Z_A = \frac{1}{2}\log\det\Delta_A, \tag{83}$$

and similarly on the other manifolds. In particular, one can use the famous result by [Cardy and Peschel, 1988]

$$F[A] = f_b V_A + f_s L_A - \frac{c}{6}\log\frac{L_A}{\varepsilon} + \mathcal{O}(1), \tag{84}$$

with f_b and f_s the bulk and surface free energies, V_A the volume and L_A the surface area of A, to infer the behavior (6) of the entanglement entropy. In particular, the volume terms cancel of in the combination $F[A] + F[B] - F[A \cup B]$ appearing in the entanglement entropy, which leads to an area law.

The functional determinants are divergent quantities and need to be regularized. Since we are only interested in the sub-leading constant terms, we don't care about the exact form of the divergences, and can calculate the determinants by means of ζ-regularization, which corresponds to finding a proper analytic continuation that doesn't diverge. We will talk

[10] Here we implicitly assume that the partition functions are regularized before taking the analytic continuation. This ensures that there are no conflicts in the limits.

a little more about this when we generalize the calculation to higher dimensions. As for the winding sector, we don't state the explicit form of the ζ-regularized determinants for the cylinder, which can be found in [Zhou et al., 2016]. We point out, however, that the complete result for the entanglement entropy consists of a scaling function, expressed in terms of aspect ratios, and a topological contribution expressed in terms of the scale invariant quantity $\sqrt{g}R$. We expect this to be valid also in higher dimensions, as it reflects the underlying criticality. For the following we emphasize that the calculation of the ground state entanglement entropy can be reduced to the calculation of two things: the functional determinants of the operator appearing in the ground state action and the winding sector. This will also be true in the higher dimensional case.

The sphere

Next, let us study the spherical case. We take the full manifold to be a sphere $M = S^2$ and cut it at the equator into the northern and southern hemispheres that we denote by $A, B = H^2$. Contrary to the cylinder the sphere doesn't have a boundary and so the action (54) enjoys the shift symmetry $S[\phi] = S[\phi + \phi^0]$ with constant ϕ^0. Since such a constant shift must be part of the classical field, we can use this symmetry to get rid of all the winding contributions in equation (69) by shifting $\phi_i^{\mathrm{cl}} \mapsto \phi_i^{\mathrm{cl}} - 2\pi R\omega_i$, that is by choosing $\phi_i^0 = -2\pi R\omega_i$. This leaves us with the boundary conditions

$$\phi_i^{\mathrm{cl}}|_\Gamma = \mathrm{cut}(x), \quad \text{for } i = 1, \dots, n. \tag{85}$$

In particular, this implies that all the classical fields are equal as they are solutions to the same differential equation with the same boundary conditions. After rotating the fields the boundary conditions become

$$\bar{\phi}_i^{\mathrm{cl}}|_{\Gamma_1}(x) = 0 \quad i = 1, \dots, n-1 \tag{86}$$

$$\bar{\phi}_n^{\mathrm{cl}}|_{\Gamma_1}(x) = \sqrt{n}\,\mathrm{cut}_1(x), \tag{87}$$

and we can write

$$\bar{W}(n) = \sum_{\bar{\phi}_i^{\mathrm{cl}}} e^{\sum_{i=1}^{n-1} S[\bar{\phi}_i^{\mathrm{cl}}]} = 1 \tag{88}$$

since the first $n-1$ rotated classical fields are unique and vanishing. The n-th rotated classical field can be stitched together with the n-th fluctuations as before, see equations (78) and (80). As was observed in [Zaletel et al., 2011, Zhou et al., 2016] the n-th rotated total field is given by $\bar{\phi}_n = \varphi_n + \sqrt{n}\phi_n^{\mathrm{cl}}$, and has an altered compactification radius:

$\bar{\phi}_n \sim \bar{\phi}_n + 2\pi R\sqrt{n}$. In the cylindrical geometry this didn't affect the result. However, since the sphere has a 0-mode, the change in compactification radius now has an effect on the partition function corresponding to $\bar{\phi}_n$ given by

$$\int \mathcal{D}\bar{\phi}_n e^{-S[\bar{\phi}_n]} = \sqrt{n}Z. \tag{89}$$

The remaining path integrals over fluctuations in (71) contribute, as before, with Dirichlet partition functions on A and B, and in total we obtain

$$\mathrm{Tr}\rho_A^n = \sqrt{n}\left(\frac{Z_A Z_B}{Z}\right)^{n-1}. \tag{90}$$

The analytic continuation is straight-forward and we can write for the entanglement entropy of a hemisphere

$$\begin{aligned} S[A] &= -\lim_{n\to 1}\partial_n \mathrm{Tr}\rho_A^n && (91)\\ &= -\log\left(\frac{Z_A Z_B}{Z}\right) - \frac{1}{2} && (92)\\ &= \frac{1}{2}\log\left(\frac{\det\Delta_{H_N^2}\det\Delta_{H_S^2}}{\det'\Delta_{S^2}}\right) + \log\left(\sqrt{4\pi g\,\mathrm{Area}(S^2)}R\right) - \frac{1}{2}. && (93)\end{aligned}$$

In the last line the extra factor is due to the 0-mode of the Laplacian on the sphere, which has to be treated carefully when rewriting the partition function as a functional determinant, see [Di Francesco et al., 1997]. After evaluating the determinants, one finds that the entanglement entropy is given by [Zhou et al., 2016]

$$S[A] = \log\left(\sqrt{8\pi g}R\right) - \frac{1}{2}. \tag{94}$$

Note that it again only depends on the scale invariant quantity $\sqrt{g}R$. Futhermore, as was pointed out in [Weisberger, 1987] and [Zhou et al., 2016], the ratio of partition functions appearing in the entanglement entropy is conformally invariant. In particular, this implies that the expression above is valid for spheres of any radius.

3.2 Higher dimensions

In section 2.2 we generalized the QLM and formulated the the GQLM on higher dimensional spheres and tori. We will now apply the replica

techniques from the last section to these higher dimensional geometries. The generalization of the replica calculation for $z = d = 2$ is, up to some minor intricacies, very straight-forward. The main difference to the previous calculations is that the operator appearing in the ground state action of the higher dimensional quantum Lifshitz model is a higher derivative operator, see 2.2 for the explicit expressions. This becomes an issue when we divide the total field into a classical part and a fluctuation, see equation (64), as giving the fluctuations Dirichlet boundary conditions and demanding that the classical field obey the equations of motions is not sufficient to ensure that the action splits as in (67). In higher dimensions we have to supplement additional boundary conditions to the fluctuations to ensure the splitting of the action. It is not hard to see from our discussion in 2.2 that the boundary conditions (41) and (46) do the trick in both spherical and toroidal symmetry.

Let us write this out explicitly. We divide each of the replicated fields on A and B into a classical part and a fluctuation

$$\phi_{X,i} = \phi^{\mathrm{cl}}_{X,i} + \varphi_{X,i}, \quad \text{for} \quad X = A, B \text{ and } i = 1, \dots, n. \tag{95}$$

From the classical field we again demand that it take up the value of the total field at the entangling cut and that it obey the equations of motion

$$\mathcal{P}_{z,M}\phi^{\mathrm{cl}}_{X,i} = 0 \quad \text{with} \quad \phi^{\mathrm{cl}}_{X,i}|_\Gamma(x) = \phi_i|_\Gamma(x). \tag{96}$$

Here, we note that the classical field is not sufficiently determined by these boundary conditions. In the case of the sphere this is not a problem, as it is reabsorbed into a full field. We will see, however, that the torus exhibits a winding sector very similar to that of the cylinder, and in order to calculate it we need an explicit expression for the classical field. For this purpose we need to supplement additional boundary conditions. Lets set the problem aside for the moment, and consider the fluctuations. Demanding that they fulfill the boundary conditions

$$\varphi_{X,i}|_\Gamma = 0, \quad \Delta^k_M \varphi_{X,i}|_\Gamma = 0, \quad k = 1, \dots, \frac{z}{2} - 1 \tag{97}$$

with Δ_M the Laplace-Beltrami operator on either the sphere or the torus, ensures that

$$S[\phi_{X,i}] = S[\phi^{\mathrm{cl}}_{X,i}] + S[\varphi_{X,i}] \quad \text{for} \quad X = A, B \text{ and } i = 1, \dots, n. \tag{98}$$

Apart from these considerations, the replica calculation goes through in a completely analogous way. Let us see what this implies for the generalized geometries.

The d-sphere

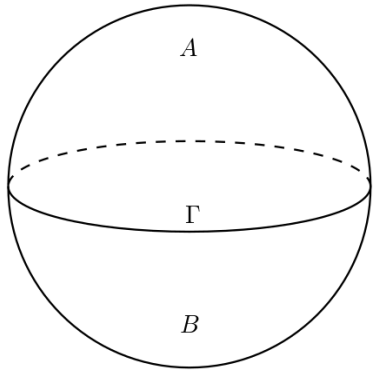

Figure 3.3. Sphere cut into two hemispheres by the entanglement cut Γ*. Figure taken from [I].*

Let $M = S^d$ and cut it at the equator into the two hemispheres $A = H_N^d$ and $B = H_S^d$, as depicted in figure 3.3, and let us set $z = d$. The replica calculation for the ground state (36) with action (38) and boundary terms (47) can be accomplished in the exact same form as before. In terms of the partition functions, the entanglement entropy takes the same form as for the 2-sphere, see (92). Thus, in terms of the functional determinants, we arrive at the generalized expression for the entanglement entropy

$$S[A] = \frac{1}{2}\log\left(\frac{\det \mathcal{P}_{d,H_N^d}\det \mathcal{P}_{d,H_S^d}}{\det' \mathcal{P}_{d,S^d}}\right) + \log\left(\sqrt{4\pi\,\mathrm{Area}(S^d)}R\right) - \frac{1}{2}, \quad (99)$$

with the GJMS-operator given in equation (45). We note that, as we have seen before, this determinants can be interpreted as the free energies of the CFT describing the ground state on the different manifolds. Calculating the functional determinants of GJMS-operators on spheres and hemispheres is not an easy task. In a series of papers [Chang and Dowker, 1993, Dowker, 1994a, Dowker, 1994b, Dowker, 2011, Dowker, 2013] these determinants were calculated by ζ-function regularization techniques for any even dimension d and any even critical exponent $z = 2k$ with $k = 1, \ldots, d/2$. In paper [I] we took these results, given in terms of multiple Γ-functions, and simplified them to be expressed as sums of Riemann ζ-functions. While the calculation of these functional determinants is quite interesting and elegant, it is does not contribute

much to the discussion of entanglement that is the focus of this thesis. We refer the interested reader to our paper [I] for a review of Dowker's calculations as well as the tedious simplification of their result. Here, we simply report the final result for the entanglement entropy

$$S[A] = \frac{1}{2}\sum_{n=0}^{d} h_n(d)\zeta'(-n) + \log\left(\sqrt{4\pi\,\mathrm{Area}(S^d)(d-1)!R}\right) - \frac{1}{2}, \quad (100)$$

where the coefficients of the Riemann ζ-functions are defined as

$$h_n(d) = \frac{1}{(d-1)!}\begin{bmatrix} d \\ n+1 \end{bmatrix} + \sum_{j=0}^{d-n} \frac{(-1)^j}{(d-j)!}\binom{d}{j-1}\begin{bmatrix} d-j+1 \\ n+1 \end{bmatrix}, \quad (101)$$

and $\left[{m \atop n}\right]$ are Stirling numbers of the first kind. For $d = z = 2$ the entanglement entropy above reduces to the expression (94) and is thus in agreement with the lower dimensional result. We further note that, while our intention was to find the entanglement entropy only at $d = z$, the framework for the calculation of the functional determinants of GJMS operators also provides analytic results in the subcritical case. In fact, the calculation of the entanglement entropy in the subcritical case turns out to be easier than in the critical case, as no 0-modes are present. This implies that in the subcritical case, that is for z even and $z < d$, the entanglement entropy is simply given by

$$S[A] = \frac{1}{2}\log\left(\frac{\det \mathcal{P}_{z,H_N^d}\det \mathcal{P}_{z,H_S^d}}{\det \mathcal{P}_{z,S^d}}\right). \quad (102)$$

We did not attempt the same type of simplification for the subcritical determinants. In order to give the reader a concrete example, the following are the entanglement entropies corresponding to all allowed GJMS

operators in 4 and 6 dimensions:

$$d = 4, z = 2: \quad S[H^4] = -\frac{\zeta(3)}{8\pi^2} \approx -0.015 \tag{103}$$

$$d = z = 4: \quad S[H^4] = \log\left(\sqrt{32\pi^2 gR}\right) - \frac{1}{2} - \frac{\zeta(3)}{4\pi^2} \approx \log(\sqrt{g}R) + 2.347 \tag{104}$$

$$d = 6, z = 2: \quad S[H^6] = \frac{\zeta(3)}{96\pi^2} + \frac{\zeta(5)}{32\pi^4} \approx 0.001 \tag{105}$$

$$d = 6, z = 4: \quad S[H^6] = -\frac{5\zeta(3)}{48\pi^2} + \frac{\zeta(5)}{16\pi^4} \approx -0.012 \tag{106}$$

$$d = z = 6: \quad S[H^6] = \log\left(\sqrt{256\pi^3 gR}\right) - \frac{1}{2} - \frac{15\zeta(3)}{32\pi^2} + \frac{3\zeta(5)}{32\pi^4} \approx \log(\sqrt{g}R) + 3.934. \tag{107}$$

As before, all expressions depend on the scale invariant quantity $\sqrt{g}R$. The dependence on both z and d is however highly non-trivial. Just as in the $2+1$-dimensional case, one can check that for smooth surgeries the ratio of determinants appearing in the entropy does not depend on the radius, and so our results are valid for spheres of any radius.

3.2.1 The d-torus

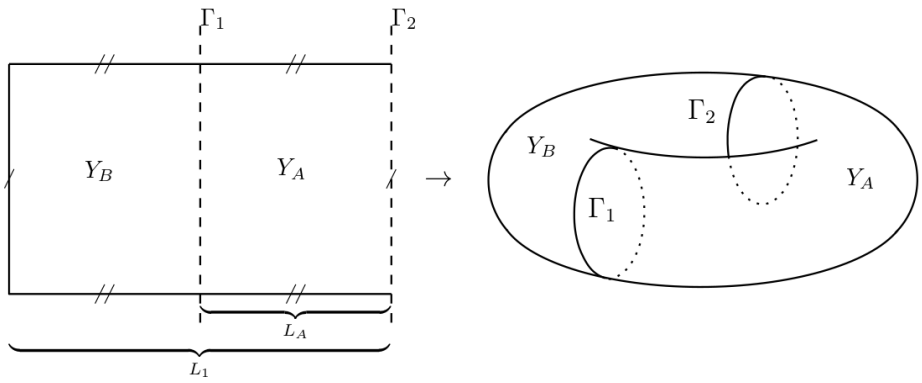

Figure 3.4. Torus cut into two cylinders by the entanglement cuts Γ_1 and Γ_2. Figure taken from [I].

Now let the total manifold be the d-dimensional flat torus defined in (39), that is $M = T^d_{L_1,\ldots,L_d}$, and cut it into the two flat d-cylinders $C_B := [-L_B, 0] \times T^d_{L_2,\ldots,L_d}$ and $C_A := [0, L_A] \times T^d_{L_2,\ldots,L_d}$. Note that

$L_1 = L_A + L_B$. As depicted in figure 3.4 this surgery introduces the two cuts Γ_1 at $x_1 = 0$ and Γ_2 at $x_1 = L_A$, which is identified with $x_1 = -L_B$. In order to perform the replica calculation for the ground state (36) on the torus under this surgery, we need to apply the lessons we learned from both the 2-sphere and the 2-cylinder, as the torus has both a 0-mode and a non-trivial winding sector. Let us briefly point out how this is done.

After applying the gluing conditions that result from the calculation of $\mathrm{Tr}\rho_A^n$, we find that all replicated fields must agree at each of the cuts Γ_1 and Γ_2. We define two functions on the cuts $\mathrm{cut}_1(x)$ and $\mathrm{cut}_2(x)$, such that all fields are equal to $\mathrm{cut}_a(x)$ at Γ_a for $a =, 1, 2$. Next, we separate the fields into a classical part and a fluctuation, enforcing the boundary conditions (97) on the fluctuations, as well as demanding that the classical fields obey the equations of motion and take up the total value of the fields at the cuts. At this point we note that at each cut the boundary conditions for the classical fields must only be satisfied up to a winding number, so we write

$$\phi^{\mathrm{cl}}_{X,i}|_a = \mathrm{cut}_a(x) + 2\pi R\omega_i^a, \quad a = 1, 2. \tag{108}$$

There are thus 2 winding numbers, one for each cut, instead of the single one we found for the cylinder. As for the sphere, the action on the torus has the shift symmetry $S[\phi_i] = S[\phi_i + \phi_i^0]$, which we are allowed to use to shift each of the classical fields. We use this symmetry to get rid of the winding numbers at the cut Γ_1. Then we use the fact that the cut functions are arbitrary and redefine cut_2 to absorb the n-th winding number at Γ_2. In total we are left with $n-1$ winding numbers at Γ_2. We emphasize here that these are the same manipulations we performed on the 2-sphere and the 2-cylinder, only now they are applied simultaneously. Next, we rotate the classical fields as $\bar{\phi}^{\mathrm{cl}} = U_n\phi^{\mathrm{cl}}$ with U_n defined in (73). In order to regain some clarity, let us write down the resulting boundary conditions for the classical fields at this key step. At Γ_1, where we got rid of all the winding numbers, the resulting situation is the same as for the spherical case

$$\bar{\phi}_i^{\mathrm{cl}}|_{\Gamma_1}(x) = 0 \quad i = 1, \ldots, n-1 \tag{109}$$

$$\bar{\phi}_n^{\mathrm{cl}}|_{\Gamma_1}(x) = \sqrt{n}\,\mathrm{cut}_1(x), \tag{110}$$

while at Γ_2 we have essentially the same situation we found for the cylinder

$$\bar{\phi}_i^{\mathrm{cl}}|_{\Gamma_2}(x) = 2\pi R\bar{\omega}_i, \quad i = 1, \ldots, n-1 \tag{111}$$

$$\bar{\phi}_n^{\mathrm{cl}}|_{\Gamma_2} = \sqrt{n}\,\mathrm{cut}_2(x) + \frac{2\pi R}{\sqrt{n}}\sum_{i=1}^{n-1}\omega_i. \tag{112}$$

Finally, we can make a change of measure in the path integrals over the cut functions like we did in (78), and glue the path integrals over the n-th fluctuations together with the path integral of the n-th classical field to form an integration over a full rotated field. As was the case for sphere, this full rotated field has an altered compactification radius, and the resulting partition function over the full torus is scaled by a factor of $\sqrt{n}$. The path integrations over the first $n-1$ fluctuations result in Dirichlet partition functions over the submanifolds C_A and C_B, and the contribution of the first $n-1$ classical fields is given by the winding sector $\bar{W}(n)$. Thus, in terms of partition functions, we get the following expression

$$\mathrm{Tr}\rho_A^n = \sqrt{n}\left(\frac{Z_A Z_B}{Z}\right)^{n-1} \bar{W}(n), \tag{113}$$

where the winding sector is explicitly given by

$$\sum_{\omega\in\mathbb{Z}^{n-1}} e^{-\sum_{i=1}^{n-1} S[\bar{\phi}_i^{\mathrm{cl}}]}. \tag{114}$$

In order to evaluate this sum, we first have to calculate the value of the classical fields, which is determined by the equations of motion on the flat torus (43), that is

$$\Delta^{\frac{z}{2}}\bar{\phi}_i^{\mathrm{cl}} = 0, \quad i = 1,\dots,n-1 \tag{115}$$

with the boundary conditions determined by the replica calculation

$$\bar{\phi}_i^{\mathrm{cl}}|_{\Gamma_1}(x) = 0 \text{ and } \bar{\phi}_i^{\mathrm{cl}}|_{\Gamma_2}(x) = 2\pi R\bar{\omega}_i, \quad i = 1,\dots,n-1. \tag{116}$$

But these are only two boundary conditions for a field that is the solution to a linear differential equation of degree z, thus for $z > 2$, the classical fields are not yet uniquely determined and we need to add additional boundary conditions to make the problem well-defined. We want to choose these boundary conditions such that they are compatible with the sort of generalized Dirichlet boundary conditions we chose for the fluctuations, see (97). Such a consistent choice is given by assigning to the classical fields the following set of generalized Neumann boundary conditions

$$\partial_n \Delta^k \bar{\phi}_i^{\mathrm{cl}}|_{\Gamma_a} = 0, \quad a = 1,2 \text{ and } k = 0,\dots,\frac{z}{2}-2, \tag{117}$$

with ∂_n the normal derivative at the boundary. With this boundary conditions the classical field is unique and can be calculated. In paper [I]

the calculation is performed and using a technique developed by [Zhou et al., 2016] the following analytic continuation for the winding sector is found

$$\bar{W}(n) = \sqrt{n}\Lambda_z^{-\frac{n-1}{2}} \int_{-\infty}^{\infty} \frac{\mathrm{d}k}{\sqrt{\pi}} \left[\sum_{\omega\in\mathbb{Z}} \exp\left(-\frac{\pi}{\Lambda_z}\omega^2 - 2i\sqrt{\frac{\pi}{\Lambda_z}}k\omega \right) \right]^{n-1}, \tag{118}$$

with

$$\Lambda_z(L_A, L_B, L_2, \ldots, L_d) := g\pi R^2 \frac{(-1)^{\frac{z}{2}} z!}{(1-2^z)B_z} \frac{L_A^{z-1} + L_B^{z-1}}{L_A^{z-1} L_B^{z-1}}, L_2 \cdots L_d \tag{119}$$

and where B_z are Bernoulli numbers. We note that for $z = d$ the winding sector is scale invariant.

We now have all the ingredients to write down a final expression for the entanglement entropy of the cut torus. In terms of functional determinants we have

$$S[C_A] = \frac{1}{2}\log\left(\frac{\det \mathcal{P}_{d,C_A} \det \mathcal{P}_{d,C_B}}{\det' \mathcal{P}_{d,T^d}} \right) + \log\left(\sqrt{4\pi \operatorname{Area}(T^d) g} R \right) - \frac{1}{2} - \bar{W}'(1), \tag{120}$$

with the operators given in section 2.2, which, since both the torus and cylinder are flat, are simply integer powers of the Laplacian. As for the sphere, considerable effort was put into evaluating and simplifying the functional determinants by ζ-function regularization techniques such as those applied to a similar problem in [Elizalde, 1998, Elizalde, 2012]. As those calculations don't contribute much to the entanglement discussion, we refer the reader to paper [I] and report here only the final result at $z = d$ which, in terms of the cross-ratios $u = \frac{L_A}{L_1}$ and $\tau_k = i\frac{L_1}{L_{k+1}}$, $k = 1, \ldots, d-1$, is given by

$$\begin{aligned} S[C_A] = {} & \frac{d}{4}\log(4u(1-u)) + \log\left(\sqrt{4\pi \operatorname{Area}(T^d) g} R \right) + \frac{d}{4}\zeta'_{T^{d-1}_{L_2,\ldots,L_d}}(0) \\ & - \frac{d}{8}G'(0; 2L_A, \ldots, L_d) - \frac{d}{8}G'(0; 2L_B, \ldots, L_d) \\ & + \frac{d}{4}G'(0; L_1, \ldots, L_d) - \frac{1}{2} - \bar{W}'(1), \end{aligned} \tag{121}$$

where $\zeta_{T^{d-1}_{L_2,\ldots,L_d}}(s)$ is the spectral ζ-function on the $d-1$-dimensional flat torus and the function G comes from the functional determinants.

In [I] we provide explicit expressions for $\zeta_{T^d_{L_1,\ldots,L_d}}(s)$ and G in terms of Riemann ζ-functions and modified Bessel functions. The derivative at 0 of G can be evaluated in a simple manner and expressed as the following fast converging multidimensional exponential sum

$$G'(0, L, L_2, \ldots, L_d) = 2 \sum_{\vec{n}_{d-1} \in \mathbb{Z}^{d-1}}{}' \sum_{n_1=1}^{\infty} \frac{\exp\left(-L\, n_1 \sqrt{\vec{n}_{d-1}^T\, \Xi_{d-1}\, \vec{n}_{d-1}}\right)}{n_1}, \tag{122}$$

with $\Xi_{d-1} = \operatorname{diag}\left((2\pi/L_2)^2, \ldots, (2\pi/L_d)^2\right)$.

As the general result for the entanglement entropy is quite involved, let us briefly take a look at the particularly simple result obtained in the thin torus limit. In two dimensions the thin torus limit is characterized by having $|\tau_1| \gg 1$ or alternatively $L_1 \gg L_2$, which is why it is also called the long torus limit. There the entanglement entropy is given by

$$S[C_A] = \log\left(8\pi g R^2\right) - 1 \tag{123}$$

which precisely double the entanglement entropy of the thin cylinder, an observation first made by [Oshikawa, 2010]. An analogous limit in higher dimensions can be defined by demanding

$$L_1, L_A \gg L_2 \gg \ldots \gg L_d. \tag{124}$$

In this limit most quantities in (121) are suppressed with respect to the term coming from the spectral ζ-function of the $d-1$-dimensional torus, which gives the following approximation for the entanglement entropy

$$S[C_A] \approx 4 \frac{(-\pi)^p}{p!} \frac{L_2 \cdots L_{2p+1}}{L_{2p+2}^{2p}} \zeta'(-2p), \quad p = \left\lfloor \frac{d-1}{2} \right\rfloor. \tag{125}$$

In paper [I] several other limits, such as the thin sliced and wide torus, and configurations, such as the halved torus, are discussed. We refer the reader to the paper for a more in-depth discussion. Although it is not always easy to see, we note that all our results for the torus are scaling invariant and can be written in terms of the aspect ratios u and τ_k as well as the combination $\sqrt{g}R$.

With this we conclude our treatment of the higher dimensional ground state entanglement entropy. Let us now return to the two dimensional case and study the entanglement entropy of the excited states of the QLM.

3.3 Excited states

The calculation of the excited state entanglement entropy is, in principle, a straight-forward generalization of the replica calculation from section 3.1 with one caveat: in the excited state density matrix the fields appear not only in the exponential of the action. In practice, this breaks some very useful factorizations that we were implicitly using for the ground state calculation and creates a combinatoric mess. In order to deal with this we will distinguish between two cases: the singly excited state and the general case. For both cases we can make the combinatorics of the problem tractable by introducing simple assumptions about the classical fields. The assumptions introduced are, as could be expected, more restricting in the general than in the singly excited case but still fulfilled on interesting geometries for both cases.

From section 2.1 we know that the state obtained by exciting the eigenmodes of the Laplacian is characterized by the set of integers $(m_{\lambda_1}, \ldots, m_{\lambda_\nu})$ describing the number of quanta of energy in each of the modes $\lambda_1, \ldots, \lambda_\nu$. The excited state is explicitly given in (30). We talk about the singly excited state if for some mode $m_\lambda = 1$ and all other occupation numbers are zero. The density matrix of the singly excited state is

$$\rho_\lambda := |m_\lambda = 1\rangle \langle m_\lambda = 1| = \frac{1}{Z} \int \mathcal{D}\phi \mathcal{D}\phi' \; \phi^\lambda \phi'^\lambda e^{-\frac{1}{2}S[\phi] - \frac{1}{2}S[\phi']} \, |\phi\rangle \langle \phi'|, \tag{126}$$

while in the general case it is given by

$$\begin{aligned} \rho_{(m_{\lambda_1},\ldots,m_{\lambda_\nu})} &= \left|(m_{\lambda_1}, \ldots, m_{\lambda_\nu})\right\rangle \left\langle (m_{\lambda_1}, \ldots, m_{\lambda_\nu})\right| \\ &= \frac{1}{Z} \int \mathcal{D}\phi \mathcal{D}\phi' \; e^{-\frac{1}{2}S[\phi] - \frac{1}{2}S[\phi']} |\phi\rangle\langle\phi'| \\ &\quad \times \left(\prod_{r=1}^{\nu} \frac{1}{2^{m_{\lambda_r}} m_{\lambda_r}!} H_{m_{\lambda_r}}\left(\frac{\phi^{\lambda_r}}{\sqrt{2}}\right) H_{m_{\lambda_r}}\left(\frac{\phi'^{\lambda_r}}{\sqrt{2}}\right) \right). \end{aligned} \tag{127}$$

We can perform the replica calculation for these density matrices pretty much in the same fashion as in section 3.1. We put the system on a manifold M and perform a surgery that divides it into the manifolds A and B where we, for simplicity, assume there is a single cut Γ between them. We take the Hilbert space to factor as $\mathcal{H} = \mathcal{H}_A \otimes \mathcal{H}_B$ and write the fields ϕ and ϕ' as products of fields with support on A and B. Then, we evaluate the reduced density matrices $\rho_{\lambda,A}$ and $\rho_{(m_{\lambda_1},\ldots,m_{\lambda_\nu}),A}$ by tracing over the B part of the Hilbert space, write down the product of n such matrices while introducing the replica index i to distinguish between

the copies, and finally take the trace of the result. Effectively, these steps introduce the gluing conditions $\phi'_{B,i} = \phi_{B,i}$ and $\phi'_{A,i} = \phi_{A,i+1}$ for $i = 1, \ldots, n$ and $n+1 \sim 1$, which have the effect of making all the fields agree at the entangling cut Γ, see (63),

$$\mathcal{B}: \quad \phi_{A,i}|_\Gamma(x) = \phi_{B,j}|_\Gamma(x) =: \mathrm{cut}(x), \quad i,j = 1, \ldots, n. \tag{128}$$

These steps result in the following expression for the trace of the n-th power of the reduced density matrix

$$\begin{aligned}
&\mathrm{Tr}\left(\rho_{(m_{\lambda_1},\ldots,m_{\lambda_\nu}),A}\right)^n = \\
&\left(\prod_{r=1}^{\nu} \frac{1}{2^{m_{\lambda_r}} m_{\lambda_r}!}\right)^n \frac{1}{Z^n} \int_{\mathcal{B}} \left[\prod_{i=1}^{n} \mathcal{D}\phi_{A,i}\mathcal{D}\phi_{B,i}\right] e^{-\sum_{i=1}^{n}(S_A[\phi_{A,i}]+S_B[\phi_{B,i}])} \\
&\quad \times \prod_{i=1}^{n}\prod_{r=1}^{\nu} H_{m_{\lambda_r}}\left(\frac{1}{\sqrt{2}}\left(\phi^{\lambda_r}_{A,i} + \phi^{\lambda_r}_{B,i}\right)\right) H_{m_{\lambda_r}}\left(\frac{1}{\sqrt{2}}\left(\phi^{\lambda_r}_{A,i+1} + \phi^{\lambda_r}_{B,i}\right)\right).
\end{aligned} \tag{129}$$

Now comes the tricky part. We would like to proceed as we did in section 3.1, separating each field into a classical component and a fluctuations, and then factoring all the path integrals to arrive at an expression like (71). However, while the action factors just as before, the product of fields, or of Hermite polynomials of fields in the general case, does not. While it should in principle be possible to perform a term by term evaluation after writing out the Hermite polynomials and expanding all the products, the combinatorics of the problem are quite daunting, and even if one could to them, it is not clear that the result would be something that can be straightforwardly analytically continued in n. In order to get around these issues we introduce the following assumptions about the classical fields (as defined in (68)). For the singly excited case it is enough to demand that the projections of the classical field onto the excited eigenmode vanishes, that is

$$\left(\phi^{\mathrm{cl}}_i\right)^{\lambda} = \sqrt{2g\lambda}\int_M \mathrm{d}^2x \; L_\lambda(x)\phi^{\mathrm{cl}}_i(x) = 0. \tag{130}$$

For the general excited state, this is not enough. Here, we need the integrals to vanish separately on the A and B subsystems for each excited eigenmode. We thus demand

$$\left(\phi^{\mathrm{cl}}_{X,i}\right)^{\lambda_r} = \sqrt{2g\lambda_r}\int_X \mathrm{d}^2x \; L_{\lambda_r}(x)\phi^{\mathrm{cl}}(x) = 0, \tag{131}$$

with $X = A, B$ and $r = 1, \ldots, \nu$. In other words, we demand that the partial projections onto the excited eigenmodes of the classical field vanish

separately on the subsystems. Two points deserve a special emphasis. First, $L_\lambda(x)$ are the eigenfunctions of the Laplacian on M, but the integral is only over a submanifold, thus for the general excited case the condition is not merely testing orthogonality of the classical field against the eigenfunctions of the Laplacian. Second, ϕ^{cl} is stitched together from separate solutions to the equations of motion on the A and B sides of M, with a specific set of boundary conditions dictated by the replica calculation in between. Hence, it generally doesn't coincide with what one would usually call the classical field on M, that is a solution to the equations of motion on M. While this assumptions might seem rather restrictive, we will later see that they are satisfied by all modes the a rectangular geometry and by all modes for the singly excited case and almost all modes in the general case on the spherical geometry. For now let us just assume the conditions for the general excited state are satisfied and continue our calculations. The calculation for the singly excited state differs a little from the general one and can be found in [III]. We leave it out here, as it doesn't add much to the discussion, and only allows us to consider a larger set of modes.

With (131) we can get rid of all the classical fields that appear outside of the exponential of the action in (129). The path integrals over the fluctuations can then be factored and rewritten as correlation functions, which then in turn can be resolved by Wick's theorem into sums of Green's functions. All this manipulations of the path integrals are reported in detail in [III]. Here, we just state the following results for the trace of the n-th power of the reduced density matrix. For the singly excited state we can write

$$\mathrm{Tr}\left(\rho_{\lambda,A}\right)^n = \mathrm{Tr}(\rho_A^n)\left[(G_A^\lambda)^{n-1}G_{A,M}^\lambda + (G_B^\lambda)^{n-1}G_{B,M}^\lambda\right], \tag{132}$$

where ρ_A is the reduced density matrix corresponding to the ground state, and the remaining terms are Green's functions integrated against eigenfunctions of the Laplacian

$$G_{X,M}^\lambda := \lambda \int_M \mathrm{d}^2x \int_X \mathrm{d}^2x' L_\lambda(x)L_\lambda(x')G_M(x,x') \tag{133}$$

$$G_X^\lambda := \lambda \int_X \mathrm{d}^2x\, \mathrm{d}^2x'\; L_\lambda(x)L_\lambda(x')G_X(x,x'), \tag{134}$$

for $X = A, B$. Here, $G_A(x,x')$ and $G_B(x,x')$ are the Green's functions with Dirichlet boundary conditions on A and B respectively and come from the path integrals over the fluctuations, while $G_M(x,x')$ is the

Green's function on M and comes from the path integral over the n-th replica field which is defined over the complete manifold.

For general excitations the structure of the expression is much more involved. As for the singly excited state, the ground state density matrix factors from the expression, and it is multiplied by an object consisting of correlation functions of the fluctuations and the n-th complete field (in the case of a single excitation only two-point functions, the Green's functions, appeared). The complete expression can be conveniently written as

$$\mathrm{Tr}\left(\rho_{(m_{\lambda_1},\ldots,m_{\lambda_\nu}),A}\right)^n = \mathrm{Tr}(\rho_A^n)\mathrm{Tr}[(\mathcal{A}\mathcal{B})^{n-1}\mathcal{M}], \tag{135}$$

where $\mathcal{A}$, $\mathcal{B}$, and $\mathcal{M}$ are rank 2ν tensors defined as

$$\mathcal{A}^{k_1',\ldots,k_\nu'}_{k_1,\ldots,k_\nu} := \left(\prod_{r=1}^{\nu}\frac{1}{2^{m_r}}\sqrt{\frac{1}{m_r!}\binom{m_r}{k_r}\binom{m_r}{k_r'}}\right)\left\langle\prod_{r=1}^{\nu}H_{m_r-k_r}(\varphi_A^{\lambda_r})H_{k_r'}(\varphi_A^{\lambda_r})\right\rangle_{A_D} \tag{136}$$

$$\mathcal{B}^{k_1',\ldots,k_\nu'}_{k_1,\ldots,k_\nu} := \left(\prod_{r=1}^{\nu}\frac{1}{2^{m_r}}\sqrt{\frac{1}{m_r!}\binom{m_r}{k_r}\binom{m_r}{k_r'}}\right)\left\langle\prod_{r=1}^{\nu}H_{m_r-k_r}(\varphi_B^{\lambda_r})H_{k_r'}(\varphi_B^{\lambda_r})\right\rangle_{B_D} \tag{137}$$

$$\mathcal{M}^{k_1',\ldots,k_\nu'}_{k_1,\ldots,k_\nu} := \left(\prod_{r=1}^{\nu}\frac{1}{2^{\frac{3m_r}{2}}m_r!}\sqrt{\binom{m_r}{k_r}\binom{m_r}{k_r'}}\right)\left\langle\prod_{r=1}^{\nu}H_{m_r}\left(\frac{1}{\sqrt{2}}\bar{\phi}^{\lambda_r}\right)H_{k_r'}(\bar{\phi}_A^{\lambda_r})H_{m_r-k_r}(\bar{\phi}_B^{\lambda_r})\right\rangle_M, \tag{138}$$

and the indices k_r and k_r' run from 0 to m_r. The tracing and product operations on these tensors are defined in the standard way

$$(\mathcal{A}\mathcal{B})^{k_1',\ldots,k_\nu'}_{k_1,\ldots,k_\nu} := \mathcal{A}^{k_1',\ldots,k_\nu'}_{j_1,\ldots,j_\nu}\mathcal{B}^{j_1,\ldots,j_\nu}_{k_1,\ldots,k_\nu} \tag{139}$$

$$\mathrm{Tr}\mathcal{A} := \mathcal{A}^{k_1,\ldots,k_\nu}_{k_1,\ldots,k_\nu}. \tag{140}$$

where we use the Einstein summation convention.

For the singly excited state the analytic continuation is straightforward. As it turns out, the general case is also relatively simple, as the tensors are sufficiently well-behaved for the matrix-logarithm to be

well-defined on them. We can thus use the matrix logarithm to define the analytic continuation in n. The issue of the existence and uniqueness of the matrix logarithm for this tensors is discussed more in detail in paper [III]. We note here that these analytic continuations all fall into the sub-exponential category that guarantees their uniqueness. Thus taking the derivative and the limit, we can write for the entanglement entropy of the singly excited state

$$S_\lambda[A] = S_{GS}[A] - \log\Big(G^\lambda_A\Big)G^\lambda_{A,M} - \log\Big(G^\lambda_B\Big)G^\lambda_{B,M} \tag{141}$$

where we used the fact that $G^\lambda_{A,M} + G^\lambda_{B,M} = G^\lambda_M$, and for the general excitation

$$S_{m_{\lambda_1},\ldots,m_{\lambda_\nu}}[A] = S_{GS}[A]\mathrm{Tr}(\mathcal{M}) + \mathrm{Tr}(\log(\mathcal{AB})\mathcal{M}). \tag{142}$$

In both cases $S_{GS}[A]$ denotes the ground state entanglement entropy. Note that in particular this implies that the entanglement entropy corresponding to this type of excited states continues to obey an area law. For the singly excited case we used the fact that $G^\lambda_M = 1$, which gets rid of the coefficient of the ground state entanglement entropy. If all excitations are put onto the same mode, a subcase that is treated in detail in [III], it turns out that $\mathrm{Tr}(\mathcal{M}) = 1$. Thus when all excitations are on the same mode the entanglement entropy has the form

$$S_{m_\lambda}[A] = S_{GS} + \mathrm{Tr}(\log(\mathcal{AB})\mathcal{M}). \tag{143}$$

This structure has been previously observed for the low-lying excited states of several theories, see [Alcaraz et al., 2011, Berganza et al., 2012, Castro-Alvaredo et al., 2018]. Furthermore, the transformed propagators (134) and (133) were already investigated under the name of Entanglement Propagator Amplitudes (EPAs) in [Parker et al., 2017]. There, a numerical analysis provided strong evidence that the EPAs are universal. In [III], we use spectral methods to calculate the transformed propagators and find our result in agreement with [Parker et al., 2017], providing further evidence for the universality of these objects. Thus, since all corrections to the ground state entanglement entropy are expressed in terms of these quantities, we can conclude that they are universal.

In order to make everything more transparent, let us consider an explicit geometry.

The sphere

Let the spatial manifold be given by a two-sphere $M = S^2$ and cut it into the two hemispheres $A, B = H^2$ at the equator. The eigenmodes of the

Laplacian on the sphere are the spherical harmonics

$$L_\lambda(x) \equiv L_{\ell,m}(x) = Y_\ell^m(x), \tag{144}$$

where $x = (\theta, \varphi)$ is a point on S^2 and

$$Y_\ell^m(x) = \sqrt{\frac{2\ell+1}{4\pi}\frac{(\ell-m)!}{(\ell+m)!}} e^{im\varphi} P_\ell^m(\cos(\theta)) \tag{145}$$

and $P_m^\ell(x)$ are associated Legendre Polynomials. With this we have

$$-\Delta_{S^2} L_\lambda(x) = -\Delta_{S^2} Y_\ell^m(x) = \ell(\ell+1). \tag{146}$$

We remind the reader that, when used as a label, λ is meant as a shorthand notation for (ℓ, m), but when it appears as a number the actual eigenvalue $\lambda = \ell(\ell+1)$ is meant. For the creation operator, for example, we can write explicitly

$$A_\lambda^\dagger \equiv A_{\ell,m}^\dagger = \frac{1}{\sqrt{g\ell(\ell+1)}} \int_{-\pi}^{\pi} \mathrm{d}\theta \int_0^{2\pi} \mathrm{d}\varphi \; Y_\ell^m(\theta,\varphi) Q^\dagger(\theta,\varphi) \sin\theta. \tag{147}$$

Up to normalization, the eigenfunctions on the hemisphere with Dirichlet boundary conditions at the equator are the spherical harmonics such that $\ell + m$ is odd. With proper normalization they are given by

$$L_\lambda^{H^2}(x) = \sqrt{2} Y_\ell^m(x), \quad \ell + m = \text{odd}. \tag{148}$$

We use spectral methods to calculate the transformed propagators. For example, we can calculate G_M^λ from equation (134) as follows. First, we use the eigenmode expansion of the Green's function on M

$$G_M(x,x') = \sum_\mu \frac{L_\mu(x) L_\mu(x')}{\mu}, \tag{149}$$

where μ labels all eigenmodes of the Laplacian on M. Then we can proceed as follows

$$G_M^\lambda = \lambda \int_M \mathrm{d}^2x \, \mathrm{d}^2x' L_\lambda(x) L_\lambda(x') \sum_\mu \frac{L_\mu(x) L_\mu(x')}{\mu} \tag{150}$$

$$= \lambda \sum_\mu \frac{1}{\mu} \left(\int_M \mathrm{d}^2x L_\lambda(x) L_\mu(x') \right)^2 = \lambda \sum_\mu \frac{\delta_{\lambda\mu}}{\mu} = 1, \tag{151}$$

which is one of the results that we mentioned towards the end of the last section. Similar techniques can be used to simplify the calculations of all transformed propagators, see [III] for details. We find that

$$G^{\lambda}_{A,M} = G^{\lambda}_{B,M} = \frac{1}{2} \tag{152}$$

$$G^{\lambda}_{A} = G^{\lambda}_{B} = \frac{1}{2}\Sigma_{\lambda} \tag{153}$$

where Σ_λ is given by

$$\Sigma_\lambda = \begin{cases} \Sigma^{\mathrm{e}}_\lambda, & \ell_\lambda + m_\lambda = \text{even} \\ 1, & \ell_\lambda + m_\lambda = \text{odd}, \end{cases} \tag{154}$$

and Σ^e_λ is given by

$$\Sigma^e_\lambda \equiv \Sigma^e_{\ell_\lambda, m_\lambda} := (2\ell_\lambda + 1)\ell_\lambda(\ell_\lambda + 1)\frac{(\ell_\lambda - m_\lambda)!}{(\ell_\lambda + m_\lambda)!} \times \sum_{\substack{\ell_\mu \geq m_\lambda \\ \ell_\mu + m_\lambda = \text{odd}}}^{\infty} \frac{(2\ell_\mu + 1)}{\ell_\mu(\ell_\mu + 1)} \frac{(\ell_\mu - m_\lambda)!}{(\ell_\mu + m_\lambda)!} \left(\int_0^1 \mathrm{d}x \; P^{m_\lambda}_{\ell_\lambda}(x) P^{m_\lambda}_{\ell_\mu}(x) \right)^2, \tag{155}$$

which is convergent and can be evaluated numerically by truncation at a sufficiently large integer.

On can check that the assumption $(\phi^{\mathrm{cl}}_i)^\lambda = 0$ is satisfied by all modes on the sphere, and that the assumptions $(\phi^{\mathrm{cl}}_{X,i})^\lambda = 0$ with $X = A, B$ are satisfied by all modes *except* those with $m = 0$ and ℓ odd. Furthermore, the ground state entanglement entropy for this geometry is [Zhou et al., 2016]

$$S_{GS}[A] = \log\left(\sqrt{8\pi g}R\right) - \frac{1}{2}. \tag{156}$$

Using equations (141) and (152) we can thus write the following expression for the entanglement entropy of the singly excited state

$$S_\lambda[A] = \log\left(\sqrt{2\pi g}R\Sigma_\lambda\right) - \frac{1}{2}, \tag{157}$$

which is valid for all modes. In particular, we can see that the entanglement entropy distinguishes between two types of modes. The first type are modes that are simultaneously eigenmodes on the sphere and hemisphere, i.e. modes with $m + \ell$ odd. The entanglement entropy is constant within this class of modes, as here $\Sigma_\lambda = 1$. The second type consists of the remaining modes. Here, the entanglement entropy has an

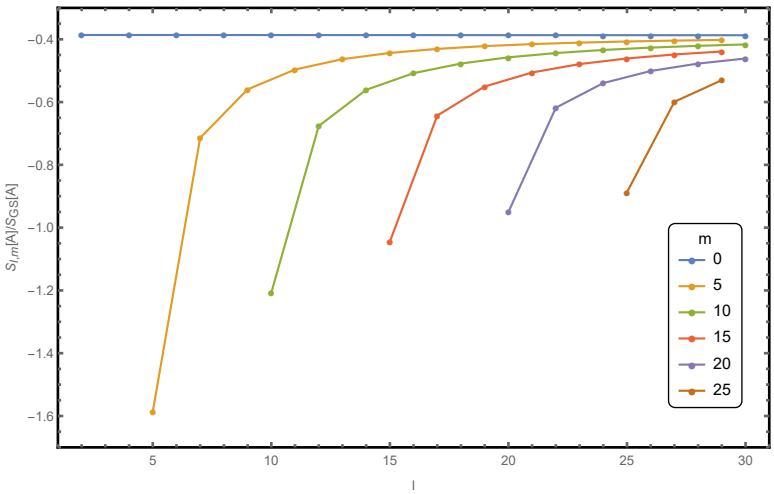

Figure 3.5. The value of the entanglement entropy $S_{\ell,m}[A]$ in units of the ground state entanglement entropy at the RK-point, i.e. $g = \frac{1}{8\pi}$, and for $R = 1$, plotted for a selection of modes with $\ell + m$ even. Figure taken from [III].

intricate dependence on the mode that is excited. The behavior of the entanglement entropy for these modes is depicted in figure 3.5

The tensors of correlation functions appearing for the most general form of excitation are quite hard to evaluate. We therefore consider the interesting subcase when all excitations are put onto the same mode. Furthermore, we concentrate on the modes of first kind, that is modes with $\ell + m$ odd, as the transformed propagators are easier to evaluate within this class. Finally, we exclude the modes with $m = 0$ and ℓ odd, as they don't satisfy the assumption needed for our calculation. In this case the entanglement entropy takes the form

$$S_{m_\lambda}[A] = \log\left(\sqrt{8\pi g}R\right) - \frac{1}{2} + \sum_{k=0}^{m_\lambda} \frac{1}{2^{m_\lambda}} \binom{m_\lambda}{k} \log\left(\frac{1}{2^{m_\lambda}}\binom{m_\lambda}{k}\right). \quad (158)$$

We refer the reader to [III] for details on the calculation above. In figure 3.6 the dependence on the excitation number of the entanglement entropy is depicted. In particular, we observe that in this case the entanglement entropy has a logarithmic dependence on the excitation number

$$S_{m_\lambda}[A] \approx S_{GS}[A] - a_1 \log m_\lambda - a_2, \quad (159)$$

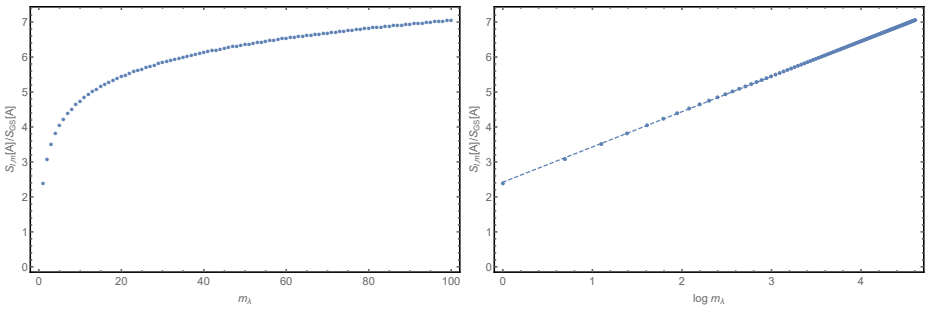

Figure 3.6. The first image shows S_{m_λ} plotted as a function of the number of excitations m_λ for any mode satisfying $\ell + m =$odd and $m \neq 0$, evaluated at the RK-point $g = \frac{1}{8\pi}$ and for $R = 1$. The second image shows a log-linear plot of the same data. The dashed line is the linear fit $y = 1.008x + 2.421$ with an R^2 value above 0.999. Figure taken from [III].

with $a_1 \approx 0.504$ and $a_2 = 0.711$. This is quite interesting, as it allows us to infer the highly excited behavior of these states, that is the limit $m_\lambda \gg 1$. In particular, we see that the logarithmic dependence on the excitation number does not affect the area law behavior of the entanglement entropy. This is somewhat surprising, as highly excited states are generically expected to obey volume laws [Page, 1993].

The rectangular geometry is also considered in [III]. There, we find same type of distinction between classes of modes, and the same type of logarithmic behavior on the excitation number. Finally, we note that all our results for the entanglement entropy of excited states depend on the scaling invariant quantity $\sqrt{g}R$ only through the ground state entanglement. The universal corrections due to the excitations contain information on the excited modes, as well as on the correlation functions on the different manifolds and submanifolds that constitute the system.

With this we close our treatment of the entanglement entropy in the quantum Lifshitz model. Next, we will analyze the entanglement of mixed states. For this purpose we will use an alternative measure: the logarithmic negativity.

4 Logarithmic negativity

We remind the reader that the entanglement entropy is not a good entanglement measure for mixed states. There, it fails to distinguish between quantum and classical correlations, and thus cannot characterize the purely quantum entanglement of the mixed state. On the other hand, the logarithmic negativity is an entanglement monotone for mixed states and thus well-suited for our purpose.

In order to simulate a generic mixed state we start with the ground state density matrix ρ of the QLM on a tripartite geometry. Concretely, we cut M into A_1, A_2, and B, and assume, as for the entanglement entropy, that the Hilbert space factors as $\mathcal{H} = \mathcal{H}_1 \otimes \mathcal{H}_2 \otimes \mathcal{H}_B$. We then perform a partial trace over B, which leaves us with a prototype for a mixed state on the bipartite geometry $A = A_1 \cup A_2$ with Hilbert space

$$\mathcal{H}_A = \mathcal{H}_1 \otimes \mathcal{H}_2 \tag{160}$$

that still captures some of the generic behavior of a mixed state. In paper [II] we perform two separate calculations of the logarithmic negativity in this setting. The first calculation is done by the correlator method [Audenaert et al., 2002, Peschel, 2003] in the discretized $1+1$-dimensional QLM at $z = 2$ defined by replacing the Laplacian and integration measure in (34) by ∂_x^2 and $\mathrm{d}x$ respectively. Furthermore, in the $1+1$-dimensional case we don't demand that the scalar be compact. We note that the calculations we performed for the $2+1$-dimensional QLM in section 2 can be applied straight-forwardly to the $1+1$-dimensional case, and in particular that the ground state also takes the form (23). The second calculation is performed by the replica approach introduced in [Calabrese et al., 2012, Calabrese et al., 2013a] for the logarithmic negativity. The approach is similar to that for the entanglement entropy and convenient for the calculations in the context of the $2+1$-dimensional QLM, as it allows us to apply the lessons we previously learned. In both calculations we find that the logarithmic negativity is heavily dependent on whether the two submanifolds A_1 and A_2 are adjacent or disjoint, vanishing exactly in the latter case.

4.1 Correlator method

In order to perform the correlator method calculation, we first need the discretized form of the Hamiltonian (17) with Laplacian $\Delta = \partial_x^2$ and one dimensional integration, that is

$$H = \frac{1}{2}\int_M \mathrm{d}^x \left(\pi^2 + g^2\left(\partial_x^2\phi\right)^2\right), \tag{161}$$

with M chosen to be the line with open or periodic boundary conditions. If we discretize the line and let it have L sites, the the corresponding discrete Hamiltonian can be written as

$$H = \frac{1}{2}\left(\pi^T\pi + \phi^T K\phi\right) \tag{162}$$

with $\pi = (\pi_1, \ldots, \pi_L)$ and $\phi = (\phi_1, \ldots, \phi_L)$, and where K is the discretized version of $\Delta^2 = \partial_x^4$. The solutions to the equations of motion in the discretized theory satisfy

$$K\phi = 0. \tag{163}$$

In addition, we need to specify a discretized version of the boundary conditions to make the problem well-defined, and , as we are dealing with a fourth degree differential operator, we have to make sure that enough boundary conditions are given. For example, we can impose a discretized version of the generalized Dirichlet boundary conditions $\phi|_{\partial M} = 0$ and $\Delta\phi|_{\partial M} = 0$. In the end, the resulting matrix K is simply the square of the discrete Laplacian matrix with Dirichlet boundary conditions or, if periodic boundary conditions were implemented instead, with periodic boundary conditions.

The correlator method is based on the observation by [Peschel, 2003] that the reduced density matrix is related to the correlation matrices X and P with elements given by the vacuum two-point functions

$$X_{ij} := \langle\phi_i\phi_j\rangle = \frac{1}{2}(K^{-\frac{1}{2}})_{ij} \text{ and } P_{ij} := \langle\pi_i\pi_j\rangle = \frac{1}{2}(K^{\frac{1}{2}})_{ij} \tag{164}$$

restricted to the subsystem A, which we denote by X_A and P_A, and in particular to the eigenvalues of the matrix $C_A = \sqrt{X_A P_A}$. Using a second observation by [Audenaert et al., 2002] that relates the partial transposition to the time reversal of the momenta in the same subsystem, we can apply Peschel's result to the calculation of the logarithmic negativity. Let $A = A_1 \cup A_2$, where the subsystems A_1 and A_2 have lengths of ℓ_1 and ℓ_2 respectively, and write the partial transposition over A_2 of P_A as

$$P_A^{T_2} = \left(\mathbb{I}_{\ell_1} \oplus (-\mathbb{I}_{\ell_2})\right) P_A \left(\mathbb{I}_{\ell_1} \oplus (-\mathbb{I}_{\ell_2})\right). \tag{165}$$

Let us further denote the spectrum of $C_A^{T_2} = \sqrt{X_A P_A^{T_2}}$ by $\{\lambda_i\}_{i=1,\dots,\ell}$ with $\ell = \ell_1 + \ell_2$ the total length of the subsystem A. Then the trace norm of the partially transposed reduced density matrix can be expressed in terms of the λ_i as

$$\|\rho_A^{T_2}\| = \prod_{i=1}^{\ell} \max\left(1, \frac{1}{2\lambda_i}\right), \tag{166}$$

and thus the logarithmic negativity as

$$\mathcal{E} = \log \|\rho_A^{T_2}\| = \sum_{i=1}^{\ell} \log\left(\max\left(1, \frac{1}{2\lambda_i}\right)\right). \tag{167}$$

We can see that the logarithmic negativity is determined by the eigenvalues of $C_A^{T_2}$ that satisfy $\lambda_i < \frac{1}{2}$.

When A_1 and A_2 are disjoint, i.e. separated by some non-zero length, it turns out that no eigenvalue satisfies the above condition in either the open or periodic system and thus, in both cases, the logarithmic negativity vanishes exactly

$$\mathcal{E}_{A_1,A_2 \text{ disjoint}} = 0. \tag{168}$$

While this is surprising and in stark contrast to CFT calculations [Calabrese et al., 2012, Calabrese et al., 2013a] that show a non-trivial logarithmic negativity in the disjoint case, the same observation for a different $1+1$-dimensional system with Lifshitz scaling was already made in [Chen et al., 2017]. Indeed, relying on a theorem proven by [Lami et al., 2018], one can show that the reduced density matrix in the disjoint non-compact case is separable, see [II], which implies the vanishing of the logarithmic negativity.

In the case of adjacent A_1 and A_2, one finds that, both for the open and periodic systems, only a small number (independent of the lengths) of eigenvalues contributes to the logarithmic negativity. In the continuum regime, reached by replacing all lengths by $\ell \to \ell/\varepsilon$, where ε is the lattice spacing, and letting $\varepsilon \to 0$, we find that for both the open and periodic system the logarithmic negativity is given by

$$\mathcal{E}_{A_1,A_2 \text{ adjacent}} = \frac{1}{2} \log\left(\frac{\ell_1 \ell_2}{\ell_1 + \ell_2}\right) + const, \tag{169}$$

where *const* is a non-universal constant that depends on the regularization. In particular, we note that the logarithmic negativity only depends on the sizes of the subsystems, and not on the total size.

The expressions for the logarithmic negativity in both the disjoint, see (168), and adjacent case, see (169), can be summarized by the following formula in terms of the Dirichlet partition functions on the subsystems A_1 and A_2

$$\mathcal{E} = -\log\left(\frac{Z_{A_1} Z_{A_2}}{Z_{A_1 \cup A_2}}\right), \tag{170}$$

where we omit non-universal terms. In the disjoint case we note that $Z_{A_1 \cup A_2} = Z_{A_1} Z_{A_2}$ since the Dirichlet boundary conditions imposed on A_1 and A_2 don't allow the submanifolds to communicate. This immediately leads to the vanishing of the logarithmic negativity. In the adjacent case we note that, again omitting non-universal terms, $Z_{A_i} = \frac{1}{2}\log(\ell_i)$ for $i = 1, 2$ and $Z_{A_1 \cup A_2} = \frac{1}{2}\log(\ell_1 + \ell_2)$, which leads to the desired result. Equation (170) is reminiscent of Fradkin and Moore's formula for the bipartite entanglement entropy of the non-compact QLM in $2+1$ dimensions. The main difference to Fradkin and Moore's formula being that here $A_1 \cup A_2$ is not the full system. It is quite interesting that the logarithmic negativity doesn't feel the part of the system that was traced over to create a mixed state, and only cares about the two components on which the mixed state is defined. Under the replica approach we will see how this similarity originates, and that the formula (170), which here is only an educated guess, is actually valid.

4.2 Replica method

Let us consider the tripartite geometry where the total manifold M is cut into A_1, A_2, B and let ρ the ground state density matrix. We construct the bipartite mixed state ρ_A by tracing over the degrees of freedom in B

$$\rho_A \equiv \rho_{A_1 \cup A_2} = \mathrm{Tr}_B \rho \tag{171}$$

and denote by $\rho_A^{T_2}$ its partial transposition over A_2. The replica approach for the logarithmic negativity relies on the observation by [Calabrese et al., 2012, Calabrese et al., 2013a] that the trace norm of $\rho_A^{T_2}$, whose eigenvalues we denote by λ, can be written as

$$\begin{aligned} \|\rho_A^{T_2}\| &= \mathrm{Tr}|\rho_A^{T_2}| = \sum_\lambda |\lambda| \\ &= \lim_{n_e \to 1} \sum_\lambda \lambda^{n_e} = \lim_{n_e \to 1} \mathrm{Tr}\left(\rho_A^{T_2}\right)^{n_e}, \end{aligned} \tag{172}$$

where n_e is an even integer. Thus, the trace norm of $\rho_A^{T_2}$ can be found by analytically continuing the even sequence $\mathrm{Tr}\left(\rho_A^{T_2}\right)^{n_e}$ and evaluating

it at $n_e = 1$. Note that while the eigenvalues of ρ_A are non-negative, this is not necessarily true for $\rho_A^{T_2}$. In fact, it is the existence of negative eigenvalues that distinguishes the odd and even sequences. In particular if we take n_o odd, the same limit leads to the normalization condition $\lim_{n_o \to 1} \mathrm{Tr}\left(\rho_A^{T_2}\right)^{n_o} = \mathrm{Tr}\rho_A^{T_2} = 1$. With this observation, the logarithmic negativity of the subsystem A_1 can be written as

$$\mathcal{E} = \log \|\rho_A^{T_2}\| = \lim_{n_e \to 1} \log \mathrm{Tr}\left(\rho_A^{T_2}\right)^{n_e}, \tag{173}$$

where n_e is an even integer. We note that up to the partial transposition, the object at the center of the calculation is the same as the one we needed to perform the replica calculation of the entanglement entropy: $\mathrm{Tr}\rho_A^n$. It is therefore instructive to consider a simpler calculation that illustrates the effect of the partial transposition before diving into the calculation of the mixed state logarithmic negativity (173).

Warming up: The bipartite pure state

Let us consider a bipartite system where the complete manifold M is cut into A_1 and A_2 with the entangling cut Γ between them, and take the QLM to be in its pure ground state described by the density matrix ρ. Before starting, let us recall the definition of the Rényi entropy

$$S^{(n)}[A_1] = \frac{1}{1-n} \log \mathrm{Tr}\rho_{A_1}^n, \tag{174}$$

where $\rho_{A_1} = \mathrm{Tr}_{A_2}\rho$. It is known that for pure states the logarithmic negativity

$$\mathcal{E} = \lim_{n_e \to 1} \log \mathrm{Tr}\left(\rho^{T_2}\right)^{n_e} \tag{175}$$

reduces to the Rényi entropy of order $n = 1/2$ [Calabrese et al., 2012, Calabrese et al., 2013a], that is $\mathcal{E} = S^{(\frac{1}{2})}[A_1]$. Let us perform the replica calculation and see if we can reconstruct this result.

The starting point is the ground state density matrix for a bipartite system given in equation (53), except with A_1 and A_2 as the subsystems instead of A and B. The partial transposition over A_2 can be easily performed in this notation, by exchanging the corresponding primed and unprimed fields. This leaves us with

$$\rho_i^{T_2} = \frac{1}{Z} \int \mathcal{D}\phi_{A_1,i} \mathcal{D}\phi'_{A_1,i} \mathcal{D}\phi_{A_2,i} \mathcal{D}\phi'_{A_2,i}\; e^{-\frac{1}{2}S[\phi] - \frac{1}{2}S[\phi']} \times |\phi_{A_1,i}\rangle \otimes |\phi'_{A_2,i}\rangle\langle\phi'_{A_1,i}| \otimes \langle\phi_{A_2,i}|, \tag{176}$$

where we also introduced the replica index $i = 1, \ldots, n$. Calculating first the product of transposed density matrices followed by the total trace as we did in section 3.1, we find the altered gluing conditions

$$\begin{aligned} \phi'_{A_1,i} &= \phi_{A_1,i+1} \\ \phi_{A_2,i} &= \phi'_{A_2,i+1} \end{aligned} \tag{177}$$

with $i = 1, \ldots, n_\mathrm{e}$ and $n_\mathrm{e} + 1 \sim 1$. This differs from the entanglement entropy calculation in that there the primed and unprimed fields on the A_2 side agreed within the same copy of the density matrix. In figure

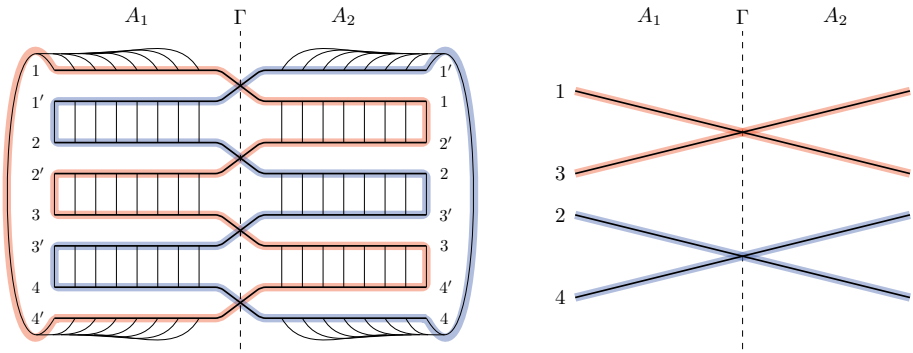

(a) Gluing conditions (b) Resulting independent sets of fields

Figure 4.7. For $n_e = 4$, the gluing conditions result in two independent sets of boundary conditions (represented in red and blue). Figure taken from [II].

4.7 the resulting situation is shown. Together with the continuity of the fields across the cut Γ, these gluing conditions force the n_e independent fields two split into two groups that separately agree at the boundary. Concretely, all fields with even indices satisfy

$$\phi_{A_1,2k}|_\Gamma(x) = \phi_{A_1,2\ell}|_\Gamma(x) =: \mathrm{cut}^\mathrm{e}(x) \tag{178}$$

while all the fields with odd indices satisfy

$$\phi_{A_1,2k-1}|_\Gamma(x) = \phi_{A_1,2\ell-1}|_\Gamma(x) =: \mathrm{cut}^\mathrm{o}(x) \tag{179}$$

for $k, \ell = 1, \ldots, \frac{n_\mathrm{e}}{2}$ and where $\mathrm{cut}^\mathrm{e}(x)$ and $\mathrm{cut}^\mathrm{o}(x)$ are separate arbitrary functions of the boundary coordinates. Since the cut functions are arbitrary and all fields are integrated over, we can after some relabeling

write

$$\mathrm{Tr}\left(\rho^{T_2}\right)^{n_\mathrm{e}} = \left(\frac{1}{Z^{\frac{n_\mathrm{e}}{2}}}\int_{\mathcal{B}}\prod_{i=1}^{\frac{n_\mathrm{e}}{2}}\mathcal{D}\phi_{A_1,i}e^{-\sum_{i=1}^{\frac{n_\mathrm{e}}{2}}S[\phi_{A_1,i}]}\int_{\mathcal{B}}\prod_{i=1}^{\frac{n_\mathrm{e}}{2}}\mathcal{D}\phi_{A_2,i}e^{-\sum_{i=1}^{\frac{n_\mathrm{e}}{2}}S[\phi_{A_2,i}]}\right)^2 \tag{180}$$

where $\mathcal{B}$ represents the same type of boundary condition as in (63), but with half the fields. Comparing this to the corresponding expression in the calculation of the entanglement entropy, see (62), we learn that the trace of the n_e-th power of the partially transposed density matrix can be expressed in terms of the reduced density matrix as

$$\mathrm{Tr}\left(\rho^{T_2}\right)^{n_\mathrm{e}} = \left(\mathrm{Tr}\rho_{A_1}^{\frac{n_\mathrm{e}}{2}}\right)^2. \tag{181}$$

For $n_\mathrm{e} \to 1$ we find that

$$\mathcal{E} = 2\log\mathrm{Tr}\rho_{A_1}^{\frac{1}{2}} = S^{(\frac{1}{2})}[A_1] \tag{182}$$

as expected.

The main lesson we learn from this calculation is that the partial transposition alters the boundary conditions satisfied by the replicated fields at the entangling cut. We also note that the effect of splitting the boundary conditions into two groups is only seen for the even sequence, whereas for the odd sequence, that is for n_o odd, we find

$$\mathrm{Tr}\left(\rho^{T_2}\right)^{n_\mathrm{o}} = \mathrm{Tr}\rho_{A_1}^{n_\mathrm{o}}. \tag{183}$$

In other words, the odd sequence is invariant under partial transposition, while the even sequence is not. This was already observed in [Calabrese et al., 2012]. We are now ready to tackle the disjoint and adjacent mixed states.

The disjoint case

Now let us return to the mixed state geometry described by the reduced ground state density matrix $\rho_{A_1\cup A_2} = \mathrm{Tr}_B\rho$, and assume that A_1 and A_2 are not adjacent. Two examples of this type configuration are depicted in figure 4.8 As we saw in section 3.1, the partial trace over B results in gluing the primed and unprimed fields of the same replica together

$$\phi_{B,i} = \phi'_{B,i} \tag{184}$$

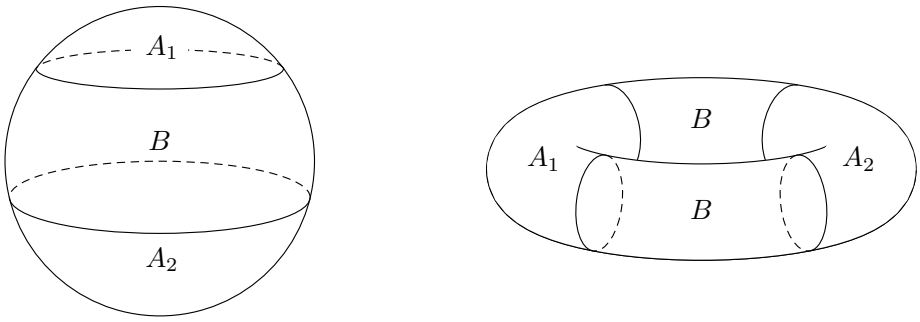

(a) Spherical geometry (b) Toroidal geometry

Figure 4.8. Two realizations of geometries where A_1 and A_2 are separated by B are depicted. Tor the torus, B consists of two disjoint components. Figure taken from [II].

for $i = 1, \ldots, n$. Once we have the reduced density matrix, we need to find an expression for the trace of an even power of its partial transposition over A_2. This calculation is analogous to our previous calculation for the pure state, and in particular it results in the same gluing conditions as before, see equation (177). The situation is depicted in figure 4.9. The

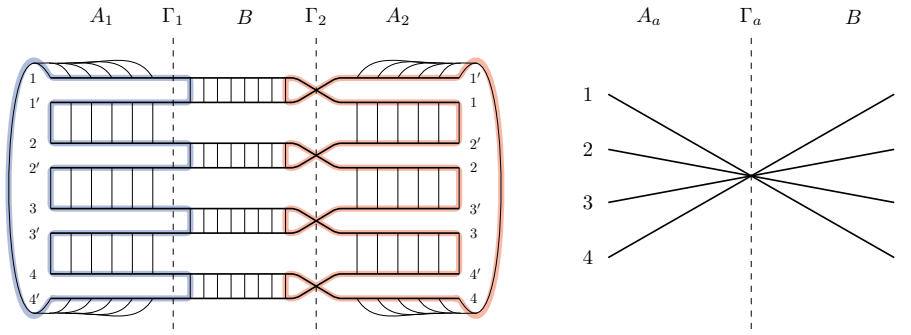

(a) Gluing conditions (b) Resulting independent sets of fields

Figure 4.9. For $n_e = 4$ the gluing conditions force all fields to agree at the boundaries between A_i and B. Figure taken from [II].

resulting boundary conditions are independent of the partial transposition, making *all* the fields agree at the boundaries between B and the A's. We

can therefore write the identity

$$\mathrm{Tr}\left(\rho_A^{T_2}\right)^{n_\mathrm{e}} = \mathrm{Tr}\rho_A^{n_\mathrm{e}}, \tag{185}$$

where the right hand side of the equation is precisely the quantity needed to calculate the tripartite entanglement entropy and was found for certain geometries in [Zhou et al., 2016]. It has the form

$$\mathrm{Tr}\rho_A^{n_\mathrm{e}} = \left(\frac{Z_{A_1}Z_{A_2}Z_B}{Z}\right)^{n_\mathrm{e}-1} W(n_\mathrm{e}), \tag{186}$$

where only the normalization $W(1) = 1$ of the winding sector $W(n_\mathrm{e})$ concerns us, not its functional form. With this, we can confirm the result obtained by the correlator method for the logarithmic negativity

$$\mathcal{E} = \lim_{n_\mathrm{e}\to 1} \log \mathrm{Tr}\left(\rho_A^{T_2}\right)^{n_\mathrm{e}} = 0. \tag{187}$$

We point out here, that the vanishing of the logarithmic negativity is not a sufficient condition for the density matrix to be separable. When we encountered this situation in the correlator method calculation, we were able invoke a theorem that allowed us to determine that the system was indeed separable. Said theorem, however, only applies to finite dimensional systems and cannot be applied in the present situation. It thus remains open to determine whether the density matrix above is separable or not. Furthermore, we note that the key steps in the calculation that determines whether the reduced density matrix is sensitive to the partial transposition do not refer to the dimension or the specific form of the action. Consequently this result is also valid for the higher dimensional generalizations of the quantum Lifshitz model discussed in section 2.2.

The adjacent non-compact case

Now let us assume that the submanifolds A_1 and A_2 are adjacent. Two examples of this configuration are shown in figure 4.10. The gluing conditions are the same as in the disjoint case, but, as depicted in figure 4.11 the resulting boundary conditions are different and not invariant under partial transposition. More concretely, without partial transposition, all fields are forced to agree at all boundaries, while the partial transposition induces a parity effect at the boundary between A_1 and A_2 like the one we saw for the pure case. Thus, the fields are split into two groups that agree separately at the boundary between A_1 and A_2, whereas *all* fields

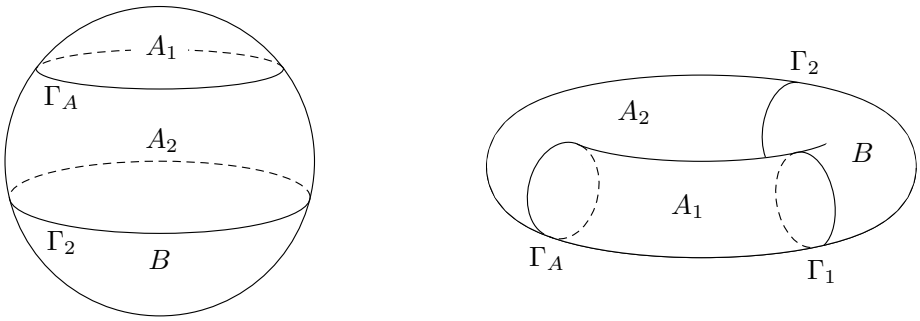

(a) Spherical geometry (b) Toroidal geometry

Figure 4.10. Two realizations of geometries where A_1 and A_2 are adjacent are depicted. Figure taken from [II].

must agree at the boundaries between B and the A's. Let us write out these boundary conditions. We denote by Γ_A the boundary between A_1 and A_2 and by Γ_α the boundary between B and A_α for $\alpha = 1, 2$. Then the boundary conditions for the path integrals are

$$\mathcal{B}: \begin{array}{ll} \phi_{A_\alpha,i}|_{\Gamma_\alpha} = \phi_{B,j}|_{\Gamma_\alpha} = \mathrm{cut}_\alpha\,, & i,j = 1,\dots,n_\mathrm{e}\,, \\ \phi_{A_1,k}|_{\Gamma_A} = \phi_{A_2,\ell}|_{\Gamma_A} = \mathrm{cut}^\mathrm{o} & \\ \phi_{A_1,n_\mathrm{e}/2+k}|_{\Gamma_A} = \phi_{A_2,n_\mathrm{e}/2+\ell}|_{\Gamma_A} = \mathrm{cut}^\mathrm{e} & k,l = 1,\dots,n_\mathrm{e}/2\,. \end{array} \tag{188}$$

We note that the fields are relabeled such that the first $n_\mathrm{e}/2$ are the odd and the second $n_\mathrm{e}/2$ the even fields. We will for the time being assume that the fields are not compact, so that we can ignore the winding contributions and return to this problem later. The path integral expression we obtain from the replica calculation at this step is

$$\begin{aligned} \mathrm{Tr}\left(\rho_A^{T_2}\right)^{n_\mathrm{e}} = \frac{1}{Z^n}\int_{\mathcal{B}}\prod_{i=1}^{n}\mathcal{D}\phi_{B,i}e^{-\sum_{i=1}^{n}S[\phi_{B,i}]} \\ \times\int_{\mathcal{B}}\prod_{i=1}^{n}\mathcal{D}\phi_{A_1,i}e^{-\sum_{i=1}^{n}S[\phi_{A_1,i}]}\int_{\mathcal{B}}\prod_{i=1}^{n}\mathcal{D}\phi_{A_2,i}e^{-\sum_{i=1}^{n}S[\phi_{A_2,i}]}. \end{aligned} \tag{189}$$

The trick to dealing with this expression, is to first apply two separate $U_{\frac{n_\mathrm{e}}{2}}$ rotations on the even and odd fields, which moves the dependence on cut^o and cut^e to only the $n_\mathrm{e}/2$-th and n_e-th fields respectively. The $n_\mathrm{e}/2$-th and n_e-th fields then respectively depend on $\sqrt{n_\mathrm{e}/2}\,\mathrm{cut}^\mathrm{o}(x)$ and $\sqrt{n_\mathrm{e}/2}\,\mathrm{cut}^\mathrm{e}(x)$ at Γ_A, and their path integrals can be glued together at

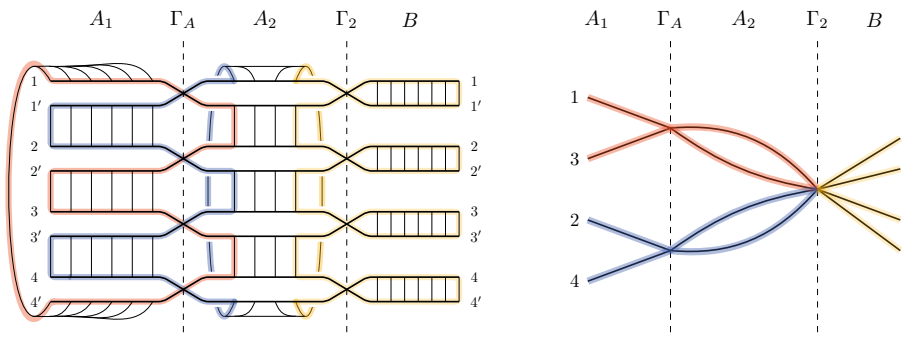

(a) Gluing conditions

(b) Resulting independent sets of fields

Figure 4.11. For $n_e = 4$ the gluing conditions force all the fields to agree at Γ_2, while two separate groups of boundary conditions are induced at Γ_A. Figure taken from [II].

that cut. At Γ_1 and Γ_2 the two fields still both depend on the functions cut_1 and cut_2 respectively. Thus, after the $U_{\frac{n_e}{2}}$ rotation and the gluing at Γ_A of these fields, it is necessary to perform yet another U_2 rotation of the $n_e/2$-th and n_e-th fields, such that afterwards only the n_e-th field depends on cut_1 and cut_2, while the $n_e/2$-th field gets Dirichlet boundary conditions at Γ_1 and Γ_2. Finally the path integrals of the n_e-th field can be glued together to form a path integral over the complete manifold. During all this gluing and rotations the boundary conditions of the remaining fields are turned into Dirichlet boundary conditions. In summary, the the n_e-th field leads to a partition function over the complete manifold Z, the $n_e/2$-th field leads to the product of Dirichlet partition functions on $A = A_1 \cup A_2$ and B, that is $Z_{A_1 \cup A_2} Z_B$, and the remaining fields lead to products of Dirichlet partition functions on each of the submanifolds $Z_{A_1} Z_{A_2} Z_B$. For a more detailed version of the calculation we refer the reader to [II]. The complete result is finally

$$\mathrm{Tr}\left(\rho_A^{T_2}\right)^{n_e} = \frac{(Z_{A_1} Z_{A_2} Z_B)^{n_e-2} Z_A Z_B}{Z^{n_e-1}}, \tag{190}$$

and taking the logarithm and the limit $n_e \to 1$ we find the same expression for the logarithmic negativity as we did with the correlator method

$$\mathcal{E} = -\log\left(\frac{Z_{A_1} Z_{A_2}}{Z_{A_1 \cup A_2}}\right). \tag{191}$$

The adjacent compact case

In the case where the field ϕ is compact, that is $\phi \sim \phi + 2\pi R$, we take the boundary conditions (188) and split the field into a classical field and a fluctuation. The fluctuations obey Dirichlet boundary conditions, while the classical fields obey the same boundary conditions as the total fields up to a factor of $2\pi R$ times an integer. Afterwards, the calculation goes through in a completely analogous way. The exact number of physical winding modes depends, as we saw in sections 3.1 and 3.2, on the geometry and surgery but, after carefully taking care of the redundancies, it is just a matter of following the winding modes around through the various manipulations. Let us take a brief look at two geometries.

Let M be a sphere and let us perform the surgery depicted on the left in figure 4.10. In particular there are only two cuts Γ_A and Γ_2, a fact that can be easily accounted for in the previous discussion by simply ignoring the cut Γ_1. Before taking care of redundancies, there is one winding number for each field at each cut adding up to a total of $2n_\mathrm{e}$ winding modes. However, each of the tree functions cut^o, cut^e, and cut_2 that determine the boundary conditions can be redefined to absorb one winding mode, and in addition, the action has a global shift symmetry that allows us to shift each replica field by a constant. We use the cut functions to remove the n_e-th winding mode at both cuts and the $n_\mathrm{e}/2$-th winding mode at Γ_A, and the shift symmetry to remove the remaining winding modes at Γ_2. Then, we can perform the same rotations of fields and restitching of path integrals as before, resulting in the expression

$$\mathrm{Tr}\left(\rho_A^{T_2}\right)^{n_\mathrm{e}} = \sqrt{n_\mathrm{e}}\frac{(Z_{A_1}Z_{A_2}Z_B)^{n_\mathrm{e}-2}Z_AZ_B}{Z^{n_\mathrm{e}-1}}W_\mathcal{E}(n_\mathrm{e}). \tag{192}$$

Here $W_\mathcal{E}(n_\mathrm{e})$ is the winding sector, and the factor of $\sqrt{n_\mathrm{e}}$ is a consequence of the altered compactification radius of the field defined on the full manifold analogous to the effect we encountered in section 3.1. For this geometry it turns out that the winding sector factors as

$$W_\mathcal{E}(n_\mathrm{e}) = W\left(\frac{n_\mathrm{e}}{2}\right)^2, \tag{193}$$

where $W(n)$ is the winding sector encountered by [Zhou et al., 2016] in the replica calculation of the entanglement entropy on the tripartite sphere. The logarithmic negativity on the spherical geometry can then finally be written as

$$\mathcal{E} = -\log\left(\frac{Z_{A_1}Z_{A_2}}{Z_{A_1\cup A_2}}\right) + 2\log W\left(\frac{1}{2}\right). \tag{194}$$

A more explicit version of this equation, where the partition functions and winding sector have been evaluated explicitly, as well as some limits can be found in paper [II].

Now let us consider the toroidal geometry depicted on the right of figure 4.10. As all the cuts are non-trivial, there are now a priori $3n_\mathrm{e}$ winding modes. But now there are four cut functions, one at Γ_1 and Γ_2 each, and two at Γ_A. Each of these is arbitrary and can be redefined to absorb a winding mode. Furthermore, as for the sphere, the action is invariant under a shift of the fields. As for the sphere, we use the cut functions to get rid of the n_e-th winding number at all cuts as well as the $n_\mathrm{e}/2$-th at Γ_A and the global shift symmetry to get rid of the remaining winding numbers at Γ_2. Note that we could equivalently get rid of the remaining winding numbers at Γ_1. After performing the rotations and restitching of path integrals we arrive at an expression that looks the same as (192), but with a new winding sector that is substantially more complex than the one for the sphere. An explicit expression can be found in paper [II]. Unfortunately, due to the complexity of the winding sector, we could not find its analytic continuation to $n_\mathrm{e} = 1$. Thus, while formally the logarithmic negativity is given by

$$\mathcal{E} = -\log\left(\frac{Z_{A_1}Z_{A_2}}{Z_{A_1\cup A_2}}\right) + \log W_{\mathcal{E}}\,(1)\,, \tag{195}$$

an explicit expression for $W_{\mathcal{E}}\,(1)$ remains to be found.

5 Discussion

In this thesis we analyzed the entanglement properties of the quantum Lifshitz model (QLM) under various circumstances. We saw that the QLM provides an excellent setting to perform analytic calculations of entanglement. The possibility to do this relied mostly on two facts. First, the ground state of the $d+1$-dimensional QLM is characterized by the d-dimensional action of a conformal field theory (CFT). This allowed us to interpret all the complicated path integrals resulting from the replica approach as CFT partition functions and, for the excited states of the model, CFT correlation functions. Second, we restricted ourselves to simple manifolds and submanifolds where the spectrum of the operators appearing in the CFT action that characterizes the ground state is well-known. This let us use ζ-function regularization techniques to evaluate the partition and correlation functions appearing in the entanglement formulas explicitly.

There are many straight-forward directions, in which our calculations can be continued. It would for example be interesting to analyze further geometries and configurations. For example, it would be interesting to consider geometries with more entangling cuts, or, especially in the higher dimensional case, with non-smooth cuts. Furthermore, we restricted ourselves to an even number of spatial dimensions as well as an even critical exponent. Generalizing to odd d and z would be quite interesting, taking into account there are $d = 3$ spatial dimensions in our universe[11] and the case of $z = 1$ is relativistic. However, both these generalizations come with non-trivial difficulties. Trying to generalize our result to odd z, for example, leads to complications in the construction of the ground state. An extension of the analysis to encompass non-compact geometries would also be desireable, although new methods would be needed for several parts of the calculations. In particular, we would not expect the spectrum of the differential operators to be discrete, meaning that the ζ-regularization techniques that we used don't straightforwardly generalize to these geometries. A replica calculation of the logarithmic negativity of mixed excited states should also be possible with the tools developed in

[11] Ignoring compact dimensions from String Theory.

our work.

A more detailed treatment of the excited states would also be desirable. In our work, for example, we only managed to perform an analysis of one type of highly excited state. In order to construct this state we excited a single eigenmode of the Laplacian – that in addition had the property of simultaneously being an eigenmode on the manifold and the submanifolds – m times, and from this deduced the behavior for $m \gg 1$. In particular, we observed that for this type of highly excited states the area law usually attributed to the ground and low-lying excited states was still conserved. It is however not clear from our analysis, whether this is a general feature of the excited states of the QLM, or only a feature of the precise state we analyzed.

Another interesting direction would be to apply the analytic insights we gained about the entanglement entropy of the quantum Lifshitz model to the agenda of holographic bulk reconstruction. In particular, it seems that, interpreting the entanglement entropy results à la Ryu-Takayanagi as information about the bulk minimal surfaces, it should be possible to reconstruct the bulk metric explicitly using results such as [Gentle and Keeler, 2016, Bao et al., 2019]. In particular, since we also have analytic results for the entanglement entropy of excited states, one could check the effect of excitations of the eigenmodes of the boundary theory to the bulk metric explicitly.

In conclusion, the QLM provided a vast and fruitful playground to better our understanding entanglement. It allowed us to perform elegant analytic calculations and provided us with simple, yet still rich and surprising results in a wide range of situations. The lessons to be learned from the QLM are by no means exhausted, and we expect the future to bring many more insights from this little corner of physics.

Acknowledgments

First of all, I would like to thank Valentina. I would not have been able to accomplish what I did without her guidance. I will miss being able to knock on her door to clear my doubts about whatever is keeping my mind busy. Similarly, I would like to thank Lárus. His advice, teeming with experience, was always insightful and helpful. I couldn't think of a better team of advisors for myself, I thoroughly enjoyed working with them.

My PhD experience was further shaped by two major events, and I would especially like to thank Valentina and Lárus for their support beyond the academic. In the first year of my PhD my mother fell ill and later died, and in my third year my son was born. During those intense and life-changing times Valentina and Lárus showed nothing but understanding and support. Thank you.

Next, I would like to thank Leon for existing and Salome for being my companion throughout this crazy adventure. Without your support I wouldn't be where I am, and I wouldn't be who I am. Thank you for being an excellent person.

I also thank the other people at HÍ who made my time here more interesting and fun. Thanks Lukas, Watse, Auðunn, Hjörtur, Aruna, Daniel, Nick, Timo, Jan and all the others (and let this list be invariant under permutations). I hope we will all keep in touch!

I thank Clément for collaborating with us. It was a pleasure and I hope we can continue to work together in the future. I am also grateful to Erik Tonni and Þórður Jónsson for being in the thesis committee, and in particular for their comments and questions at the midway evaluation.

Finally, I thank my family. No matter the distance, we will always be close. I grew up feeling loved supported and that feeling never stopped. I am truly lucky.

Thanks everyone, thanks Iceland!

Juanfernando Angel-Ramelli

References

[Alba et al., 2009] Alba, V., Fagotti, M., and Calabrese, P. (2009). Entanglement entropy of excited states. *Journal of Statistical Mechanics: Theory and Experiment*, 2009(10):P10020.

[Alcaraz et al., 2011] Alcaraz, F. C., Berganza, M. I. n., and Sierra, G. (2011). Entanglement of low-energy excitations in conformal field theory. *Phys. Rev. Lett.*, 106:201601.

[Amico et al., 2008] Amico, L., Fazio, R., Osterloh, A., and Vedral, V. (2008). Entanglement in many-body systems. *Rev. Mod. Phys.*, 80:517–576.

[Angel-Ramelli, 2020] Angel-Ramelli, J. (2020). Entanglement entropy of excited states in the quantum lifshitz model. *arXiv:2009.02283 [hep-th]*.

[Angel-Ramelli et al., 2020] Angel-Ramelli, J., Berthiere, C., Puletti, V. G. M., and Thorlacius, L. (2020). Logarithmic negativity in quantum lifshitz theories. *Journal of High Energy Physics*, 2020(9):11.

[Angel-Ramelli et al., 2019] Angel-Ramelli, J., Puletti, V. G. M., and Thorlacius, L. (2019). Entanglement entropy in generalised quantum lifshitz models. *Journal of High Energy Physics*, 2019(8):72.

[Ardonne et al., 2004] Ardonne, E., Fendley, P., and Fradkin, E. (2004). Topological order and conformal quantum critical points. *Annals of Physics*, 310(2):493 – 551.

[Aspect et al., 1982] Aspect, A., Dalibard, J., and Roger, G. (1982). Experimental test of bell's inequalities using time-varying analyzers. *Phys. Rev. Lett.*, 49:1804–1807.

[Audenaert et al., 2002] Audenaert, K., Eisert, J., Plenio, M. B., and Werner, R. F. (2002). Entanglement properties of the harmonic chain. *Phys. Rev. A*, 66:042327.

[Bao et al., 2019] Bao, N., Cao, C., Fischetti, S., and Keeler, C. (2019). Towards bulk metric reconstruction from extremal area variations. *Classical and Quantum Gravity*, 36(18):185002.

[Bekenstein, 1973] Bekenstein, J. D. (1973). Black holes and entropy. *Phys. Rev. D*, 7:2333–2346.

[Bell, 1964] Bell, J. S. (1964). On the einstein podolsky rosen paradox. *Physics Physique Fizika*, 1:195–200.

[Bennett et al., 1996a] Bennett, C. H., Bernstein, H. J., Popescu, S., and Schumacher, B. (1996a). Concentrating partial entanglement by local operations. *Phys. Rev. A*, 53:2046–2052.

[Bennett et al., 1993] Bennett, C. H., Brassard, G., Crépeau, C., Jozsa, R., Peres, A., and Wootters, W. K. (1993). Teleporting an unknown quantum state via dual classical and einstein-podolsky-rosen channels. *Phys. Rev. Lett.*, 70:1895–1899.

[Bennett et al., 1996b] Bennett, C. H., DiVincenzo, D. P., Smolin, J. A., and Wootters, W. K. (1996b). Mixed-state entanglement and quantum error correction. *Phys. Rev. A*, 54:3824–3851.

[Berganza et al., 2012] Berganza, M. I., Alcaraz, F. C., and Sierra, G. (2012). Entanglement of excited states in critical spin chains. *Journal of Statistical Mechanics: Theory and Experiment*, 2012(01):P01016.

[Bombelli et al., 1986] Bombelli, L., Koul, R. K., Lee, J., and Sorkin, R. D. (1986). Quantum source of entropy for black holes. *Phys. Rev. D*, 34:373–383.

[Brust and Hinterbichler, 2017] Brust, C. and Hinterbichler, K. (2017). Free $\Box^k$-scalar conformal field theory. *Journal of High Energy Physics*, 2017(2):66.

[Calabrese and Cardy, 2004] Calabrese, P. and Cardy, J. (2004). Entanglement entropy and quantum field theory. *J. Stat. Mech.*

[Calabrese and Cardy, 2009] Calabrese, P. and Cardy, J. (2009). Entanglement entropy and conformal field theory. *J. Phys. A*.

[Calabrese et al., 2012] Calabrese, P., Cardy, J., and Tonni, E. (2012). Entanglement negativity in quantum field theory. *Phys. Rev. Lett.*, 109:130502.

[Calabrese et al., 2013a] Calabrese, P., Cardy, J., and Tonni, E. (2013a). Entanglement negativity in extended systems: a field theoretical approach. *Journal of Statistical Mechanics: Theory and Experiment*, 2013(02):P02008.

[Calabrese et al., 2014] Calabrese, P., Cardy, J., and Tonni, E. (2014). Finite temperature entanglement negativity in conformal field theory. *Journal of Physics A: Mathematical and Theoretical*, 48(1):015006.

[Calabrese and Cardy, 2006] Calabrese, P. and Cardy, J. L. (2006). Entanglement entropy and quantum field theory: A non-technical introduction. *Int. J. Quant. Inf.*, 4:429. Workshop on Quantum Entanglement in Physical and Information Sciences Pisa, Italy, December 14-18, 2004.

[Calabrese et al., 2013b] Calabrese, P., Tagliacozzo, L., and Tonni, E. (2013b). Entanglement negativity in the critical ising chain. *Journal of Statistical Mechanics: Theory and Experiment*, 2013(05):P05002.

[Callan and Wilczek, 1994] Callan, C. and Wilczek, F. (1994). On geometric entropy. *Physics Letters B*, 333(1):55 – 61.

[Cardy and Peschel, 1988] Cardy, J. L. and Peschel, I. (1988). Finite-size dependence of the free energy in two-dimensional critical systems. *Nuclear Physics B*, 300:377 – 392.

[Carlson, 1914] Carlson, F. (1914). *Sur une classe de séries de Taylor*. Uppsala.

[Casini and Huerta, 2009] Casini, H. and Huerta, M. (2009). Entanglement entropy in free quantum field theory. *J. Phys. A*.

[Castelnovo et al., 2005] Castelnovo, C., Chamon, C., Mudry, C., and Pujol, P. (2005). From quantum mechanics to classical statistical physics: Generalized rokhsar–kivelson hamiltonians and the "stochastic matrix form" decomposition. *Annals of Physics*, 318(2):316 – 344.

[Castro-Alvaredo et al., 2018] Castro-Alvaredo, O. A., De Fazio, C., Doyon, B., and Szécsényi, I. M. (2018). Entanglement content of quantum particle excitations. part i. free field theory. *Journal of High Energy Physics*, 2018(10):39.

[Chang and Dowker, 1993] Chang, P. and Dowker, J. (1993). Vacuum energy on orbifold factors of spheres. *Nuclear Physics B*, 395(1):407 – 432.

[Chen et al., 2015] Chen, X., Cho, G. Y., Faulkner, T., and Fradkin, E. (2015). Scaling of entanglement in 2 + 1-dimensional scale-invariant field theories. *Journal of Statistical Mechanics: Theory and Experiment*, 2015(2):P02010.

[Chen et al., 2017] Chen, X., Fradkin, E., and Witczak-Krempa, W. (2017). Quantum spin chains with multiple dynamics. *Phys. Rev. B*, 96:180402.

[Coser et al., 2016] Coser, A., Tonni, E., and Calabrese, P. (2016). Towards the entanglement negativity of two disjoint intervals for a one dimensional free fermion. *Journal of Statistical Mechanics: Theory and Experiment*, 2016(3):033116.

[Di Francesco et al., 1997] Di Francesco, P., Mathieu, P., and Senechal, D. (1997). *Conformal Field Theory*. Graduate Texts in Contemporary Physics. Springer-Verlag, New York.

[Dowker, 1994a] Dowker, J. S. (1994a). Effective action in spherical domains. *Commun. Math. Phys.*, 162:633–648.

[Dowker, 1994b] Dowker, J. S. (1994b). Functional determinants on spheres and sectors. *J. Math. Phys.*, 35:4989–4999. [Erratum: J. Math. Phys.36,988(1995)].

[Dowker, 2011] Dowker, J. S. (2011). Determinants and conformal anomalies of gjms operators on spheres. *J. Phys.*, A44:115402.

[Dowker, 2013] Dowker, J. S. (2013). Numerical evaluation of spherical GJMS determinants for even dimensions. *arXiv hep-th*.

[Einstein et al., 1935] Einstein, A., Podolsky, B., and Rosen, N. (1935). Can quantum-mechanical description of physical reality be considered complete? *Phys. Rev.*, 47:777–780.

[Eisert et al., 2010] Eisert, J., Cramer, M., and Plenio, M. B. (2010). Area laws for the entanglement entropy - a review. *Rev. Mod. Phys.*, 82:277–306.

[Ekert, 1991] Ekert, A. K. (1991). Quantum cryptography based on bell's theorem. *Phys. Rev. Lett.*, 67:661–663.

[Elizalde, 1998] Elizalde, E. (1998). Multidimensional extension of the generalized chowla-selberg formula. *Commun. Math. Phys.*, 198:83–95.

[Elizalde, 2012] Elizalde, E. (2012). *Ten Physical Applications of Spectral Zeta Functions*, volume 855 of *Lecture Notes in Physics*. Springer-Verlag Berlin Heidelberg, 2 edition.

[Fendley, 2008] Fendley, P. (2008). Topological order from quantum loops and nets. *Annals of Physics*, 323(12):3113 – 3136.

[Fradkin and Moore, 2006] Fradkin, E. and Moore, J. E. (2006). Entanglement entropy of 2d conformal quantum critical points: Hearing the shape of a quantum drum. *Phys. Rev. Lett.*, 97:050404.

[Freedman et al., 2005] Freedman, M., Nayak, C., and Shtengel, K. (2005). Extended hubbard model with ring exchange: A route to a non-abelian topological phase. *Phys. Rev. Lett.*, 94:066401.

[Freedman and Clauser, 1972] Freedman, S. J. and Clauser, J. F. (1972). Experimental test of local hidden-variable theories. *Phys. Rev. Lett.*, 28:938–941.

[Fursaev et al., 2013] Fursaev, D. V., Patrushev, A., and Solodukhin, S. N. (2013). Distributional geometry of squashed cones. *Phys. Rev. D*, 88:044054.

[Gentle and Keeler, 2016] Gentle, S. A. and Keeler, C. (2016). On the reconstruction of lifshitz spacetimes. *Journal of High Energy Physics*, 2016(3):195.

[Gentle and Vandoren, 2018] Gentle, S. A. and Vandoren, S. (2018). Lifshitz entanglement entropy from holographic cmera. *Journal of High Energy Physics*, 2018(7):13.

[Gover and Hirachi, 2004] Gover, A. R. and Hirachi, K. (2004). Conformally invariant powers of the laplacian: A complete non-existence theorem. *Journal of the American Mathematical Society*, 17(02):389–406.

[Graham et al., 1992] Graham, C. R., Jenne, R., Mason, L. J., and Sparling, G. A. J. (1992). Conformally invariant powers of the laplacian, i: Existence. *Journal of the London Mathematical Society*, s2-46(3):557–565.

[Gubser et al., 1998] Gubser, S., Klebanov, I., and Polyakov, A. (1998). Gauge theory correlators from non-critical string theory. *Physics Letters B*, 428(1):105 – 114.

[Hawking, 1976] Hawking, S. W. (1976). Particle creation by black holes. *Communications in Mathematical Physics*, 46(2):206–206.

[He et al., 2017] He, T., Magan, J. M., and Vandoren, S. (2017). Entanglement Entropy in Lifshitz Theories. *SciPost Phys.*, 3:034.

[Henley, 1997] Henley, C. L. (1997). Relaxation time for a dimer covering with height representation. *Journal of Statistical Physics*, 89(3):483–507.

[Holzhey et al., 1994] Holzhey, C., Larsen, F., and Wilczek, F. (1994). Geometric and renormalized entropy in conformal field theory. *Nuclear Physics B*, 424(3):443 – 467.

[Horodecki et al., 2009] Horodecki, R., Horodecki, P., Horodecki, M., and Horodecki, K. (2009). Quantum entanglement. *Rev. Mod. Phys.*, 81:865–942.

[Hsu and Fradkin, 2010] Hsu, B. and Fradkin, E. (2010). Universal behavior of entanglement in 2d quantum critical dimer models. *Journal of Statistical Mechanics: Theory and Experiment*, 2010(09):P09004.

[Hsu et al., 2009] Hsu, B., Mulligan, M., Fradkin, E., and Kim, E.-A. (2009). Universal entanglement entropy in two-dimensional conformal quantum critical points. *Phys. Rev. B*, 79:115421.

[Hubeny et al., 2007] Hubeny, V. E., Rangamani, M., and Takayanagi, T. (2007). A covariant holographic entanglement entropy proposal. *Journal of High Energy Physics*, 2007(07):062–062.

[Juhl, 2009] Juhl, A. (2009). On conformally covariant powers of the laplacian.

[Juhl, 2011] Juhl, A. (2011). Explicit formulas for gjms-operators and q-curvatures.

[Kachru et al., 2008] Kachru, S., Liu, X., and Mulligan, M. (2008). Gravity duals of lifshitz-like fixed points. *Phys. Rev. D*, 78:106005.

[Keränen et al., 2017] Keränen, V., Sybesma, W., Szepietowski, P., and Thorlacius, L. (2017). Correlation functions in theories with lifshitz scaling. *Journal of High Energy Physics*, 2017(5):33.

[Keränen and Thorlacius, 2015] Keränen, V. and Thorlacius, L. (2015). Holographic geometries for condensed matter applications. In *13th Marcel Grossmann Meeting on Recent Developments in Theoretical and Experimental General Relativity, Astrophysics, and Relativistic Field Theories*, pages 902–921.

[Kivelson et al., 1987] Kivelson, S. A., Rokhsar, D. S., and Sethna, J. P. (1987). Topology of the resonating valence-bond state: Solitons and high-T_c superconductivity. *Phys. Rev. B*, 35:8865–8868.

[Laflorencie, 2016] Laflorencie, N. (2016). Quantum entanglement in condensed matter systems. *Physics Reports*, 646:1 – 59. Quantum entanglement in condensed matter systems.

[Lami et al., 2018] Lami, L., Serafini, A., and Adesso, G. (2018). Gaussian entanglement revisited. *New Journal of Physics*, 20(2):023030.

[Maldacena, 1999] Maldacena, J. (1999). The large-n limit of superconformal field theories and supergravity. *International Journal of Theoretical Physics*, 38(4):1113–1133.

[Masanes, 2009] Masanes, L. (2009). Area law for the entropy of low-energy states. *Phys. Rev. A*, 80:052104.

[Moessner et al., 2001] Moessner, R., Sondhi, S. L., and Fradkin, E. (2001). Short-ranged resonating valence bond physics, quantum dimer models, and ising gauge theories. *Phys. Rev. B*, 65:024504.

[Mozaffar and Mollabashi, 2017] Mozaffar, M. R. M. and Mollabashi, A. (2017). Entanglement in lifshitz-type quantum field theories. *Journal of High Energy Physics*, 2017(7):120.

[Mozaffar and Mollabashi, 2018] Mozaffar, M. R. M. and Mollabashi, A. (2018). Logarithmic negativity in lifshitz harmonic models. *Journal of Statistical Mechanics: Theory and Experiment*, 2018(5):053113.

[Nishioka, 2018] Nishioka, T. (2018). Entanglement entropy: Holography and renormalization group. *Rev. Mod. Phys.*, 90:035007.

[Nishioka et al., 2009] Nishioka, T., Ryu, S., and Takayanagi, T. (2009). Holographic entanglement entropy: an overview. *Journal of Physics A: Mathematical and Theoretical*, 42(50):504008.

[Osborne and Nielsen, 2002] Osborne, T. J. and Nielsen, M. A. (2002). Entanglement in a simple quantum phase transition. *Phys. Rev. A*, 66:032110.

[Oshikawa, 2010] Oshikawa, M. (2010). Boundary conformal field theory and entanglement entropy in two-dimensional quantum lifshitz critical point.

[Osterloh et al., 2002] Osterloh, A., Amico, L., Falci, G., and Fazio, R. (2002). Scaling of entanglement close to a quantum phase transition. *Nature*, 416(6881):608–610.

[Page, 1993] Page, D. N. (1993). Average entropy of a subsystem. *Phys. Rev. Lett.*, 71:1291–1294.

[Parker et al., 2017] Parker, D. E., Vasseur, R., and Moore, J. E. (2017). Entanglement entropy in excited states of the quantum lifshitz model. *Journal of Physics A: Mathematical and Theoretical*, 50(25):254003.

[Peres, 1996] Peres, A. (1996). Separability criterion for density matrices. *Phys. Rev. Lett.*, 77:1413–1415.

[Peschel, 2003] Peschel, I. (2003). Calculation of reduced density matrices from correlation functions. *Journal of Physics A: Mathematical and General*, 36(14):L205–L208.

[Plenio and Virmani, 2007] Plenio, M. B. and Virmani, S. (2007). An Introduction to entanglement measures. *Quant. Inf. Comput.*, 7:1–51.

[Rangamani and Takayanagi, 2017] Rangamani, M. and Takayanagi, T. (2017). Holographic entanglement entropy. *Lecture Notes in Physics*, 931.

[Rokhsar and Kivelson, 1988] Rokhsar, D. S. and Kivelson, S. A. (1988). Superconductivity and the quantum hard-core dimer gas. *Phys. Rev. Lett.*, 61:2376–2379.

[Rubel, 1956] Rubel, L. A. (1956). Necessary and sufficient conditions for carlson's theorem on entire functions. *Transactions of the American Mathematical Society*, 83(2):417–429.

[Ryu and Takayanagi, 2006a] Ryu, S. and Takayanagi, T. (2006a). Aspects of holographic entanglement entropy. *Journal of High Energy Physics*, 2006(08):045–045.

[Ryu and Takayanagi, 2006b] Ryu, S. and Takayanagi, T. (2006b). Holographic derivation of entanglement entropy from the anti–de sitter space/conformal field theory correspondence. *Phys. Rev. Lett.*, 96:181602.

[Schrödinger, 1935] Schrödinger, E. (1935). Discussion of probability relations between separated systems. *Mathematical Proceedings of the Cambridge Philosophical Society*, 31(4):555–563.

[Shapourian and Ryu, 2019] Shapourian, H. and Ryu, S. (2019). Finite-temperature entanglement negativity of free fermions. *Journal of Statistical Mechanics: Theory and Experiment*, 2019(4):043106.

[Solodukhin, 2008] Solodukhin, S. N. (2008). Entanglement entropy, conformal invariance and extrinsic geometry. *Physics Letters B*, 665(4):305 – 309.

[Srednicki, 1993] Srednicki, M. (1993). Entropy and area. *Phys. Rev. Lett.*, 71:666–669.

[Stéphan et al., 2013] Stéphan, J.-M., Ju, H., Fendley, P., and Melko, R. G. (2013). Entanglement in gapless resonating-valence-bond states. *New Journal of Physics*, 15(1):015004.

[Susskind, 1995] Susskind, L. (1995). The world as a hologram. *Journal of Mathematical Physics*, 36(11):6377–6396.

['t Hooft, 1993] 't Hooft, G. (1993). Dimensional reduction in quantum gravity. *Conf. Proc. C*, 930308:284–296.

[Taylor, 2008] Taylor, M. (2008). Non-relativistic holography.

[Van Raamsdonk, 2009] Van Raamsdonk, M. (2009). Comments on quantum gravity and entanglement.

[Vidal et al., 2003] Vidal, G., Latorre, J. I., Rico, E., and Kitaev, A. (2003). Entanglement in quantum critical phenomena. *Phys. Rev. Lett.*, 90:227902.

[Vidal and Werner, 2002] Vidal, G. and Werner, R. F. (2002). Computable measure of entanglement. *Phys. Rev. A*, 65:032314.

[Weisberger, 1987] Weisberger, W. I. (1987). Conformal invariants for determinants of laplacians on riemann surfaces. *Communications in Mathematical Physics*, 112(4):633–638.

[Witten, 1998] Witten, E. (1998). Anti-de Sitter space and holography. *Adv. Theor. Math. Phys.*, 2:253–291.

[Witten, 2018] Witten, E. (2018). Aps medal for exceptional achievement in research: Invited article on entanglement properties of quantum field theory. *Rev. Mod. Phys.*, 90:045003.

[Zaletel et al., 2011] Zaletel, M. P., Bardarson, J. H., and Moore, J. E. (2011). Logarithmic terms in entanglement entropies of 2d quantum critical points and shannon entropies of spin chains. *Phys. Rev. Lett.*, 107:020402.

[Zhou, 2016] Zhou, T. (2016). Entanglement entropy of local operators in quantum lifshitz theory. *Journal of Statistical Mechanics: Theory and Experiment*, 2016(9):093106.

[Zhou et al., 2016] Zhou, T., Chen, X., Faulkner, T., and Fradkin, E. (2016). Entanglement entropy and mutual information of circular entangling surfaces in the $2+1$-dimensional quantum lifshitz model. *Journal of Statistical Mechanics: Theory and Experiment*, 2016(9):093101.

Paper I

Entanglement in generalised quantum Lifshitz models

Angel-Ramelli, J., Puletti, V.G.M. & Thorlacius, L.

J. High Energ. Phys. **2019**, 72 (2019).

Note: The margins of the paper were trimmed to better fit the format of this thesis.

Published for SISSA by Springer

Received: *June 28, 2019*
Accepted: *July 28, 2019*
Published: *August 13, 2019*

Entanglement entropy in generalised quantum Lifshitz models

J. Angel-Ramelli,[a] **V. Giangreco M. Puletti**[a] **and L. Thorlacius**[a,b]

[a] *University of Iceland, Science Institute, Dunhaga 3, 107 Reykjavík, Iceland*

[b] *The Oskar Klein Centre for Cosmoparticle Physics & Department of Physics, Stockholm University, AlbaNova, 106 91 Stockholm, Sweden*

E-mail: jfa1@hi.is, vgmp@hi.is, lth@hi.is

Abstract: We compute universal finite corrections to entanglement entropy for generalised quantum Lifshitz models in arbitrary odd spacetime dimensions. These are generalised free field theories with Lifshitz scaling symmetry, where the dynamical critical exponent z equals the number of spatial dimensions d, and which generalise the 2+1-dimensional quantum Lifshitz model to higher dimensions. We analyse two cases: one where the spatial manifold is a d-dimensional sphere and the entanglement entropy is evaluated for a hemisphere, and another where a d-dimensional flat torus is divided into two cylinders. In both examples the finite universal terms in the entanglement entropy are scale invariant and depend on the compactification radius of the scalar field.

Keywords: Conformal Field Theory, Field Theories in Higher Dimensions

ArXiv ePrint: 1906.08252

https://doi.org/10.1007/JHEP08(2019)072

Contents

1 Introduction

Quantum entanglement refers to a correlation of a purely quantum mechanical nature between degrees of freedom in a physical system. Consider a quantum system that can be divided into two subsystems A and B, such that the Hilbert space can be written as a direct product of the Hilbert spaces of the subsystems, $\mathcal{H} = \mathcal{H}_A \otimes \mathcal{H}_B$, and take the full system to be in a state described by a density matrix ρ. The entanglement entropy of subsystem A is then defined as the von Neumann entropy of the reduced density matrix, obtained by taking a trace over the degrees of freedom in subsystem B, i.e.

$$S[A] = -\mathrm{Tr}\left(\rho_A \log \rho_A\right) , \tag{1.1}$$

with $\rho_A = \mathrm{Tr}_B\, \rho$. We will take ρ to be the ground state density matrix of the full system but our results can be extended to more general states.

Entanglement entropy is a useful theoretical probe that encodes certain universal properties of field theories describing critical systems, see e.g. [1–5]. A well known example in this respect is the entanglement entropy of a two-dimensional conformal field theory (CFT) [6–8], which has a *universal* logarithmic term,

$$S[A] = \frac{c}{3} \log\left(\frac{L_A}{\varepsilon}\right) , \tag{1.2}$$

where c is the central charge of the CFT in question, L_A is the spatial size of the subsystem A, and ε is a UV-cutoff. Here we are assuming that A is connected and that its size is small compared to the full system size $L_A \ll L$. The logarithmic UV behaviour of the entanglement entropy tells us that the system has long-range entangled degrees of freedom (in contrast to an area-law where short-range entanglement would mainly contribute).

In recent years considerable effort has been devoted to investigating such universal terms in the entanglement entropy of CFTs in arbitrary dimensions (see [9, 10] for reviews). What will be important for us is the following general UV behavior of entanglement entropy in even D-dimensional CFTs,

$$S[A] = c_{D-2} \frac{\Sigma_{D-2}}{\varepsilon^{D-2}} + \cdots + c_0 \log\left(\frac{L_A}{\varepsilon}\right) + \ldots , \tag{1.3}$$

where Σ_{D-2} is the area of the $(D-2)$-dimensional entangling surface ∂A and L_A is a characteristic length associated with ∂A. Only c_0 is universal in this expression. The other coefficients depend on the regularisation scheme used. One also finds a universal subleading term in odd-dimensional CFTs but in this case it is finite rather than logarithmic, see e.g. [10] and references therein. The coefficient of the universal term is a function of topological and geometric invariants, such as the Euler density and Weyl invariants constructed from the entangling (hyper)-surface [11, 12]. This reflects the fact that the logarithmic term in $S[A]$ is related to the conformal anomaly of the stress-energy tensor of the corresponding CFT.

In the present work we will study entanglement entropy, including universal finite terms (i.e. of order $\mathcal{O}(1)$ with respect to L_A), in a family of $d+1$-dimensional scale invariant

quantum field theories introduced in [13]. The scale symmetry is a non-relativistic Lifshitz symmetry that acts asymmetrically on the time and spatial coordinates,

$$\vec{x} \to \lambda\, \vec{x}, \qquad \tau \to \lambda^z \tau\,, \tag{1.4}$$

with a dynamical critical exponent equal to the number of spatial dimensions $z = d$. These theories are closely related to the well known quantum Lifshitz model (QLM), first studied in the seminal work [14]. This is a scale invariant free field theory in $2 + 1$-dimensional spacetime with a $z = 2$ dynamical critical exponent. It is an effective field theory for certain quantum dimer models (and their universality class) in square lattices at a critical point and involves a *compactified* free massless scalar field [14]. Non-trivial Lifshitz scaling is achieved via a kinetic term that is asymmetric between time and space (with higher derivatives acting in the spatial directions). The higher-derivative construction can easily be extended to free scalar field theories in any number of spatial dimensions d with $z = d$ Lifshitz scaling. In [13] such theories were dubbed generalised quantum Lifshitz models (GQLMs) and several interesting symmetry properties were revealed in correlation functions of scaling operators. The periodic identification of the scalar field did not figure in that work but turns out be important when one considers entanglement entropy in a GQLM defined on a topologically nontrivial geometry.

A key property of the QLM and GQLM theories is that the ground state wave functional is invariant under conformal transformations involving *only* the spatial dimensions [13, 14]. The spatial conformal symmetry is a rather special feature (the corresponding critical points are called conformal quantum critical points [14]) and it manifests in the scaling properties of entanglement entropy. In essence, the symmetry allows us to map a $(d+1)$-dimensional Lifshitz field theory with $z = d$ to a d-dimensional Euclidean CFT. In the $d = 2$ QLM the CFT is the standard free boson CFT but for $d > 2$ GQLM's the spatial CFT is a higher-derivative generalised free field theory. Such higher-derivative CFTs have been discussed in a number of contexts, for instance in relation to higher spin theories, e.g. [15, 16], as models in elastic theory e.g. [17], in a high-energy physics setting in connection with the naturalness problem e.g. [18, 19], and in the context of dS/CFT duality e.g. [20, 21]. These theories are not unitary but their n-point correlation functions are well defined in Euclidean spacetime and being free field theories they have no interactions that trigger instability.

Entanglement entropy and its scaling properties have been extensively studied in the QLM [1, 22–27].[1] The replica method in the QLM was first developed in [22], where it was found that for a smooth entanglement boundary, the scaling behaviour of the entanglement entropy in the QLM (and more generally for conformal quantum critical points in $(2+1)$-dimensions) is of the form

$$S[A] = c_1 \frac{L_A}{\varepsilon} + \frac{c}{6} \Delta\chi \log \frac{L_A}{\varepsilon} + \dots\,, \tag{1.5}$$

where c_1 depends on the regulator and $\Delta\chi$ is the change in the Euler characteristic (upon dividing the the system in two), which in turns depends on the topology of the system and

[1] See also [28] for related study of Rényi entropies in quantum dimer models.

on the entangling surface. The above behavior follows from general expectations for the free energy of a two-dimensional CFT with boundary [29]. This result is for the entanglement entropy of a non-relativistic (2+1)-dimensional theory, however its computation starts from a ground state which is a "time-independent" conformal invariant. As the time coordinate only appears as a spectator, the final result displays features of a two-dimensional CFT. This is in line with the results of [13, 14], where it was shown that equal-time correlation functions of local scaling operators in the QLM and GQLM can be expressed in terms of correlation functions of a d-dimensional Euclidean CFT.

Furthermore, by choosing a smooth partition, such that we have no contribution from the logarithm (i.e. $\Delta\chi = 0$), a further sub-leading (of order one in L_A) universal term appears in the entanglement entropy for the QLM [1], that is

$$S_{\mathrm{EE}} = c_1 \frac{L_A}{\varepsilon} + \gamma_{\mathrm{QCP}} + \dots \,. \tag{1.6}$$

The universal term γ_{QCP}, where QCP stands for quantum critical point, depends both on the geometry and topology of the manifolds [23, 25–27]. It depends on the geometry in the sense that it includes a scaling function written in terms of aspect ratios typical of the given subsystem, and on the topology through a contribution from zero modes and non-trivial winding modes. In this sense, the entanglement entropy of the QLM is able to capture long-range (non-local) properties of the system. In particular, γ_{QCP} was computed by various methods for a spatial manifold in the form of a cylinder in [24–27, 30], for a sphere in [27], and the toroidal case was treated in [25] by means of a boundary field theory approach. The toroidal case was further investigated in [31], where analytic results were obtained for Rényi entropies.[2]

Our aim is to extend the study of these finite universal terms in the entanglement entropy to generalised quantum Lifshitz models. In particular, we analyse their scaling properties in full generality, in any number of spatial dimensions d with Lifshitz exponent $z = d$. For technical reasons (which we explain below) we restrict attention to the case of even integer d. More concretely, we obtain universal terms in the entanglement entropy in GQLM on two classes of manifolds. On the one hand, we divide a d-dimensional sphere into two d-dimensional hemispheres, on the other hand we consider a d-dimensional flat torus, sliced into two d-dimensional cylinders.[3] Our computations are purely field theoretical. The theories we consider represent rare examples of non-relativistic critical theories, for which entanglement entropy can be obtained analytically. We view them as toy-models where we can explore quantum entanglement for different values of the dynamical critical exponent z. Further motivation comes from a puzzling aspect of Lifshitz holography, where one considers gravitational solutions that realise the Lifshitz scaling (1.4), see e.g. [34, 35]. In AdS/CFT the entanglement entropy is computed by means of the Ryu-Takayanagi formula [36, 37]. The usual working assumption is to apply the RT prescription also in Lifshitz holography, but in a static Lifshitz spacetime the holographic entanglement entropy does not depend on the critical exponent at all (see e.g. [38]). From a field theory point of

[2] For related studies of the scaling properties of entanglement entropy for a toroidal manifold in scale invariant (2+1)-dimensional systems, see also [32, 33].

[3] Here a d-dimensional cylinder refers to the product of an interval and a $(d-1)$-dimensional flat torus.

view, however, one expects the higher-derivative terms to dominate at short distances, and thus the UV behaviour of entanglement should reflect the value of the dynamical critical exponent. The absence of z from the holographic entanglement entropy is puzzling if Lifshitz spacetime is the gravitational dual of a strongly coupled field theory with Lifshitz symmetry. Similar considerations motivated the work in [39–41]. While we clearly see a dependence on z, it is difficult to compare our results directly to those of these authors as we are not working within the same class of field theories and we focus on universal sub-leading terms rather than the leading area terms.

The paper is arranged as follows. In section 2 we briefly review the construction of generalised quantum Lifshitz models and extend their definition to two specific compact manifolds. These are higher-derivative field theories so we must ensure that the variational problem is well posed. This amounts to imposing z conditions on the variations (2.8), (2.15) and including a boundary action (2.10) for the d-torus or (2.16) for the d-sphere. In section 3 we discuss the replica method, which we use to compute the entanglement entropy. In essence, this approach maps the problem of computing the nth-power of the reduced density matrix to a density matrix of an n times replicated field theory. The goal is to produce a result that can be analytically continued in n, in order to calculate the entanglement entropy according to (3.1). As we explain in section 3, the replica method forces all the replicated fields to be equal at the cut, since the cut is not physical and our original field theory only has one field. There is an additional subtlety in implementing this condition due to the periodic identification of the scalar field in the GQLM and in order to ensure the correct counting of degrees of freedom we separate the replicated fields into classical and fluctuating parts. The fluctuating fields obey Dirichlet boundary conditions as well as the vanishing of the conformal Laplacian and its integer powers at the cut. Their contribution is encoded in partition functions computed via functional determinants defined on the sphere and torus respectively. The classical fields give rise to winding sectors that are encoded in the function $W(n)$ described in section 3. For the spherical case this contribution is simple and only amounts to a multiplicative factor $\sqrt{n}$. For the toroidal case, the contribution from the classical fields is less trivial, and requires summing over classical vacua of the action. For higher-derivative theories some further conditions have to be implemented in the classical sector, and we argue that a compatible prescription is to use Neumann boundary conditions for these fields. At this point no freedom and/or redundancy is left, and it is straightforward to compute the sum over winding modes. We collect the contributions from the classical and fluctuating fields to the universal finite term of the entanglement entropy for a d-sphere and a d-torus in sections 4 and 5 respectively. We conclude with some open questions in section 6.

Most of the technical details are relegated to appendices. In appendix A we review the computation of the functional determinant contribution for the spherical case, which was originally worked out in [42]. In appendix B we develop an alternative expression for the formulae presented in appendix A, which we find more transparent and better suitable for numerical evaluation. In appendix C we compute the functional determinant contribution for the toroidal case. Finally we compute the winding sector contribution for the d-torus in appendix D.

2 Generalised quantum Lifshitz models in (d+1)-dimensions

The 2+1-dimensional quantum Lifshitz model [14] can be generalised to d+1-dimensions [13]. Whenever the dynamical critical exponent z is equal to the number of spatial dimensions, the ground state wave-functional is invariant under d-dimensional conformal transformations acting in the spatial directions, extending the connection between the quantum Lifshitz model and a free conformal field theory in one less dimension to any d. We recall that in the 2+1-dimensional case the scalar field is compactified [14], and below we will also compactify the scalar field in the GQLM at general d on a circle of radius R_c, that is identify $\phi \sim \phi + 2\pi R_c$.

The ground state wave functional of the GQLM is [13]

$$|\psi_0\rangle = \frac{1}{\sqrt{Z}} \int [\mathcal{D}\phi] e^{-\frac{1}{2}S[\phi]} |\phi\rangle \,, \tag{2.1}$$

where $\{|\phi\rangle\}$ is an orthonormal basis of states in the Hilbert space made up of eigenstates of the field operator, and the partition function Z is given by

$$Z = \int [\mathcal{D}\phi]\, e^{-S[\phi]} \,. \tag{2.2}$$

We are interested in computing the sub-leading universal finite term of the entanglement entropy (1.1) in the ground state, i.e. with $\rho = |\psi_0\rangle\langle\psi_0|$, when the manifold $\mathcal{M}$ is a d-sphere or a d-torus. The subsystem A will consist of field degrees of freedom on a submanifold of $\mathcal{M}$. For technical reasons we restrict attention to the case where d is an even (positive) integer.

We follow the normalisation convention of [27] and write the action as

$$S[\phi] = S_0[\phi] + S_{\partial\mathcal{M}}[\phi] = \frac{\kappa}{4\pi} \int_{\mathcal{M}} \mathrm{d}^d x \sqrt{G}\, \phi\, \mathcal{P}_{z,\mathcal{M}}\, \phi + S_{\partial\mathcal{M}}[\phi] \,, \tag{2.3}$$

where $G = \det G_{ab}$ $(a, b = 1, \ldots, d)$ is the determinant of the Euclidean metric on the manifold $\mathcal{M}$, and $\mathcal{P}_{z,\mathcal{M}}$ is a proper conformal differential operator of degree z in d dimensions. The specific form of $\mathcal{P}_{z,\mathcal{M}}$ depends on $\mathcal{M}$, as we will discuss at the end of this section. In order to have a well-defined variational problem, the action has to include a suitable boundary term $S_{\partial\mathcal{M}}$ whose specific form is also given below. Note that the scalar field ϕ has dimension zero under Lifshitz scaling in the GQLM at general d. We find it convenient to use the shorthand $g = \frac{\kappa}{4\pi}$.[4] We note that for a flat manifold, the compactification of the field implies a global shift symmetry compatible with conformal symmetry [43, 44]. This is also true for the $z = d$ theory on the d-sphere (and more generally on any Einstein manifold) provided the action includes appropriate terms that generalise the notion of conformal coupling to a higher-derivative setting.

Let us consider how the action in (2.3) is constructed concretely for the two cases, mentioned above. To keep the discussion somewhat general, we assume that both z and d

[4] The normalisation of the action in (2.3) and the compactification radius R_c are not independent. A rescaling of the scalar field will affect both g and R_c, while physical quantities that are independent of rescaling are expressed in terms of $2\pi R_c \sqrt{g}$ [43, 44].

are even positive integers and do not insist on $z = d$ for the time being. The case when d is an odd integer is also interesting but raises a number of technical issues that we do not address in this work. The boundary terms in the action will be important once we divide the system into subsystems and apply the replica method (cf. section 3).

***d*-torus.** In section 5, we consider a torus obtained as the quotient space of $\mathbb{R}^d$ and a d-dimensional lattice. The manifold is flat, and in this case the operator appearing in the action $S_0[\phi]$ in (2.3) is simply the $z/2$ power of the Laplace-Beltrami operator,

$$\mathcal{P}_{z,T^d} = (-1)^{z/2+1}\Delta^{z/2} = (-1)^{z/2+1}\left(-\partial_a\partial^a\right)^{z/2}\,, \tag{2.4}$$

that is

$$S_0[\phi] = (-1)^{z/2+1} g \int_M d^d x\, \phi \Delta^{z/2}\phi\,. \tag{2.5}$$

For $d = z = 2$ this reduces to $S = g\int(\nabla\phi)^2$ as in [14] (after integrating by parts). Varying $S_0[\phi]$ we obtain

$$\begin{aligned}\delta S_0[\phi] =& 2(-1)^{z/2+1} g \int_M d^d x\, (\Delta^{z/2}\phi)\delta\phi \\ &+ (-1)^{z/2+1} g \int_{\partial M} d^{d-1}x \sum_{k=0}^{z-1}(-1)^k(\partial_n^k\phi)(\partial_n^{z-1-k}\delta\phi)\end{aligned} \tag{2.6}$$

where the partial derivatives should be understood as follows

$$\partial_n^{2\ell} = \left(\partial_a\partial^a\right)^\ell\,, \qquad \partial_n^{2\ell+1} = n_a\partial^a\left(\partial_b\partial^b\right)^\ell\,, \tag{2.7}$$

with n_a an oriented unit vector normal to the boundary. We need to choose appropriate boundary conditions for the variations. One possibility is to demand that

$$\partial_n^{2\ell}\delta\phi\big|_{\partial\mathcal{M}} = 0\,, \qquad \ell = 0, \ldots, \frac{z}{2} - 1\,. \tag{2.8}$$

The reason behind this choice is that we will be interested in the eigenvalue problem of $\Delta^{z/2}$, for which we require the operator to be self-adjoint and to have a complete set of consistent boundary conditions. The replica method forces us to choose Dirichlet conditions on the field at the boundary (cf. section 3) and the remaining conditions are chosen to be consistent with the self-adjointness of the operator. Equipped with (2.8), the variation of the Lagrangian reduces to

$$\begin{aligned}\delta S_0[\phi] =& 2(-1)^{z/2+1} g \int_M d^d x\, (\Delta^{z/2}\phi)\delta\phi \\ &+ (-1)^{z/2+1} g \int_{\partial M} d^{d-1}x \sum_{\ell=0}^{\frac{z}{2}-1}(\partial_n^{2\ell}\phi)(\partial_n^{z-1-2\ell}\delta\phi)\,.\end{aligned} \tag{2.9}$$

Hence, defining the following boundary action

$$S_\partial[\phi] = (-1)^{z/2+1} g \int_{\partial M} d^{d-1}x \sum_{k=0}^{\frac{z}{2}-1}(\partial_n^{2k}\phi)(\partial_n^{z-2k-1}\phi), \tag{2.10}$$

with variation given by

$$\delta S_\partial[\phi] = (-1)^{z/2+1} g \int_{\partial M} d^{d-1}x \sum_{k=0}^{\frac{z}{2}-1} (\partial_n^{2k}\phi)(\partial_n^{z-2k-1}\delta\phi), \tag{2.11}$$

clearly gives a well-defined variation for the total action $S[\phi] = S_0[\phi] + S_\partial[\phi]$ and leads to the following equations of motion

$$\Delta^{z/2}\phi = 0, \quad \text{and} \quad \partial_n^{2k}\delta\phi\big|_{\partial M} = 0, \quad \text{for } k = 0, \dots, \frac{z}{2} - 1\,. \tag{2.12}$$

***d*-sphere.** When the manifold $\mathcal{M}$ is a unit d-sphere, the operator in (2.3) is the so-called GJMS operator on a d-sphere [45]. In essence, GJMS operators generalise the conformal Laplacian to higher derivatives and d-dimensional curved manifolds [45] (see [46–54] for more references on the subject). This means that a GJMS operator of degree $2k$ in d-dimensions (where k is a positive integer) is constructed so that it transforms in a simple way under a Weyl transformation of the metric, $G_{ab} \to e^{2\omega}G_{ab}$,

$$\mathcal{P}_{2k}(e^{2\omega}G) = e^{-(d/2+k)\omega}\mathcal{P}_{2k}(G)\, e^{(d/2-k)\omega}\,. \tag{2.13}$$

In general, the operator $\mathcal{P}_{2k}$ is well defined for $k = 1, \dots d/2$ for even d, in the sense that it reduces to the standard Laplacian of degree k in flat space [47]. For odd d-dimensional manifolds operators satisfying (2.13) exist for all $k \geq 1$ [47, 52, 53].

On a unit d-sphere the GJMS operator of degree $2k$ explicitly reads as

$$\mathcal{P}_{2k,S^d} = \prod_{j=1}^{k} \left[\Delta_{S^d} + \left(\frac{d}{2} - j\right)\left(\frac{d}{2} + j - 1\right)\right], \tag{2.14}$$

where $\Delta_{S^d} = -\frac{1}{\sqrt{G}}\partial_a\left(\sqrt{G}\, G^{ab}\partial_b\right)$, with $a, b = 1, \dots d$, is the Laplace-Beltrami operator. The case of most interest to us is to consider a GJMS operator of degree $2k = d$. This is known in the literature as the critical case, while $k < d/2$ is referred to as the subcritical case. It is straightforward to check, using (2.13), that the final action S_0 (2.3) is invariant under Weyl transformations. The factorisation in (2.14) is a general characteristic of Einstein manifolds. Since the eigenfunctions of the Laplace-Beltrami operator on a compact Riemannian manifold form an orthonormal basis, one can easily obtain the spectrum of the GJMS operator on the sphere from the factorisation above. This will play an important role later in the computation of partition functions in section 4.

When S^d is divided into hemispheres, the action $S_0[\phi]$ has to be complemented by boundary terms. As before, in order to have a well-defined variational problem, we compute the variation of the action δS_0, impose z boundary conditions on $\delta\phi$ and its derivatives, and then cancel any remaining terms against appropriate boundary terms. We impose the following boundary conditions

$$\delta\phi\big|_{\partial\mathcal{M}} = 0\,, \quad \Delta^k\delta\phi\big|_{\partial\mathcal{M}} = 0 \qquad k = 1, \dots \frac{z}{2} - 1\,, \tag{2.15}$$

that is Dirichlet boundary conditions on the variation $\delta\phi$ and vanishing of its Laplacian and its powers at the boundary. This is analogous to (2.8) for a curved manifold. The explicit expression for $S_\partial[\phi]$ is

$$S_\partial[\phi] = g\sum_{\ell=1}^{d/2}\int_{\mathcal{M}} d^dx\ \partial_a\Bigg\{\sqrt{G}G^{ab}\Bigg[\prod_{j=1}^{d/2-\ell}\left(\Delta+\left(\frac{d}{2}-j\right)\left(\frac{d}{2}+j-1\right)\right)\phi\Bigg] \times\partial_b\Bigg[\prod_{k=d/2-\ell+2}^{d/2}\left(\Delta+\left(\frac{d}{2}-k\right)\left(\frac{d}{2}+k-1\right)\right)\phi\Bigg]\Bigg\}, \tag{2.16}$$

where the products in the above expression are taken to be empty when the upper extreme is less than the lower extreme. Finally, the classical equation of motion is

$$\mathcal{P}_{d,S^d}\,\phi = \prod_{j=1}^{d/2}\left[\Delta_{S^d}+\left(\frac{d}{2}-j\right)\left(\frac{d}{2}+j-1\right)\right]\phi = 0\,. \tag{2.17}$$

3 Replica method

The entanglement entropy of subsystem A can be defined as

$$S[A] = -\lim_{n\to 1}\partial_n \mathrm{Tr}(\rho_A^n)\,, \tag{3.1}$$

where an analytic continuation of the index n is assumed. This definition is equivalent to the von Neumann entropy of ρ_A (1.1). Following [8, 55], we will use the replica approach to evaluate (3.1). At the heart of this method is to view each appearance of the density matrix ρ in $\mathrm{Tr}(\rho_A^n)$ as coming from an independent copy of the original theory, so that one ends up working with n replicated scalar fields. The process of taking partial traces and multiplying the replicas of ρ then induces a specific set of boundary conditions at the entanglement cuts on the replica fields.

In this section we adapt the replica trick to generalised quantum Lifshitz theories. For the QLM the replica method was reviewed in [26, 27]. Our starting point is the ground state density matrix $\rho = |\psi_0\rangle\langle\psi_0|$, with $|\psi_0\rangle$ as in (2.1). Now divide the manifold into two regions A and B and assume that the Hilbert space splits as $\mathcal{H} = \mathcal{H}_A\otimes\mathcal{H}_B$. This allows us to write the density matrix as

$$\rho = \frac{1}{Z}\int[\mathcal{D}\phi^A][\mathcal{D}\phi^B][\mathcal{D}\phi'^A][\mathcal{D}\phi'^B] \times e^{-\frac{1}{2}S[\phi^A]-\frac{1}{2}S[\phi^B]-\frac{1}{2}S[\phi'^A]-\frac{1}{2}S[\phi'^B]}|\phi^A\rangle\otimes|\phi^B\rangle\langle\phi'^A|\otimes\langle\phi'^B|, \tag{3.2}$$

where the field eigenstates $\{|\phi^A\rangle\}$ and $\{|\phi^B\rangle\}$ provide orthonormal bases in $\mathcal{H}_A$ and $\mathcal{H}_B$, respectively, and we have used that ϕ^A and ϕ^B are free fields with support on non-overlapping subsets of $\mathcal{M}$ to write $S[\phi] = S[\phi^A]+S[\phi^B]$. We then construct ρ_A^n by the gluing procedure represented in figure 1. Each copy of ρ is represented by a path integral as in (3.2) with

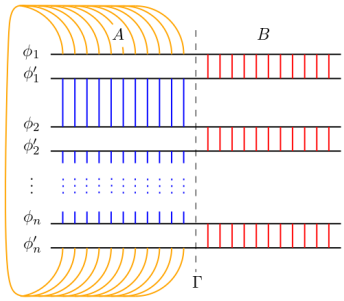

Figure 1. The gluing procedure due to the replica trick. Gluing due to the partial trace over B is represented in red, due to multiplication of the reduced density matrices ρ_A in blue, and due to the final total trace in yellow.

fields labelled by a replica index $i = 1, \ldots, n$. The partial trace over field degrees of freedom with support in B gives the following reduced density matrix for the i-th replica,

$$\begin{aligned}\rho_A &= \mathrm{Tr}_B\,(\rho) \\ &= \frac{1}{Z}\int [\mathcal{D}\phi_i^A][\mathcal{D}\phi_i'^A][\mathcal{D}\phi_i^B] e^{-\frac{1}{2}S[\phi_i^A]-\frac{1}{2}S[\phi_i'^A]-S[\phi_i^B]} |\phi_i^A\rangle\langle\phi_i'^A|.\end{aligned} \tag{3.3}$$

Multiplying together two adjacent copies of the reduced density matrix gives

$$\begin{aligned}\rho_A^2 = \frac{1}{Z^2}\int &[\mathcal{D}\phi_i^A][\mathcal{D}\phi_{i+1}'^A][\mathcal{D}\phi_{i+1}^A][\mathcal{D}\phi_i^B][\mathcal{D}\phi_{i+1}^B] \\ &\times e^{-\frac{1}{2}S[\phi_i^A]-\frac{1}{2}S[\phi_{i+1}'^A]-S[\phi_{i+1}^A]-S[\phi_i^B]-S[\phi_{i+1}^B]} |\phi_i^A\rangle\langle\phi_{i+1}'^A|\,.\end{aligned} \tag{3.4}$$

The δ-function coming from $\langle\phi_i'^A|\phi_{i+1}^A\rangle$ forces the identification $\phi_i'^A = \phi_{i+1}^A$, effectively gluing together the primed field from replica i and the unprimed field from replica $i+1$, as indicated in figure 1. It follows that multiplying n copies of the reduced density matrix gives rise to pairwise gluing conditions $\phi_i'^A = \phi_{i+1}^A$ for $i = 1, \ldots, n-1$, and when we take the trace of the complete expression we get a gluing condition between the first and last replicas, $\phi_1^A = \phi_n'^A$. Combining this with the gluing condition $\phi_i^B = \phi_i'^B$ for $i = 1, \ldots, n$ from the partial trace in (3.3), and the boundary condition $\phi_i^A\big|_\Gamma = \phi_i^B\big|_\Gamma$, where Γ denotes the entangling surface separating A and B, we see that *all* the replica fields are forced to agree on Γ. The final result for ρ_A^n is then

$$\mathrm{Tr}_A\,(\rho_A^n) = \frac{1}{Z_{A\cup B}^n}\int_{\mathrm{bc}}\prod_{i=1}^n [\mathcal{D}\phi_i^A] e^{-\sum_{i=1}^n S[\phi_i^A]} \int_{\mathrm{bc}}\prod_{i=1}^n [\mathcal{D}\phi_i^B]\, e^{-\sum_{i=1}^n S[\phi_i^B]} \tag{3.5}$$

with

$$\mathrm{bc} \quad : \quad \phi_i^A\big|_\Gamma(x) = \phi_j^B\big|_\Gamma(x) \equiv \mathrm{cut}(x)\,, \quad i,j = 1,\ldots,n\,, \tag{3.6}$$

where $\mathrm{cut}(x)$ is some function of the boundary coordinates. We write the denominator in (3.5) as $Z_{A\cup B}^n$ to emphasise that it contains n copies of the partition function of the

original system before any subdivision into fields on A and B. In the numerator, however, the field configurations of the different replicas are integrated over independently, except that the replicated fields are subject to the boundary conditions (3.6) (up to the periodic identification $\phi \sim \phi + 2\pi R_c$).

In order to take the periodic identification into account when applying boundary conditions, we separate each replicated field into a classical mode and a fluctuation, following a long tradition, see e.g. [43, 44],

$$\phi_i^{A(B)} = \phi_{i,\mathrm{cl}}^{A(B)} + \varphi_i^{A(B)}\,, \qquad i = 1, \ldots, n\,. \tag{3.7}$$

The modes $\phi_{i,\mathrm{cl}}$ satisfy the following classical equations of motion and boundary conditions,

$$\mathcal{P}_z \phi_{i,\mathrm{cl}}^{A(B)}(x) = 0\,, \qquad \phi_{i,\mathrm{cl}}^{A(B)}(x)\big|_\Gamma = \mathrm{cut}(x) + 2\pi R_c w_i^{A(B)}\,, \qquad i = 1, \ldots, n\,, \tag{3.8}$$

where $w_i^{A(B)}$ are integers indicating the winding sector. The classical field determines the total field value at the entanglement cut, while the fluctuating field φ satisfies Dirichlet boundary conditions,

$$\varphi_i^{A(B)}(x)\big|_\Gamma = 0 \qquad i = 1, \ldots, n\,. \tag{3.9}$$

In two dimensions this condition, along with the equation of motion of the classical fields, ensures that the action factorises [27],[5]

$$S[\phi_i^{A(B)}] = S[\phi_{i,\mathrm{cl}}^{A(B)}] + S[\varphi_i^{A(B)}]\,, \qquad i = 1, \ldots, n\,. \tag{3.10}$$

The decomposition of the action is less trivial in higher dimensions but it can be achieved if the Dirichlet boundary condition on the fluctuating field at the entanglement cut is augmented by further conditions. It is straightforward to check that imposing (3.9) along with (2.8)–(2.15) on the fluctuating fields at the cut leads to a well-posed variational problem as well as self-adjointness of the operator $\mathcal{P}_{z,\mathcal{M}}$ on $\mathcal{M}$. As was discussed earlier, this combination of conditions amounts to the vanishing of the Laplace operator and its integer powers acting on the fluctuating fields at the boundary. This turns out to be enough to ensure that the *total* action splits according to (3.10) (once again the equations of motion for the classical fields have to be used to achieve factorization). We note, that with this prescription and using the classical equations of motion, the boundary terms in the action can be written in a form that only depends on the classical part of the field,

$$S_\partial[\phi_i^{A(B)}] = S_\partial[\phi_{i,\mathrm{cl}}^{A(B)}]\,. \tag{3.11}$$

In the presence of winding modes, there remains some redundancy in the classical part of the action, as further discussed in appendix D where we compute the contribution from the classical winding sector for the d-torus.

As a consequence of (3.10), the fluctuating modes φ_i simply contribute as n independent fields obeying Dirichlet boundary conditions (3.9) at the entanglement cut. For the

[5] Derivatives of the classical fields are in general discontinuous at the cut, but the left- and right-derivatives remain bounded.

classical modes, on the other hand, we can solve for the A and B sectors simultaneously, as the boundary value problem (3.8) has a unique solution in $A \cup B \setminus \Gamma$, up to winding numbers. At the entanglement cut only relative winding numbers matter and we can choose to write the boundary conditions for the classical fields as [26]

$$\phi_{i,\mathrm{cl}}\big|_{\Gamma}(x) = \mathrm{cut}(x) + 2\pi R_c w_i\,, \qquad i = 1, \ldots, n-1\,, \qquad \phi_{n,\mathrm{cl}}\big|_{\Gamma}(x) = \mathrm{cut}(x)\,. \tag{3.12}$$

Thus, the trace of the n-th power of the reduced density matrix reads

$$\mathrm{Tr}_A\,(\rho_A^n) = \frac{1}{Z^n_{A\cup B}} \prod_{i=1}^{n} \int_{\mathrm{D}} [\mathcal{D}\varphi_i^A] e^{-S[\varphi_i^A]} \prod_{i=1}^{n} \int_{\mathrm{D}} [\mathcal{D}\varphi_i^B]\, e^{-S[\varphi_i^B]}\, W(n)\,, \tag{3.13}$$

where $W(n)$ is the contribution coming from summing over all classical field configurations satisfying the boundary conditions (3.12). The subscript D on the integral sign is a reminder that the the fluctuating fields obey Dirichlet boundary conditions.

At this point we need to distinguish the spherical case from the toroidal one. We start by analysing the problem on the d-sphere, which turns out to be particularly simple.

***d*-sphere.** We closely follow the treatment of the two-dimensional case in [27]. The crucial observation here is that the winding mode can be reabsorbed by the global shift symmetry of the action, $S[\phi_i] = S[\phi_i + \phi_i^0]$ with constant ϕ_i^0, as mentioned in section 2. Indeed, since the fields satisfying the classical equation of motion include any constant part of the total field, we can use the symmetry to rewrite their boundary conditions as

$$\phi^{\mathrm{cl}}_{i|\Gamma}(x) = \mathrm{cut}(x) + 2\pi\, R_c\, \omega_i + \phi_i^0\,. \tag{3.14}$$

We then choose $\phi_i^0 = -2\pi\, R_c\, \omega_i$ to cancel out all winding numbers. The boundary conditions then become

$$\phi^{\mathrm{cl}}_{i|\Gamma}(x) = \mathrm{cut}(x)\,, \qquad i = 1, \ldots, n\,, \tag{3.15}$$

and the sum over classical configurations can be written as

$$W(n) = \sum_{\phi_{i,\mathrm{cl}}} e^{-\sum_i S[\phi_{i,\mathrm{cl}}]} = \sum_{\phi_{n,\mathrm{cl}}} e^{-n\, S[\phi_{n,\mathrm{cl}}]} = \sum_{\phi_{n,\mathrm{cl}}} e^{-S[\sqrt{n}\,\phi_{n,\mathrm{cl}}]}\,. \tag{3.16}$$

Consequently, we have for the d-sphere

$$\mathrm{Tr}_A\,(\rho_A^n) = \frac{1}{Z^n_{A\cup B}} \prod_{i=1}^{n} \int_{\mathrm{D}} [\mathcal{D}\varphi_i^A] e^{-S[\varphi_i^A]} \prod_{i=1}^{n} \int_{\mathrm{D}} [\mathcal{D}\varphi_i^B]\, e^{-S[\varphi_i^B]} \sum_{\phi_{n,\mathrm{cl}}} e^{-S[\sqrt{n}\,\phi_{n,\mathrm{cl}}]}\,. \tag{3.17}$$

We can now combine the n-th fluctuating fields with support on A and B and the n-th classical field to define

$$\Phi_n = \varphi_n + \sqrt{n}\,\phi_{n,\mathrm{cl}}\,, \tag{3.18}$$

with $\varphi_n = \varphi_n^{A(B)}$ in $A(B)$. Notice that the effective compactification radius of Φ_n is now $\sqrt{n}R_c$ [26, 27]. The path integral over φ_n^A and φ_n^B along with the contribution $W(n)$ from

the rescaled classical field amounts to the partition function on the whole d-sphere for the combined field Φ_n, which is equal to the partition function of the original field up to a factor of $\sqrt{n}$ due to the different compactification radius, and it therefore almost exactly cancels one power of the original partition function in the denominator in (3.17),

$$\begin{aligned} \mathrm{Tr}_A\left(\rho_A^n\right) &= \frac{1}{Z_{A\cup B}^n}\prod_{i=1}^{n-1}\int_{\mathrm{D}}[\mathcal{D}\varphi_i^A]e^{-S[\varphi_i^A]}\prod_{i=1}^{n-1}\int_{\mathrm{D}}[\mathcal{D}\varphi_i^B]\,e^{-S[\varphi_i^B]}\,\sqrt{n}\,Z_{A\cup B} \\ &= \sqrt{n}\left(\frac{Z_{D,A}Z_{D,B}}{Z_{A\cup B}}\right)^{n-1}, \end{aligned} \tag{3.19}$$

where $Z_{D,A(B)} \equiv \int_{\mathrm{D}}[\mathcal{D}\varphi_i^{A(B)}]e^{-S[\varphi_i^{A(B)}]}$ denotes the Dirichlet partition function on $A(B)$. Hence, the entanglement entropy is given by

$$S_{\mathrm{EE}} = -\lim_{n\to 1}\partial_n \mathrm{Tr}_A\left(\rho_A^n\right) = -\log\left(\frac{Z_{D,A}Z_{D,B}}{Z_{A\cup B}}\right) - \frac{1}{2}, \tag{3.20}$$

and the original problem has been reduced to the computation of partition functions with appropriate boundary conditions on the regions A and B and $A\cup B$.

We will consider the case where the d-sphere is divided into two hemispheres. Then we only have to compute the partition function on the full sphere and a Dirichlet partition function on a hemisphere. These are in turn given by determinants of the appropriate GJMS operators. The detailed computation is described in section 4 and appendices A and B.

***d*-torus.** We now apply the replica method in the case of a d-torus. We cut the torus into two parts, thus introducing two boundaries which are given by two disjoint periodically identified $(d-1)$-intervals (in $d=2$ this is simply an S^1). As explained before, all the fields have to agree at the cuts Γ_a (where now the index $a=1,2$ labels each cut). For the quantum fields this simply implies that they need to satisfy Dirichlet boundary conditions, that is

$$\varphi_i^{A(B)}\big|_{\Gamma_a} = 0\,, \qquad i=1,\dots,n, \qquad a=1,2\,. \tag{3.21}$$

As explained earlier, further conditions are necessary in dimensions $d>2$, and we demand that the conditions (2.8) hold at the cut for the fluctuating fields.

Now consider the classical fields on the torus. We can use the global shift symmetry discussed in section 2 to write the boundary conditions for the classical fields as

$$\phi_{i,\mathrm{cl}}\big|_{\Gamma_a}(x) = \mathrm{cut}_a(x) + 2\pi R_c\,\omega_i^a + \phi_i^0 \tag{3.22}$$

with ϕ_i^0 constant on the whole torus. As in the spherical case, we can choose the ϕ_i^0 so that they absorb the winding numbers from one of the cuts,

$$\phi_{i,\mathrm{cl}}\big|_{\Gamma_1}(x) = \mathrm{cut}_1(x)\,, \qquad i=1,\dots,n\,, \tag{3.23}$$

$$\phi_{i,\mathrm{cl}}\big|_{\Gamma_2}(x) = \mathrm{cut}_2(x) + 2\pi R_c\,\omega_i\,, \qquad i=1,\dots,n\,, \tag{3.24}$$

where $\omega_i := \left(\omega_i^2 - \omega_i^1\right)$. We are effectively left to deal with winding sectors at a single entanglement cut and since only the relative winding number between adjacent replicas matters we can eliminate one more winding number to obtain

$$\phi_{i,\mathrm{cl}}\big|_{\Gamma_1}(x) = \mathrm{cut}_1(x)\,, \qquad i = 1,\dots,n \tag{3.25}$$

$$\phi_{i,\mathrm{cl}}\big|_{\Gamma_2}(x) = \mathrm{cut}_2(x) + 2\pi R_c\,\omega_i\,, \quad i = 1,\dots,n-1, \qquad \phi_{n,\mathrm{cl}}\big|_{\Gamma_2}(x) = \mathrm{cut}_2(x)\,. \tag{3.26}$$

At this point, we can use the same unitary rotation U_n as in [26, 27], to bring the classical fields $\phi_{i,\mathrm{cl}}$ $i = 1,\dots,n$ into a canonical form constructed to separate the contribution from the winding modes from the contribution from modes subject to boundary conditions given by the functions $\mathrm{cut}_{1,2}(x)$. Concretely, we define the matrices

$$U_n = \begin{bmatrix} \frac{1}{\sqrt{2}} & -\frac{1}{\sqrt{2}} & 0 & & \dots \\ \frac{1}{\sqrt{6}} & -\frac{1}{\sqrt{6}} & -\frac{2}{\sqrt{6}} & 0 & \dots \\ \vdots & & & & \\ \frac{1}{\sqrt{n(n-1)}} & \frac{1}{\sqrt{n(n-1)}} & \dots & \dots & -\sqrt{1-\frac{1}{n}} \\ \frac{1}{\sqrt{n}} & \frac{1}{\sqrt{n}} & \dots & \dots & \frac{1}{\sqrt{n}} \end{bmatrix}, \tag{3.27}$$

and

$$M_{n-1} = \mathrm{diag}\left(1,\dots,1,\frac{1}{n}\right) U_{n-1}\,, \tag{3.28}$$

so that we have

$$\bar{\phi}_i^{\mathrm{cl}}|_{\Gamma_1}(x) = 0 \qquad\qquad i = 1,\dots,n-1\,,$$

$$\bar{\phi}_n^{\mathrm{cl}}|_{\Gamma_1}(x) = \sqrt{n}\,\mathrm{cut}_1(x)\,, \tag{3.29}$$

$$\bar{\phi}_i^{\mathrm{cl}}|_{\Gamma_2}(x) = 2\pi R_c\,\left(M_{n-1}\right)_{ij}\omega_j\,, \qquad i = 1,\dots,n-1\,,$$

$$\bar{\phi}_n^{\mathrm{cl}}|_{\Gamma_2}(x) = \sqrt{n}\,\mathrm{cut}_2(x) + \frac{2\pi\,R_c}{\sqrt{n}}\sum_{i=1}^{n-1}\omega_i\,. \tag{3.30}$$

Hence, the sum over all the classical configurations reduces to a sum over the vector $\mathbf{w} = (\omega_1,\dots,\omega_{n-1}) \in \mathbb{Z}^{n-1}$ and an integral over the n-th classical mode. Notice that, as for the spherical case, the n-th classical mode $\bar{\phi}_n^{\mathrm{cl}}$ has a compactification radius amplified by $\sqrt{n}$, due to the rotation (3.27). We want to use this mode to reconstruct a full partition function on the torus, that is define

$$\Phi_n = \varphi_n + \bar{\phi}_n^{\mathrm{cl}}\,, \tag{3.31}$$

so that

$$\int_{\mathrm{D}}[d\varphi_n^A]e^{-S[\varphi_n^A]}\int_{\mathrm{D}}[d\varphi_n^B]e^{-S[\varphi_n^B]}\int[d\bar{\phi}_n^{\mathrm{cl}}]e^{-S[\bar{\phi}_n^{\mathrm{cl}}]} = \sqrt{n}\,Z_{A\cup B}\,, \tag{3.32}$$

where the $\sqrt{n}$ factor on the right-hand-side of (3.32) accounts for the different compactification radius. Thus, the replica method finally gives

$$\mathrm{Tr}_A\left(\rho_A^n\right) = \sqrt{n}\left(\frac{Z_{D,A}Z_{D,B}}{Z_{\mathrm{free,A\cup B}}}\right)^{n-1}\overline{W}(n)\,, \tag{3.33}$$

where $\overline{W}(n)$ contains the contributions from the first $n-1$ classical configurations satisfying the boundary conditions in (3.29) at $\Gamma_{1(2)}$.

In two dimensions the classical fields are uniquely determined by the equations of motion and the boundary conditions (3.29), and thus the classical action has only one vacuum. The contribution from the winding sector is then simply given by the sum over the corresponding winding modes [26, 27],

$$\overline{W}(n) = \sum_{\mathbf{w}\in\mathbb{Z}^{n-1}} e^{-\sum_{i=1}^{n-1} S[\bar{\phi}_i^{\mathrm{cl}}]}\,. \tag{3.34}$$

However, in higher dimensions ($d > 2$) the conditions (3.29) do not uniquely specify the vacua of the classical action. In other words, our construction is consistent for more than one set of boundary conditions applied on derivatives of the classical fields and the value of the boundary action depends on the boundary conditions. This is the redundancy mentioned in section 2.

The classical field satisfies a higher-derivative equation of motion, whose general solution is parametrised by $z/2$ constants. The boundary condition imposed on Φ_n will fix one of these constants but we need to add $z/2-1$ further boundary conditions for the classical field to fix the rest. The value of the boundary terms in the action will in general depend on the choice of boundary conditions.

In the present work we impose a generalised form of Neumann boundary conditions on derivatives of the classical fields,

$$\partial_n \Delta^k \bar{\phi}_i^{\mathrm{cl}}\big|_{\partial_r} = 0 \quad k = 0, \ldots, \frac{z}{2} - 2. \tag{3.35}$$

This prescription is compatible with the conditions imposed on the fluctuations,

$$\Delta^k \phi_i\big|_{\partial M} = \Delta^k(\bar{\phi}_i^{\mathrm{cl}} + \varphi_i)\big|_{\partial M} = \Delta^k \bar{\phi}_i^{\mathrm{cl}}\big|_{\partial M}, \quad \text{for } k = 1, \ldots, \frac{z}{2} - 1\,, \tag{3.36}$$

and, at the same time, it gives a non-vanishing classical boundary action, which is important in order for the sum over winding modes to converge. The contribution from winding modes is then accounted for in any number dimentions by computing

$$\overline{W}(n) = \sum_{\mathbf{w}\in\mathbb{Z}^{n-1}} e^{-\sum_{i=1}^{n-1} S[\bar{\phi}_i^{\mathrm{cl}}]}\,, \tag{3.37}$$

where the classical fields $\bar{\phi}_i^{\mathrm{cl}}$ satisfy the boundary conditions (3.29) and the Neumann conditions in (3.35). The details of the computation are reported in appendix D.

Finally, the entanglement entropy for the d-torus is given by

$$S_{\mathrm{EE}} = -\log\left(\frac{Z_{D,A}Z_{D,B}}{Z_{A\cup B}}\right) - \frac{1}{2} - \overline{W}'(1)\,, \tag{3.38}$$

since the winding sector is normalised such that $\overline{W}(1) = 1$. The computation of the partition functions for the d-torus is presented in section 5 below.

We close this section by noting that even though winding numbers come into play across entanglement cuts in our computation, we are restricting our attention to a single topological sector of the original theory on the d-torus. Indeed, since we periodically identify the field, we could consider winding sectors on the d-torus itself,

$$\phi(x_1 + L_1, \ldots, x_d + L_d) = \phi(x_1, \ldots, x_d) + 2\pi L^I m_I, \quad I = 1, \ldots, d\,, \quad m_I \in \mathbb{Z}\,. \tag{3.39}$$

We have set $m_I = 0$ in our calculations in the present paper but a more general study can be carried out, evaluating the contribution from winding sectors $W(n, m_L)$ associated with an entanglement cut for each topological configuration, and then summing over the m_I. The corresponding topological contributions to entanglement entropy in a scalar field theory on a two-dimensional cylinder, are obtained in [26].

4 Entanglement entropy on a hemisphere

In this section we calculate the universal finite terms of entanglement entropy in GQLM resulting from the division of a d-sphere into two d-hemispheres A and B by an entanglement cut at the equator as shown in figure 2. According to the replica calculation in section 3, we have to compute (3.20), where now A and B are the two d-hemispheres, and the bulk action contains the GJMS operator (2.14) with $2k = d$. The partition function on the whole manifold ($Z_{A\cup B}$ in (3.20)) contains a zero mode, which should be treated separately [43, 44],

$$Z_{A\cup B} = 2\pi R_c \sqrt{\frac{g}{\pi}\mathcal{A}_d}\left(\det{}'\left(\frac{g}{\pi}\mathcal{P}_{d,S^d}\right)\right)^{-\frac{1}{2}} \tag{4.1}$$

where $\mathcal{A}_d$ is the area of the d-sphere and the $\sqrt{\frac{g}{\pi}\mathcal{A}_d}$ factor comes from the normalisation of the eigenfunction corresponding to the zero eigenvalue. The functional determinant $\det'$ is the (regularised) product of the non-zero eigenvalues. The operator (2.14) on the unit d-hemisphere with Dirichlet boundary conditions does not have a zero eigenvalue, so the partition functions on the subsystems A and B can be directly computed via regularised functional determinants. Hence we can write (3.20) as

$$S[A] = \frac{1}{2}\log\left(\frac{\det\mathcal{P}_{d,H^d_D}\,\det\mathcal{P}_{d,H^d_D}}{\det{}'\mathcal{P}_{d,S^d}}\right) + \log\left(\sqrt{4\pi g\mathcal{A}_d}R_c\right) - \frac{1}{2}, \tag{4.2}$$

where the D subscript on H^d_D indicates Dirichlet boundary conditions on the fields at the boundary of the d-hemisphere H^d. At the end of the day, the entanglement entropy can only depend on the combination $g\mathcal{A}_d$. All factors of g/π inside functional determinants must therefore cancel out in the final result and going forward we simply leave them out of our formulas.

We now turn to the explicit computation of the functional determinants appearing in (4.2). In a series of papers [42, 56–58], Dowker calculates determinants of GJMS operators on spheres in any even dimension d and for any degree $k \leq d/2$ via ζ-function

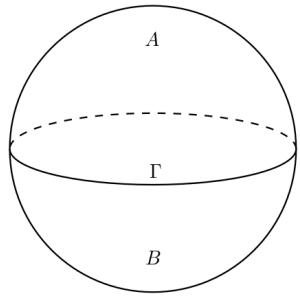

Figure 2. The sphere is cut into hemispheres A and B by an entangling cut at the equator.

methods. We give a self-contained review of these calculations in appendix A, partly to adapt them to our notation and partly to have all the results we want to use in one place. Determinants of critical GJMS operators (where the degree $2k$ of the operator matches d) on spheres and hemispheres are expressed in terms of multiple Γ-functions in [42]. A simplified version of these results, expressing them in terms of the more familiar Riemann ζ-function, is presented in appendix B.

The starting point of Dowker's computation is the observation that the determinant of the GJMS operator on a d-sphere, given in terms of the spectral ζ-function, can be obtained as a sum of the corresponding determinant on a d-hemisphere with Dirichlet and Neumann boundary conditions [42, 59] (again expressed in terms of spectral ζ-functions). On the hemisphere with Dirichlet boundary conditions the log-determinant of the GJMS operator is given by

$$\log\det \mathcal{P}_{d,H^d_D} = -Z'_d(0, a_D, d/2) = -\sum_{n=0}^{d} h^D_n(d)\zeta'(-n) - f^D(d), \tag{4.3}$$

where $Z_d(s, a_D, d/2)$ is the spectral ζ-function corresponding to the GJMS operator of degree $2k = d$, cf. (A.1) and (A.2). Here ζ is the Riemann ζ-function, and h^D_n, f^D are given by

$$h^D_n(d) = -\frac{1}{(d-1)!}\begin{bmatrix} d \\ n+1 \end{bmatrix} + \frac{1}{d!}\begin{bmatrix} d+1 \\ n+1 \end{bmatrix} - \sum_{j=0}^{d-n} \frac{(-1)^j}{(d-j)!}\binom{d+1}{j}\begin{bmatrix} d-j+1 \\ n+1 \end{bmatrix}, \tag{4.4}$$

$$f^D(d) = -\frac{1}{d!}\sum_{l=1}^{d-1} \log(l)(l-d)_{d+1} + M(d). \tag{4.5}$$

The $\begin{bmatrix} d \\ k \end{bmatrix}$ are Stirling numbers of the first kind, $(z)_k$ is a Pochhammer symbol, and $M(d)$ is a sum of harmonic numbers and generalised Bernoulli polynomials whose explicit form is not important to us, as it cancels in the final expression for the entanglement entropy. The derivations of h^D_n and f^D can be found in appendix B.2, while the derivation of $M(d)$ can be found in A.3, its explicit form is given in equation (A.58). These functions may seem

quite complicated at first sight, but they all consist of well understood algebraic functions that can easily be evaluated using a computer. For the determinant of a critical GJMS operator on a hemisphere with Neumann boundary conditions we find a similar result

$$\log\det \mathcal{P}_{d,H^d_N} = -Z'_d(0,a_N,d/2) = -\sum_{n=0}^{d} h_n^N(d)\zeta'(-n) - f^N(d), \tag{4.6}$$

with h_n^N and f^N given by

$$h_n^N(d) = \frac{1}{d!}\begin{bmatrix} d+1 \\ n+1 \end{bmatrix} - \sum_{j=0}^{d-n} \frac{(-1)^j}{(d-j)!}\binom{d}{j}\begin{bmatrix} d-j+1 \\ n+1 \end{bmatrix}, \tag{4.7}$$

$$f^N(d) = \log(d-1)! + f^D(d). \tag{4.8}$$

We note that our result in (4.6) differs from [42] by a sign in the term $\log(d-1)!$. This is because we treat the zero mode separately as is apparent in (4.1) and (4.2).

As mentioned above, the log-determinant on the whole sphere is the sum of the log-determinants on the hemisphere with Dirichlet and Neumann boundary conditions [42],

$$\log\det{}'\mathcal{P}_{d,S^d} = \log\det \mathcal{P}_{d,H^d_N} + \log\det \mathcal{P}_{d,H^d_D}\,. \tag{4.9}$$

With an eye towards the entropy formula (4.2), we express the ratio of determinants as

$$\begin{aligned} 2\log\det \mathcal{P}_{d,H^d_D} - \log\det{}'\mathcal{P}_{d,S^d} &= -\sum_{n=0}^{d}\left(h_n^D(d) - h_n^N(d)\right)\zeta'(-n) - f^D(d) + f^N(d) \\ &= \sum_{n=0}^{d} h_n(d)\zeta'(-n) + \log(d-1)!\,, \end{aligned} \tag{4.10}$$

where, using the properties of the binomial coefficients, one can write h_n in the the following form

$$h_n(d) = \frac{1}{(d-1)!}\begin{bmatrix} d \\ n+1 \end{bmatrix} + \sum_{j=0}^{d-n}\frac{(-1)^j}{(d-j)!}\begin{pmatrix} d \\ j-1 \end{pmatrix}\begin{bmatrix} d-j+1 \\ n+1 \end{bmatrix}. \tag{4.11}$$

Putting everything together, we obtain a surprisingly simple expression for the entanglement entropy of a hemisphere,

$$S[H^d] = \frac{1}{2}\sum_{n=0}^{d} h_n(d)\zeta'(-n) + \log\left(\sqrt{4\pi g\mathcal{A}_d(d-1)!}R_c\right) - \frac{1}{2}, \tag{4.12}$$

with $h_n(d)$ given above in (4.11). For dimensions $d = 2, 4, 6$, and 8, in the critical case $z = d$, the entropy is given explicitly by

$$d = z = 2: \quad S_{\rm EE} = \log\left(\sqrt{8\pi g}R_c\right) - \frac{1}{2} \tag{4.13}$$

$$d = z = 4: \quad S_{\rm EE} = \log\left(4\sqrt{2g}\pi R_c\right) - \frac{1}{2} - \frac{\zeta(3)}{4\pi^2} \tag{4.14}$$

$$d = z = 6: \quad S_{\rm EE} = \log\left(16\sqrt{\pi^3 g}R_c\right) - \frac{1}{2} - \frac{15\,\zeta(3)}{32\pi^2} + \frac{3\,\zeta(5)}{32\pi^4} \tag{4.15}$$

$$d = z = 8: \quad S_{\rm EE} = \log\left(32\sqrt{3g}\pi^2 R_c\right) - \frac{1}{2} - \frac{469\,\zeta(3)}{720\pi^2} + \frac{7\,\zeta(5)}{24\pi^4} - \frac{\zeta(7)}{32\pi^6}, \tag{4.16}$$

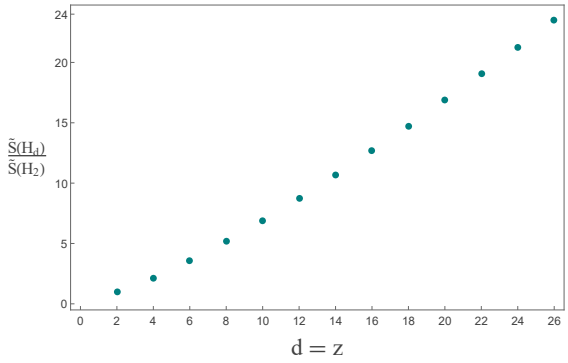

Figure 3. The universal finite term (4.12) in the entanglement entropy of GQLM on a hemisphere plotted against the number of spatial dimension d (which is equal to the critical exponent z). We normalise $S[H_d]$ with respect to the two-dimensional case, and set $g = R_c = 1$.

and more values are plotted in figure 3. The two-dimensional case agrees with the result presented in [27]. Notice that the logarithmic term depends on the product $R_c\sqrt{g}$, which is independent of rescaling of the fields. Hence, in the case of a d-sphere cut into two d-hemispheres, the finite universal terms of the entanglement entropy (4.12) are constant, they only depend on the physical compactification radius $R_c\sqrt{g}$ of the target space, which appears in the above expression through the zero modes.

Explicit results can also be obtained for the subcritical case, i.e. when $z < d$. In this case, the entanglement entropy on a hemisphere is simply given by the difference of log-determinants on the hemisphere with Dirichlet and Neumann boundary conditions. In [60] this difference was shown to be equal to a "boundary free energy", initially defined for hemispheres in 4-dimensional CFTs in [61]. Its value for $d = 4$ and $z = 2$ was calculated in [60–62], while the value for $d = 6$ and $z = 2$ appeared in [60].[6]

Here we list a few examples of the entanglement entropy on a hemisphere in the subcritical case with z and d both even integers,

$$\begin{aligned} d = 4, z = 2: &\qquad S_{EE} = -\frac{\zeta(3)}{8\pi^2}\,, \\ d = 6, z = 2: &\qquad S_{EE} = \frac{\zeta(3)}{96\pi^2} + \frac{\zeta(5)}{32\pi^4}\,, \\ d = 6, z = 4: &\qquad S_{EE} = -\frac{5\zeta(3)}{48\pi^2} + \frac{\zeta(5)}{16\pi^4}, \\ d = 8, z = 2: &\qquad S_{EE} = -\frac{\zeta(3)}{720\pi^2} - \frac{\zeta(5)}{192\pi^4} - \frac{\zeta(7)}{128\pi^6}\,. \end{aligned} \tag{4.17}$$

The relevant functional determinants (for z and d even integers) were computed originally in [42] and are included in appendix A.

[6] We thank Stuart Dowker for bringing these results and references to our attention.

The result in (4.12) only depends on "topological data" represented by the scale invariant compactification radius of the target space and not on other geometric features. One might object that this is because we initially set the radius of the d-sphere to one, and thus our computations are insensitive to the geometry. Indeed, as mentioned in the Introduction, for smooth entangling cuts in even-dimensional CFTs, the entanglement entropy is expected to have a universal term proportional to the logarithm of a characteristic scale of the system with a constant of proportionality which depends on the central charge and on the Euler characteristic. It can be checked that introducing a radius R of the d-sphere in our problem modifies the above results by adding a term proportional to

$$\Delta\chi \log R\,, \tag{4.18}$$

where $\Delta\chi$ is the change in the Euler characteristic due to dividing the d-sphere along the entanglement cut. For the two-dimensional case this was understood in [1]. Just as for a two-dimensional sphere, the change in the Euler characteristic vanishes for the chosen entanglement cut (while having a non-smooth entangling surface can introduce further universal logarithmic terms). Indeed, on a non-unit sphere all eigenvalues entering our determinants are rescaled, and upon regularising this contributes,

$$\begin{aligned}\log\det\mathcal{P}_{2k,H^d} &= -d\,Z_d(0,a_D,k)\log R - Z'_d(0,a_D,k)\,, \\ \log\det\mathcal{P}_{2k,S^d} &= -d\,(Z_d(0,a_D,k)+Z_d(0,a_N,k))\log R - Z'_d(0,a_D,k) - Z'_d(0,a_N,k)\,,\end{aligned} \tag{4.19}$$

instead of equations (A.2), (A.3). Including the contribution coming from the normalisation of the zero-mode this would leave us with

$$\frac{d}{2}\,(1+Z_d(0,a_N,k)-Z_d(0,a_D,k))\log R\,, \tag{4.20}$$

but it is straightforward to check, using (A.45) and (A.54), that this combination vanishes. In fact, Dowker's construction of the determinant for the sphere as sum of determinants on hemispheres with Dirichlet and Neumann boundary conditions makes this quite transparent, since the spectral ζ-function in the Neumann case is nothing but the Dirichlet one after subtracting the zero mode.[7] Finally, we should stress that the sub-leading universal terms as (4.18) (which vanish here due to the chosen entanglement surface) are those expected in a d-dimensional CFT. The quantum field theory we are considering lives on a $(d+1)$-dimensional manifold, and yet due to the enhanced d-dimensional symmetries in the critical $d=z$ case, it has entanglement properties typical of d-dimensional CFTs.

5 Entanglement entropy on cut d-torus

We now turn our attention to the sub-leading universal terms in the entanglement entropy on a flat d-dimensional torus with circumferences $L_1,\ldots,L_d$,

$$T^d_{L_1,\ldots,L_d} := \mathbb{R}^d/(L_1\mathbb{Z}\times\ldots\times L_d\mathbb{Z}), \tag{5.1}$$

that is cut into two d-cylinders: $Y_B := [-L_B,0]\times T^{d-1}_{L_2,\ldots,L_d}$ and $Y_A := [0,L_A]\times T^{d-1}_{L_2,\ldots,L_d}$, where our conventions are $L_B>0$ and $L_1 = L_A+L_B$. The two-dimensional case is shown

[7] See [42, 63, 64] for related studies of conformal anomalies for GJMS operators on spherical manifolds.

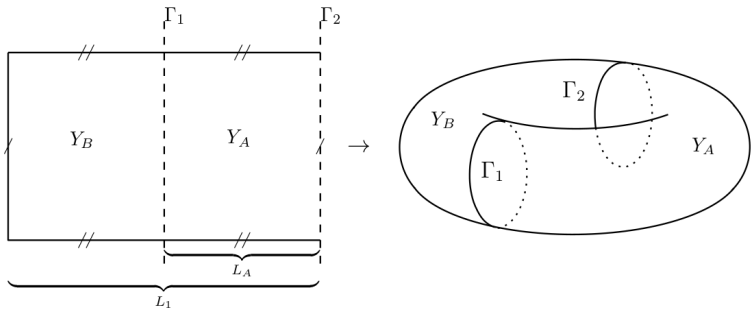

Figure 4. The torus is cut into cylinders Y_A and Y_B by the two entangling cuts Γ_1 and Γ_2.

in figure 4. The replica method for the entanglement entropy on the torus was discussed in section 3, and it requires us to compute (3.38), where the winding sector contribution is given by (3.37), with the classical fields satisfying the equations of motion and boundary conditions expressed in (3.29) and (3.35). For the d-torus, the bulk and boundary terms in the action are given by (2.5) and (2.10), respectively. The operator $\mathcal{P}_{d,T^d}$ in (2.4) is simply an integer power of the Laplacian. We first compute the quantum contribution to the entanglement entropy arising from the partition functions in (3.38), and after that we tackle the winding sector contribution. All the detailed calculations of functional determinants are relegated to appendix C, and those regarding the winding sector to appendix D. In this section we collect the results and discuss some interesting limits.

The operator $\mathcal{P}_{d,T^d}$ has a zero mode and as result the torus partition function is given by

$$Z_{A\cup B} = 2\pi R_c \sqrt{\frac{g}{\pi} A_d}\, \left(\det{}'\Big(\frac{g}{\pi}\mathcal{P}_{d,T^d}\Big)\right)^{-\frac{1}{2}}, \tag{5.2}$$

where A_d is the area of the d-torus. As was the case for the sphere, the $\frac{g}{\pi}$ factor in the determinant only amounts to a rescaling of the torus to which the entanglement entropy is not sensitive, and we can ignore it in our calculations. On the d-cylinder with Dirichlet boundary conditions, on the other hand, there is no zero mode and we can write the (sub-leading terms of) entanglement entropy as

$$S[A] = \frac{1}{2}\log\left(\frac{\det \mathcal{P}_{d,Y_{A,D}} \det \mathcal{P}_{d,Y_{B,D}}}{\det{}'\mathcal{P}_{d,T^d}}\right) + \log\left(\sqrt{4\pi g\, A_d} R_c\right) - \frac{1}{2} - \overline{W}'(1)\,. \tag{5.3}$$

The required functional determinants are evaluated in appendix C.

By means of equations (C.30a) and (C.6), we find that the determinant on the full torus is given by

$$\begin{aligned}\log\det{}'\Delta^{d/2}_{T^d_{L_1,\dots,L_d}} &= -\frac{d}{2}\zeta'_{T^d_{L_1,\dots,L_d}}(0)\\ &= d\log(L_1) + \frac{d}{2}L_1\,\zeta_{T^{d-1}_{L_2,\dots,L_d}}(-1/2) - \frac{d}{2}G'(0;L_1,\dots,L_d)\,,\end{aligned} \tag{5.4}$$

where $\zeta_{T^{d-1}_{L_2,\dots,L_d}}(s)$ is the spectral ζ-function on the $(d-1)$-torus. The auxiliary function G is defined in appendix C.1, as

$$G(s;L_1,L_2,\dots,L_d) := \frac{2^{3/2-s}L_1^{s+1/2}}{\Gamma(s)\sqrt{\pi}} \sum_{\vec{n}_{d-1}\in\mathbb{Z}^{d-1}}{}' \sum_{n_1=1}^{\infty} \left(\frac{n_1}{\sqrt{\vec{n}_{d-1}^T\,\Xi_{d-1}\,\vec{n}_{d-1}}}\right)^{s-1/2} \times K_{s-1/2}\left(L_1 n_1 \sqrt{\vec{n}_{d-1}^T\,\Xi_{d-1}\,\vec{n}_{d-1}}\right), \tag{5.5}$$

where the primed sum indicates the omission of the zero mode, $K_\nu(z)$ is a modified Bessel function of the second kind and $\Xi_{d-1} = \operatorname{diag}\left((2\pi/L_2)^2,\dots,(2\pi/L_d)^2\right)$ is a diagonal matrix. We have explicit expressions both for the spectral ζ-function on the torus in (C.13) and its derivative evaluated at $s=0$ in (C.18), but at this stage we find it more convenient to use the above expression, and only insert explicit formulae at the end, after some cancellations.

For d-cylinders with Dirichlet boundary conditions, using (C.30b) and (C.24), we obtain

$$\begin{aligned}\log\det\Delta^{d/2}_{[0,L]\times T^{d-1}_{L_2,\dots,L_d}} &= \frac{d}{2}\log(2L) + \frac{d}{4}\zeta'_{T^{d-1}_{L_2,\dots,L_d}}(0) \\ &\quad + \frac{d}{2}L\zeta_{T^{d-1}_{L_2,\dots,L_d}}(-1/2) - \frac{d}{4}G'(0;2L,\dots,L_d),\end{aligned} \tag{5.6}$$

where $L = L_A$ for Y_A and $L = L_1 - L_A$ for Y_B. We can rewrite the difference between the log-determinants as

$$\begin{aligned}&\log\det\Delta^{d/2}_{[0,L_1-L_A]\times T^{d-1}_{L_2,\dots,L_d}} + \log\det\Delta^{d/2}_{[0,L_A]\times T^{d-1}_{L_2,\dots,L_d}} - \log\det{}'\Delta^{d/2}_{T^d_{L_1,\dots,L_d}} \\ &\quad= \frac{d}{2}\log(4u(1-u)) + \frac{d}{2}\zeta'_{T^{d-1}_{L_2,\dots,L_d}}(0) - \frac{d}{4}G'(0;2L_A,\dots,L_d) \\ &\qquad - \frac{d}{4}G'(0;2(L_1-L_A),\dots,L_d) + \frac{d}{2}G'(0;L_1,\dots,L_d),\end{aligned} \tag{5.7}$$

where the parameter $u = L_A/L_1$ characterises the relative size of the two d-cylinders.

The explicit expression for $\zeta'_{T^{d-1}_{L_2,\dots,L_d}}(0)$ is given by (C.18) with the replacement $d\to d-1$ and a relabelling of the sides L_i. As discussed in appendix C, despite its appearance the above expression is rather convenient to handle, thanks to the fast convergence of the modified Bessel functions contained in the auxiliary function G. The derivative of the function G with respect to s, evaluated at $s=0$, is given by

$$\begin{aligned}G'(0,L,L_2,\dots,L_d) &= \sqrt{\frac{8L}{\pi}} \sum_{\vec{n}_{d-1}\in\mathbb{Z}^{d-1}}{}' \sum_{n_1=1}^{\infty} \frac{(\vec{n}_{d-1}^T\,\Xi_{d-1}\,\vec{n}_{d-1})^{1/4}}{\sqrt{n_1}} \\ &\quad\times K_{-1/2}\big(L\,n_1\sqrt{\vec{n}_{d-1}^T\,\Xi_{d-1}\,\vec{n}_{d-1}}\big) \\ &= 2\sum_{\vec{n}_{d-1}\in\mathbb{Z}^{d-1}}{}' \sum_{n_1=1}^{\infty} \frac{\exp\left(-L\,n_1\sqrt{\vec{n}_{d-1}^T\,\Xi_{d-1}\,\vec{n}_{d-1}}\right)}{n_1},\end{aligned} \tag{5.8}$$

where we have used the explicit expression (E.4) for the modified Bessel function $K_{-\frac{1}{2}}$.

As an explicit example of the above result, the determinant ratio for $z = d = 2$ is explicitly given by

$$\begin{aligned}
&\log\det\Delta_{[0,L_1-L_A]\times S^1_{L_2}} + \log\det\Delta_{[0,L_A]\times S^2_{L_2}} - \log\det\Delta_{T^2_{L_1,L_2}} \\
&\quad = \log\left(2u|\tau_1|\eta^2(2u\tau_1)\right) + \log\left(2(1-u)|\tau_1|\eta^2(2(1-u)\tau_1)\right) - \log\left(L_1^2\eta^4(\tau_1)\right) \\
&\quad = -2\log L_1 + \log\left(4u(1-u)|\tau_1|^2\right) + 2\log\left(\frac{\eta(2(1-u)\tau_1)\,\eta(2u\tau_1)}{\eta^2(\tau_1)}\right), \qquad (5.9)
\end{aligned}$$

where we used (C.20) and (C.28) and introduced the notation $\tau_k = i\frac{L_1}{L_{k+1}}$, for $k = 1,\dots,d-1$, for the aspect ratios of the general d-torus.

For the winding sector, the computations are detailed in appendix D. The end result, given in (D.13), is

$$-\overline{W}'(1) = \log\sqrt{\Lambda_z} - \frac{1}{2} - \int_{-\infty}^{\infty}\frac{dk}{\sqrt{\pi}}e^{-k^2}\log\left(\sum_{\omega\in\mathbb{Z}}\exp\left(-\frac{\pi}{\Lambda_z}\omega^2 - 2i\sqrt{\frac{\pi}{\Lambda_z}}k\,\omega\right)\right), \qquad (5.10)$$

with Λ_z given by

$$\Lambda_z = g\,\pi\,R_c^2\frac{(-1)^{z/2}z!}{(1-2^z)B_z}\left(u^{1-z}+(1-u)^{1-z}\right)\frac{1}{|\tau_1|\dots|\tau_{d-1}|}. \qquad (5.11)$$

where B_z are the Bernoulli numbers. For instance, in $d = 2$ we have

$$\Lambda_2 = 4\pi\,g\,R_c^2\,\frac{1}{u(1-u)}\frac{1}{|\tau_1|}. \qquad (5.12)$$

Finally, putting together the contributions from the functional determinants and the winding sector, (5.7) and (5.10) respectively, we get the following (rather long) expression for the entanglement entropy (5.3),

$$\begin{aligned}
S[A] = {}& \frac{d}{4}\log(4u(1-u)) + \frac{d}{4}\zeta'_{T^{d-1}_{L_2,\dots,L_d}}(0) - \frac{d}{8}G'(0;2L_A,\dots,L_d) - \frac{d}{8}G'(0;2L_B,\dots,L_d) \\
&+ \frac{d}{4}G'(0;L_1,\dots,L_d) + \log\left(4\pi g\,R_c^2\right) + \log\sqrt{A_d} - 1 - \frac{1}{2}\log|\tau_1\dots\tau_{d-1}| \\
&+ \frac{1}{2}\log\left(\frac{(-1)^{d/2}d!}{4(1-2^d)B_d}\left(u^{1-d}+(1-u)^{1-d}\right)\right) \\
&- \int_{-\infty}^{\infty}\frac{dk}{\sqrt{\pi}}e^{-k^2}\log\left(\sum_{\omega\in\mathbb{Z}}\exp\left(-\frac{\pi}{\Lambda_d}\omega^2 - 2i\sqrt{\frac{\pi}{\Lambda_d}}k\,\omega\right)\right). \qquad (5.13)
\end{aligned}$$

It can be verified that the entanglement entropy is symmetric under the transformation $u \to 1-u$ [33] as required for a pure state of the full system.

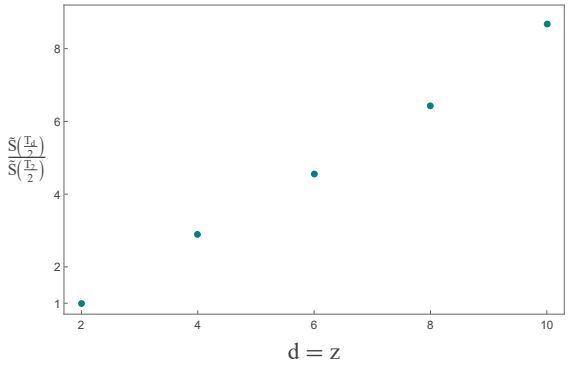

Figure 5. We plot the final expression for the universal finite term in the entanglement entropy on a half torus (5.17) against the number of spatial dimension d (which is equal to the critical exponent z). We normalise $S[T_d/2]$ with respect to the two-dimensional case, and set $g = R_c = L_1 = \cdots = L_d = 2L_A = 1$ in the plot.

For the special case of $d = z = 2$ we obtain (using (5.9) and (D.16))

$$\begin{aligned} S[A_2] = &-\frac{1}{2}\log|\tau_1| + \frac{1}{2}\log\left(4u(1-u)|\tau_1|^2\right) + \log\left(\frac{\eta(2(1-u)\tau_1)\,\eta(2u\tau_1)}{\eta^2(\tau_1)}\right) \\ &-1 + \log\left(4\pi\, g\, R_c^2\right) - \frac{1}{2}\log(u(1-u)) - \frac{1}{2}\log|\tau_1| \\ &-\int_{-\infty}^{\infty}\frac{dk}{\sqrt{\pi}}e^{-k^2}\log\left(\sum_{\omega\in\mathbb{Z}}\exp\left(-\frac{\pi}{\Lambda_2}\omega^2 - 2i\sqrt{\frac{\pi}{\Lambda_2}}k\,\omega\right)\right) \\ =&\log\left(\frac{\eta(2(1-u)\tau_1)\,\eta(2u\tau_1)}{\eta^2(\tau_1)}\right) - 1 + \log\left(8\pi\, g\, R_c^2\right) \\ &-\int_{-\infty}^{\infty}\frac{dk}{\sqrt{\pi}}e^{-k^2}\log\left(\sum_{\omega\in\mathbb{Z}}\exp\left(-\frac{\pi}{\Lambda_2}\omega^2 - 2i\sqrt{\frac{\pi}{\Lambda_2}}k\,\omega\right)\right), \end{aligned} \tag{5.14}$$

where $\Lambda_2 = 4\pi\, g\, R_c^2\, \frac{1}{u(1-u)}\frac{1}{|\tau_1|}$. The final result looks relatively simple due to some cancellations between the classical and quantum contributions. To our knowledge, this is the first time that universal finite terms in the entanglement entropy on a torus have been obtained in closed form using path integral methods, even for the two-dimensional case. They have been computed numerically in [30] and by means of a boundary field method in [25].

We will now check some interesting limits of our general expressions.

Halved *d*-torus. The first simplifying special case that that we consider is when the torus is divided into two equal parts:

$$L_A = L_B\,, \qquad L_1 = 2L_A\,, \qquad u = \frac{1}{2}\,. \tag{5.15}$$

The contribution from the functional determinants (5.7) simplifies tremendously, leaving only a single term,

$$\log\det\Delta^{d/2}_{[0,L_A]\times T^{d-1}_{L_2,\dots,L_d}}+\log\det\Delta^{d/2}_{[0,L_A]\times T^{d-1}_{L_2,\dots,L_d}}-\log\det{}'\Delta^{d/2}_{T^d_{2L_A,\dots,L_d}}=\frac{d}{2}\zeta'_{T^{d-1}_{L_2,\dots,L_d}}(0)\,, \tag{5.16}$$

and we obtain for the universal terms in the entanglement entropy

$$\begin{aligned}S[A]=&\frac{d}{4}\zeta'_{T^{d-1}_{L_2,\dots,L_d}}(0)+\log\left(4\pi g\,R_c^2\right)+\frac{d}{2}\log L_1-1-\log|\tau_1\dots\tau_{d-1}|\\&+\frac{1}{2}\log\left(\frac{(-1)^{d/2}\,d!}{4(1-2^{-d})B_d}\right)-\int_{-\infty}^{\infty}\frac{dk}{\sqrt{\pi}}e^{-k^2}\log\left(\sum_{\omega\in\mathbb{Z}}\exp\left(-\frac{\pi}{\Lambda_d}\omega^2-2i\sqrt{\frac{\pi}{\Lambda_d}}k\,\omega\right)\right),\end{aligned} \tag{5.17}$$

where now

$$\Lambda_d(u=1/2)=g\,\pi\,R_c^2\frac{(-1)^{d/2}2^d d!}{(1-2^d)\,B_d}\,\frac{1}{|\tau_1|\dots|\tau_{d-1}|}\,. \tag{5.18}$$

In $d=2$ this reduces to

$$S[A_2]=-1+\log\left(8\pi\,g\,R_c^2\right)-\int_{-\infty}^{\infty}\frac{dk}{\sqrt{\pi}}e^{-k^2}\log\left(\sum_{\omega\in\mathbb{Z}}\exp\left(-\frac{\pi}{\Lambda_2}\omega^2-2i\sqrt{\frac{\pi}{\Lambda_2}}k\,\omega\right)\right), \tag{5.19}$$

since the contributions from the Dedekind-eta functions in (5.14) cancel against each other when $u=1/2$. Moreover, Λ_2 is given here by

$$\Lambda_2(u=1/2)=16\,g\,\pi\,R_c^2\,\frac{1}{|\tau_1|}\,. \tag{5.20}$$

Thin *d*-torus. In $d=2$, the infinitely thin torus limit (sometimes called also the long torus limit) amounts to $|\tau_1|\gg 1$ and u fixed. It can be helpful to think of this limit as $L_2\to 0$ while all the other lengths (L_1,L_A) are kept fixed. In this case, the contribution from the integral in the expression (5.14) is exponentially suppressed, and moreover, we have the asymptotic behaviour (E.7) for the Dedekind η function. It is then clear that all the contributions from the Dedekind η-functions vanish in this limit, and we are left with the simple result

$$S[A_2]=\log\left(8\pi\,g\,R_c^2\right)-1\,, \tag{5.21}$$

which agrees with [25]. In this limit the entanglement entropy for the thin torus is *twice* the entanglement entropy for the thin cylinder [25], since the entropy still carries information about the two boundaries of the torus.

We can take a look at the same limit for the d-torus. In the d-dimensional case we assume that L_1, L_A are fixed and of order one, while all the other sides are approaching zero, that is $L_2,\dots,L_d\to 0$. There is an ambiguity in how to take this limit, so as a first step we consider the case

$$L_1, L_A\gg L_2\gg\dots\gg L_d\,, \tag{5.22}$$

which can also be written as

$$1 \ll |\tau_1| \ll \cdots \ll |\tau_{d-1}| \,. \tag{5.23}$$

Let us examine how the different terms in (5.13) behave when the inequalities in (5.22) hold. First, all the functions $G'(0, L, L_2, \ldots, L_d)$ (5.8) with $L = 2L_A, 2(L_1 - L_A), L_1$ are exponentially suppressed, since all the elements of the matrix Ξ_{d-1} diverge, while L is kept fixed. Now consider the term $\zeta'_{T^{d-1}_{L_2,\ldots,L_d}}(0)$ in (5.13). This term is defined in (C.18) with a shift $d \to d-1$ and subsequent relabelling of the torus sides. With the choice (5.22) all the Bessel functions contained in (C.17), and thus in $\zeta'_{T^{d-1}_{L_2,\ldots,L_d}}(0)$, are exponentially suppressed. It then follows that the leading piece of $\zeta'_{T^{d-1}_{L_2,\ldots,L_d}}(0)$ in (C.18) is given by the highest term in the sums, that is

$$\begin{aligned}\zeta'_{T^{d-1}_{L_2,\ldots,L_d}}(0) &\approx 4\frac{(-\pi)^p}{p!}\frac{L_2\ldots L_{2p+1}}{L_{2p+2}^{2p}}\zeta'(-2p) + 2\frac{L_2\ldots L_{2p}}{L_{2p+1}^{2p-1}}\frac{(-2\pi)^p}{(2p-1)!!}\zeta(-2p+1)\\ &\approx 4\frac{(-\pi)^p}{p!}\frac{L_2\ldots L_{2p+1}}{L_{2p+2}^{2p}}\zeta'(-2p)\,,\end{aligned} \tag{5.24}$$

where $p = \lceil \frac{d-1}{2} \rceil - 1 = \lfloor \frac{d-1}{2} \rfloor$ for even d. We can rewrite the term more elegantly as a function of the aspect ratios,[8]

$$\zeta'_{T^{d-1}_{L_2,\ldots,L_d}}(0) \approx \frac{2\,\Gamma\left(p+\frac{1}{2}\right)}{\pi^{p+\frac{1}{2}}}\zeta\left(p+\frac{1}{2}\right)\frac{|\tau_{2p+1}|^{2p}}{|\tau_1|\ldots|\tau_{2p}|}\,.$$

Finally, the integral over k in (5.13) is also exponentially suppressed and will not contribute to the final expression. Then, keeping only the most divergent term according to (5.22), we obtain

$$S[A_d] \approx \frac{d\,\Gamma\left(p+\frac{1}{2}\right)}{2\,\pi^{p+\frac{1}{2}}}\zeta\left(p+\frac{1}{2}\right)\frac{|\tau_{2p+1}|^{2p}}{|\tau_1|\ldots|\tau_{2p}|}\,, \qquad p = \left\lfloor \frac{d-1}{2} \right\rfloor . \tag{5.25}$$

Similar limits were discussed in [33] for the Renyi entropies of 3+1-dimensional relativistic fields theories with various twisted boundary conditions. Except for having the same power-law divergence, our results appear not to agree with their findings. The comparison is tricky though, as there are effectively three length scales in the $d = 4$, and since we are looking at the regularised entanglement entropy we do not have an explicit cut-off as in [33].

We should stress that when $d = 2$ all the sums in $\zeta'_{T^{d-1}_{L_2,\ldots,L_d}}(0)$ in (C.18) are empty and the only contribution from this term is the logarithm $-2\log L_2$. Then the only divergent contributions are coming from the log terms (see e.g. (5.14)) and they cancel, leaving the finite term shown in (5.21).

The thin sliced *d*-torus. In $d = 2$ this limit corresponds to $L_A \to 0$ while all the other length scales involved remain fixed, that is $u \to 0$ while $|\tau_1|$ is kept fixed. The

[8] Where we have used the ζ-function identity $\zeta'(-2n) = (-1)^n \frac{(2n)!}{2(2\pi)^{2n}}\zeta(2n+1)\,, \quad n \in \mathbb{N}$.

integral in (5.14) can then be evaluated, for instance by means of the Poisson summation formula (E.2), and at leading order it gives $\frac{1}{2}\log u$. Considering only the leading term in the expansion of the Dedekind function (E.6), we obtain, for $u \to 0$,

$$S[A_2] = -\tfrac{\pi}{24|\tau_1|u} + \dots \,, \tag{5.26}$$

which agrees with the entanglement entropy for the infinite long and thin sliced cylinder computed in [27]. Indeed, in this limit the torus and the cylinder are indistinguishable at leading order.

We can proceed with similar arguments in higher dimensions, assuming $u \to 0$ while all the aspect ratios $|\tau_i|$, with $i = 1, \dots, d-1$ are kept fixed. In order to simplify the computation we assume all the aspect ratios to be equal, $|\tau_i| = \sigma$ for all $i = 1, \dots, d-1$. Then, the leading divergent terms are contained in $G'(0, 2L_A, L_2, \dots, L_d)$ in (5.13), and by estimating the $d-1$-dimensional sum in $G'(0, 2L_A, L_2, \dots, L_d)$ (cf. (5.8)) with an integral we obtain the following leading behaviour for the entanglement entropy,

$$S[A_d] \approx \frac{\kappa_d}{u^{d-1}\sigma^{d-1}} \,, \tag{5.27}$$

where κ_d is a numerical coefficient that depends on the number of dimensions d. Similar behaviour was obtained for the three-dimensional torus in conformal field theories in [65] (see also [66]), and also in [67] from a holographic approach.

The wide *d*-torus. As our final example, we consider the so-called wide torus limit, that is when the directions transverse to the cut are very large while L_A, L_1 are kept fixed. Let us start by considering this limit for $d = 2$. This means that $|\tau_1| \to 0$ while u is kept fixed. Using the expansion of the Dedekind-eta function (E.6), we see that the term containing the logarithm of the ratio of Dedekind-eta functions in (5.14) produces the leading divergence. Hence, from the general expression for the entanglement entropy in $d = 2$ (5.14), we obtain

$$S[A_2] \approx -\frac{\pi}{24u(1-u)|\tau_1|} + \frac{\pi}{6|\tau_1|} \,. \tag{5.28}$$

This asymptotic behaviour is also expected for the universal function of the Renyi entropies of the two-dimensional torus, cf. [33] and references therein, and was found in holographic CFTs in [32].

In higher dimensions we can consider the limit when u is kept fixed, and all the transverse directions are very large compared to L_1, L_A, but all the aspect ratios approach zero at the same rate, that is $|\tau_i| = \varepsilon$, with $i = 1, \dots, d-1$ and $\varepsilon \to 0$. In this case, the expressions in (5.13) simplify, and, as in the two-dimensional case, the leading divergent contribution is contained in the functions $G'(0, L, L_2, \dots, L_d)$ (cf. (5.8)), where L can be $L_1, 2L_A$ or $2(L_1 - L_A)$. Using a similar expansion as performed in the thin sliced torus limit, we obtain

$$S[A_d] \approx \frac{f_d(u)}{\varepsilon^{d-1}} \,, \tag{5.29}$$

where $f_d(u)$ is a function symmetric under the exchange $u \to 1-u$.

In the above discussion, the case $u = \frac{1}{2}$ is special for any dimension d, since the function $f_d(u = 1/2) = 0$, so that the sub-leading but still diverging terms become important. Looking directly at (5.17) and (5.19), there is no contribution now coming from $G'(0, L, L_2, \ldots, L_d)$, and the next divergent term is logarithmic in the aspect ratios τ_i, which in the two-dimensional torus is entirely coming from the integral in (5.19), while in higher dimensions it receives contributions also from the area term $\log \sqrt{A_d}$ and $\zeta'_{T^{d-1}}(0)$. In our simplified limit where all the ratios $|\tau_i|$ approach zero at the same rate, we see that

$$S[A_d] \approx \frac{1}{2} \log \varepsilon \,, \qquad u = \frac{1}{2} \,, \quad d \geq 2 \,. \tag{5.30}$$

This is consistent with the findings of [33], where for the $z = 2$ free boson field theory in 3+1 dimensions the universal function of Renyi entropies J_n satisfies the relation $\lim_{|\tau|\to 0} J_n(u = 1/2, |\tau|)|\tau| = 0$.[9] This clearly holds in our case since the universal term of the entanglement entropy has a logarithmic divergence. Rather different behaviour was observed in free two-dimensional CFTs for Renyi entropies [33] and also in holographic CFTs in two and three space dimensions for entanglement entropy [67], where also for $u = 1/2$ the universal part continues to have a power-law divergence similar to (5.28) and (5.29). The disagreement was already observed in [33].

6 Discussion

In this work we have analytically computed the universal finite corrections to the entanglement entropy for GQLMs in arbitrary d+1 dimensions, for even integer d, and on either a d-sphere cut into two d-dimensional hemispheres or a d-torus cut into two d-dimensional cylinders. GQLMs are free field theories where the Lifshitz exponent is equal to the number of spatial dimensions, and they are described in terms of compactified massless scalars. When $d = z = 2$ the GQLM reduces to the quantum Lifshitz model [14], and our findings confirm the known results of [25–27]. The calculations are performed by means of the replica method. Caution is required when performing the cut as the massless scalar field in the GQLM is compactified. It is useful to discern between the role of the fluctuating fields and the classical modes. In essence, the periodical identification mixes with the boundary conditions imposed at the cut on the replicated fields [23, 25–27, 30], and disentangling the winding modes from the rest leads to an additional universal sub-leading contribution to the entanglement entropy. The fluctuating fields satisfy Dirichlet conditions at the cut (as well as further conditions imposed on their even-power derivatives), while the classical fields take care of the periodic identification. The contribution from the fluctuating fields comes from the ratio of functional determinants of the relevant operators, which we compute via spectral ζ-function methods. The classical fields contribute via the zero-mode and via the winding sector summarised in the function $W(n)$.

For the spherical case, the full analytic expression of the universal finite terms turned out to be a constant, depending only on the scale invariant compactification radius, cf. (4.12). This is a consequence of the presence of zero modes, and their normalisation.

[9] Note that the bosons are not compactified in [33].

For the toroidal case, the story is rather rich. The general expression is (5.13), while (5.17) is valid when we cut the torus by half. In both cases, the universal term is comprised of a scaling function, which depends on the relevant aspect ratios of the subsystems, and a constant term, which contains the "physical" compactification radius. The last one comes from the zero mode of the partition function of the d-torus as well as from the winding sector. We considered various limits, such as the thin torus limit, which results in the simple expressions (5.21) and (5.25) in two and d dimensions respectively, the thin sliced d-torus, cf. (5.26) and (5.27), and finally we examined the wide torus limit, cf. (5.28), (5.29), and (5.30) where the last expression is valid for $u = 1/2$. Notice that in the toroidal case, where the winding sector is non trivial, it also contributes to the scaling function. For example, in the thin torus limit its contribution is decisive in order to cancel divergences and leave a finite result, cf. (5.21) and (5.25). Our findings confirm expectations from the study of the (2+1)-dimensional QLM [24–27], that also for critical non-relativistic theories entanglement entropy can encode both local and non-local information of the whole system. Moreover, our results give substance to the field theoretic intuition that entanglement entropy should depend on the dynamical critical exponent, see also [39–41] for analogous results in this direction. The specific dependence is rather non-trivial already in the simplest spherical case.

The next step would be to extend our analysis to even-dimensional spacetime, that is when d is an odd integer. Progress has been recently made in e.g. [68] (and references therein), in computing determinants of GJMS operators on odd-dimensional spheres, see also [69] for a different approach based on heat kernel techniques. It would also be interesting to broaden our study of GQLMs by examining entanglement entropy for non-smooth entangling surfaces. In the QLM for non-smooth boundaries, sharp corners source a universal logarithmic contribution (i.e. $\log L_A$), with a coefficient that depends on the central charge and the geometry of the surgery [22, 29]. For d-dimensional CFTs and in presence of non-smooth entangling surfaces further UV divergences also appear whose coefficients are controlled by the opening angle. In particular, for a conical singularity, the nearly smooth expansion of the universal corner term (seen as a function of the opening angle θ) is simply proportional to the central charge of the given CFT [70–77].[10] Another relevant direction to pursue is the study of post-quench time evolution of entanglement in these systems, see e.g. [80] for recent results in QLM and [81] for Lifshitz-type scalar theories.[11] In this respect, GQLMs can provide an interesting and rich playground where one can answer many questions in a full analytic manner.

Acknowledgments

We acknowledge useful discussions with J. Bardarson, P. Di Vecchia, J. S. Dowker, D. Friedan, B. Gouteraux, K. Grosvenor, D. Medina-Rincon, R. Leigh, D. Seminara, W. Sybesma, S. Vandoren, and M. Zaletel. This research was supported in part by the Icelandic Research Fund under contracts 163419-053 and 163422-053, and by grants from the University of Iceland Research Fund.

[10] See also [78, 79] for related holographic results.
[11] See also the work [82] for a study of signatures of chaos in the QLM.

A The determinant of GJMS operators on spheres and hemispheres

In this appendix we review the calculation of the determinants of GJMS operators on spherical domains, originally performed by Dowker in [42], and rewrite his results in a way we find more transparent. Building on his previous work, in particular [56] and [57], Dowker writes the following expression for the spectral ζ-function of a GJMS operator of degree $2k$, which we denote by P_{2k}, on the hemisphere,

$$Z_d(s, a_{D/N}, k) = \sum_{\mathbf{m}\in\mathbb{N}^d} \prod_{j=0}^{k-1} \left((\mathbf{m}\cdot\mathbf{d} + a_{D/N})^2 - \alpha_j^2\right)^{-s}, \tag{A.1}$$

with $\mathbf{d} = (1, \ldots, 1) \in \mathbb{R}^d$, $\alpha_j = j + 1/2$, $a_D = (d+1)/2$ for Dirichlet boundary conditions, and $a_N = (d-1)/2$ for Neumann boundary conditions. The GJMS operators are well defined for $k = 1, \ldots, d/2$ and we distinguish between the subcritical case $k < d/2$ and the critical case $k = d/2$. Using the above form of the spectral ζ-function the log determinant of P_{2k} on the d-hemisphere H^d with either Neumann or Dirichlet boundary conditions can be found as

$$\log\det P_{2k,H^d_{D/N}} = -Z_d'(0, a_{D/N}, k). \tag{A.2}$$

The expression $Z_d'(0, a_{D/N}, k)$ should be interpreted as $\lim_{s\to 0}\partial_s Z_d(s, a_{D/N}, k)$. Given (A.2), one can then add the Neumann and the Dirichlet cases to find the log determinant of P_{2k} on the whole sphere

$$\log\det P_{2k,S^d} = -Z_d'(0, a_D, k) - Z_d'(0, a_N, k). \tag{A.3}$$

Our task therefore is to evaluate $Z_d'(0, a_{D/N}, k)$. In order to do so, we first review the definition and key properties of the Barnes ζ-function. We then turn to the evaluation of the spectral ζ-function of one of the factors in (A.1) and finally put everything together to get the desired log determinants.

A.1 Definition and properties of the Barnes ζ-function

The Barnes ζ function is defined for $s > d$ as

$$\zeta(s, a|\mathbf{d}) := \sum_{\mathbf{m}\in\mathbb{N}^d} (a + \mathbf{m}\cdot\mathbf{d})^{-s} = \sum_{m_1,\ldots,m_d=0}^{\infty} (a + m_1 d_1 + \ldots m_d d_d)^{-s}. \tag{A.4}$$

For the special case of $\mathbf{d} = \mathbf{1} = (1, \ldots, 1)$ we use the simplified notation,

$$\zeta_d(s, a) := \zeta(s, a|\mathbf{1}). \tag{A.5}$$

Analytic continuation of $\zeta_d(s, a)$ is facilitated by the relation (see [83], page 149),

$$\zeta_d(s, a) = \Gamma(1-s) I_d(s, a), \tag{A.6}$$

with $I_d(s, a)$ given by the integral

$$I_d(s, a) = -\frac{1}{2\pi i}\int_{\infty}^{0^+} \frac{(-z)^{s-1} e^{-az}}{(1-e^{-z})^n} dz. \tag{A.7}$$

$I_d(s,a)$ is an entire function in s. The new definition of $\zeta_d(s,a)$ is analytic for all s except for simple poles at $s = 1,\dots,d$ where it has residues

$$\begin{aligned}\operatorname*{Res}_{s=k}\zeta_d(s,a) &= \frac{1}{(d-k)!(k-1)!}\lim_{z\to 0}\frac{d^{d-k}}{dz^{d-k}}\frac{z^d e^{-az}}{(1-e^{-z})^d}\\ &= \frac{(-1)^{d-k}B^{(d)}_{d-k}(a)}{(d-k)!(k-1)!}\\ &= \frac{(-1)^k}{(k-1)!}I_d(k,a), \qquad k=1,\dots,d\end{aligned} \tag{A.8}$$

where $B^{(d)}_l(a)$ are generalised Bernoulli polynomials. For future convenience we define

$$R_d(k,a) := \frac{(-1)^{d-k}B^{(d)}_{d-k}(a)}{(d-k)!(k-1)!}, \tag{A.9}$$

such that for $k = 1,\dots,d$ we can simply write $\operatorname{Res}_{s=k}\zeta_d(s,a) = R_d(k,a)$. In particular this means that we have the following expansion around $s = 0$ for $k = 1,\dots,d$,

$$\zeta_d(k+s,a) = \frac{1}{s}R_d(k,a) + C_d(k,a) + \mathcal{O}(s). \tag{A.10}$$

Calculating $\partial_s s\zeta_d(k+s,a)|_{s=0}$ using the analytic continuation (A.6) one finds that

$$C_d(k,a) = R'_d(k,a) - \psi(k)R_d(k,a), \tag{A.11}$$

where the derivative of R should be read as $R'_d(k,a) = \lim_{s\to 0}\partial_s R_d(k+s,a)$, and ψ is the digamma function. For non-negative k, $\zeta_d(-k,a)$ can be evaluated using its analytic continuation (A.6). On page 151 of [83] the following expression is given

$$\zeta_d(-k,a) = (-1)^d\frac{k!}{(d+k)!}B^{(d)}_{d+k}(a), \tag{A.12}$$

where again $B^{(d)}_l(a)$ are generalised Bernoulli polynomials.

A.2 A first step towards Z_d

In order to calculate $Z'_d(0,a_{D/N},k)$ with Z_d as in (A.1), we need to evaluate the derivative at $s = 0$ of ζ-functions of the form

$$\zeta_D(s) := \sum_{\mathbf{m}\in\mathbb{N}^d}\left((a_D + \mathbf{m}\cdot\mathbf{d})^2 - \alpha^2\right)^{-s}, \tag{A.13}$$

with $\alpha = (d-1)/2$ and $a_D = \sum d_i - (d-1)/2$, with $\mathbf{d} \in \mathbb{N}^d$ for Dirichlet boundary conditions, as such functions roughly correspond to the factors of Z_d. From now on we set $\mathbf{d} \equiv (1,\dots,1)$ as this is the only case relevant to our discussion. In particular, this implies that $a_D = (d+1)/2$. For Neumann boundary conditions we have to set $a_N = (d-1)/2$

instead of a_D, which makes the term coming from the origin $\mathbf{0} \in \mathbb{N}^d$ ill-defined. For the Neumann case we thus have to omit the origin from the summation,

$$\begin{aligned}\bar{\zeta}_N(s) &:= \zeta_N(s) - (a_N^2 - \alpha^2)^{-s} \\ &= \sum_{\mathbf{m}\in\mathbb{N}^d\setminus\{\mathbf{0}\}} \left((a_N + \mathbf{m}\cdot\mathbf{d})^2 - \alpha^2\right)^{-s}.\end{aligned} \tag{A.14}$$

Below, we derive the following two identities

$$\zeta_D'(0) = \zeta_d'(0, a_D + \alpha) + \zeta_d'(0, a_D - \alpha) + \sum_{r=1}^{d/2} \frac{\alpha^{2r}}{r} H_1(r) R_d(2r, a_D)\,, \tag{A.15}$$

$$\bar{\zeta}_N'(0) = \zeta_d'(0, a_N + \alpha) - \log\rho_d - \log(a_N + \alpha) + \sum_{r=1}^{d/2} \frac{\alpha^{2r}}{r} H_1(r) R_d(2r, a_N). \tag{A.16}$$

Here the R_d are residues of the Barnes ζ-function given in (A.8), $\log\rho_d$ is a Γ-modular form as described in equations (A.34) and (A.33) below, and $H_n(r)$ is a harmonic function defined in terms of harmonic numbers H_r via

$$H_n(r) := \frac{H_{r-1}}{2n} - H_{2r-1}. \tag{A.17}$$

A.2.1 Dirichlet boundary conditions

We now proceed with the derivation of (A.15). Since we will only be dealing with Dirichlet boundary conditions throughout this section, we will omit the D-index in a_D and only reintroduce it when we reach the final result. The first step in the evaluation is to perform a binomial expansion of $\zeta_D(s)$. The expansion converges because $(a + \mathbf{m}\cdot\mathbf{d})^2 \geq \alpha^2$ for $\mathbf{d} = \mathbf{1}$ in both the Dirichlet and Neumann cases, with equality only arising for the zero mode of the Neumann case, which is omitted anyway. We thus get

$$\begin{aligned}\zeta_D(s) &= \sum_{\mathbf{m}\in\mathbb{N}^d} \sum_{r=0}^{\infty} \frac{(s)_r}{r!} \alpha^{2r} \left(a + \mathbf{m}\cdot\mathbf{d}\right)^{-(2s+2r)} \\ &= \sum_{r=0}^{\infty} \frac{(s)_r}{r!} \alpha^{2r} \sum_{\mathbf{m}\in\mathbb{N}^d} \left(a + \mathbf{m}\cdot\mathbf{d}\right)^{-(2s+2r)} \\ &= \zeta_d(2s, a) + \sum_{r=1}^{\infty} \frac{sf(s)}{r!} \alpha^{2r} \zeta_d(2s + 2r, a),\end{aligned} \tag{A.18}$$

where we used the definition of the Barnes ζ-function for $\mathbf{d} = \mathbf{1}$ given in (A.5) and rewrote the Pochhammer symbol for $r > 0$ as $(s)_r = s(s+1)\cdots(s+r-1) =: sf(s)$ to make the behaviour around $s = 0$ more transparent. We also note that $f(0) = (r-1)!$. Considering that $\zeta_d(2r)$ has simple poles at $r = 1, \ldots, d/2$ and converges for higher r, we can immediately write down the following expression at $s = 0$

$$\zeta_D(0) = \zeta_d(0, a) + \frac{1}{2} \sum_{r=1}^{d/2} \frac{\alpha^{2r}}{r} R_d(2r, a) \tag{A.19}$$

with $R_d(k, a)$ defined in equation (A.8).

The next step is to evaluate $\zeta_D'(0)$. In order to do this, we first take a partial derivative with respect to s at general values of s and then let $s \to 0$,

$$\partial_s \zeta_D(s) = \partial_s \zeta_d(2s,a) + \sum_{r=1}^{\infty} \frac{\alpha^{2r}}{r!} \Big(f'(s) s \zeta_d(2s+2r,a) + f(s)\zeta_d(2s+2r,a) + s f(s) \partial_s \zeta_d(2s+2r,a) \Big). \tag{A.20}$$

We note that $f'(0) = (r-1)! H_{r-1}$, where H_{r-1} is a harmonic number, and remind the reader that for $r = 1, \ldots, d/2$ and small s

$$\zeta_d(2s+2r,a) = \frac{R_d(2r,a)}{2s} + C_d(2r,a) + \mathcal{O}(s),$$

and similarly

$$\zeta_d'(2s+2r,a) = -\frac{R_d(2r,a)}{2s^2} + \mathcal{O}(s).$$

Thus at $s = 0$ we can write

$$\big[f'(s) s \zeta_d(2s+2r,a) \big]_{s=0} = (r-1)! \frac{H_{r-1}}{2} R_d(2r,a) \tag{A.21}$$

$$\big[f(s)\zeta_d(2s+2r,a) + s f(s) \partial_s \zeta_d(2s+2r,a) \big]_{s=0} = (r-1)! C_d(2r,a) \tag{A.22}$$

Putting these expressions together we find

$$\zeta_D'(0) = 2\zeta_d'(0,a) + \sum_{r=1}^{d/2} \frac{\alpha^{2r}}{r} \frac{H_{r-1}}{2} R_d(2r,a) + \sum_{r=1}^{d/2} \frac{\alpha^{2r}}{r} C_d(2r,a) + \sum_{r=d/2+1}^{\infty} \frac{\alpha^{2r}}{r} \zeta_d(2r,a). \tag{A.23}$$

There is no contribution to ζ_d' after $r = d/2$, since all such terms in the sum get set to 0 by the s factor.

The next task is to compute the remaining infinite series in (A.23). In order to do this we first note that $\zeta_d(s,a)$ admits the following integral representation for $s > d$

$$\zeta_d(s,a) = \frac{1}{\Gamma(s)} \int_0^{\infty} dt \; \frac{e^{-at}\; t^{s-1}}{(1-e^{-t})^d}. \tag{A.24}$$

Using this we can rewrite

$$\begin{aligned}
\sum_{r=u+1}^{\infty} \frac{\alpha^{2r}}{r} \zeta_d(2r,a) &= 2 \int_0^{\infty} dt \frac{t^{-1}\; e^{-at}}{(1-e^{-t})^d} \sum_{r=d/2+1}^{\infty} \frac{(\alpha t)^{2r}}{(2r)!} \\
&= \int_0^{\infty} dt \frac{t^{-1}\; e^{-at}}{(1-e^{-t})^d} \left(\underbrace{2\cosh(\alpha t)}_{=e^{\alpha t}+e^{-\alpha t}} - 2 \sum_{r=0}^{d/2} \frac{(\alpha t)^{2r}}{(2r)!} \right) \\
&= \lim_{\sigma \to 0} \left(\int_0^{\infty} dt \frac{t^{\sigma-1}\; e^{-(a+\alpha)t}}{(1-e^{-t})^d} + \int_0^{\infty} dt \frac{t^{\sigma-1}\; e^{-(a-\alpha)t}}{(1-e^{-t})^d} \right. \\
&\qquad \left. - 2 \sum_{r=0}^{d/2} \frac{(\alpha)^{2r}}{(2r)!} \int_0^{\infty} dt \frac{t^{2r+\sigma-1}\; e^{-at}}{(1-e^{-t})^d} \right)
\end{aligned}$$

$$= \lim_{\sigma\to 0}\Bigg(\Gamma(\sigma)\left(\zeta_d(\sigma,a+\alpha)+\zeta_d(\sigma,a-\alpha)-2\zeta_d(\sigma,a)\right) - 2\sum_{r=1}^{d/2}\frac{\alpha^{2r}}{(2r)!}\Gamma(2r+\sigma)\zeta_d(2r+\sigma,a)\Bigg), \tag{A.25}$$

where we introduced a convergence parameter σ in order for the integral representation to make sense. For the $\sigma \to 0$ limit we will need to use the analytic continuation of ζ_d. We now take a closer look at the different parts of the expression above around $\sigma = 0$. The ζ_d functions on the first line of (A.25) are convergent at $\sigma = 0$ while the Gamma function has a simple pole. Expanding order by order in σ gives

$$\begin{aligned}\Gamma(\sigma)&\left(\zeta_d(\sigma,a+\alpha)+\zeta_d(\sigma,a-\alpha)-2\zeta_d(\sigma,a)\right)\\ &= \frac{1}{\sigma}\left(\zeta_d(0,a+\alpha)+\zeta_d(0,a-\alpha)-2\zeta_d(0,a)\right)\\ &\quad+\zeta_d'(0,a+\alpha)+\zeta_d'(0,a-\alpha)-2\zeta_d'(0,a)\\ &\quad-\gamma\left(\zeta_d(0,a+\alpha)+\zeta_d(0,a-\alpha)-2\zeta_d(0,a)\right)+\mathcal{O}(\sigma).\end{aligned} \tag{A.26}$$

Carrying out the corresponding expansion on the second line of (A.25) gives

$$\begin{aligned}-2\sum_{r=1}^{d/2}\frac{\alpha^{2r}}{(2r)!}&\left(\Gamma(2r)+\Gamma(2r)\psi(2r)\sigma+\mathcal{O}(\sigma^2)\right)\left(\frac{1}{\sigma}R_d(2r,a)+C_d(2r,a)+\mathcal{O}(\sigma)\right)\\ &= -\frac{1}{\sigma}\sum_{r=1}^{d/2}\frac{\alpha^{2r}}{r}R_d(2r,a)-\sum_{r=1}^{d/2}\frac{\alpha^{2r}}{r}\psi(2r)R_d(2r,a)-\sum_{r=1}^{d/2}\frac{\alpha^{2r}}{r}C_d(2r,a)+\mathcal{O}(\sigma).\end{aligned} \tag{A.27}$$

To get a finite end result we need the pole to vanish when we add (A.26) and (A.27).[12] This is equivalent to the condition

$$\zeta_d(0,a+\alpha)+\zeta_d(0,a-\alpha) = 2\zeta_d(0,a)+\sum_{r=1}^{d/2}\frac{\alpha^{2r}}{r}R_d(2r,a). \tag{A.28}$$

We can then take the limit and write

$$\begin{aligned}(\text{A.25}) &= -\gamma\left(\zeta_d(0,a+\alpha)+\zeta_d(0,a-\alpha)-2\zeta_d(0,a)\right)\\ &\quad+\zeta_d'(0,a+\alpha)+\zeta_d'(0,a-\alpha)-2\zeta_d'(0,a)\\ &\quad-\sum_{r=1}^{d/2}\frac{\alpha^{2r}}{r}\psi(2r)R_d(2r,a)-\sum_{r=1}^{d/2}\frac{\alpha^{2r}}{r}C_d(2r,a)\\ &= \zeta_d'(0,a+\alpha)+\zeta_d'(0,a-\alpha)-2\zeta_d'(0,a)\\ &\quad-\gamma\sum_{r=1}^{d/2}\frac{\alpha^{2r}}{r}R_d(2r,a)-\sum_{r=1}^{d/2}\frac{\alpha^{2r}}{r}\psi(2r)R_d(2r,a)-\sum_{r=1}^{d/2}\frac{\alpha^{2r}}{r}C_d(2r,a)\end{aligned}$$

[12] More rigorously one would first prove the convergence of the infinite sum (A.25), which after rewriting implies the vanishing of the pole and in turn (A.28).

$$= \zeta_d'(0, a+\alpha) + \zeta_d'(0, a-\alpha) - 2\zeta_d'(0,a) \\ - \sum_{r=1}^{d/2} \frac{\alpha^{2r}}{r} H_{2r-1} R_d(2r,a) - \sum_{r=1}^{d/2} \frac{\alpha^{2r}}{r} C_d(2r,a), \tag{A.29}$$

where $H_{2r-1} := \psi(2r) + \gamma$ is a harmonic number. For clarity and later convenience we write down the following identity resulting from the above discussion in the case of Dirichlet boundary conditions explicitly

$$\partial_s \sum_{r=1}^{\infty} \frac{(s)_r}{r!} \alpha^{2r} \zeta_d(2s+2r,a)\Big|_{s=0} = \zeta_d'(0,a+\alpha) + \zeta'(0,a-\alpha) - 2\zeta_d'(0,a) \\ + \sum_{r=1}^{d/2} \frac{\alpha^{2r}}{r} \left(\frac{H_{r-1}}{2} - H_{2r-1} \right) R_d(2r,a)\,. \tag{A.30}$$

Putting everything back together into (A.23) we can write for the complete ζ-function in the Dirichlet case

$$\zeta_D'(0) := \zeta'(0) = \zeta_d'(0, a_D+\alpha) + \zeta_d'(0,a_D-\alpha) + \sum_{r=1}^{d/2} \frac{\alpha^{2r}}{r} \left(\frac{H_{r-1}}{2} - H_{2r-1} \right) R_d(2r, a_D) \\ = \zeta_d'(0, a_D+\alpha) + \zeta_d'(0,a_D-\alpha) + \sum_{r=1}^{d/2} \frac{\alpha^{2r}}{r} H_1(r) R_d(2r, a_D), \tag{A.31}$$

where $H_1(r)$ is a special case of

$$H_n(r) := \frac{H_{r-1}}{2n} - H_{2r-1}\,. \tag{A.32}$$

defined for any integer $n \geq 1$. Higher values of n will be relevant when carrying out the corresponding analysis for a zeta function of the form $\zeta_d(2ns+2r,a)$ instead of $\zeta_d(2s+2r,a)$.

A.2.2 Neumann boundary conditions

Calculating the Neumann case is equivalent to setting $a_N - \alpha = \varepsilon$ and letting ε go to 0. In this limit Barnes [84] calculated that

$$\zeta_d'(0,\varepsilon) = -\log\varepsilon - \log\rho_d + \mathcal{O}(\varepsilon), \tag{A.33}$$

where $\rho_d \equiv \rho_d(\mathbf{1})$ is called a Γ-modular form and obeys the following identity involving the multiple Gamma function

$$\frac{\Gamma_d(a)}{\rho_d} = \frac{\Gamma_{d+1}(a)}{\Gamma_{d+1}(a+1)}. \tag{A.34}$$

The multiple Gamma function $\Gamma_d(a|\mathbf{d})$ is defined,

$$\frac{\Gamma_d(a|\mathbf{d})}{\rho_d(\mathbf{d})} := e^{\zeta_d'(0,a|\mathbf{d})} \tag{A.35}$$

and we write $\Gamma_d(a) := \Gamma_d(a|\mathbf{1})$. Equipped with these tools we can compute the derivative of the ζ-function in the Neumann case (A.14),

$$\begin{aligned}\bar{\zeta}'_N(0) &:= \zeta'_N(0) - \partial_s(a_N^2-\alpha^2)^{-s}\big|_{s=0} \\ &= \zeta'_d(0,a_N+\alpha) - \log\rho_d - \log(a_N-\alpha) + \log\big(a_N^2-\alpha^2\big) + \sum_{r=1}^{d/2}\frac{\alpha^{2r}}{r}H_1(r)R_d(2r,a_N) \\ &= \zeta'_d(0,a_N+\alpha) - \log\rho_d + \log(a_N+\alpha) + \sum_{r=1}^{d/2}\frac{\alpha^{2r}}{r}H_1(r)R_d(2r,a_N), \end{aligned} \tag{A.36}$$

where ζ_N is just ζ_D but with a_D replaced by a_N. We can also write the following Neumann version of the identity (A.30)

$$\begin{aligned}\partial_s\left(\sum_{r=1}^{\infty}\frac{(s)_r}{r!}\alpha^{2r}\zeta_d(2s+2r,a_N) - (a_N^2-\alpha^2)^{-s}\right)\Bigg|_{s=0} \\ = \zeta'_d(0,a_N+\alpha) - \log\rho_d + \log(a_N+\alpha) - 2\zeta'_d(0,a_N) \\ + \sum_{r=1}^{d/2}\frac{\alpha^{2r}}{r}H_1(r)R_d(2r,a_N).\end{aligned} \tag{A.37}$$

A.3 Determinant of GJMS operators

We are now prepared to tackle the calculation of the log-determinants.

In section A.3.1, for the case of Dirichlet boundary conditions on the hemisphere, we obtain

$$\log\det P_{2k,H_D^d} = -\zeta'_{d+1}(0,d/2-k+1) + \zeta'_{d+1}(0,d/2+k+1) - M(d,k), \tag{A.38}$$

where the function $M(d,k)$ is defined via equations (A.46), (A.47), and (A.49). Equation (A.38) is valid for $k=1,\dots,d/2$.

In section A.3.2, we discuss the Neumann case, which is a little more involved, as the zero mode makes the log-determinant ill-defined in the critical case $k=d/2$. For the subcritical case $k=1,\dots,d/2-1$ we get

$$\log\det P_{2k,H_N^d} = -\zeta'_{d+1}(0,d/2-k) + \zeta'_{d+1}(0,d/2+k) - M(d,k), \tag{A.39}$$

while for the critical case we get the slightly more complicated result

$$\log\det P_{d,H_N^d} = -\log(d-1)! + \log\rho_{d+1} + \zeta'_{d+1}(0,d) - M(d), \tag{A.40}$$

where $M(d) = M(d,d/2)$ and ρ_{d+1} is a Γ-modular form as defined in (A.34).

In section A.3.3 we assemble these results to construct the determinant of GJMS operators on a sphere, summarised in (A.60).

A.3.1 Determinant on the hemisphere with Dirichlet boundary conditions

We will now generalise the results of the last section. Our starting point is the spectral ζ-function defined in (A.1). As before, we start by doing a binomial expansion for every term in the product,

$$\begin{aligned}
Z_d(s,a,k) &= \sum_{\mathbf{m}\in\mathbb{N}^d}\prod_{j=0}^{k-1}\sum_{r_j=0}^{\infty}\frac{(s)_{r_j}}{r_j!}\frac{\alpha_j^{2r_j}}{(\mathbf{m}\cdot\mathbf{d}+a)^{2s+2r_j}} \\
&= \sum_{\mathbf{r}\in\mathbb{N}^k}^{\infty}\left(\prod_{j=0}^{k-1}\frac{(s)_{r_j}}{r_j!}\alpha_j^{2r_j}\right)\sum_{\mathbf{m}\in\mathbb{N}^d}\frac{1}{(\mathbf{m}\cdot\mathbf{d}+a)^{2ks+2\sum_{j=0}^{k-1}r_j}} \\
&= \sum_{\mathbf{r}\in\mathbb{N}^k}^{\infty}\left(\prod_{j=0}^{k-1}\frac{(s)_{r_j}}{r_j!}\alpha_j^{2r_j}\right)\zeta_d\left(2ks+2\mathbf{r}\cdot\mathbf{d},a\right) \\
&= \underbrace{\zeta_d(2ks,a)}_{\mathbf{r}=\mathbf{0}} + \sum_{i=0}^{k-1}\underbrace{\sum_{r_i=1}^{\infty}\frac{(s)_{r_i}}{r_i!}\alpha_i^{2r_i}\zeta_d(2ks+2r_i,a)}_{\mathbf{r}=(0,\ldots,0,r_i,0,\ldots,0)} \\
&\quad + \sum_{i=1}^{k-1}\sum_{j=0}^{i-1}\underbrace{\sum_{r_i,r_j=1}^{\infty}\frac{(s)_{r_i}}{r_i!}\frac{(s)_{r_j}}{r_j!}\alpha_i^{2r_i}\alpha_j^{2r_j}\zeta_d(2ks+2r_i+2r_j,a)}_{\mathbf{r}=(0,\ldots,0,r_i,0,\ldots,0,r_j,0,\ldots,0)} + R(s).
\end{aligned} \tag{A.41}$$

We remind the reader that $\alpha_j = j+\frac{1}{2}$, $\mathbf{d}=\mathbf{1}$, and $a_D = (d+1)/2$ for Dirichlet boundary conditions. For simplicity we write a instead of a_D throughout this section.

The remaining sums, denoted by $R(s)$ above, will vanish for Z_d and Z_d' around $s=0$. This is easy to see, as $(s)_r = \mathcal{O}(s)$ while the ζ_d functions will contribute with simple poles and ζ' with double poles. When more than two Pochhammer symbols are present, they overcome the poles and give zero in the limit. We can make further simplifications in some of the sums above by noting that the r_i are dummy indices and rewrite (A.41) as

$$\begin{aligned}
Z_d(s,a,k) = \zeta_d(ds,a) &+ \sum_{r=1}^{\infty}\frac{(s)_r}{r!}\left(\sum_{j=0}^{k-1}\alpha_j^{2r}\right)\zeta_d(2ks+2r,a) \\
&+ \sum_{r,r'=1}^{\infty}\frac{(s)_r}{r!}\frac{(s)_{r'}}{r'!}\left(\sum_{i=1}^{k-1}\sum_{j=0}^{i-1}\alpha_i^{2r}\alpha_j^{2r'}\right)\zeta_d(2ks+2r+2r',a) + R(s).
\end{aligned} \tag{A.42}$$

The double sum vanishes at $s=0$ as ζ_d only contributes a pole proportional to $1/s$ while the Pochhammer symbols each contribute a factor of s. The rest of the expression looks just like the ζ-functions in the previous section, so the result follows directly from (A.19) and (A.18),

$$Z_d(0,a,k) = \zeta_d(0,a) + \frac{1}{2k}\sum_{r=1}^{d/2}\frac{1}{r}\left(\sum_{j=0}^{k-1}\alpha_j^{2r}\right)R_d(2r,a)\,. \tag{A.43}$$

Using equation (A.28) we can rewrite this as

$$Z_d(0,a,k) = \frac{1}{2k}\sum_{j=0}^{k-1}\left(\zeta_d(0,a+\alpha_j)+\zeta_d(0,a-\alpha_j)\right). \tag{A.44}$$

By virtue of (A.12) evaluated at $k=0$, this can in turn be written in terms of generalised Bernoulli polynomials [42],

$$Z_d(0,a,k) = \frac{1}{2k\,d!}\sum_{j=0}^{k-1}\left(B_d^{(d)}(d/2+j+1)+B_d^{(d)}(d/2-j)\right). \tag{A.45}$$

Evaluating the derivative at $s=0$ is also relatively painless now. For the first two terms the result follows directly from the discussion in the previous sections, in particular from equation (A.30) in the Dirichlet and (A.37) in the Neumann case. In the Dirichlet case we thus have

$$\begin{aligned}
&\partial_s\left(\zeta_d(2ks,a)+\sum_{r=1}^{\infty}\frac{(s)_r}{r!}\left(\sum_{j=0}^{k-1}\alpha_j^{2r}\right)\zeta_d(2ks+2r,a)\right)\Bigg|_{s=0}\\
&\quad=\sum_{j=0}^{k-1}\left(\zeta_d'(0,a+\alpha_j)+\zeta_d'(0,a-\alpha_j)\right)+\sum_{r=1}^{d/2}\frac{1}{r}\left(\sum_{j=0}^{k-1}\alpha_j^{2r}\right)H_k(r)R_d(2r,a)\\
&\quad=:\sum_{j=0}^{k-1}\left(\zeta_d'(0,a+\alpha_j)+\zeta_d'(0,a-\alpha_j)\right)+M_1(d,a,k),
\end{aligned} \tag{A.46}$$

where we defined M_1 in the last line to simplify the notation. To calculate the contribution from the double sum in (A.42) we remind the reader that $\zeta_d(s+n,a)=\frac{1}{s}R_d(n,a)+\mathcal{O}(s^0)$ and $\zeta_d'(s+n,a)=\frac{-1}{s^2}R_d(n,a)+\mathcal{O}(s)$ for $n=1,\dots,d$. Since $(s)_r =: sf(s)=\mathcal{O}(s)$ with $f(0)=(r-1)!$, this means that the only terms in the sum that will survive are those for which $2r+2r'\le d$. Also noting that $\partial_s(s)_r\big|_{s=0}=(r-1)!$ we get the following result

$$\begin{aligned}
&\partial_s\sum_{r,r'=1}^{\infty}\frac{(s)_r}{r!}\frac{(s)_{r'}}{r'!}\underbrace{\left(\sum_{i=0}^{k-1}\sum_{j=0}^{i-1}\alpha_i^{2r}\alpha_j^{2r'}\right)}_{\equiv A(r,r')}\zeta_d(2ks+2r+2r',a)\Bigg|_{s=0}\\
&\quad=\sum_{r=1}^{d/2}\sum_{r'=1}^{d/2-r}\frac{1}{r}\frac{1}{r'}A(r,r')\left[s^2\partial_s\zeta_d(2ks+2r+2r',a)\right]_{s=0}\\
&\qquad+2\sum_{r=1}^{d/2}\sum_{r'=1}^{d/2-r}\frac{1}{r}\frac{1}{r'}A(r,r')\left[s\zeta_d(2ks+2r+2r',a)\right]_{s=0}\\
&\quad=\sum_{r=1}^{d/2}\sum_{r'=1}^{d/2-r}\frac{1}{r}\frac{1}{r'}A(r,r')\left(-\frac{1}{2k}R_d(2r+2r',a)+\frac{2}{2k}R_d(2r+2r',a)\right)\\
&\quad=\frac{1}{2k}\sum_{r=1}^{d/2}\sum_{r'=1}^{d/2-r}\frac{1}{r}\frac{1}{r'}A(r,r')R_d(2r+2r',a)=:M_2(d,a,k).
\end{aligned} \tag{A.47}$$

Putting (A.46) and (A.47) together we get the result

$$\begin{aligned} Z'_d(0,a,k) &= \sum_{j=0}^{k-1} \left(\zeta'_d(0,a+\alpha_j) + \zeta'_d(0,a-\alpha_j)\right) + M(d,a,k) \\ &= \log\left(\frac{1}{\rho_d^{2k}} \prod_{j=0}^{k-1} \Gamma_d(a+\alpha_j)\Gamma_d(a-\alpha_j)\right) + M(d,a,k), \end{aligned} \tag{A.48}$$

where in the last line we used the definition of the multiple Gamma function (A.34) to rewrite the result, and where we defined

$$M(d,k) := M_1(d,a,k) + M_2(d,a,k). \tag{A.49}$$

We omitted a in $M(d,k)$, because the property $B_n^{(\alpha)}(x) = (-1)^n B_n^{(\alpha)}(\alpha - x)$ [83] of generalised Bernoulli polynomials implies, according to (A.9), that $R_d(2r, a_N) = R_d(2r, a_D)$ for even dimension, which in turn implies that $M(d,k)$ does not depend on whether we chose a_D or a_N. It is possible to further simplify the result by using (A.34) and noting that $\alpha_j + n = \alpha_{j+n}$. This induces a telescope-like cancellation in the product,

$$\begin{aligned} \log\left(\frac{1}{\rho_d^{2k}} \prod_{j=0}^{k-1} \Gamma_d(a+\alpha_j)\Gamma_d(a-\alpha_j)\right) &= \log\left(\prod_{j=0}^{k-1} \frac{\Gamma_d(a+\alpha_j)}{\rho_d} \frac{\Gamma_d(a-\alpha_j)}{\rho_d}\right) \\ &= \log\left(\prod_{j=0}^{k-1} \frac{\Gamma_{d+1}(a+\alpha_j)}{\Gamma_{d+1}(a+\alpha_{j+1})} \frac{\Gamma_{d+1}(a-\alpha_j)}{\Gamma_{d+1}(a-\alpha_{j-1})}\right) \\ &= \log\left(\frac{\Gamma_{d+1}(a+\alpha_0)}{\Gamma_{d+1}(a+\alpha_k)} \frac{\Gamma_{d+1}(a-\alpha_{k-1})}{\Gamma_{d+1}(a-\alpha_{-1})}\right) \\ &= \log\left(\frac{\Gamma_{d+1}(d/2-k+1)}{\Gamma_{d+1}(d/2+k+1)}\right). \end{aligned} \tag{A.50}$$

Putting everything together we get the following expression for the log-determinant

$$\begin{aligned} \log\det P_{2k,H_D^d} &= -Z'_d(0,a_D,k) \\ &= -\log\left(\frac{\Gamma_{d+1}(d/2-k+1)}{\Gamma_{d+1}(d/2+k+1)}\right) - M(d,k) \\ &= -\zeta'_{d+1}(0,d/2-k+1) + \zeta'_{d+1}(0,d/2+k+1) - M(d,k), \end{aligned} \tag{A.51}$$

which is valid for $k = 1, \ldots, d/2$, i.e. in the critical as well as subcritical case.

A.3.2 Determinant on the hemisphere with Neumann boundary conditions

In the subcritical case there is no zero mode and we can continue from (A.50), inserting the appropriate a for Neumann boundary conditions, i.e. $a_N = (d-1)/2$. Then the expression for the spectral ζ-function is as in (A.45), thanks to the above mentioned property of the generalised Bernoulli polynomials [42], and the subcritical expression for the determinant is

$$\begin{aligned} \log\det P_{2k,H_N^d} &= -Z'_d(0,a_N,k) \\ &= -\log\left(\frac{\Gamma_{d+1}(d/2-k)}{\Gamma_{d+1}(d/2+k)}\right) - M(d,k) \\ &= -\zeta'_{d+1}(0,d/2-k) + \zeta'_{d+1}(0,d/2+k) - M(d,k). \end{aligned} \tag{A.52}$$

In the critical case $k = d/2$ the calculation is more subtle. In order to get a well-defined expression, we must subtract the zero mode contribution from the sum,

$$\begin{aligned}\bar{Z}_d(s, a_N, k) &= \sum_{\mathbf{m}\in\mathbb{N}^d\setminus\{0\}} \prod_{j=0}^{k-1} \left((\mathbf{m}\cdot\mathbf{d} + a_N)^2 - \alpha_j^2\right)^{-s} \\ &= Z_d(s, a_N, k) - \prod_{j=0}^{k-1} \left(a_N^2 - \alpha_j^2\right)^{-s}.\end{aligned} \tag{A.53}$$

At $s = 0$ we have for the critical case $k = d/2$ [42]

$$\bar{Z}_d(0, a_N, k) = \frac{1}{2k\, d!} \sum_{j=0}^{k-1} \left(B_d^{(d)}(d/2 - j - 1) + B_d^{(d)}(d/2 + j)\right) - 1\,. \tag{A.54}$$

We can now use (A.48) as well as (A.33), to write down the following expression,

$$\begin{aligned}\bar{Z}'(0, a_N, k) = \lim_{\varepsilon\to 0} \sum_{j=0}^{k-2} \left(\zeta_d'(0, a_N + \alpha_j) + \zeta_d'(0, a_N - \alpha_j)\right) + \zeta_d'(0, a_N + \alpha_{k-1}) - \log(\varepsilon) \\ - \log(\rho_d) + M(d, k) + \underbrace{\log\left(a_N^2 - \alpha_{k-1}^2\right)}_{=\log(a_N+\alpha_{k-1})+\log(\varepsilon)} + \sum_{j=0}^{k-2} \log\left(a_N^2 - \alpha_j^2\right) + \mathcal{O}(\varepsilon),\end{aligned} \tag{A.55}$$

where we denote $\varepsilon = a_N - \alpha_{k-1}$. The logarithmic divergence cancels and we obtain

$$\begin{aligned}\bar{Z}'(0, a_N, k) &= \sum_{j=0}^{k-2} \left(\zeta_d'(0, a_N + \alpha_j) + \zeta_d'(0, a_N - \alpha_j) + \log\left(a_N^2 - \alpha_j^2\right)\right) \\ &\qquad + \zeta_d'(0, a_N + \alpha_{k-1}) - \log(\rho_d) + \log(d-1) + M(d, k) \\ &= \sum_{j=0}^{k-2} \left(\zeta_d'(0, a_N + \alpha_j) + \zeta_d'(0, a_N - \alpha_j)\right) + \zeta_d'(0, d-1) \\ &\qquad - \log(\rho_d) + \log((d-1)!) + M(d, k) \\ &= \log\left(\frac{(d-1)!}{\rho_d^{2k}} \Gamma_d(d-1) \prod_{j=0}^{k-2} \Gamma_d(a_N + \alpha_j)\Gamma(a_N - \alpha_j)\right) + M(d, k)\end{aligned} \tag{A.56}$$

where we used the fact that $a_N + \alpha_{k-1} = d - 1$ and $\sum_{j=0}^{k-2} \log\left(a_N^2 - \alpha_j^2\right) = \log((d-2)!)$ for Neumann boundary conditions. As before, we can use identities involving the multiple Gamma function to induce cancellations. This leads us to the final result in the critical case,

$$\begin{aligned}\log\det P_{d,H_N^d} &= -\bar{Z}_d'(0, a_N, d/2) \\ &= -\log\left(\frac{(d-1)!}{\rho_d} \frac{\Gamma_{d+1}(1)}{\Gamma_{d+1}(d)}\right) - M(d) \\ &= -\log\left(\frac{(d-1)!}{\Gamma_{d+1}(d)}\right) - M(d) \\ &= -\log((d-1)!) + \log\rho_{d+1} + \zeta_{d+1}'(0, d) - M(d),\end{aligned} \tag{A.57}$$

where we used $\rho_d = \Gamma_{d+1}(1)$, and the abbreviated notation $M(d, d/2) =: M(d)$. Since the critical case is the most relevant to this paper, we give the explicit form of $M(d)$,

$$M(d) = \sum_{r,l=1}^{d/2} \frac{1}{r(d-2r)!(2r-1)!} \left(l+\frac{1}{2}\right)^{2r} \left(\frac{H_{r-1}}{d} - H_{2r-1}\right) B^{(d)}_{d-2r}\left(\frac{d+1}{2}\right) + \frac{1}{d} \sum_{r,l=1}^{d/2} \sum_{t=1}^{d/2-r} \sum_{m=1}^{l} \frac{1}{rt(d-2r-2t)!(2r+2t-1)!} \left(l+\frac{1}{2}\right)^{2r} \left(m+\frac{1}{2}\right)^{2t} B^{(d)}_{d-2r-2t}\left(\frac{d+1}{2}\right). \tag{A.58}$$

As mentioned in the main body, our result differs by Dowker's result due to the different sign in front of the $\log(d-1)!$ term because we are considering the functional determinant of the GJMS operators on the sphere with the zero mode removed.

A.3.3 Determinant on the sphere

The log-determinant on the sphere is obtained by adding the log-determinants on the hemisphere for Dirichlet and Neumann boundary conditions. In the critical case, the spectral ζ-function for the sphere at $s = 0$ is given by (A.45) and (A.54), [42], so that

$$Z_d(0,k) = \frac{1}{k\,d!} \sum_{j=0}^{k-1} \left(B^{(d)}_d(d/2+j+1) + B^{(d)}_d(d/2+j) \right) - 1\,, \tag{A.59}$$

and the log-determinant on the sphere is thus given by

$$\begin{aligned} \log\det P_{d,S^d} &= \log\det P_{d,H^d_D} + \log\det P_{d,H^d_N} \\ &= -\log\left((d-1)! \frac{\Gamma_{d+1}(1)}{\Gamma_{d+1}(d)\Gamma_{d+1}(d+1)} \right) - 2M(d) \\ &= -\zeta'_{d+1}(0,1) + \zeta'_{d+1}(0,d+1) + \zeta'_{d+1}(0,d) \\ &\quad - \log((d-1)!) + \log\rho_{d+1} - 2M(d). \end{aligned} \tag{A.60}$$

In the subcritical case we instead have

$$Z_d(0,k) = \frac{1}{k\,d!} \sum_{j=0}^{k-1} \left(B^{(d)}_d(d/2+j+1) + B^{(d)}_d(d/2+j) \right)\,, \tag{A.61}$$

and the functional determinant reads

$$\begin{aligned} \log\det P_{2k,S^d} &= \log\det P_{2k,H^d_D} + \log\det P_{2k,H^d_N} \\ &= -\log\left(\frac{\Gamma_{d+1}(d/2-k)}{\Gamma_{d+1}(d/2+k)} \frac{\Gamma_{d+1}(d/2-k+1)}{\Gamma_{d+1}(d/2+k+1)} \right) - 2M(d,k) \\ &= -\zeta'_{d+1}(0,d/2-k) + \zeta'_{d+1}(0,d/2+k) \\ &\quad - \zeta'_{d+1}(0,d/2-k+1) + \zeta'_{d+1}(0,d/2+k+1) - 2M(d,k). \end{aligned} \tag{A.62}$$

B An alternative form for determinants of GJMS operators on spheres and hemispheres

In this appendix we will show how to rewrite Dowker's expressions (A.51) and (A.57) for the log-determinants of GJMS operators on hemispheres as

$$\begin{aligned}\log\det P_{2k,H^d_D} &= -\sum_{n=0}^{d} h^D_n(d,k)\zeta'(-n) - f^D(d,k),\\ \log\det P_{2k,H^d_N} &= -\sum_{n=0}^{d} h^N_n(d,k)\zeta'(-n) - f^N(d,k),\end{aligned} \tag{B.1}$$

where ζ is the Riemann ζ-function, and h_n and f are functions that we derive and that depend on the boundary conditions, the dimension, and the degree of the GJMS-operator. The spherical case then follows directly as the sum of Dirichlet and Neumann hemispherical results,

$$\log\det P_{2k,S^d} = -\sum_{n=0}^{d}\left(h^D_n(d,k) + h^N_n(d,k)\right)\zeta'(-n) - f^D(d,k) - f^N(d,k). \tag{B.2}$$

B.1 Rewriting ζ_d in terms of the Riemann ζ-function

In [85], Adamchik gives a closed form of the Barnes ζ-function in terms of a series of Riemann ζ-functions. His calculation is summarized by equations (14), (17), and (23) in the reference, which in our slightly different notation and after a bit of rearranging read

$$\zeta'_d(0,z) = (-1)^{d+1}\log G_d(z) + \sum_{k=0}^{d-1}(-1)^k\binom{z}{k}R_{d-k}, \tag{B.3}$$

where we note that the $G_d(z)$ are multiple Gamma functions with a different normalization compared to the one used by Dowker. We have the following explicit closed forms for all the parts of the above expression,

$$\begin{aligned}\log G_d(z) &= \frac{(-1)^d}{(d-1)!}\sum_{k=0}^{d-1} P_{k,d}(z)\left(\zeta'(-k) - \zeta'(-k,z)\right), \quad \mathrm{Re}(z) > 0\\ R_{d-k} &= \frac{1}{(d-k-1)!}\sum_{l=0}^{d-k-1}\begin{bmatrix} d-k \\ l+1\end{bmatrix}\zeta'(-l).\end{aligned} \tag{B.4}$$

For our purposes, it is not necessary to know how the polynomials $P_{k,d}(z)$ are defined, it suffices to know that they satisfy [85]

$$\sum_{k=0}^{d-1} P_{k,d}(z)n^k = (n-z+1)_d = \prod_{k=1}^{d-1}(n+k-z). \tag{B.5}$$

We are only interested in the special case of the above formula, for which z is a positive integer. For $z = 1$ it is clear that $\log G_d(1) = 0$. For $z > 1$ we can use the fact that

$$\zeta(s,z) = \zeta(s) - \sum_{n=1}^{z-1}\frac{1}{n^s} \tag{B.6}$$

to simplify

$$\zeta'(-k) - \zeta'(-k,z) = -\sum_{n=1}^{z-1} n^k \log n. \tag{B.7}$$

We can now define the following quantity

$$\begin{aligned} A(d,z) &:= (-1)^{d+1} \log G_d(z) \\ &= \frac{1}{(d-1)!} \sum_{k=0}^{d-1} P_{k,d}(z) \sum_{n=1}^{z-1} n^k \log n \\ &= \frac{1}{(d-1)!} \sum_{n=1}^{z-1} \log(n)(n-z+1)_d\,, \quad z>1\,. \end{aligned} \tag{B.8}$$

It is further clear from $\zeta(s) = \zeta(s,1)$ that $A(d,1) = 0$. Another very useful simplification comes from rewriting the R_{d-k} sum in (B.3) as

$$\begin{aligned} \sum_{k=0}^{d-1} (-1)^k \binom{z}{k} R_{d-k} &= \sum_{k=0}^{d-1} \binom{z}{k} \frac{(-1)^k}{(d-k-1)!} \sum_{l=0}^{d-k-1} \begin{bmatrix} d-k \\ l+1 \end{bmatrix} \zeta'(-l) \\ &= \sum_{l=0}^{d-1} \left(\sum_{k=0}^{d-l-1} \frac{(-1)^k}{(d-k-1)!} \binom{z}{k} \begin{bmatrix} d-k \\ l+1 \end{bmatrix} \right) \zeta'(-l) \\ &=: \sum_{l=0}^{d-1} D_l(d,z) \zeta'(-l), \end{aligned} \tag{B.9}$$

where we define $D_k(d,z)$ in the last line as

$$D_k(d,z) := \sum_{j=0}^{d-k-1} \frac{(-1)^j}{(d-j-1)!} \binom{z}{j} \begin{bmatrix} d-j \\ k+1 \end{bmatrix}. \tag{B.10}$$

With these definitions it possible to write down the $\zeta'_d(0,z)$ in the following very simple way

$$\zeta'_d(0,z) = A(d,z) + \sum_{k=0}^{d-1} D_k(d,z) \zeta'(-k), \quad z \in \mathbb{N}^+. \tag{B.11}$$

B.2 Determinants in terms of Riemann ζ-functions

Dirichlet boundary conditions on the hemisphere. We can now use the above technology to rewrite the log-determinant (A.51) on the hemisphere for Dirichlet boundary conditions,

$$\begin{aligned} \log\det P_{2k,H_D^d} &= -\zeta'_{d+1}(0, d/2-k+1) + \zeta'_{d+1}(0, d/2+k+1) - M(d) \\ &= -A(d+1, d/2-k+1) + A(d+1, d/2+k+1) - M(d) \\ &\quad - \sum_{n=0}^{d} \left(D_n(d+1, d/2-k+1) - D_n(d+1, d/2+k+1) \right) \zeta'(-n) \\ &=: -\sum_{n=0}^{d} h_n^D(d,k) \zeta'(-n) - f^D(d,k). \end{aligned} \tag{B.12}$$

Here we have defined two functions

$$h_n^D(d,k) := D_n(d+1, d/2-k+1) - D_n(d+1, d/2+k+1), \tag{B.13}$$
$$f^D(d,k) := A(d+1, d/2-k+1) - A(d+1, d/2+k+1) + M(d). \tag{B.14}$$

Since the critical case $k = d/2$ is of particular interest to us, we give the explicit form of h_n^D and f^D in that case,

$$\begin{aligned} h_n^D(d) &:= h_n^D(d, d/2) \\ &= -\frac{1}{(d-1)!}\begin{bmatrix} d \\ n+1 \end{bmatrix} + \frac{1}{d!}\begin{bmatrix} d+1 \\ n+1 \end{bmatrix} - \sum_{j=0}^{d-n} \frac{(-1)^j}{(d-j)!}\binom{d+1}{j}\begin{bmatrix} d-j+1 \\ n+1 \end{bmatrix}, \end{aligned} \tag{B.15}$$

$$\begin{aligned} f^D(d) &:= f^D(d, d/2) \\ &= -\frac{1}{d!}\sum_{j=1}^{d-1} \log(j)(j-d)_{d+1} + M(d). \end{aligned} \tag{B.16}$$

Neumann boundary conditions on the hemisphere. Writing the subcritical, i.e. $k = 1, \ldots, d/2-1$, determinant (A.52) for Neumann boundary conditions is straightforward,

$$\begin{aligned} \log\det P_{2k,H_N^d} &= -\zeta'_{d+1}(0, d/2-k) + \zeta'_{d+1}(0, d/2+k) - M(d) \\ &= -A(d+1, d/2-k) + A(d+1, d/2+k) - M(d) \\ &\quad - \sum_{n=0}^{d} \left(D_n(d+1, d/2-k) - D_n(d+1, d/2+k)\right)\zeta'(-n) \\ &=: -\sum_{n=0}^{d} h_n^N(d,k)\zeta'(-n) - f^N(d,k), \end{aligned} \tag{B.17}$$

with the functions $h_n^N(d,k)$ and $f^N(d,k)$ defined in the last line as

$$h_n^N(d,k) := D_n(d+1, d/2-k) - D_n(d+1, d/2+k), \tag{B.18}$$
$$f^N(d,k) := A(d+1, d/2-k) - A(d+1, d/2+k) + M(d). \tag{B.19}$$

The critical case (A.57) is slightly harder, as we also need to rewrite $\log\rho_{d+1}$. In order to do this, we use the following formula from [85],

$$\log\rho_d = -\frac{1}{(d-1)!}\sum_{n=0}^{d-1}\begin{bmatrix} d \\ n+1 \end{bmatrix}\zeta'(-n). \tag{B.20}$$

Reminding the reader that $\begin{bmatrix} d \\ d+1 \end{bmatrix} = 0$ we can thus write

$$\begin{aligned} \log\det P_{d,H_N^d} &= -\log(d-1)! + \log\rho_{d+1} + \zeta'_{d+1}(0,d) - M(d) \\ &= -\sum_{n=0}^{d}\left(\frac{1}{d!}\begin{bmatrix} d+1 \\ n+1 \end{bmatrix} - D_n(d+1,d)\right)\zeta'(-n) \\ &\quad - \log(d-1)! + A(d+1,d) - M(d) \\ &=: -\sum_{n=0}^{d} h_n^N(d)\zeta'(-n) - f^N(d) \end{aligned} \tag{B.21}$$

where we define $h_n^N(d)$ and $f^N(d)$ in the last line. In analogy to the Dirichlet case we can define $h_n^N(d, d/2) := h_n^N(d)$ and $f^N(d, d/2) := f^N(d)$, as with this definition equation (B.17) becomes valid for for all k. Again we write these functions explicitly for the critical case,

$$h_n^N(d) = \frac{1}{d!}\begin{bmatrix} d+1 \\ n+1 \end{bmatrix} - \sum_{j=0}^{d-n} \frac{(-1)^j}{(d-j)!}\binom{d}{j}\begin{bmatrix} d-j+1 \\ n+1 \end{bmatrix}, \tag{B.22}$$

$$f^N(d) = \log(d-1)! - \frac{1}{d!}\sum_{j=1}^{d-1} \log(j)(j-d)_{d+1} + M(d). \tag{B.23}$$

C Functional determinants on the flat d-torus

In this appendix we calculate functional determinants of the Laplacian on the flat torus (appendix C.1) and on a cylinder obtained by cutting the torus along a cycle and imposing Dirichlet boundary conditions along the cut (appendix C.2). After that, in appendix C.3, we derive the functional determinant of k-powers of the Laplacian both on the flat torus as well as on the cylinder.

C.1 Determinant of the Laplacian on the flat torus

The d-dimensional flat torus can be defined as the hyperinterval with side lengths given by L_i and opposing sides identified,

$$T^d_{L_1,\dots,L_d} := \mathbb{R}^d/(L_1\mathbb{Z} \times \ldots \times L_d\mathbb{Z}). \tag{C.1}$$

Since the manifold is flat, the Laplace-Beltrami operator is just the standard Laplacian on Euclidean space.

We compute the functional determinant for the Laplacian on the d-torus via a spectral ζ-function method. The eigenvalues of the Laplace operator $-\partial_a\partial^a$, are given by

$$\lambda_{n_1,\dots,n_d} = \left(\frac{2\pi n_1}{L_1}\right)^2 + \cdots + \left(\frac{2\pi n_d}{L_d}\right)^2, \qquad n_1,\dots,n_d \in \mathbb{Z}\,. \tag{C.2}$$

As usual, the zero mode, with $n_1 = n_2 = \cdots = n_d = 0$, needs to be removed in the computation of the spectral ζ-function. In order to calculate the determinant of the Laplacian, we need to evaluate

$$\begin{aligned} \zeta_{T^d_{L_1,\dots,L_d}}(s) &:= {\sum_{\vec{n}\in\mathbb{Z}^d}}' \left(\left(\frac{2\pi n_1}{L_1}\right)^2 + \cdots + \left(\frac{2\pi n_d}{L_d}\right)^2\right)^{-s} \\ &= {\sum_{\vec{n}\in\mathbb{Z}^d}}' \left(\vec{n}_d^{\,T}\,\Xi\,\vec{n}_d\right)^{-s}, \end{aligned} \tag{C.3}$$

where $\vec{n}_d := (n_1,\dots,n_d)$ is a d-vector, $\Xi := \mathrm{diag}\big(\,(2\pi/L_1)^2,\dots,(2\pi/L_d)^2\,\big)$ a $d\times d$ matrix, and the prime on the sum denotes the omission of the zero mode.

In section 2.2 of [86] the analytic continuation of the sum (C.3) is evaluated recursively. In our notation the result is given by

$$\zeta_{T^d_{L_1,\dots,L_d}}(s) = 2\left(\frac{L_1}{2\pi}\right)^{2s}\zeta(2s) + L_1\frac{\Gamma(s-1/2)}{2\sqrt{\pi}\Gamma(s)}\zeta_{T^{d-1}_{L_2,\dots,L_d}}(s-1/2) + G(s;L_1,\dots,L_d)\,, \tag{C.4}$$

where we define the function

$$\begin{aligned} G(s;L_1,L_2,\dots,L_d) := \frac{2^{3/2-s}L_1^{s+1/2}}{\Gamma(s)\sqrt{\pi}}\sum_{\vec{n}_{d-1}\in\mathbb{Z}^{d-1}}{}'\sum_{n_1=1}^{\infty}\left(\frac{n_1}{\sqrt{\vec{n}^T_{d-1}\,\Xi_{d-1}\,\vec{n}_{d-1}}}\right)^{s-1/2} \\ \times K_{s-1/2}\left(L_1 n_1\sqrt{\vec{n}^T_{d-1}\,\Xi_{d-1}\,\vec{n}_{d-1}}\right), \end{aligned} \tag{C.5}$$

with $K_\nu(z)$ being the modified Bessel function of the second kind, $\vec{n}_{d-1} = (n_2,\dots,n_d)$, and $\Xi_{d-1} = \mathrm{diag}\left((2\pi/L_2)^2,\dots,(2\pi/L_d)^2\right)$.

We can directly evaluate the log-determinant on the flat torus, as the analytic continuation (C.4) has only a pole at $s=\frac{d}{2}$ in the whole complex plane,

$$\begin{aligned} \log\det\mathcal{P}_{2,T^d} &= \log\det\Delta_{T^d_{L_1,\dots,L_d}} = -\zeta'_{T^d_{L_1,\dots,L_d}}(0) \\ &= 2\log(L_1) + L_1\,\zeta_{T^{d-1}_{L_2,\dots,L_d}}(-1/2) - G'(0;L_1,\dots,L_d)\,. \end{aligned} \tag{C.6}$$

This expression is recursive, and thus not in a closed form yet, however, it turns out to be useful in the evaluation of the functional determinant contribution to the entanglement entropy in section 5.

We now solve the recursion directly and provide a closed form for the ζ-function. Our calculation of the closed form is slightly more direct than the one carried out in section 4.2.3 of [87] but the end result is the same. In order to make the calculation more transparent, let us for a while rewrite (C.4) as

$$\zeta_d(s) = h_1(s) + f_1(s)\zeta_{d-1}\left(s-\frac{1}{2}\right) + g_d(s), \tag{C.7}$$

where the functions above summarize the information in the recursion:

$$\zeta_{d-k}(s) := \zeta_{T^{d-k}_{L_{k+1},\dots,L_d}}(s)\,, \tag{C.8a}$$

$$h_k(s) := 2\left(\frac{L_k}{2\pi}\right)^{2s}\zeta(2s)\,, \tag{C.8b}$$

$$f_k(s) := L_k\frac{\Gamma(s-1/2)}{2\sqrt{\pi}\Gamma(s)}\,, \tag{C.8c}$$

$$g_{d-k}(s) := G(s;L_{k+1},\dots,L_d)\,. \tag{C.8d}$$

In this notation it is not difficult to see, that after k steps we get

$$\begin{aligned}\zeta_d(s) = h_1(s) &+ \sum_{j=2}^{k} h_j\left(s-\frac{j-1}{2}\right)\prod_{i=1}^{j-1} f_i\left(s-\frac{i-1}{2}\right) + g_d(s)\\ &+ \sum_{j=2}^{k} g_{d-j+1}\left(s-\frac{j-1}{2}\right)\prod_{i=1}^{j-1} f_i\left(s-\frac{i-1}{2}\right)\\ &+ \zeta_{d-k}\left(s-\frac{k}{2}\right)\prod_{j=1}^{k} f_j\left(s-\frac{j-1}{2}\right).\end{aligned} \tag{C.9}$$

The anchor for the recursion is

$$\zeta_1(s) := \sum_{n\in\mathbb{Z}}{}' \left(\frac{2\pi n}{L_d}\right)^{-2s} = 2\left(\frac{L_d}{2\pi}\right)^{2s}\zeta(2s) =: h_d(s). \tag{C.10}$$

We note that the products of f_k functions in (C.9) simplify to

$$\prod_{i=1}^{j-1} f_i\left(s-\frac{i-1}{2}\right) = L_1L_2\cdots L_{j-1}\left(\frac{1}{2\sqrt{\pi}}\right)^{j-1}\frac{\Gamma\left(s-\frac{j-1}{2}\right)}{\Gamma(s)}, \tag{C.11}$$

hence, performing the recursion for $k = d-1$ steps and reinserting the definitions then gives us the following expression

$$\begin{aligned}\zeta_{T^d_{L_1,\ldots,L_d}}(s) = &\frac{2}{\sqrt{\pi}}\left(\frac{1}{2\pi}\right)^{2s}\sum_{j=1}^{d}\pi^{\frac{j}{2}}\frac{\Gamma\left(s-\frac{j-1}{2}\right)}{\Gamma(s)}\zeta(2s-j+1)L_1\cdots L_{j-1}L_j^{2s-j+1}\\ &+\frac{1}{\Gamma(s)}\sum_{j=1}^{d-1}L_1\cdots L_{j-1}\left(\frac{1}{2\sqrt{\pi}}\right)^{j-1}\Gamma\left(s-\frac{j-1}{2}\right)G\left(s-\frac{j-1}{2};L_j,\ldots,L_d\right),\end{aligned} \tag{C.12}$$

with the understanding that for $j=1$ the product $L_1\ldots L_{j-1}$ is simply 1. If we in addition insert the definition of G we can rewrite the complete expression as

$$\begin{aligned}\zeta_{T^d_{L_1,\ldots,L_d}}(s) = &\frac{2}{\sqrt{\pi}}\left(\frac{1}{2\pi}\right)^{2s}\sum_{j=1}^{d}\pi^{\frac{j}{2}}\frac{\Gamma\left(s-\frac{j-1}{2}\right)}{\Gamma(s)}\zeta(2s-j+1)L_1\cdots L_{j-1}L_j^{2s-j+1}\\ &+\frac{2^{2-s}}{\Gamma(s)}\sum_{j=1}^{d-1}L_1\cdots L_{j-1}\frac{L_j^{s-\frac{j-2}{2}}}{(2\pi)^{j/2}}\sum_{\vec{n}\in\mathbb{Z}^{d-j}}{}'\sum_{n_j=1}^{\infty}\left(\frac{n_j}{\sqrt{\vec{n}_{d-j}^{\,T}\,\Xi_{d-j}\,\vec{n}_{d-j}}}\right)^{s-j/2}\\ &\times K_{s-j/2}\left(L_jn_j\sqrt{\vec{n}_{d-j}^{\,T}\,\Xi_{d-j}\,\vec{n}_{d-j}}\right),\end{aligned} \tag{C.13}$$

where in this notation Ξ_{d-j} is $(d-j)\times(d-j)$-matrix obtained from Ξ by removing the first j columns and j rows. From this expression we can now directly calculate $\zeta'_{T^d_{L_1,\ldots,L_d}}(0)$,

as needed for the determinant. Calculating the derivative of the second sum at $s = 0$ is simple, since

$$\frac{1}{\Gamma(\varepsilon)} = \varepsilon + \dots, \qquad \frac{d}{ds}\frac{1}{\Gamma(s)}_{|s=\varepsilon} = 1 + \dots, \qquad \varepsilon \ll 1, \tag{C.14}$$

so the only term that survives is the one where the derivative hits the Γ-function, and we effectively set $s = 0$ everywhere and the Γ-function to 1. For the first sum the situation is a bit trickier, as there are two Γ-functions involved, whose poles cancel only for even j, meaning that we have to separate even and odd j for the calculation. Let us first take a look at the even j part of the first sum, that is $j = 2\ell$, we have

$$\begin{aligned}\frac{d}{ds}\frac{2}{\sqrt{\pi}}\left(\frac{1}{2\pi}\right)^{2s}\sum_{\ell=1}^{\lfloor d/2\rfloor}\pi^{\ell}\frac{\Gamma\left(s-\frac{2\ell-1}{2}\right)}{\Gamma(s)}\zeta(2s-2\ell+1)L_1\cdots L_{2\ell-1}L_{2\ell}^{2s-2\ell+1}\Big|_{s=0}\\ = 2\sum_{\ell=1}^{\lfloor d/2\rfloor}\pi^{\ell-\frac{1}{2}}\frac{L_1\cdots L_{2\ell-1}}{L_{2\ell}^{2\ell-1}}\Gamma\left(\frac{1}{2}-\ell\right)\zeta(1-2\ell).\end{aligned} \tag{C.15}$$

When j is odd, that is $j = 2\ell - 1$, we get

$$\begin{aligned}\frac{d}{ds}\frac{2}{\sqrt{\pi}}\left(\frac{1}{2\pi}\right)^{2s}\sum_{\ell=1}^{\lceil d/2\rceil}\pi^{\ell-1/2}\frac{\Gamma\left(s-\ell+1\right)}{\Gamma(s)}\zeta(2s-2\ell+2)L_1\cdots L_{2\ell-2}L_{2\ell-1}^{2s-2\ell+2}\Big|_{s=0}\\ = -2\log(L_1) + 4\sum_{\ell=1}^{\lceil d/2\rceil-1}\frac{L_1\cdots L_{2\ell}}{L_{2\ell+1}^{2\ell}}\frac{(-\pi)^{\ell}}{\ell!}\zeta'(-2\ell).\end{aligned} \tag{C.16}$$

Before putting everything together, we note that the sums over the modified Bessel functions converge exponentially at $s = 0$ [86]. We can thus introduce the following notation for their limits

$$\begin{aligned}S_{d-j}(L_j,\dots,L_d) := \frac{1}{(2\pi)^{j/2}}\sum_{\vec{n}\in\mathbb{Z}^{d-j}}{}'\sum_{n_j=1}^{\infty}\left(\frac{\sqrt{\vec{n}_{d-j}^{\,T}\,\Xi_{d-j}\,\vec{n}_{d-j}}}{n_j}\right)^{\frac{j}{2}}\\ \times K_{-j/2}\left(L_j n_j\sqrt{\vec{n}_{d-j}^{\,T}\,\Xi_{d-j}\,\vec{n}_{d-j}}\right),\end{aligned} \tag{C.17}$$

where S_{d-j} is convergent for $d > j > 0$. Finally, we obtain

$$\begin{aligned}\zeta'_{T^d_{L_1,\dots,L_d}}(0) = &-2\log(L_1) + 4\sum_{j=1}^{\lceil d/2\rceil-1}\frac{L_1\cdots L_{2j}}{L_{2j+1}^{2j}}\frac{(-\pi)^j}{j!}\zeta'(-2j)\\ &+ 2\sum_{j=1}^{\lfloor d/2\rfloor}\frac{L_1\cdots L_{2j-1}}{L_{2j}^{2j-1}}\frac{(-2\pi)^j}{(2j-1)!!}\zeta(-(2j-1))\\ &+ 4\sum_{j=1}^{d-1}\frac{L_1\cdots L_{j-1}}{L_j^{\frac{j}{2}-1}}S_{d-j}(L_{j+1},\dots,L_d).\end{aligned} \tag{C.18}$$

The expression above gives us the functional determinant for a d-dimensional torus, and despite its intimidating appearance, it is rather straightforward to handle, since the modified Bessel functions hidden in S converge rapidly to zero as the integers n_i increase.

It is instructive to evaluate the $d = 2$ case. First of all, we note that the sum on the first line of (C.18) is empty for $d = 2$. The remaining two sums in (C.18) consist only of the $j = 1$ term, giving us

$$\begin{aligned}\zeta'_{T^2_{L_1,L_2}}(0) &= -2\log L_1 + \frac{\pi}{3}\frac{L_1}{L_2} + 4\sqrt{L_1}S_1(L_2) \\ &= -2\log L_1 + \frac{\pi}{3}\frac{L_1}{L_2} + 2{\sum_{n_2\in\mathbb{Z}}}' \sum_{n_1=1}^{\infty} \frac{e^{-2\pi n_1|n_2|\frac{L_1}{L_2}}}{n_1}\,.\end{aligned}$$

Using more standard conventions, see e.g. [43], introducing the modular parameter $\tau = iL_1/L_2$, as well as defining $q := e^{2\pi i\tau}$, and then performing the sum over n_1, we obtain

$$\begin{aligned}\zeta'_{T^2_{L_1,L_2}}(0) &= -2\log L_1 + \frac{\pi}{3}\frac{L_1}{L_2} + 2{\sum_{n_2\in\mathbb{Z}}}' \sum_{n_1=1}^{\infty} \frac{e^{-2\pi n_1|n_2|\frac{L_1}{L_2}}}{n_1} \\ &= -2\log L_1 - \frac{i\pi}{3}\tau - 4\sum_{m=1}^{\infty}\log\left(1-q^m\right) = -\log\big(L_1^2\eta^4(\tau)\big),\end{aligned} \tag{C.19}$$

where η is the Dedekind η-function, defined as in (E.5). If we denote the area of the 2-torus by A, where $A = L_1L_2$ in our convention,[13] then taking into account the contribution from the zero-mode, the log-determinant and the partition function on the torus can be written as

$$\begin{aligned}\log\det\Delta_{T^2} &= -\zeta'_{T^2_{L_1,L_2}}(0) = \log\big(L_1^2\eta^4(\tau)\big), \\ Z(\tau) &= \sqrt{A}\exp\left(\frac{1}{2}\zeta'_{T^2_{L_1,L_2}}(0)\right) = \frac{1}{\sqrt{\mathrm{Im}(\tau)}\eta^2(\tau)},\end{aligned} \tag{C.20}$$

which is a well known result, see e.g. [43].

C.2 Determinant of the Laplacian on the cut d-torus

We now consider cutting the torus $T^d_{L_1,\ldots,L_d}$ at $x_1 = 0$ and $x_1 = L < L_1$, as shown in figure 4. As discussed in the main body, this gives rise to two subsystems, each of which is a cylinder represented by an interval times a $d-1$-dimensional torus. Imposing Dirichlet boundary conditions (3.21) the eigenvalues of the Laplacian $-\partial_a\partial^a$ are

$$\mu_{m,n_2,\ldots,n_d} = \left(\frac{m\pi}{L}\right)^2 + \lambda_{n_2,\ldots,n_d}, \quad m\in\mathbb{N}^+, \quad n_2,\ldots,n_d\in\mathbb{Z}\,, \tag{C.21}$$

[13] We set here the coupling $g = 1$ as well as $2\pi R_c = 1$, since we are only interested here in checking that our calculations reproduce well known results in literature.

with $\lambda_{n_2,\dots,n_d}$ the eigenvalue on $T^{d-1}_{L_2,\dots,L_d}$. Notice that there is no zero mode now. The spectral ζ-function on this geometry thus takes the form

$$\begin{aligned}\zeta_{[0,L]\times T^{d-1}_{L_2,\dots,L_d}}(s) &:= \sum_{\lambda}\sum_{m=1}^{\infty}\left(\lambda+\left(\frac{m\pi}{L}\right)^2\right)^{-s}\\ &= \left(\frac{L}{\pi}\right)^{2s}\zeta(2s)+\sum_{\lambda}{}'\sum_{m=1}^{\infty}\left(\lambda+\left(\frac{m\pi}{L}\right)^2\right)^{-s},\end{aligned}$$

where we schematically write λ for the $(d-1)$-dimensional toroidal part of the eigenvalue, and we explicitly separate the $(d-1)$-dimensional toroidal zero mode from the rest in the last passage. We can now evaluate the primed sum by means of the identities (E.1), (E.2), and (E.3) collected in appendix E, and we obtain

$$\begin{aligned}&\sum_{\lambda}{}'\sum_{m=1}^{\infty}\left(\lambda+\left(\frac{m\pi}{L}\right)^2\right)^{-s}\\ &\quad=\frac{1}{\Gamma(s)}\sum_{\lambda}{}'\sum_{m=1}^{\infty}\int_0^\infty dt\; t^{s-1}e^{-t\left(\lambda+\left(\frac{m\pi}{L}\right)^2\right)}\\ &\quad=\frac{1}{\Gamma(s)}\sum_{\lambda}{}'\int_0^\infty dt\; t^{s-1}e^{-t\lambda}\sum_{m=1}^{\infty}e^{-t\left(\frac{m\pi}{L}\right)^2}\\ &\quad=\frac{1}{\Gamma(s)}\sum_{\lambda}{}'\int_0^\infty dt\; t^{s-1}e^{-t\lambda}\left(-\frac{1}{2}+\frac{L}{2\sqrt{\pi}}t^{-\frac{1}{2}}+\frac{L}{\sqrt{\pi}}t^{-\frac{1}{2}}\sum_{m=1}^{\infty}e^{-\frac{(mL)^2}{t}}\right)\\ &\quad=-\frac{1}{2}\zeta_{T^{d-1}_{L_2,\dots,L_d}}(s)+\frac{L}{2\sqrt{\pi}}\frac{\Gamma(s-1/2)}{\Gamma(s)}\zeta_{T^{d-1}_{L_2,\dots,L_d}}(s-1/2)\\ &\qquad+\frac{2L^{s+\frac{1}{2}}}{\Gamma(s)\sqrt{\pi}}\sum_{\lambda}{}'\sum_{m=1}^{\infty}\left(\frac{m}{\sqrt{\lambda}}\right)^{s-\frac{1}{2}}K_{s-1/2}\left(2Lm\sqrt{\lambda}\right).\end{aligned}\tag{C.22}$$

Notice that λ is nothing but $\vec{n}_{d-1}\,\Xi_{d-1}\,\vec{n}_{d-1}$ as defined in appendix C.1. Hence, adopting the same notation here, the above term containing the modified Bessel function can be written in terms of the function G as defined in (C.5), and we can finally write the expression for the ζ-function on the cut torus as follows,

$$\begin{aligned}\zeta_{[0,L]\times T^{d-1}_{L_2,\dots,L_d}}(s) &= \left(\frac{L}{\pi}\right)^{2s}\zeta(2s)-\frac{1}{2}\zeta_{T^{d-1}_{L_2,\dots,L_d}}(s)+\frac{L}{2\sqrt{\pi}}\frac{\Gamma(s-1/2)}{\Gamma(s)}\zeta_{T^{d-1}_{L_2,\dots,L_d}}(s-1/2)\\ &\quad+\frac{1}{2}G(s;2L,L_2,\dots,L_d).\end{aligned}\tag{C.23}$$

Finally, the log-determinant is given by

$$\begin{aligned}&\log\det\Delta_{[0,L]\times T^{d-1}_{L_2,\dots,L_d}}\\ &\quad=-\zeta'_{[0,L]\times T^{d-1}_{L_2,\dots,L_d}}(0)\\ &\quad=\log(2L)+\frac{1}{2}\zeta'_{T^{d-1}_{L_2,\dots,L_d}}(0)+L\,\zeta_{T^{d-1}_{L_2,\dots,L_d}}(-1/2)-\frac{1}{2}G'(0;2L,\dots,L_d).\end{aligned}\tag{C.24}$$

Our expression (C.24) agrees with the results of [88] obtained by contour integration.

Let us check that for $d = 2$ we obtain the well-known result for the log determinant of the Laplacian on a cylinder. In this case $T^1_{L_2}$ is nothing but a circle of length L_2, and according to (C.10), we have

$$\zeta_{T^1_{L_2}}(s) = 2\left(\frac{L_2}{2\pi}\right)^{2s}\zeta(2s)\,. \tag{C.25}$$

Hence, we obtain

$$\begin{aligned}\log\det\Delta_{[0,L]\times S^1_{L_2}} &= -\zeta'_{[0,L]\times S^1_{L_2}}(0) = \log\left(2\frac{L}{L_2}\right) - \frac{\pi}{3}\frac{L}{L_2} - 2\sum_{n_2=1}^{\infty}\sum_{n_1=1}^{\infty}\frac{e^{-4\pi\frac{L}{L_2}n_1n_2}}{n_1}\\ &= \log\left(2\frac{L}{L_2}\right) - \frac{\pi}{3}\frac{L}{L_2} + 2\sum_{n_2=1}^{\infty}\log\left(1-e^{-4\pi\frac{L}{L_2}n_2}\right)\,.\end{aligned} \tag{C.26}$$

Introducing modular parameters,

$$\tau = i\frac{L_1}{L_2}\,,\qquad\text{and}\qquad \alpha := \frac{L}{L_1}\,, \tag{C.27}$$

as well as the Dedekind function as in (E.5), we see that we can rewrite the functional determinant on the cylinder as

$$\log\det\Delta_{[0,L]\times S^1_{L_2}} = \log\left(2\alpha|\tau|\,\eta^2(2\alpha\tau)\right)\,. \tag{C.28}$$

This is a well-known result in literature, see e.g. [43, 44]. It is convenient to leave α general, so that we can easily use the above results for the functional determinants for arbitrary cuts.

C.3 Determinant of powers of the Laplacian on the torus

When calculating the entanglement entropy of the GQLM on a d-torus with d even, the determinants that arise are those of even powers of the Laplacian. On the flat d-torus geometry the higher-derivative conformal operator $\mathcal{P}_z$ is indeed just the $z/2$-th power of the standard Laplacian, cf. equation (2.4) in section 2. In order to generalise our previous result, we first make the observation that, since the flat torus as well as the cut torus are compact manifolds, the spectrum of Δ^k is just given by the set of λ^k, where λ is an eigenvalue of Δ as in (C.2) or (C.21) in the case of the d-torus or the cut d-torus respectively. In particular, the spectral ζ-function corresponding to Δ^k is given by

$$\zeta_T(s,k) := {\sum_{\lambda}}'\left(\lambda^k\right)^{-s} = \zeta_T(ks), \tag{C.29}$$

where we write schematically T for either $T^d_{L_1,\ldots,L_d}$ or $[0,L]\times T^{d-1}_{L_2,\ldots,L_d}$, and λ for the corresponding eigenvalues (C.2) or (C.21) respectively. This leads to the simple result for the determinants [89]

$$\log\det\Delta^k_{T^d_{L_1,\ldots,L_d}} = k\log\det\Delta_{T^d_{L_1,\ldots,L_d}}\,, \tag{C.30a}$$

$$\log\det\Delta^k_{[0,L]\times T^{d-1}_{L_2,\ldots,L_d}} = k\log\det\Delta_{[0,L]\times T^{d-1}_{L_2,\ldots,L_d}}\,, \tag{C.30b}$$

where the critical case is found by setting $k = d/2$.

D The winding sector for the *d*-torus

The goal of this appendix is to compute the winding sector contribution (3.37) that originates from cutting the d-torus, as discussed in section 3. In order to do so, we first need to solve the classical equations of motions for the $n-1$ classical fields, (2.12), obeying the boundary conditions (3.29) as well as (3.35). As discussed in section 3, the n-th classical field is reabsorbed into the constrained partition functions to create a free one, cf (3.32), thus here we are only concerned with $n-1$ classical fields.

To facilitate reading, we list here again equations of motion and explicit conditions which the $n-1$ classical fields have to fulfill. The equations of motion are given by

$$\Delta^{z/2}\bar{\phi}_i^{\rm cl} = 0 \quad i = 1, \dots, n-1. \tag{D.1}$$

We solve these equations on the flat torus given by $[-L_B, L_A] \times [0, L_2] \times \ldots \times [0, L_d]$ with the ends of each of the intervals identified and place the cuts Γ_1 at $x_1 = 0$ and Γ_2 at $x_1 = L_A$ (and thus $x_1 = -L_B$). With this, the boundary conditions along the x_1 direction (3.29) for $i = 1, \dots, n-1$ can be rewritten as

$$\bar{\phi}_i^{\rm cl}|_{\Gamma_1}(x) = \bar{\phi}_i^{\rm cl}(0, y) = 0\,, \tag{D.2a}$$
$$\bar{\phi}_i^{\rm cl}|_{\Gamma_2}(x) = 2\pi R_c\, \bar{\omega}_i = \bar{\phi}_i^{\rm cl}(L_A, y) = \bar{\phi}_i^{\rm cl}(-L_B, y) = 2\pi R_c\, \bar{\omega}_i, \tag{D.2b}$$

where we denote $x = (x_1, y) = (x_1, x_2, \dots x_d)$ and $\bar{\omega}_i := (M_{n-1})_{ij}\omega_j$ throughout this section. Notice that the above conditions (D.2a)–(D.2b) have to hold for all the coordinates y in the $d-1$-dimensional torus, i.e. $y \in [0, L_2] \times \ldots \times [0, L_d]$. Along the $d-1$-toroidal directions we have the periodicity conditions

$$\bar{\phi}_i^{\rm cl}(x_1, y) = \bar{\phi}_i^{\rm cl}(x_1, y + \beta)\,, \qquad \beta := (L_2, \dots, L_d)\,. \tag{D.3}$$

The standard way of solving such a partial differential equation is by separation of variables, and here it suffices to separate only the first variable x_1 from the remaining orthogonal $d-1$ directions y, as e.g.

$$\bar{\phi}_i^{\rm cl}(x_1, y) = f_i(x_1)\, g_i(y)\,, \qquad i = 1, \dots, n-1\,. \tag{D.4}$$

The boundary condition (D.2b) shows that $g_i(y)$ can only be a constant for all $i = 1, \dots, n-1$, and from now on we set $g_i(y) = 1$ and work only with the functions $f_i(x_1)$. Hence, the equations of motion and boundary conditions expressed on f_i $(i = 1, \dots, n-1)$ are simply

$$\Delta^{z/2}\bar{\phi}_i^{\rm cl}(x, y) = 0 \quad \Rightarrow \quad \partial_{x_1}^z f_i(x_1) = 0\,, \tag{D.5a}$$
$$\bar{\phi}_i^{\rm cl}(0, y) = 0 \quad \Rightarrow \quad f_i(0) = 0\,, \tag{D.5b}$$
$$\bar{\phi}_i^{\rm cl}(L_A, y) = \bar{\phi}_i^{\rm cl}(-L_B, y) = 2\pi R_c\, \bar{\omega}_i \quad \Rightarrow \quad f_i(L_A) = f_i(-L_B) = 2\pi R_c\, \bar{\omega}_i\,. \tag{D.5c}$$

Notice that the last condition above has to be imposed either at $x_1 = L_A$ or at $x_1 = -L_B$, or, in other words, we solve for classical fields in the region A and in the region B separately and then we glue the solutions at the boundary. As we discussed in section 3,

these conditions (D.5b)–(D.5c) are not sufficient to specify a solution of the equation of motion (D.5a), which is in general a polynomial of degree $z-1$, expressed in terms of z coefficients. A choice of supplementary boundary conditions are given by (3.35), which now imply

$$\begin{aligned}
&\partial_n \Delta^k \bar{\phi}_i^{\rm cl}\big|_{\Gamma_1} = 0 \quad k = 0, \dots, \frac{z}{2}-2\,, \\
&\qquad \Rightarrow\ \partial_{x_1}^{2\ell-1} f_i(0) = 0\,, \quad \ell = 1, \dots, \frac{z}{2}-1, && \text{(D.6a)} \\
&\partial_n \Delta^k \bar{\phi}_i^{\rm cl}\big|_{\Gamma_2} = 0 \quad k = 0, \dots, \frac{z}{2}-2\,, \\
&\qquad \Rightarrow\ \partial_{x_1}^{2\ell-1} f_i(L_A) = \partial_{x_1}^{2\ell-1} f_i(-L_B) = 0\,, \quad \ell = 1, \dots, \frac{z}{2}-1\,. && \text{(D.6b)}
\end{aligned}$$

We then solve the equations respectively in A and B, and glue the solutions at the two cuts, that is the whole solution is given by

$$f_i(x_1) = \begin{cases} f_{i,A}(x_1), & x_1 \in [0, L_A]\,, \\ f_{i,B}(x_1), & x_1 \in [-L_B, 0]\,, \end{cases} \tag{D.7}$$

where

$$f_{i,A(B)}(x_1) = 2\pi R_c\, \bar{\omega}_i \left(a_{z-1} \left(\frac{|x_1|}{L_{A(B)}} \right)^{z-1} + \sum_{k=1}^{z/2-1} a_{2k} \left(\frac{x_1}{L_{A(B)}} \right)^{2k} \right). \tag{D.8}$$

While the explicit value of the coefficients is quite complicated, their i dependence is simple. For instance, for the first few values of z, the functions $f_{i,A}$ read

$$f_{i,A}(x_1) = \begin{cases} 2\pi R_c\, \bar{\omega}_i \frac{|x_1|}{L_A}, & z = 2, \\ 2\pi R_c\, \bar{\omega}_i \Big(-2 \left(\frac{|x_1|}{L_A} \right)^3 + 3 \left(\frac{x_1}{L_A} \right)^2 \Big), & z = 4, \\ 2\pi R_c\, \bar{\omega}_i \Big(\left(\frac{|x_1|}{L_A} \right)^5 - \frac{5}{2} \left(\frac{x_1}{L_A} \right)^4 + \frac{5}{2} \left(\frac{x_1}{L_A} \right)^2 \Big), & z = 6, \\ 2\pi R_c\, \bar{\omega}_i \Big(-\frac{4}{17} \left(\frac{|x_1|}{L_A} \right)^7 + \frac{14}{17} \left(\frac{x_1}{L_A} \right)^6 - \frac{35}{17} \left(\frac{x_1}{L_A} \right)^4 + \frac{42}{17} \left(\frac{x_1}{L_A} \right)^2 \Big), & z = 8, \end{cases}$$

and the same for the functions $f_{i,B}$ after the replacement $L_A \to L_B$. Notice that the functions f_i are continuous everywhere on $A \cup B$, but they are not differentiable at the cuts Γ_1, Γ_2, even though the left and right derivatives exist and are finite. This is not unusual, and it is true already in $d = 2$, see for example the cylindric case in [26, 27].

Now we are ready to evaluate the winding sector contribution (3.37), that is the function

$$\overline{W}(n) = \sum_{\bar{\phi}_i^{\rm cl}} e^{-\sum_{i=1}^{n-1} S[\bar{\phi}_i^{\rm cl}]}\,.$$

The action is given by the bulk term S_0 (2.5) and the boundary part S_∂ (2.10), and it is clear that only the latter will contribute to $\overline{W}(n)$. As it turns out, evaluating $S_\partial[\bar{\phi}_i^{\rm cl}]$ results in the following rather simple closed expression (notice that only the highest derivative term

contributes to the action (2.10)),[14]

$$S[\bar{\phi}_i^c] = g\,\pi^2 R_c^2\,\bar{\omega}_i\cdot\,\bar{\omega}^i\,\frac{(-1)^{z/2}z!}{(1-2^z)B_z}\left(1+\left(\frac{L_A}{L_B}\right)^{z-1}\right)\frac{L_2\cdots L_d}{L_A^{z-1}}\,, \tag{D.9}$$

where the B_z are Bernoulli numbers. Notice that only the case $z = d$ gives a scale invariant winding sector contribution as expected from a critical theory. With this result, we can use the analytic continuation found in appendix F of [27] to write

$$\overline{W}(n) = \sum_{\omega\in\mathbb{Z}^{n-1}} \exp\!\big(-\pi\;\Lambda_z(L_A,L_B,L_2,\ldots,L_d)\;\omega^T\cdot T_{n-1}\omega\big) \tag{D.10}$$

$$= \sqrt{n}\Lambda_z^{-\frac{n-1}{2}}\int_{-\infty}^{\infty}\frac{dk}{\sqrt{\pi}}e^{-k^2}\left[\sum_{\omega\in\mathbb{Z}}\exp\!\left(-\frac{\pi}{\Lambda_z}\omega^2-2i\sqrt{\frac{\pi}{\Lambda_z}}k\,\omega\right)\right]^{n-1}, \tag{D.11}$$

where $T_{n-1} := M_{n-1}^T M_{n-1}$ and

$$\Lambda_z(L_A,L_B,L_2,\ldots,L_d) := g\,\pi\,R_c^2\frac{(-1)^{z/2}z!}{(1-2^z)B_z}\;\frac{L_A^{z-1}+L_B^{z-1}}{L_A^{z-1}L_B^{z-1}}\;L_2\cdots L_d\,. \tag{D.12}$$

The derivative with respect to n at 1 is finally given by

$$-\,\overline{W}'(1) = \log\sqrt{\Lambda_z}-\frac{1}{2}-\int_{-\infty}^{\infty}\frac{dk}{\sqrt{\pi}}e^{-k^2}\log\left(\sum_{\omega\in\mathbb{Z}}\exp\!\left(-\frac{\pi}{\Lambda_z}\omega^2-2i\sqrt{\frac{\pi}{\Lambda_z}}k\,\omega\right)\right). \tag{D.13}$$

In order to make comparison in a more transparent way it is useful to rewrite Λ_z in terms of the aspect ratios of the d-torus. Introducing the dimensionless parameters τ, as well as u the parameter controlling the cut, as follows

$$\tau_k = i\frac{L_1}{L_{k+1}}\,,\qquad k=1\,,\ldots\,,d-1\,,\qquad u=\frac{L_A}{L_1}\,, \tag{D.14}$$

and noticing that $L_B = L_1 - L_A$, we can write

$$\Lambda_z = g\,\pi\,R_c^2\frac{(-1)^{z/2}z!}{(1-2^z)B_z}\;\left(u^{1-z}+(1-u)^{1-z}\right)\frac{1}{|\tau_1|\ldots|\tau_{d-1}|}\,. \tag{D.15}$$

In particular, for $d = 2$ and $z = 2$, we obtain

$$\Lambda_2 = 4\pi\,g\,R_c^2\,\frac{1}{u(1-u)}\frac{1}{|\tau_1|}\,. \tag{D.16}$$

In the semi-infinite limit, that is when $|\tau_1| \gg 1$, the integral in $\overline{W}'(1)$ (D.13) is exponentially suppressed, hence at the leading order in Λ_2 we have

$$-\overline{W}'(1) = \frac{1}{2}\log\left(4\pi\,g\,R_c^2\right)-\frac{1}{2}\log(u(1-u))-\frac{1}{2}\log|\tau_1|-\frac{1}{2}+\ldots\,, \tag{D.17}$$

and for $u = \frac{1}{2}$ this reduces to

$$-\overline{W}'(1) = \frac{1}{2}\log\left(16\pi\,g\,R_c^2\right)-\frac{1}{2}\log|\tau_1|-\frac{1}{2}+\ldots\,. \tag{D.18}$$

[14] As we discussed the classical fields are not differentiable at the cuts, however left and right derivatives exist and they are finite, so here the integrals are evaluated using left and right limits, exactly as in $d = 2$ dimensions.

E Useful formulae

Here we collect some useful formulae and definitions of special functions used in the paper.

The integral representation of the Gamma function immediately leads to

$$\ell^{-s} = \frac{1}{\Gamma(s)} \int_0^\infty dt\; t^{s-1}\; e^{-\ell t}\,. \tag{E.1}$$

The Poisson summation formula is given by

$$\begin{aligned} \sum_{n=1}^{\infty} e^{-an^2} &= -\frac{1}{2} + \frac{1}{2}\sqrt{\frac{\pi}{a}} + \sqrt{\frac{\pi}{a}} \sum_{n=1}^{\infty} e^{-\frac{n^2\pi^2}{a}}\,, \\ \sum_{n=-\infty}^{\infty} e^{-\pi n^2 A + 2\pi n A s} &= \frac{1}{\sqrt{A}} e^{\pi A s^2} \sum_{m=-\infty}^{\infty} e^{-\frac{\pi}{A} m^2 - 2i\pi m s}\,. \end{aligned} \tag{E.2}$$

The integral representation of a modified Bessel function is

$$K_\nu(z) = \frac{1}{2} \int_0^\infty du\; e^{-\frac{z}{2}\left(u+\frac{1}{u}\right)}\; u^{\nu-1}\,, \tag{E.3}$$

and the explicit expression for the special case $\nu = -\frac{1}{2}$ is

$$K_{-\frac{1}{2}}(x) = \sqrt{\frac{\pi}{2}} \frac{e^{-x}}{\sqrt{x}}\,. \tag{E.4}$$

The Dedekind function is defined as follows

$$\eta(\tau) := q^{1/24} \prod_{n=1}^{\infty} (1 - q^n)\,, \qquad q := e^{2i\pi\tau}\,. \tag{E.5}$$

Its expansion for small imaginary argument is given by

$$\eta(i|\tau|) \approx \frac{e^{-\frac{\pi}{12|\tau|}}}{\sqrt{|\tau|}}\,, \qquad \text{as} \qquad |\tau| \to 0^+\,, \tag{E.6}$$

while for large imaginary argument we have

$$\eta(i|\tau|) \sim e^{-\frac{\pi}{12}|\tau|}\,, \qquad \text{as} \qquad |\tau| \to \infty\,. \tag{E.7}$$

References

[1] B. Hsu, M. Mulligan, E. Fradkin and E.-A. Kim, *Universal entanglement entropy in 2D conformal quantum critical points*, *Phys. Rev.* **B 79** (2009) 115421 [arXiv:0812.0203] [INSPIRE].

[2] P. Calabrese and J.L. Cardy, *Entanglement entropy and quantum field theory: a non-technical introduction*, *Int. J. Quant. Inf.* **4** (2006) 429 [quant-ph/0505193] [INSPIRE].

[3] L. Amico, R. Fazio, A. Osterloh and V. Vedral, *Entanglement in many-body systems*, *Rev. Mod. Phys.* **80** (2008) 517 [quant-ph/0703044] [INSPIRE].

[4] J. Eisert, *Colloquium: area laws for the entanglement entropy*, *Rev. Mod. Phys.* **82** (2010) 277.

[5] N. Laflorencie, *Quantum entanglement in condensed matter systems*, *Phys. Rept.* **646** (2016) 1.

[6] C.G. Callan Jr. and F. Wilczek, *On geometric entropy*, *Phys. Lett.* **B 333** (1994) 55 [hep-th/9401072] [INSPIRE].

[7] C. Holzhey, F. Larsen and F. Wilczek, *Geometric and renormalized entropy in conformal field theory*, *Nucl. Phys.* **B 424** (1994) 443 [hep-th/9403108] [INSPIRE].

[8] P. Calabrese and J.L. Cardy, *Entanglement entropy and quantum field theory*, *J. Stat. Mech.* **0406** (2004) P06002 [hep-th/0405152] [INSPIRE].

[9] M. Rangamani and T. Takayanagi, *Holographic entanglement entropy*, *Lect. Notes Phys.* **931** (2017) 1 [arXiv:1609.01287].

[10] T. Nishioka, *Entanglement entropy: holography and renormalization group*, *Rev. Mod. Phys.* **90** (2018) 035007 [arXiv:1801.10352] [INSPIRE].

[11] S.N. Solodukhin, *Entanglement entropy, conformal invariance and extrinsic geometry*, *Phys. Lett.* **B 665** (2008) 305 [arXiv:0802.3117] [INSPIRE].

[12] D.V. Fursaev, A. Patrushev and S.N. Solodukhin, *Distributional geometry of squashed cones*, *Phys. Rev.* **D 88** (2013) 044054 [arXiv:1306.4000] [INSPIRE].

[13] V. Keranen, W. Sybesma, P. Szepietowski and L. Thorlacius, *Correlation functions in theories with Lifshitz scaling*, *JHEP* **05** (2017) 033 [arXiv:1611.09371] [INSPIRE].

[14] E. Ardonne, P. Fendley and E. Fradkin, *Topological order and conformal quantum critical points*, *Annals Phys.* **310** (2004) 493 [cond-mat/0311466] [INSPIRE].

[15] C. Brust and K. Hinterbichler, *Free $\Box^k$ scalar conformal field theory*, *JHEP* **02** (2017) 066 [arXiv:1607.07439] [INSPIRE].

[16] M. Beccaria and A.A. Tseytlin, *Partition function of free conformal fields in 3-plet representation*, *JHEP* **05** (2017) 053 [arXiv:1703.04460] [INSPIRE].

[17] Y. Nakayama, *Hidden global conformal symmetry without Virasoro extension in theory of elasticity*, *Annals Phys.* **372** (2016) 392 [arXiv:1604.00810] [INSPIRE].

[18] T. Griffin, K.T. Grosvenor, P. Hořava and Z. Yan, *Scalar field theories with polynomial shift symmetries*, *Commun. Math. Phys.* **340** (2015) 985 [arXiv:1412.1046] [INSPIRE].

[19] T. Griffin, K.T. Grosvenor, P. Hořava and Z. Yan, *Cascading multicriticality in nonrelativistic spontaneous symmetry breaking*, *Phys. Rev. Lett.* **115** (2015) 241601 [arXiv:1507.06992] [INSPIRE].

[20] A. Strominger, *The dS/CFT correspondence*, *JHEP* **10** (2001) 034 [hep-th/0106113] [INSPIRE].

[21] D. Anninos, T. Hartman and A. Strominger, *Higher spin realization of the dS/CFT correspondence*, *Class. Quant. Grav.* **34** (2017) 015009 [arXiv:1108.5735] [INSPIRE].

[22] E. Fradkin and J.E. Moore, *Entanglement entropy of 2D conformal quantum critical points: hearing the shape of a quantum drum*, *Phys. Rev. Lett.* **97** (2006) 050404 [cond-mat/0605683] [INSPIRE].

[23] B. Hsu and E. Fradkin, *Universal behavior of entanglement in 2D quantum critical dimer models*, *J. Stat. Mech.* **1009** (2010) P09004 [arXiv:1006.1361] [INSPIRE].

[24] J.-M. Stéphan, *Shannon and entanglement entropies of one- and two-dimensional critical wave functions*, *Phys. Rev.* **B 80** (2009) 184421.

[25] M. Oshikawa, *Boundary conformal field theory and entanglement entropy in two-dimensional quantum Lifshitz critical point*, arXiv:1007.3739 [INSPIRE].

[26] M.P. Zaletel, J.H. Bardarson and J.E. Moore, *Logarithmic terms in entanglement entropies of 2D quantum critical points and Shannon entropies of spin chains*, *Phys. Rev. Lett.* **107** (2011) 020402 [arXiv:1103.5452] [INSPIRE].

[27] T. Zhou, X. Chen, T. Faulkner and E. Fradkin, *Entanglement entropy and mutual information of circular entangling surfaces in the $2+1$-dimensional quantum Lifshitz model*, *J. Stat. Mech.* **1609** (2016) 093101 [arXiv:1607.01771] [INSPIRE].

[28] J.-M. Stephan, G. Misguich and V. Pasquier, *Renyi entanglement entropies in quantum dimer models: from criticality to topological order*, *J. Stat. Mech.* **1202** (2012) P02003 [arXiv:1108.1699] [INSPIRE].

[29] J.L. Cardy and I. Peschel, *Finite size dependence of the free energy in two-dimensional critical systems*, *Nucl. Phys.* **B 300** (1988) 377 [INSPIRE].

[30] J.M. Stéphan, S. Furukawa, G. Misguich and V. Pasquier, *Shannon and entanglement entropies of one- and two-dimensional critical wave functions*, *Phys. Rev.* **B 80** (2009) 184421.

[31] J.M. Stéphan, H. Ju, P. Fendley and R.G. Melko, *Entanglement in gapless resonating-valence-bond states*, *New J. Phys.* **15** (2013) 015004.

[32] X. Chen, G.Y. Cho, T. Faulkner and E. Fradkin, *Scaling of entanglement in $2+1$-dimensional scale-invariant field theories*, *J. Stat. Mech.* **1502** (2015) P02010 [arXiv:1412.3546] [INSPIRE].

[33] X. Chen, W. Witczak-Krempa, T. Faulkner and E. Fradkin, *Two-cylinder entanglement entropy under a twist*, *J. Stat. Mech.* **1704** (2017) 043104.

[34] S. Kachru, X. Liu and M. Mulligan, *Gravity duals of Lifshitz-like fixed points*, *Phys. Rev.* **D 78** (2008) 106005 [arXiv:0808.1725] [INSPIRE].

[35] M. Taylor, *Non-relativistic holography*, arXiv:0812.0530 [INSPIRE].

[36] S. Ryu and T. Takayanagi, *Aspects of holographic entanglement entropy*, *JHEP* **08** (2006) 045 [hep-th/0605073] [INSPIRE].

[37] S. Ryu and T. Takayanagi, *Holographic derivation of entanglement entropy from AdS/CFT*, *Phys. Rev. Lett.* **96** (2006) 181602 [hep-th/0603001] [INSPIRE].

[38] V. Keränen and L. Thorlacius, *Holographic geometries for condensed matter applications*, in the proceedings of the 13th *Marcel Grossmann Meeting on Recent Developments in Theoretical and Experimental General Relativity, Astrophysics and Relativistic Field Theories (MG13)*, July 1–7, Stockholm, Sweden (2015), arXiv:1307.2882 [INSPIRE].

[39] S.A. Gentle and S. Vandoren, *Lifshitz entanglement entropy from holographic cMERA*, *JHEP* **07** (2018) 013 [arXiv:1711.11509] [INSPIRE].

[40] T. He, J.M. Magan and S. Vandoren, *Entanglement entropy in Lifshitz theories*, *SciPost Phys.* **3** (2017) 034 [arXiv:1705.01147] [INSPIRE].

[41] M.R. Mohammadi Mozaffar and A. Mollabashi, *Entanglement in Lifshitz-type quantum field theories*, *JHEP* **07** (2017) 120 [arXiv:1705.00483] [INSPIRE].

[42] J.S. Dowker, *Determinants and conformal anomalies of GJMS operators on spheres*, *J. Phys.* **A 44** (2011) 115402 [arXiv:1010.0566] [INSPIRE].

[43] P. Di Francesco, P. Mathieu and D. Senechal, *Conformal field theory*, Graduate Texts in Contemporary Physics, Springer, Germany (1997).

[44] P.H. Ginsparg, *Applied conformal field theory*, in the proceedings of the *Les Houches Summer School in Theoretical Physics: Fields, Strings, Critical Phenomena*, June 28-August 5, Les Houches, France (1988), hep-th/9108028 [INSPIRE].

[45] L.J.M. C.R. Graham, R. Jenne and G.A.J. Sparling, *Conformally invariant powers of the laplacian. I: existence*, *J. London Math. Soc.* **S2-46** (1992) 557.

[46] T.P. Branson, P.B. Gilkey and D.V. Vassilevich, *The asymptotics of the Laplacian on a manifold with boundary. 2*, *Boll. Union. Mat. Ital.* **11B** (1997) 39 [hep-th/9504029] [INSPIRE].

[47] A.R. Gover and K. Hirachi, *Conformally invariant powers of the Laplacian: a complete non-existence theorem*, *J. Amer. Math. Soc.* **17** (2004) 389.

[48] A. Gover, *Laplacian operators and q-curvature on conformally einstein manifolds*, math/0506037.

[49] C.R. Graham, *Conformal powers of the laplacian via stereographic projection*, *SIGMA* **3** (2007) 121 [arXiv:0711.4798].

[50] C. Fefferman and C. R. Graham, *Juhl's formulae for gjms operators and q-curvatures*, arXiv:1203.0360.

[51] S. Paneitz, *A quartic conformally covariant differential operator for arbitrary pseudo-riemannian manifolds (summary)*, *SIGMA* **4** (2008) 036 [arXiv:0803.4331].

[52] A. Juhl, *On conformally covariant powers of the laplacian*, arXiv:0905.3992.

[53] A. Juhl, *Explicit formulas for GJMS-operators and Q-curvatures*, arXiv:1108.0273 [INSPIRE].

[54] H. Baum and A. Juhl, *Conformal differential geometry*, Birkhäuser, Basel Switzerland (2010).

[55] P. Calabrese and J. Cardy, *Entanglement entropy and conformal field theory*, *J. Phys.* **A 42** (2009) 504005 [arXiv:0905.4013] [INSPIRE].

[56] P. Chang and J. Dowker, *Vacuum energy on orbifold factors of spheres*, *Nucl. Phys.* **B 395** (1993) 407.

[57] J.S. Dowker, *Effective action in spherical domains*, *Commun. Math. Phys.* **162** (1994) 633 [hep-th/9306154] [INSPIRE].

[58] J.S. Dowker, *Numerical evaluation of spherical GJMS determinants for even dimensions*, arXiv:1310.0759 [INSPIRE].

[59] J.S. Dowker, *Functional determinants on spheres and sectors*, *J. Math. Phys.* **35** (1994) 4989 [*Erratum ibid.* **36** (1995) 988] [hep-th/9312080] [INSPIRE].

[60] J.S. Dowker, *The boundary F-theorem for free fields*, arXiv:1407.5909 [INSPIRE].

[61] D. Gaiotto, *Boundary F-maximization*, arXiv:1403.8052 [INSPIRE].

[62] I.R. Klebanov, S.S. Pufu and B.R. Safdi, *F-theorem without supersymmetry*, *JHEP* **10** (2011) 038 [arXiv:1105.4598] [INSPIRE].

[63] D.E. Diaz, *Polyakov formulas for GJMS operators from AdS/CFT*, *JHEP* **07** (2008) 103 [arXiv:0803.0571] [INSPIRE].

[64] F. Bugini and D.E. Díaz, *Holographic Weyl anomaly for GJMS operators: one Laplacian to rule them all*, *JHEP* **02** (2019) 188 [arXiv:1811.10380] [INSPIRE].

[65] W. Witczak-Krempa, L.E. Hayward Sierens and R.G. Melko, *Cornering gapless quantum states via their torus entanglement*, *Phys. Rev. Lett.* **118** (2017) 077202 [arXiv:1603.02684] [INSPIRE].

[66] H. Casini and M. Huerta, *Entanglement entropy in free quantum field theory*, *J. Phys.* **A 42** (2009) 504007 [arXiv:0905.2562] [INSPIRE].

[67] P. Bueno and W. Witczak-Krempa, *Holographic torus entanglement and its renormalization group flow*, *Phys. Rev.* **D 95** (2017) 066007 [arXiv:1611.01846] [INSPIRE].

[68] J.S. Dowker, *A technical note on the calculation of GJMS (Rac and Di) operator determinants*, arXiv:1807.11872 [INSPIRE].

[69] A.O. Barvinsky et al., *Heat kernel methods for lifshitz theories*, *JHEP* **06** (2017) 063.

[70] P. Bueno and R.C. Myers, *Universal entanglement for higher dimensional cones*, *JHEP* **12** (2015) 168 [arXiv:1508.00587] [INSPIRE].

[71] P. Bueno, R.C. Myers and W. Witczak-Krempa, *Universality of corner entanglement in conformal field theories*, *Phys. Rev. Lett.* **115** (2015) 021602 [arXiv:1505.04804] [INSPIRE].

[72] P. Bueno, R.C. Myers and W. Witczak-Krempa, *Universal corner entanglement from twist operators*, *JHEP* **09** (2015) 091 [arXiv:1507.06997] [INSPIRE].

[73] P. Bueno and R.C. Myers, *Corner contributions to holographic entanglement entropy*, *JHEP* **08** (2015) 068 [arXiv:1505.07842] [INSPIRE].

[74] P. Bueno and W. Witczak-Krempa, *Bounds on corner entanglement in quantum critical states*, *Phys. Rev.* **B 93** (2016) 045131 [arXiv:1511.04077] [INSPIRE].

[75] I.R. Klebanov, T. Nishioka, S.S. Pufu and B.R. Safdi, *On shape dependence and RG flow of entanglement entropy*, *JHEP* **07** (2012) 001 [arXiv:1204.4160] [INSPIRE].

[76] H. Elvang and M. Hadjiantonis, *Exact results for corner contributions to the entanglement entropy and Rényi entropies of free bosons and fermions in 3d*, *Phys. Lett.* **B 749** (2015) 383 [arXiv:1506.06729] [INSPIRE].

[77] R.-X. Miao, *A holographic proof of the universality of corner entanglement for CFTs*, *JHEP* **10** (2015) 038 [arXiv:1507.06283] [INSPIRE].

[78] D.-W. Pang, *Corner contributions to holographic entanglement entropy in non-conformal backgrounds*, *JHEP* **09** (2015) 133 [arXiv:1506.07979] [INSPIRE].

[79] M. Alishahiha, A.F. Astaneh, P. Fonda and F. Omidi, *Entanglement Entropy for Singular Surfaces in Hyperscaling violating Theories*, *JHEP* **09** (2015) 172 [arXiv:1507.05897] [INSPIRE].

[80] T. Zhou, *Entanglement entropy of local operators in quantum Lifshitz theory*, *J. Stat. Mech.* **1609** (2016) 093106.

[81] M.R. Mohammadi Mozaffar and A. Mollabashi, *Entanglement evolution in Lifshitz-type scalar theories*, *JHEP* **01** (2019) 137 [arXiv:1811.11470] [INSPIRE].

[82] E. Plamadeala and E. Fradkin, *Scrambling in the quantum Lifshitz model*, *J. Stat. Mech.* **1806** (2018) 063102.

[83] H. Srivastava and J. Choi, *Zeta and q-zeta functions and associated series and integrals*, Elsevier, The Netherlands (2012).

[84] E. Barnes, *The theory of the moltiple Gamma function*, *Trans. Camb. Philos. Soc.* **19** (1904) 374.

[85] V.S. Adamchik, *Multiple gamma function and its application to computation of series*, submitted to *Ramanujan J.* (2003), math/0308074.

[86] E. Elizalde, *Multidimensional extension of the generalized Chowla-Selberg formula*, *Commun. Math. Phys.* **198** (1998) 83 [hep-th/9707257] [INSPIRE].

[87] E. Elizalde, *Ten physical applications of spectral zeta functions*, Lecture Notes in Physics volume 855, Springer, Germany (2012).

[88] K. Kirsten, P. Loya and J. Park, *Zeta functions of Dirac and Laplace-type operators over finite cylinders*, *Annals Phys.* **321** (2006) 1814 [INSPIRE].

[89] E. Elizalde and M. Tierz, *Multiplicative anomaly and zeta factorization*, *J. Math. Phys.* **45** (2004) 1168 [hep-th/0402186] [INSPIRE].

Paper II

Logarithmic negativity in quantum Lifshitz theories

Angel-Ramelli, J., Berthiere, C., Puletti, V.G.M. & Thorlacius, L.
J. High Energ. Phys. **2020**, 11 (2020).

Note: The margins of the paper were trimmed to better fit the format of this thesis.

Published for SISSA by Springer

Received: *February 24, 2020*
Accepted: *July 31, 2020*
Published: *September 1, 2020*

Logarithmic negativity in quantum Lifshitz theories

J. Angel-Ramelli,[a] **C. Berthiere,**[b] **V. Giangreco M. Puletti**[a] **and L. Thorlacius**[a]

[a] *University of Iceland, Science Institute, Dunhaga 3, 107 Reykjavík, Iceland*
[b] *Department of Physics, Peking University, Beijing 100871, China*

E-mail: jfa1@hi.is, clement.berthiere@pku.edu.cn, vgmp@hi.is, lth@hi.is

Abstract: We investigate quantum entanglement in a non-relativistic critical system by calculating the logarithmic negativity of a class of mixed states in the quantum Lifshitz model in one and two spatial dimensions. In 1+1 dimensions we employ a correlator approach to obtain analytic results for both open and periodic biharmonic chains. In 2+1 dimensions we use a replica method and consider spherical and toroidal spatial manifolds. In all cases, the universal finite part of the logarithmic negativity vanishes for mixed states defined on two disjoint components. For mixed states defined on adjacent components, we find a non-trivial logarithmic negativity reminiscent of two-dimensional conformal field theories. As a byproduct of our calculations, we obtain exact results for the odd entanglement entropy in 2+1 dimensions.

Keywords: Field Theories in Higher Dimensions, Field Theories in Lower Dimensions, Conformal Field Theory

ArXiv ePrint: 2002.05713

https://doi.org/10.1007/JHEP09(2020)011

Contents

1 Introduction

Over the past decade, quantum information theory has led to important insights and advances in several areas of physics including quantum field theory, condensed matter physics, and quantum gravity. Central to these developments is the concept of quantum entanglement, which constitutes a fundamental characteristic distinguishing quantum systems from classical ones. Quantum entanglement can be characterised in different ways and there is no single measure that captures all aspects of entanglement for all quantum systems. One particular measure, that has been the focus of numerous studies, is the entanglement entropy associated with a state described by a density matrix ρ, and a subsystem A of the full system $A \cup B$. It is defined as $S_A = -\mathrm{Tr}\,(\rho_A \log \rho_A)$, where the reduced density matrix is $\rho_A = \mathrm{Tr}_B\, \rho$ and the Hilbert space of the full system is assumed to factorise, $\mathcal{H} = \mathcal{H}_A \otimes \mathcal{H}_B$. This last assumption fails in practice for systems described by local quantum field theories, and this is manifested by short distance divergences appearing in the entanglement entropy. The leading divergence is usually a power law in the UV cutoff with a coefficient proportional to the area of the entangling surface that separates the subsystems. In the case of quantum critical theories, the entanglement entropy typically has a sub-leading logarithmic divergence with a scheme independent *universal* coefficient that encodes information about long-range entanglement in the system. In the present paper we will consider a class of quantum critical theories and focus our attention exclusively on the universal terms.

The entanglement entropy is particularly useful when the full system is in a pure quantum state, but this is rather restrictive. In practice, one often has limited information about the system in question and needs to work with mixed quantum states. Thermal states are archetypal examples of such states, and, in this case, the entanglement entropy is no longer a good measure of quantum entanglement in the sense that it includes contributions from both quantum and classical correlations. Other ways of quantifying entanglement besides entanglement entropy should then be introduced — and they are legion [1–3]. A few important representatives are the entanglement cost and distillable entanglement [4], the entanglement of formation [5], and the logarithmic negativity [6, 7]. In the crowded field of measures of bipartite entanglement for mixed states, the logarithmic negativity stands out as being actually computable. Indeed, most of the other entanglement measures, including the aforementioned, involve a minimisation over infinitely many quantum states, thus rendering them extremely difficult (if not impossible) to evaluate analytically in a quantum field theory setting.

In the present work we consider the quantum entanglement of mixed states in a class of critical quantum field theories. For technical reasons we focus on mixed states that are simple to construct starting from a pure state but still reflect the essential issues arising for generic mixed states. Beginning with a system in a pure state, we take two non-overlapping subsystems, A_1 and A_2, that are not complements of one another (i.e. their complement defines a third subsystem B) and consider the reduced density matrix on $A = A_1 \cup A_2$, which is in general that of a mixed state. In a finite-dimensional Hilbert space, any mixed state can be purified by viewing it as a reduction of a pure state in a larger Hilbert space. In a quantum field theory the corresponding question is more subtle, but the states we consider are purified by construction.

The logarithmic negativity introduced in [7] is defined as follows. Let ρ_A be the density matrix of a bipartite system $A = A_1 \cup A_2$ in a pure or mixed state. We further suppose that the Hilbert space corresponding to our system factorises as $\mathcal{H} = \mathcal{H}_{A_1} \otimes \mathcal{H}_{A_2}$, and define $|e_i^{(1)}\rangle$ and $|e_i^{(2)}\rangle$ to be orthonormal basis states of $\mathcal{H}_{A_1}$ and $\mathcal{H}_{A_2}$, respectively, such that their tensor products $|e_i^{(1)}\rangle \otimes |e_j^{(2)}\rangle \equiv |e_i^{(1)} e_j^{(2)}\rangle$ form a basis of $\mathcal{H}$. The partial transposition of the density matrix, with respect to $\mathcal{H}_{A_2}$, is an operator $\rho_A^{T_2}$ acting on $\mathcal{H}_{A_1} \otimes \mathcal{H}_{A_2}$ with matrix elements in the $|e_i^{(1)} e_j^{(2)}\rangle$ basis given by

$$\langle e_i^{(1)} e_j^{(2)}| \, \rho_A^{T_2} \, |e_k^{(1)} e_l^{(2)}\rangle \equiv \langle e_i^{(1)} e_l^{(2)}| \, \rho_A \, |e_k^{(1)} e_j^{(2)}\rangle \,. \tag{1.1}$$

In other words, the matrix elements of $\rho_A^{T_2}$ are obtained from those of ρ_A by simply swapping basis elements $|e_j^{(2)}\rangle \leftrightarrow |e_l^{(2)}\rangle$ in $\mathcal{H}_{A_2}$. Then the logarithmic negativity is obtained as

$$\mathcal{E} = \log ||\rho_A^{T_2}|| \,, \tag{1.2}$$

where the trace norm $||\mathcal{O}|| \equiv \mathrm{Tr}\sqrt{\mathcal{O}^\dagger \mathcal{O}}$ is the sum of the absolute values of the eigenvalues of the operator $\mathcal{O}$. Its relevance relies on a crucial observation [8, 9]: A necessary condition for the separability of the density matrix ρ_A (that is for the system to be in a non-entangled state) is that its partial transpose (as e.g. $\rho_A^{T_2}$) is also a density matrix, which means that its spectrum is non-negative. Partial transposition is not a unitary operation, and a non-vanishing $\mathcal{E}$ in (1.2) detects when the system fails to be separable. The logarithmic negativity, despite not being convex, is an entanglement monotone [10], both under local quantum operations and classical communication (LOCC) and under positive partial transpose preserving operations (PPT). It is also additive and provides bounds on certain other measures [7]. For pure states, the logarithmic negativity does not reduce to the entanglement entropy but instead coincides with the Rényi entropy of order 1/2.

A replica method was developed in [11, 12] for calculating the logarithmic negativity in many-body systems. In essence, the replica method relates the negativity to the traces of integer powers of $\rho_A^{T_2}$. Since the eigenvalues of $\rho_A^{T_2}$ are not guaranteed to be positive, the traces $\mathrm{Tr}\left(\rho_A^{T_2}\right)^n$ are sensitive to the parity of n. Denoting by n_e (n_o) the even (odd) integers, we obtain the trace norm by analytic continuation of the even sequence at $n_e \to 1$, so that the logarithmic negativity reads

$$\mathcal{E} = \lim_{n_e \to 1} \log \mathrm{Tr}\left(\rho_A^{T_2}\right)^{n_e} . \tag{1.3}$$

This approach has been extensively applied to ground states in conformal field theory (CFT) [11–16], but also at finite temperature [17, 18] and in out-of-equilibrium situations [19–21], as well as to topological systems [22, 23].

In this paper, we are interested in a certain class of non-relativistic quantum field theories — those admitting Lifshitz symmetry. Lifshitz field theories exhibit anisotropic scaling between space and time,

$$t \to \lambda^z \, t \,, \qquad \mathbf{x} \to \lambda \, \mathbf{x} \,, \tag{1.4}$$

with characteristic dynamical exponent $z > 1$. Non-relativistic theories are especially relevant in the context of condensed matter physics. In particular, the Lifshitz theory in

$2+1$ dimensions with dynamical exponent $z = 2$, referred to as the quantum Lifshitz model (QLM) [24], is known to describe a quantum phase transition in systems, such as quantum dimer models [24, 25], between a uniform phase and a phase with spontaneously broken translation invariance in two spatial dimensions. The $(2+1)$-dimensional QLM was generalised to $d+1$ dimensions with a critical exponent $z = d$ in [26] where this special class of Lifshitz theories was named generalised quantum Lifshitz models (GQLMs). A key feature of these $(d+1)$-dimensional Lifshitz field theories with (even) positive integer z is that the ground state wave-functional takes a local form, given in terms of the action of a d-dimensional Euclidean CFT. The local nature of the ground state makes these theories rare examples of non-relativistic theories which admit analytic treatment. The entanglement properties of ground states of quantum Lifshitz theories have been extensively studied [27–35] using analytic and numerical methods.

In the present paper, we extend the work on entanglement in Lifshitz field theories by evaluating analytically the logarithmic negativity for a class of bipartite mixed states in the quantum Lifshitz model. The mixed states are obtained by tracing out the degrees of freedom of one of the subsystems in a tripartite pure state, which for us will be the ground state of the QLM. We adopt two different approaches to the calculation of logarithmic negativity. First, we employ the so-called correlator method [36, 37], which in essence discretises the theory on a lattice. For this part we consider the $(1+1)$-dimensional version of the theory with Lifshitz exponent $z = 2$. We then compute the logarithmic negativity by means of the replica method [11, 12], with focus on the $(2+1)$-dimensional QLM defined on two different spatial manifolds, a 2-sphere and a 2-torus.

In both approaches, we start the discussion by considering a bipartite system in its ground state and confirm that in this case the logarithmic negativity reduces to the $n = 1/2$ Rényi entropy, as it should for a system in a pure state [11, 12]. After that, we investigate a system in a more general mixed state, obtained by partially tracing over the ground state of a bipartite system, resulting in a reduced density matrix ρ_A. We then further divide the subsystem A into A_1 and A_2 and partially transpose over A_2 in order to compute the logarithmic negativity. At this point, we analyse two different cases, depending on whether the subsystems A_1 and A_2 are disjoint or adjacent when viewed as part of the original tripartite system.

Interestingly, the logarithmic negativity turns out to vanish for disjoint subsystems in the QLM, both in one and two spatial dimensions. This is unexpected in a gapless system and is in sharp contrast with 2d CFT [11, 12]. The physical origin of this effect is not clear to us but it is a robust result that we obtain using two different approaches: a correlator method for a discrete theory in one spatial dimension and a replica method for a continuum theory in two spatial dimensions. In the discrete non-compact theory, the reduced density matrix on disjoint intervals for the open chain is separable,[1] which is in general a stronger result than the vanishing of the logarithmic negativity. It remains an open question whether the corresponding reduced density matrix for disjoint submanifolds, obtained via the replica method is also separable. Similar results were found previously

[1] Perhaps this has its origin in the local nature of the ground state.

for the topological logarithmic negativity in Chern-Simons theory [22, 23], as well as in a $(1+1)$-dimensional system with $z = 2$ Lifshitz scaling [38], that is closely related to our discrete theory. The resemblance between QLM and topological theories was first noted in [27, 29, 33], where the entanglement entropy for the QLM was found to exhibit a finite sub-leading universal term analogous to the topological entanglement entropy. For adjacent subsystems we obtain a non-trivial logarithmic negativity, which is somewhat closer to $2d$ CFT results [11, 12].

A numerical study of logarithmic negativity in Lifshitz theories in one and two spatial dimensions for arbitrary z was carried out in [39]. Our findings partially confirm their results, but we emphasise that our approach is entirely analytical. By concentrating on the QLM with $z = 2$, we are able to obtain closed form expressions for the logarithmic negativity, both in the correlator approach and the replica method. As far as we know, this is the first time the replica method is used to compute the logarithmic negativity in Lifshitz theories, and, for the discrete theory in one spatial dimension, we have obtained moments of the $z = 2$ QLM reduced density matrix and its partial transpose in analytic form — something that is still beyond reach for the relativistic boson ($z = 1$). In the present work, we have chosen to focus on the special case of $z = 2$ and $d = 1$ or 2, but several of our results generalise to other values of z and d and we comment on this along the way.

As a by-product of our study we also obtain the so-called odd entanglement entropy, or odd entropy for short, in the $(2+1)$-dimensional QLM. The main motivation for considering the odd entropy is to have an entanglement measure that directly computes the entanglement wedge cross section in holographic two-dimensional CFTs [40].

The paper is organised as follows. In section 2.1 we briefly review key definitions for the QLM. In section 2 we obtain the logarithmic negativity in a $(1+1)$-dimensional model by means of the correlator method. We then proceed in section 3 to calculate the logarithmic negativity via a replica method using path integrals. Our results on odd entropy are presented in section 4 and in section 5 we conclude with a discussion and some open questions. Some technical details related to the correlator method appear in appendix B, and details related to the replica approach are found in appendices C and D. Appendix E completes section 4 on odd entropy, and this work.

2 Logarithmic negativity from correlation functions

2.1 The quantum Lifshitz model

The (2+1)-dimensional quantum Lifshitz model, with critical exponent $z = 2$ on the spatial manifold $\mathcal{M}$, is a quantum field theory involving a compact scalar field $\phi \sim \phi + 2\pi R_c$ defined by the Hamiltonian [24]

$$H = \frac{1}{2}\int_{\mathcal{M}} \mathrm{d}^2x \left(\pi^2 + g^2(\triangle\phi)^2\right), \tag{2.1}$$

where $\pi = -i\delta/\delta\phi$ is the momentum conjugate to the field, $\triangle$ is the Laplacian on $\mathcal{M}$, and g is a free parameter of the model. The ground state can be expressed in terms of a path

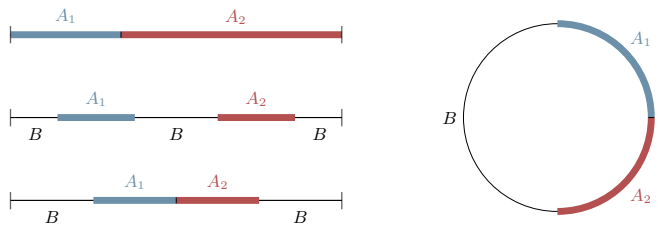

Figure 1. Entanglement between two intervals A_1 and A_2 embedded in the ground state of a (larger) system formed by the union of A_1, A_2 and the complement B. Left: open system with Dirichlet boundary conditions at both ends. Right: Periodic system.

integral of a two-dimensional Euclidean theory [24],

$$|\Psi_0\rangle = \frac{1}{\sqrt{Z_{\mathcal{M}}}} \int \mathcal{D}\phi \; e^{-\frac{1}{2}S[\phi]} |\phi\rangle, \qquad S[\phi] = g \int_{\mathcal{M}} \mathrm{d}^2x \; (\nabla\phi)^2, \tag{2.2}$$

with the partition function given by $Z_{\mathcal{M}} := \int \mathcal{D}\phi \; e^{-S[\phi]}$. We denote the corresponding density matrix by

$$\rho := |\Psi_0\rangle\langle\Psi_0| = \frac{1}{Z_{\mathcal{M}}} \int \mathcal{D}\phi \mathcal{D}\phi' \; e^{-\frac{1}{2}(S[\phi]+S[\phi'])} |\phi\rangle\langle\phi'|. \tag{2.3}$$

A $1+1$-dimensional quantum Lifshitz model with $z = 2$ can be defined in analogous fashion, with the Laplacian replaced by ∂_x^2 and the integration measure by $\mathrm{d}x$. We will take the scalar field to be *non-compact* in the $1+1$-dimensional case.

Generalisations to higher spatial dimensions d and even integer critical exponents z are possible, with some restrictions [26, 34]. For instance, when the spatial manifold is a d-sphere the even critical exponent z is required to satisfy $z \leq d$ in order to guarantee a well-defined GJMS-operator [34, 41]. Generalizations to higher odd integer values of z are less understood and will not be considered here. Since the physically relevant systems are in one and two spatial dimensions, we will restrict our calculations to $d = 1$ and $d = 2$, but point out whenever our results are valid beyond those cases.

2.2 Logarithmic negativity from correlator method

The correlator method for computing the entanglement entropy or logarithmic negativity of Gaussian states has a long tradition [12, 36, 37, 39, 42–48]. This method has been almost exclusively employed as a numerical one, often as a check of field theory predictions. Here, we focus on the $(1+1)$-dimensional free Lifshitz scalar field with dynamical exponent $z = 2$ in its ground state. We obtain simple closed form results for the Rényi entropies and logarithmic negativity for the discrete theory on a one-dimensional lattice, which are then easily translated to the continuum.

Discrete theory and boundary conditions. The Hamiltonian of a non-compact free massless scalar field ϕ with dynamical exponent $z = 2$ in $1 + 1$ dimensions is given by

$$H = \frac{1}{2} \int_{\mathcal{M}} dx \left(\pi^2 + \phi \, \partial_x^4 \, \phi \right) , \tag{2.4}$$

where $\mathcal{M}$ is the one-dimensional line with open or periodic boundary condition. Without loss of generality, we have set to unity the constant g appearing in front of the spatial derivatives. Discretising the theory on a lattice with L sites, the above Hamiltonian is replaced by

$$H = \frac{1}{2} \left(\pi^T \pi + \phi^T K \phi \right) , \tag{2.5}$$

where $\phi^T = (\phi_1, \phi_2, \cdots, \phi_L)$, $\pi^T = (\pi_1, \pi_2, \cdots, \pi_L)$, and the matrix K is a discrete version of the spatial biharmonic operator $\triangle^2 \equiv \partial_x^4$. Static solutions of the Hamiltonians (2.4) and (2.5) satisfy

$$\triangle^2 \phi = 0 , \qquad \text{and} \qquad K\phi = 0 , \tag{2.6}$$

respectively, with some specified boundary conditions at the boundary $\partial\mathcal{M}$ of the space/lattice. The biharmonic equation requires additional boundary conditions compared to the standard Laplace equation. In the continuum theory a natural "Dirichlet" boundary condition is given by

$$\phi|_{\partial\mathcal{M}} = 0 , \quad \text{and} \quad \triangle\phi|_{\partial\mathcal{M}} = 0 . \tag{2.7}$$

A lattice version of this Dirichlet condition can be implemented as follows. First, introduce degrees of freedom on fictitious lattice sites at the boundaries, ϕ_{-1}, ϕ_0, ϕ_{L+1}, ϕ_{L+2} and impose the lattice biharmonic equation of motion,

$$\phi_{i-2} - 4\phi_{i-1} + 6\phi_i - 4\phi_{i+1} + \phi_{i+2} = 0 , \tag{2.8}$$

for $i = 1, \ldots L$, where we have set the lattice spacing ϵ to unity for simplicity. The fictitious fields appear in the equations for ϕ_1, ϕ_2, ϕ_{L-1} and ϕ_L but they can be eliminated by imposing a discrete version of the Dirichlet conditions $\phi|_{\partial\mathcal{M}} = 0$ and $\triangle\phi|_{\partial\mathcal{M}} = 0$, given by

$$\phi_0 = 0 , \quad \text{and} \quad -\phi_{-1} + 2\phi_0 - \phi_1 = 0 , \tag{2.9}$$

at $i = 0$, and similarly at $i = L + 1$. With these boundary conditions, the matrix K is indeed simply the square of the discrete Laplacian matrix with standard Dirichlet boundary conditions. Alternatively, one can impose periodic boundary conditions on the lattice. The resulting K is the square of the usual discrete Laplacian matrix with periodic boundary conditions. Note, however, that the matrix K has a vanishing eigenvalue for a periodic chain and is non-invertible unless a mass term is added to the Hamiltonian (2.5).

Correlation functions, reduced density matrix and partial transpose. Vacuum two-point functions are given by

$$X_{ij} \equiv \langle \phi_i \phi_j \rangle = \frac{1}{2} (K^{-1/2})_{ij} , \quad \text{and} \quad P_{ij} \equiv \langle \pi_i \pi_j \rangle = \frac{1}{2} (K^{1/2})_{ij} . \tag{2.10}$$

The reduced density matrix ρ_A can easily be related [37] to the correlation matrices X and P restricted to the subsystem A (denoted hereafter X_A and P_A). In particular, from the eigenvalues $\{\nu_i\}_{i=1,\cdots,\ell}$ of $C_A = \sqrt{X_A P_A}$ for a region A of size ℓ, the trace of the n^{th} power of the reduced density matrix ρ_A reads

$$\mathrm{Tr}\,\rho_A^n = \prod_{i=1}^{\ell} \left[\left(\nu_i + \frac{1}{2}\right)^n - \left(\nu_i - \frac{1}{2}\right)^n \right]^{-1}, \tag{2.11}$$

from which one easily obtains the Rényi entropies

$$S_A^{(n)} = \frac{1}{1-n} \log \mathrm{Tr}\,\rho_A^n \,. \tag{2.12}$$

Now consider a tripartite system with $A = A_1 \cup A_2$. The partial transposition with respect to, e.g., A_2, for a bosonic Gaussian state, corresponds to time reversal applied only on the momenta corresponding to the subsystem A_2 [36]. The partially transposed reduced density matrix $\rho_A^{T_2}$ thus remains a Gaussian matrix. We introduce the matrices

$$P_A^{T_2} = T_2 \cdot P_A \cdot T_2 \,, \tag{2.13}$$

$$T_2 = \mathbb{1}_{\ell_1} \oplus (-\mathbb{1}_{\ell_2}) \,, \tag{2.14}$$

where ℓ_1, ℓ_2 are the lengths of the intervals A_1, A_2, respectively, such that $\ell = \ell_1 + \ell_2$. The trace of the n^{th} power of $\rho_A^{T_2}$ can then be computed from the eigenvalues $\{\lambda_i\}_{i=1,\cdots,\ell}$ of $C_A^{T_2} \equiv \sqrt{X_A P_A^{T_2}}$ as

$$\mathrm{Tr}\left(\rho_A^{T_2}\right)^n = \prod_{i=1}^{\ell} \left[\left(\lambda_i + \frac{1}{2}\right)^n - \left(\lambda_i - \frac{1}{2}\right)^n \right]^{-1}, \tag{2.15}$$

from which the trace norm follows straightforwardly

$$||\rho_A^{T_2}|| = \prod_{i=1}^{\ell} \left[\left|\lambda_i + \frac{1}{2}\right| - \left|\lambda_i - \frac{1}{2}\right| \right]^{-1} = \prod_{i=1}^{\ell} \max\left(1, \frac{1}{2\lambda_i}\right). \tag{2.16}$$

Finally, the logarithmic negativity is given by

$$\mathcal{E} = \sum_{i=1}^{\ell} \log\left[\max\left(1, \frac{1}{2\lambda_i}\right) \right]. \tag{2.17}$$

Notice that only the eigenvalues that satisfy $\lambda_i < 1/2$ contribute to the logarithmic negativity.

2.3 Rényi entropies

We start by computing Rényi entropies for a single interval in a bipartite pure state. This allows us to carry out a simple consistency check of our calculations in the discrete model by evaluating the logarithmic negativity for the same interval and confirming that it reduces to the Rényi entropy of order $n = 1/2$, as it should for a pure state.

Open system. For a finite chain of L lattice sites with Dirichlet boundary conditions at both ends, the vacuum two-point functions (2.10) take a simple form,

$$X_{ij} = \frac{1}{2(L+1)} \begin{cases} i(L-j+1)\,, & i \le j \\ j(L-i+1)\,, & i > j \end{cases} \tag{2.18}$$

$$P_{ij} = \delta_{ij} - \frac{1}{2}(\delta_{i,j-1} + \delta_{i-1,j})\,. \tag{2.19}$$

Taking an interval $A_1 = [1, \ell]$ adjacent to one of the boundaries ($A_2 = \bar{A}_1$, see figure 1 top-left panel), one finds that the matrix C_{A_1} is triangular with spectrum

$$\text{Spectrum}(C_{A_1}) = \left\{ \frac{1}{2}\sqrt{\frac{(\ell+1)(L-\ell+1)}{L+1}},\, \frac{1}{2},\, \cdots,\, \frac{1}{2} \right\}. \tag{2.20}$$

Quite remarkably, only one eigenvalue, $\nu \equiv \nu_1$, contributes to the entropy. Plugging ν in (2.12) yields exact expressions for the Rényi entropies.

We can access the continuum regime of the theory by reintroducing the lattice spacing ϵ into the notation via $L \to L/\epsilon$ and $\ell \to \ell/\epsilon$, and taking the limit $\epsilon \to 0$. The continuum Rényi entropies read

$$S^{(n)}_{A_1} = \frac{1}{2}\log\left(\frac{\ell(L-\ell)}{\epsilon L}\right) + \frac{1}{n-1}\log\left(2^{1-n}n\right). \tag{2.21}$$

The leading term in (2.21) is independent of the Rényi index n as expected [27], and agrees with the results of [38, 49] where the Renyi entropies were obtained by mapping the ground state of the $z = 2$ boson to that of a path integral for a quantum mechanical particle. The finite part is non universal and depends on how one regulates the theory in the UV.

Periodic system. For periodic boundary conditions, the K matrix of a finite biharmonic chain is a circulant matrix. It is non-invertible due to a zero eigenvalue but the zero mode can be lifted by adding a mass term, $\frac{1}{2}m^4\phi^2$, to the Hamiltonian (2.4) resulting in

$$K = \text{circ}(6 + m^4, -4, 1, 0, \cdots, 0, 1, -4)\,. \tag{2.22}$$

The mass m has dimensions of inverse length and is measured in units of the inverse lattice spacing ϵ^{-1}, which has been set to one as before.

We are interested in the critical regime, that is $m \to 0$ and $mL \ll 1$, for which the eigenvalues of C_{A_1} constructed from the circulant matrix K on a single interval A_1 of size ℓ reduce to

$$\text{Spectrum}(C_{A_1}) = \left\{ \frac{1}{\sqrt{2m^2L}},\, \frac{1}{2}\sqrt{\frac{(\ell+1)(L-\ell+1)}{2L}},\, \frac{1}{2},\, \cdots,\, \frac{1}{2} \right\}. \tag{2.23}$$

If we reinstate the lattice spacing ϵ and take the continuum limit as before, we obtain the following expression for the single interval Rényi entropies,

$$S^{(n)}_{A_1} = \frac{1}{2}\log\left(\frac{\ell(L-\ell)}{\epsilon L}\right) - \frac{1}{2}\log\left(\epsilon m^2 L\right) + \frac{2}{n-1}\log\left(2^{1-n}n\right) + \cdots, \tag{2.24}$$

where the ellipsis denotes terms vanishing in the limits $mL \ll 1$, $\epsilon \to 0$.

2.4 Logarithmic negativity

Let us now turn to the logarithmic negativity. We have to compute the eigenvalues of the matrix $C_A^{T_2}$, defined above (2.15), for a bipartite (sub)system $A = A_1 \cup A_2$ of the $z = 2$ chain. We first consider the pure state case, for which A is the whole system, then we move on to the configuration of two disjoint intervals A_1 and A_2, and finally we let A_1 and A_2 be adjacent.

2.4.1 Pure states

When ρ_A is pure, A_2 is the complement of A_1, and $\ell_1 = L - \ell_2$, see figure 1 top-left panel. In that case, for the open chain, there is only one eigenvalue of $C_A^{T_2}$ that satisfies $\lambda_i < 1/2$, that is

$$\lambda^2 = 2\nu\Big(\nu - \sqrt{\nu^2 - 1/4}\Big) - 1/4\,, \tag{2.25}$$

where ν is the single eigenvalue of C_{A_1} in (2.20), with $\ell \equiv \ell_1$, that is distinct from $1/2$. After some algebra, one obtains that the logarithmic negativity of this bipartite pure state is, as expected, the Rényi entropy of order $1/2$, i.e. $\mathcal{E}(\rho_{A_1\cup A_2}) = S_{A_1}^{(1/2)}$.

Similarly, for the periodic chain in the critical regime, only two eigenvalues of $C_A^{T_2}$ contribute to the logarithmic negativity, i.e.

$$\lambda_1^2 = \frac{m^2 L}{32}\,, \qquad \lambda_2^2 = 2\nu\Big(\nu - \sqrt{\nu^2 - 1/4}\Big) - 1/4\,, \tag{2.26}$$

where ν is the second eigenvalue of C_{A_1} in (2.23), with $\ell \equiv \ell_1$. One can then check that for the periodic case as well, the logarithmic negativity reduces to the $(1/2)$-Rényi entropy of A_1.

2.4.2 Two disjoint intervals

Now let A be a subsystem of the $z = 2$ open chain of length L and further divide A into two subsystems, $A = A_1 \cup A_2$ with A_1 and A_2 disjoint, as for example depicted in figure 1 middle-left panel. First, take A_1 and A_2 to be of the same size $\ell_1 = \ell_2 = \ell$ and each adjacent to one of the boundaries of the total system. The distance between A_1 and A_2 is then $d = L - 2\ell > 0$. We find in that case,

$$\text{Spectrum}(C_A^{T_2}) = \left\{ \frac{\sqrt{\ell+1}}{2}, \frac{1}{2}\sqrt{\frac{(\ell+1)(L-2\ell+1)}{L+1}}, \frac{1}{2}, \cdots, \frac{1}{2} \right\}. \tag{2.27}$$

A quick inspection of the spectrum (2.27) of $C_A^{T_2}$ reveals that not a single eigenvalue is smaller than $1/2$. We thus conclude that the logarithmic negativity vanishes, $\mathcal{E} = 0$, for this configuration of two disjoint intervals. This result may seem surprising. It is, however, a consequence of the separability of the reduced density matrix. To arrive at that conclusion, we rely on the following statement proven in [50]: A bipartite non-compact Gaussian state that is invariant under partial transposition of one of the two subsystems is separable. It is easy to see that for two disjoint regions in the $z = 2$ chain, the corresponding reduced density matrix is indeed invariant under partial transposition, cf. appendix A, and thus separable. It follows that the logarithmic negativity is zero.

A vanishing logarithmic negativity on disjoint intervals was observed previously in a closely related (1+1)-dimensional system with Lifshitz scaling in [38]. These authors study the ground state of the Motzkin Hamiltonian subject to the constraint $\phi \geq 0$, which renders the density matrix non-Gaussian. However, for two intervals far away from the boundaries of the system, the constraint becomes unimportant and the model reduces to the $z = 2$ free boson studied in the present paper. In contrast to [38], our result applies regardless of whether the two disjoint regions are located near or far away from the boundaries of the system, and also on a circle of finite length. We will see below that the same result is found in the (2+1)-dimensional quantum Lifshitz model and extends to higher-dimensional models with Lifshitz scaling as well.

In a slightly more general case, where A_1 and A_2 are symmetric with respect to the center of the chain, but not necessarily adjacent to the boundaries and separated by a distance $d > 0$, the eigenvalues of $C_A^{T_2}$ distinct from $1/2$ are the (positive) solutions of the following two equations:

$$32\lambda^4 - 8(L - \ell - d + 2)\lambda^2 + (\ell + 1)(L - 2\ell - d + 2) = 0\,, \tag{2.28}$$

$$32(L+1)\lambda^4 - 8(L + 2 - d^2 + (\ell + d)(L - 2\ell + 1))\lambda^2 + (\ell + 1)(d + 1)(L - 2\ell - d + 2) = 0\,. \tag{2.29}$$

As before, the UV cutoff can be restored by making the changes $L \to L/\epsilon$, $\ell \to \ell/\epsilon$ and $d \to d/\epsilon$. For both L and ℓ arbitrary, the two solutions of the first equation above are always larger or equal to $1/2$, while for the second equation one finds that its solutions may be smaller than $1/2$, but only provided $d < \epsilon$. However, since the UV cutoff ϵ is arbitrarily small in the continuum regime, neither of the eigenvalues can actually be smaller than $1/2$, thus implying, again that $\mathcal{E} = 0$. More generally, we find that the logarithmic negativity vanishes for arbitrary configurations of two disjoint intervals. This may also easily be verified numerically. The same conclusion carries through to the periodic chain.

In [39], it was observed based on numerical computations that for high values of the dynamical exponent z, there exist a critical distance between two disjoint intervals below which the logarithmic negativity is non-vanishing. We believe this to be a lattice effect. In our analytic calculation above, we found that in the continuum regime and upon restoring the UV cutoff ϵ, the critical distance is actually proportional to ϵ. We saw this explicitly for $z = 2$, but it is also true for $z > 2$ where the critical distance can be shown to be $d_c = (z/2)\epsilon$. Later on we will see, using path integrals and the replica method, that the logarithmic negativity vanishes for two disjoint systems for any even positive integer z.

2.4.3 Two adjacent intervals

Open system. Now consider two intervals of same length ℓ joined at the center of the full system (assuming L even), as shown in the bottom-left panel of figure 1. In this case, the only eigenvalue of $C_A^{T_2}$ satisfying $\lambda < 1/2$ reads

$$\lambda^2 = \frac{(2\ell+1)(L-2\ell+2)+2}{16(L+1)}\left(1 - \sqrt{1 - \frac{8(L+1)(L-2\ell+2)}{((2\ell+1)(L-2\ell+2)+2)^2}}\right). \tag{2.30}$$

In the continuum regime, with all lengths measured in units of the UV cutoff ϵ from now on, we have $\lambda^{-1} = \sqrt{8\ell}$, from which follows the logarithmic negativity

$$\mathcal{E} = \frac{1}{2}\log(2\ell)\,. \tag{2.31}$$

Notice that for $\ell = L/2$, the negativity (2.31) reduces to the (1/2)-Rényi entropy (2.21). Indeed, in that case ρ_A is pure.

In the most general case, that is for two adjacent intervals of arbitrary lengths and relative position in the total system, there are at most four eigenvalues of $C_A^{T_2}$ distinct from 1/2. These four eigenvalues are the roots of a certain quartic equation presented in appendix B. What is important here is that only one eigenvalue, call it λ, among these four roots is smaller than 1/2, and we find in the continuum regime that

$$\lambda = \sqrt{\frac{\ell_1 + \ell_2}{16\ell_1\ell_2}}\,. \tag{2.32}$$

The logarithmic negativity of two adjacent intervals in a finite system with Dirichlet boundary conditions is thus given in general by

$$\mathcal{E} = \frac{1}{2}\log\left(\frac{\ell_1\ell_2}{\ell_1+\ell_2}\right) + \text{const}\,, \tag{2.33}$$

where const $= \log 2$ in our setup here, but is not a universal quantity and depends on the regularisation scheme. For $\ell_1 = \ell_2 = \ell$ we recover (2.31).

Periodic system. Let us now consider a finite system of length L with periodic boundary conditions, and two adjacent intervals of lengths ℓ_1 and ℓ_2 such that $\ell_1 + \ell_2 \leq L$, as in the right-hand panel of figure 1. As discussed above, the discrete theory has a divergence due to a zero mode that we circumvent by introducing a non-zero mass. Working in the limit of very small mass, one might expect a term logarithmic in the mass parameter to appear in the negativity, as is indeed the case for pure states with $\ell_1 + \ell_2 = L$ where the logarithmic negativity equals the (1/2)-Rényi entropy given by (2.24). It turns out, however, for a mixed state such that $\ell_1 + \ell_2 < L$, no divergent term appears in the logarithmic negativity. In the simplest case where $\ell_1 = \ell_2 = \ell < L/2$, the spectrum of $C_A^{T_2}$ in the continuum limit is found to be

$$\text{Spectrum}(C_A^{T_2}) = \left\{\sqrt{\frac{1}{8\ell}}, \sqrt{\frac{\ell}{6}}, \sqrt{\frac{\ell(L-2\ell)}{8L}}, \sqrt{\frac{3}{2m^2L}}, \frac{1}{2}, \cdots, \frac{1}{2}\right\}. \tag{2.34}$$

In the critical regime, where $mL \ll 1$, the only eigenvalue that contributes to the logarithmic negativity is $\lambda_1 = \sqrt{1/(8\ell)}$ and we get $\mathcal{E} = (1/2)\log(2\ell)$, the same as for the open chain with Dirichlet boundary conditions. Note that this result is only reliable for a mixed state where the strict inequality $\ell < L/2$ holds. Indeed, for $\ell = L/2$, the third eigenvalue in the expression (2.34) for the spectrum vanishes, indicating that the regulator mass needs to be retained and in this case the logarithmic mass dependence of the pure state result (2.24) is recovered.

In the general case, with arbitrary $\ell_1+\ell_2 < L$, the spectrum of $C_A^{T_2}$ in the critical limit is given in appendix B. The spectrum contains only one eigenvalue smaller than $1/2$, which in the continuum regime reads $\lambda^2 = (\ell_1+\ell_2)/(16\ell_1\ell_2)$, and we find the same logarithmic negativity as for the open system.

2.4.4 A hint at a general formula

Let us first emphasise that, for the $z = 2$ free boson, we find the expression

$$\mathcal{E} = \frac{1}{2}\log\left(\frac{\ell_1\ell_2}{\ell_1+\ell_2}\right) + \text{const} \tag{2.35}$$

for the continuum logarithmic negativity of two adjacent intervals in a finite or infinite system, with or without (Dirichlet) boundaries. This is in contrast to the $z = 1$ relativistic free scalar field for which the logarithmic negativity of two adjacent intervals depends in general on the size of the total system as, e.g. for periodic boundary conditions

$$\mathcal{E}^{(z=1)} = \frac{1}{4}\log\left(\frac{L}{\pi}\frac{\sin\left(\frac{\pi\ell_1}{L}\right)\sin\left(\frac{\pi\ell_2}{L}\right)}{\sin\left(\frac{\pi(\ell_1+\ell_2)}{L}\right)}\right) + \text{const}\,, \tag{2.36}$$

and only for an infinite system $L\to\infty$ one obtains

$$\mathcal{E}^{(z=1)} = \frac{1}{4}\log\left(\frac{\ell_1\ell_2}{\ell_1+\ell_2}\right) + \text{const}\,. \tag{2.37}$$

Since a picture is worth a thousand words, we plot in figure 2 the logarithmic negativities of two adjacent intervals of same length ℓ in a periodic chain of length L for a $z = 2$ and a $z = 1$ scalar. One can appreciate the difference in behaviour between the two theories, particularly close to $\ell \simeq L/2$ where $\mathcal{E}^{(z=2)} \propto \log L$ while $\mathcal{E}^{(z=1)} \propto \log\big(L^2/(L-2\ell)\big)$.

Fradkin and Moore [27] taught us that the bipartite Rényi entropies for ground states of non-compact scalar fields with critical dynamical exponent $z = 2$ can be simply expressed in terms of partition functions of a free Euclidean CFT in one dimension lower, namely

$$S_A^{(n)} = -\log\left(\frac{Z_A Z_B}{Z_{A\cup B}}\right), \tag{2.38}$$

and is actually independent of the Rényi index n. Z_A and Z_B are the CFT partition functions on regions A and B, respectively, with Dirichlet boundary conditions on the entangling cut. $Z_{A\cup B}$ is the partition function on the entire space, with specified boundary conditions, for example Dirichlet, at the boundary $\partial\mathcal{M}$. Returning to the logarithmic negativity for mixed states of two adjacent intervals, we have found that the negativity (2.35) does not depend on the size of the total system. Furthermore, we know that for a pure state it reduces to the Rényi entropy of order $n = 1/2$, which for the $z = 2$ scalar is given by (2.38) independently of n. We are thus led to conjecture the following general formula for the logarithmic negativity of the $z = 2$ non-compact free scalar field:

$$\mathcal{E} = -\log\left(\frac{Z_{A_1} Z_{A_2}}{Z_{A_1\cup A_2}}\right), \tag{2.39}$$

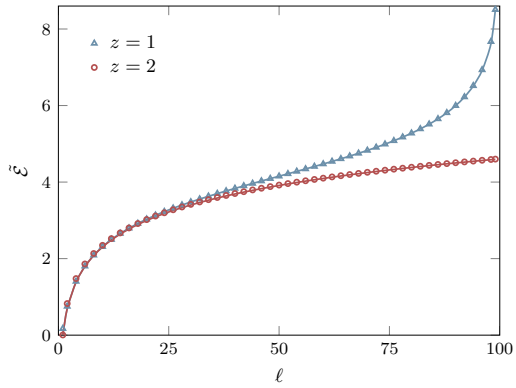

Figure 2. Logarithmic negativities of two adjacent intervals of same length ℓ in the periodic chain of length $L = 200$ and mass $m = 10^{-5}$ for the relativistic ($z = 1$) and Lifshitz ($z = 2$) bosons. To allow an easy comparison between the two theories, the logarithmic negativities are normalised in such a way that for $\ell \ll L$ they behave as $\tilde{\mathcal{E}} \simeq \log \ell$. The data are perfectly consistent with the (normalised) continuum expressions (2.35) and (2.36), shown as solid lines.

where Z_{A_i} is the partition function of the Euclidean CFT in one dimension lower on A_i with Dirichlet boundary conditions on the entangling cut(s), and $Z_{A_1 \cup A_2}$ is the partition function on $A_1 \cup A_2$ with similar boundary conditions. Clearly, when A_2 is the complement of A_1, formula (2.39) reduces to the entropy (2.38). When A_1 and A_2 are disjoint, these regions do not talk to each other because of the Dirichlet boundary conditions, thus one has $Z_{A_1 \cup A_2} = Z_{A_1} Z_{A_2}$, hence $\mathcal{E} = 0$. Finally, if A_1 and A_2 are adjacent, using heat kernel techniques one can easily compute in $1d$ (omitting non-universal parts): $-\log Z_{A_{1,2}} = (1/2) \log \ell_{1,2}$ and $-\log Z_{A_1 \cup A_2} = (1/2) \log(\ell_1 + \ell_2)$, such that we recover (2.35).

In the following section, we show that (2.39) is indeed correct in the (2+1)-dimensional quantum Lifshitz model. It also holds for non-compact $(d+1)$-dimensional Lifshitz theories with even exponent z on flat space and up to some subtleties on curved manifolds as well. We derive (2.39) and its generalisation to compact fields using path integrals and the replica trick.

3 Logarithmic negativity from a replica approach

In this section, we apply replica techniques to evaluate the logarithmic negativity in the (2+1)-dimensional QLM. The calculation is closely patterned on [27, 32, 33], where a replica method was developed to calculate the entanglement entropy in the QLM. As its name suggests, this method introduces independent copies of the original theory — the replicas — and a surgery procedure to join them together. The crucial step is to identify the correct set of boundary conditions to be imposed at the entangling cuts on the replica fields. We will adapt the technique to evaluate the logarithmic negativity in quantum

Lifshitz theories on different spatial manifolds by means of an expression of the form (1.3), for mixed state density matrices constructed from the ground state by partially tracing over a subsystem.

3.1 Pure states

We begin, as in section 2.4, by considering the logarithmic negativity of pure states, which should reduce to the Rényi entropy of order 1/2. In this case, the spatial manifold $\mathcal{M}$ is divided into two submanifolds A_1 and A_2, with boundary Γ between them, and we assume the Hilbert space on the full manifold factorises as $\mathcal{H} = \mathcal{H}_{A_1} \otimes \mathcal{H}_{A_2}$. We then introduce a replica index $i = 1, \dots, n_e$ for the density matrices and rewrite (2.3) on the bipartite manifold as

$$\rho_i = \frac{1}{Z_{A_1 \cup A_2}} \int \mathcal{D}\phi_i^{A_1} \mathcal{D}\phi_i'^{A_1} \mathcal{D}\phi_i^{A_2} \mathcal{D}\phi_i'^{A_2} \, e^{-\frac{1}{2}(S[\phi_i^{A_1}]+S[\phi_i'^{A_1}]+S[\phi_i^{A_2}]+S[\phi_i'^{A_2}])} \\ \times |\phi_i^{A_1}\rangle \otimes |\phi_i^{A_2}\rangle\langle\phi_i'^{A_1}| \otimes \langle\phi_i'^{A_2}| \, . \tag{3.1}$$

Note that since the replicated fields are all dummy fields we have $\rho_i \equiv \rho$. We stress that in the replica method we always work with the action of a free conformal compactified bosonic field for $z = 2$, that is the action S appearing in the above density matrix is given by the expression (2.2). This means that for $z = 2$ it is enough to impose Dirichlet boundary conditions on the fields to have a self-adjoint Laplacian operator. The partial transposition over, e.g., A_2, then amounts to exchanging the primed and unprimed A_2-fields in (3.1):

$$\rho_i^{T_2} = \frac{1}{Z_{A_1 \cup A_2}} \int \mathcal{D}\phi_i^{A_1} \mathcal{D}\phi_i'^{A_1} \mathcal{D}\phi_i^{A_2} \mathcal{D}\phi_i'^{A_2} \, e^{-\frac{1}{2}(S[\phi_i^{A_1}]+S[\phi_i'^{A_1}]+S[\phi_i^{A_2}]+S[\phi_i'^{A_2}])} \\ \times |\phi_i^{A_1}\rangle \otimes |\phi_i'^{A_2}\rangle\langle\phi_i'^{A_1}| \otimes \langle\phi_i^{A_2}| \, . \tag{3.2}$$

We can now compute the trace of the n_e-th power of the partial transpose density matrix, $\mathrm{Tr}\left(\rho^{T_2}\right)^{n_e} \equiv \mathrm{Tr}\left(\rho_1^{T_2} \cdots \rho_{n_e}^{T_2}\right)$. For $i = 1, \dots, n_e - 1$, each adjacent matrix product $\rho_i^{T_2} \rho_{i+1}^{T_2}$ leads to two δ-functions coming from $\langle\phi_i'^{A_1}|\phi_{i+1}^{A_1}\rangle$ and $\langle\phi_i^{A_2}|\phi_{i+1}'^{A_2}\rangle$. The final total trace of the product of density matrices adds another two δ-functions $\langle\phi_n'^{A_1}|\phi_1^{A_1}\rangle$ and $\langle\phi_n^{A_2}|\phi_1'^{A_2}\rangle$. Resolving all the δ-functions leads to the gluing conditions

$$\left.\begin{aligned} \phi_i'^{A_1} &= \phi_{i+1}^{A_1} \\ \phi_i^{A_2} &= \phi_{i+1}'^{A_2} \end{aligned}\right\} \qquad i = 1, \dots, n_e \, , \tag{3.3}$$

with $\phi_{n_e+1} \equiv \phi_1$. Furthermore, the continuity conditions among the fields at the entangling cut read

$$\phi_i^{A_1}|_\Gamma = \phi_i^{A_2}|_\Gamma \, , \qquad \phi'^{A_1}_i|_\Gamma = \phi'^{A_2}_i|_\Gamma, \tag{3.4}$$

as can be seen in figure 3. A closer look at these conditions reveals that all even and all odd fields must agree separately at the entangling cut Γ, leaving us with n_e independent fields with boundary conditions

$$\left.\begin{aligned} \phi_{2k}^{A_1}|_\Gamma = \ \phi_{2l}^{A_2}|_\Gamma \ &\equiv \chi^e \\ \phi_{2k-1}^{A_1}|_\Gamma = \phi_{2l-1}^{A_2}|_\Gamma &\equiv \chi^o \end{aligned}\right\} \qquad k, l = 1, \dots, n_e/2, \tag{3.5}$$

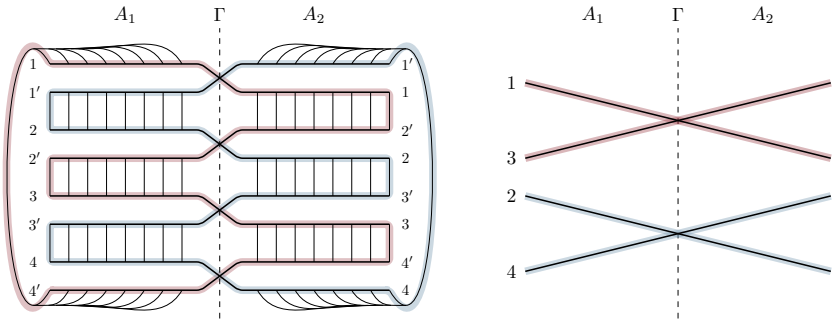

(a) Gluing conditions (b) Resulting independent sets of fields

Figure 3. Gluing conditions for $n_e = 4$. Gluing results in two independent sets of boundary conditions represented in red and blue.

where χ^e and χ^o are two independent functions of the boundary coordinates. The partial transposition thus has the effect of creating two independent sets of $n_e/2$ fields. Since the boundary functions $\chi^{e,o}$ and the fields are all dummy integration variables, we can relabel them as $\phi^{A_i}_{2k}, \phi^{A_i}_{2k-1} \mapsto \phi^{A_i}_k$ and $\chi^e, \chi^o \mapsto \chi$ to get

$$\mathrm{Tr}\left(\rho^{T_2}\right)^{n_e} = \left(\frac{1}{Z^{n_e/2}_{A_1\cup A_2}} \int_{\mathcal{B}} \prod_{k=1}^{n_e/2} \mathcal{D}\phi^{A_1}_k \, e^{-S[\phi^{A_1}_k]} \int_{\mathcal{B}} \prod_{k=1}^{n_e/2} \mathcal{D}\phi^{A_2}_k \, e^{-S[\phi^{A_2}_k]}\right)^2 , \tag{3.6}$$

where the boundary conditions $\mathcal{B}$ are now given by

$$\mathcal{B}: \qquad \phi^{A_1}_k|_\Gamma = \phi^{A_2}_l|_\Gamma = \chi, \qquad k,l = 1,\ldots,n_e/2\,. \tag{3.7}$$

Upon closer inspection, one can recognise in (3.6) the expression for $\mathrm{Tr}\,\rho^{n_e/2}_{A_1}$ derived in [32–34], where $\rho_{A_1} = \mathrm{Tr}_{A_2}\,\rho$ is the reduced density matrix obtained by tracing out the degrees of freedom in A_2,[2] meaning that the following equation holds

$$\mathrm{Tr}\left(\rho^{T_2}\right)^{n_e} = \left(\mathrm{Tr}\,\rho^{n_e/2}_{A_1}\right)^2 . \tag{3.8}$$

In particular this gives $\lim_{n_e\to 2}\mathrm{Tr}\left(\rho^{T_2}\right)^{n_e} = 1$, as it should [12]. For a compact field on a circle of radius R_c, the fields are subject to the boundary conditions (3.7) up to the periodic identification $\phi \sim \phi + 2\pi R_c$. In [32–34] it was found that

$$\mathrm{Tr}\,\rho^{n_e/2}_{A_1} = \left(\frac{Z_{A_1}Z_{A_2}}{Z_{A_1\cup A_2}}\right)^{n_e/2-1} W(n_e/2)\,, \tag{3.9}$$

where Z_{A_i} is the partition function on A_i with Dirichlet boundary conditions at the entangling cut Γ and $W(n)$ is a sum over different classical configurations of the compactified

[2]Note that we could have written the expression in terms of $\rho_{A_2} = \mathrm{Tr}_{A_1}\,\rho$, since the system is in a pure state.

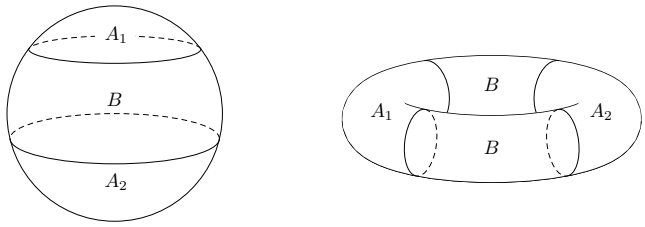

(a) Spherical geometry (b) Toroidal geometry

Figure 4. Examples of geometries where A_1 and A_2 are separated by B. Note that for the torus, B consists of two disjoint components.

fields. Applying the replica formula (1.3), we obtain for the logarithmic negativity of a pure state

$$\mathcal{E} = -\log\left(\frac{Z_{A_1}Z_{A_2}}{Z_{A_1\cup A_2}}\right) + 2\log W(1/2) \tag{3.10}$$

which, as expected [12], is indeed the (1/2)–Rényi entropy $S^{(1/2)}_{A_1}$.

It is also worth looking at the odd n_o sequence $\mathrm{Tr}\left(\rho^{T_2}\right)^{n_o}$. In that case, all the fields have to be equal at the entangling cut Γ, that is

$$\phi_i^{A_1}|_\Gamma = \phi_j^{A_2}|_\Gamma = \chi, \qquad i,j = 1,\dots,n_o\,. \tag{3.11}$$

We thus have

$$\mathrm{Tr}\left(\rho^{T_2}\right)^{n_o} = \mathrm{Tr}\,\rho_{A_1}^{n_o}\,, \tag{3.12}$$

which yields the normalization

$$\lim_{n_o\to 1}\mathrm{Tr}\left(\rho^{T_2}\right)^{n_o} = W(1) = 1\,. \tag{3.13}$$

3.2 Disjoint submanifolds

We now turn to the more interesting case of entanglement between two regions of a system in a mixed state. In this section, we illustrate the replica approach for the case of a mixed state when A_1 and A_2 are disjoint and separated by B, as illustrated in figure 4.

The mixed state we consider is obtained by tracing over the degrees of freedom on B, with the full system in its ground state, and is thus described by the reduced density matrix $\rho_A \equiv \rho_{A_1\cup A_2}$. In order to calculate the logarithmic negativity, we then transpose the density matrix over A_2 resulting in $\rho_A^{T_2}$. The trace on B leads to conditions of the form

$$\phi_i^B = \phi_i'^B\,, \tag{3.14}$$

that is the primed and unprimed copies of the fields are sewed within the same replica of the density matrix. The gluing conditions that result for the fields on A_1 and A_2 are the same as before, that is (3.3), so they connect the density matrices cyclically. The continuity conditions at the entangling cut between A_a and B (indicated as Γ_a) require that

$$\phi_i^{A_a}|_{\Gamma_a} = \phi_i^B|_{\Gamma_a}\,, \qquad \phi'^{A_a}_i|_{\Gamma_a} = \phi'^B_i|_{\Gamma_a}\,,$$

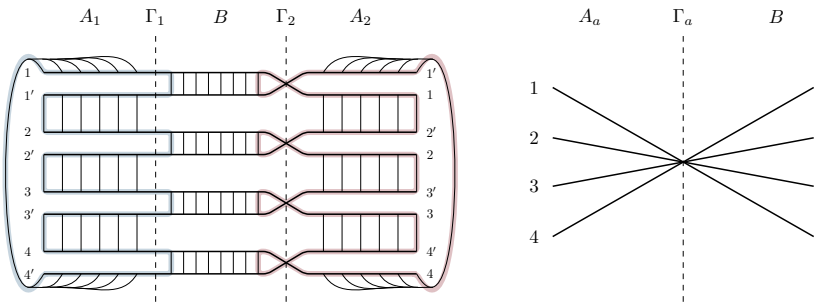

(a) Gluing conditions (b) Resulting independent sets of fields

Figure 5. Gluing conditions around the boundaries between B and the two components of A for $n_e = 4$. The resulting boundary conditions, depicted on the right, are the same for A_1 and A_2.

for all $i = 1, \ldots, n_e$ and $a = 1, 2$. Putting everything together, all replica fields must agree at the boundary between B and any of the A_a's, as depicted in figure 5. In particular, this means that the geometry is *not* sensitive to the partial transposition, and we obtain the identity

$$\mathrm{Tr}\left(\rho_A^{T_2}\right)^{n_e} = \mathrm{Tr}\,\rho_A^{n_e}\,. \tag{3.15}$$

The latter quantity appears in the calculation of the tripartite entanglement entropy [33] and is given by

$$\mathrm{Tr}(\rho_A)^{n_e} = \left(\frac{Z_{A_1} Z_{A_2} Z_B}{Z_{A\cup B}}\right)^{n_e-1} W(n_e). \tag{3.16}$$

For disjoint subsystems the partial transposition is not sensitive to the parity of n, i.e. equations (3.15) and (3.16) are also valid for odd n_o. It then immediately follows from the unit normalization of the density matrix in the odd sequence at $n_o = 1$ that the winding sector contribution is trivial, $W(1) = 1$. We thus find the striking result,

$$\mathcal{E} = \lim_{n_e \to 1} \log \mathrm{Tr}\left(\rho_A^{T_2}\right)^{n_e} = 0\,. \tag{3.17}$$

While this result differs from the expectation for a conformal field theory [12], it agrees with the correlator method calculations in section 2.4.2. We stress that the vanishing of the logarithmic negativity is a necessary but not sufficient condition for the separability of the density matrix [8]. The theorem of [50] only applies to finite dimensional systems, so it remains an open question whether the reduced density matrix constructed via the replica method is separable for disjoint subsystems.

The expression (3.16) also holds in higher dimensions for generalised quantum Lifshitz models with even z as discussed in [26, 34], as long as the cuts are smooth and a direct generalisation of figure 4. The relation (3.15) is therefore still valid for smooth partitions of the ground state of such theories, which implies that the main conclusion in (3.17) remains correct. In the case of $d = z = 2$ it suffices to impose Dirichlet boundary conditions on

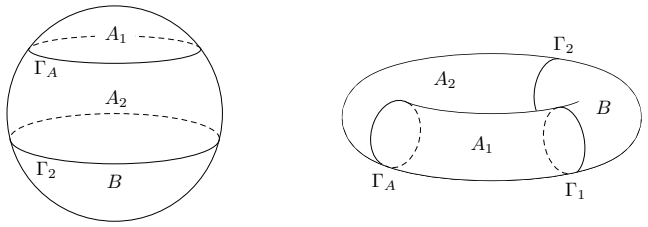

(a) Spherical geometry (b) Toroidal geometry

Figure 6. Realisations of the situation when A_1 and A_2 are adjacent on the sphere and torus.

the fluctuations to ensure that the variational problem is well-posed and the Laplacian self-adjoint after surgery, leading to a consistent replica calculation. For curved higher-dimensional manifolds and higher z, further restrictions apply in order to have a well-defined higher-derivative operator in the action S in (2.2). On a d-sphere, for instance, the operator in question is only well-defined for even $z \leq d$. For the construction of consistent operators on tori and spheres, and details on the corresponding replica calculation see [34] and references therein.

The fact that in Lifshitz theories with even dynamical exponent the entanglement negativity vanishes for disjoint subsystems is surprising but it is not unheard of. Similar behaviour was already noted in a closely related $z = 2$ system in [38] and in Chern-Simons field theories in $2 + 1$ dimensions the topological logarithmic negativity vanishes for disjoint subsystems [22, 23]. In this respect, Lifshitz theories exhibit similarities to topological theories.

3.3 Adjacent submanifolds without winding

Next, we consider the case where the submanifolds A_1 and A_2 are adjacent, as in figure 6. To keep the discussion as general as possible, we assume the maximal number of non-trivial entangling cuts Γ_1, Γ_2, and Γ_A. The spherical case, which requires only two cuts, is recovered by trivially identifying fields across the third cut. We take ϕ to be non-compact throughout this section and postpone addressing the additional complications that arise from the winding structure of a compact ϕ until section 3.4.

As in section 3.2, we perform a trace over the degrees of freedom on B at the beginning and then compute $\mathrm{Tr}\left(\rho_A^{T_2}\right)^{n_e}$ with a transposition on A_2. The partial trace on B leads to the gluing conditions (3.14), while the product and final trace over A_1, A_2 leads to the conditions (3.3). At the entangling cut between A_1 and A_2, denoted by Γ_A, the continuity conditions are

$$\phi_i^{A_1}|_{\Gamma_A} = \phi_i^{A_2}|_{\Gamma_A}\,, \qquad \phi'^{A_2}_i|_{\Gamma_A} = \phi'^{A_1}_i|_{\Gamma_A}\,, \qquad i = 1, \ldots, n_e\,, \tag{3.18}$$

and at the cut between A_a and B, denoted Γ_a, they are

$$\phi_i^{A_a}|_{\Gamma_a} = \phi_i^{B}|_{\Gamma_a}\,, \qquad \phi'^{A_a}_i|_{\Gamma_a} = \phi'^{B}_i|_{\Gamma_a}\,, \qquad a = 1, 2\,, \quad i = 1, \ldots, n_e\,. \tag{3.19}$$

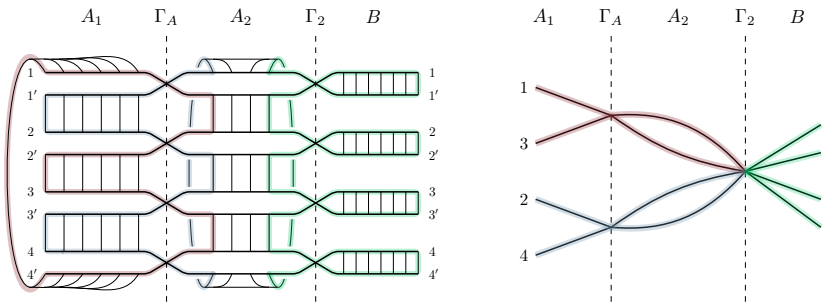

(a) Gluing conditions (b) Resulting independent sets of fields

Figure 7. Realisations ($n_e = 4$) of the situation when A_1 and A_2 are adjacent on the sphere and torus.

When we combine the gluing and continuity conditions, we see that the fields must satisfy

$$\mathcal{B}: \quad \left.\begin{aligned} &\phi_i^{A_a}|_{\Gamma_a} = \phi_j^B|_{\Gamma_a} = \chi_a\,, \\ &\phi_k^{A_1}|_{\Gamma_A} = \phi_\ell^{A_2}|_{\Gamma_A} = \chi_A^o \\ &\phi_{n_e/2+k}^{A_1}|_{\Gamma_A} = \phi_{n_e/2+\ell}^{A_2}|_{\Gamma_A} = \chi_A^e \end{aligned}\right\} \quad \begin{aligned} &a = 1,2\,, \quad i,j = 1,\dots,n_e\,, \\ &k,l = 1,\dots,n_e/2\,, \end{aligned} \tag{3.20}$$

as depicted in figure 7. Notice that we have relabelled the n_e independent fields in order to have the odd fields ranging from 1 to $n_e/2$ and the even fields from $n_e/2+1$ to n_e. The functions $\chi_a, \chi_A^o, \chi_A^e$ are arbitrary and only defined at the corresponding entangling cuts, essentially by the above conditions.

The main difference compared to the case of disjoint submanifolds now becomes apparent: We have two independent sets of $n_e/2$ boundary conditions at the entangling cut between A_1 and A_2, while at the other cuts Γ_1 and Γ_2 we still have a single set of n_e conditions. This means that, contrary to the disjoint case, the adjacent geometry is sensitive to the partial transposition.

Using the boundary conditions $\mathcal{B}$ given in (3.20), we can now directly write

$$\mathrm{Tr}\left(\rho_A^{T_2}\right)^{n_e} = \frac{1}{Z_{A\cup B}^{n_e}} \int_{\mathcal{B}} \prod_{i=1}^{n_e} \mathcal{D}\phi_i^{A_1}\, e^{-S[\phi_i^{A_1}]} \int_{\mathcal{B}} \prod_{i=1}^{n_e} \mathcal{D}\phi_i^{A_2}\, e^{-S[\phi_i^{A_2}]} \int_{\mathcal{B}} \prod_{i=1}^{n_e} \mathcal{D}\phi_i^{B}\, e^{-S[\phi_i^{B}]}\,. \tag{3.21}$$

For a pure state, the path integrals factorise in a straightforward way at this point. The situation here is a little more complicated since the entangling cuts carry different numbers of degrees of freedom — one at $\Gamma_{1,2}$ and two at Γ_A. However, this difficulty may be circumvented by rotating the fields as described originally in [27, 32, 33]. Let us first define

a unitary rotation matrix U_n [33] as follows

$$U_n = \begin{bmatrix} \frac{1}{\sqrt{2}} & -\frac{1}{\sqrt{2}} & 0 & & \dots \\ \frac{1}{\sqrt{6}} & \frac{1}{\sqrt{6}} & -\frac{2}{\sqrt{6}} & 0 & \dots \\ \vdots & & & & \\ \frac{1}{\sqrt{n(n-1)}} & \frac{1}{\sqrt{n(n-1)}} & \dots & \dots & -\sqrt{1-\frac{1}{n}} \\ \frac{1}{\sqrt{n}} & \frac{1}{\sqrt{n}} & \dots & \dots & \frac{1}{\sqrt{n}} \end{bmatrix} . \tag{3.22}$$

It is chosen such that the first $n-1$ rotated fields vanish on the entanglement cuts. Two rotations are then performed independently on the first and on the last $n_e/2$ fields with the help of the block diagonal matrix $\tilde{U}_{n_e} = U_{n_e/2} \oplus U_{n_e/2}$. In vector notation this rotation reads $\tilde{\phi} = \tilde{U}_{n_e}\phi$ and results in the boundary conditions

$$\begin{aligned} & \tilde{\phi}_i^{A_a}|_{\Gamma_a} = \tilde{\phi}_j^{B}|_{\Gamma_a} = \sqrt{\frac{n_e}{2}}\chi_a\,, \qquad a=1,2\,, \quad i,j = n_e/2, n_e \\ \tilde{\mathcal{B}}: \quad & \tilde{\phi}_{n_e/2}^{A_1}|_{\Gamma_A} = \tilde{\phi}_{n_e/2}^{A_2}|_{\Gamma_A} = \sqrt{\frac{n_e}{2}}\chi_A^o\,, \\ & \tilde{\phi}_{n_e}^{A_1}|_{\Gamma_A} = \tilde{\phi}_{n_e}^{A_2}|_{\Gamma_A} = \sqrt{\frac{n_e}{2}}\chi_A^e\,, \end{aligned} \tag{3.23}$$

with the remaining fields vanishing at all cuts. We then perform an additional U_2 rotation on the fields $\tilde{\phi}_{n_e/2}, \tilde{\phi}_{n_e}$ as to obtain

$$\begin{aligned} & \bar{\phi}_{n_e}^{A_a}|_{\Gamma_a} = \bar{\phi}_{n_e}^{B}|_{\Gamma_a} = \sqrt{n_e}\chi_a\,, \qquad a=1,2\,, \\ \bar{\mathcal{B}}: \quad & \bar{\phi}_{n_e}^{A_1}|_{\Gamma_A} = \bar{\phi}_{n_e}^{A_2}|_{\Gamma_A} = \sqrt{\frac{n_e}{2}}\chi_+\,, \\ & \bar{\phi}_{n_e/2}^{A_1}|_{\Gamma_A} = \bar{\phi}_{n_e/2}^{A_2}|_{\Gamma_A} = \sqrt{\frac{n_e}{2}}\chi_-\,, \end{aligned} \tag{3.24}$$

where

$$\chi_\pm := \frac{1}{\sqrt{2}}(\chi_A^o \pm \chi_A^e)$$

are again arbitrary and independent functions, and the n_e-2 remaining fields have Dirichlet boundary conditions at all entangling cuts.

Each of these n_e-2 fields thus produces three Dirichlet partition functions in (3.21): on A_1, A_2 and B. Further inspection of the boundary conditions (3.24) reveals that the n_e-th field is free on the whole manifold $A \cup B$. It is not constrained to vanish at any cut, and the cut functions χ are arbitrary, which allows us to write[3]

$$\begin{aligned} & Z_{A\cup B} = \\ & \int_{\bar{\mathcal{B}}} \mathcal{D}\bar{\phi}_{n_e}^{A_1} e^{-S[\bar{\phi}_{n_e}^{A_1}]} \int_{\bar{\mathcal{B}}} \mathcal{D}\bar{\phi}_{n_e}^{A_2} e^{-S[\bar{\phi}_{n_e}^{A_2}]} \int_{\bar{\mathcal{B}}} \mathcal{D}\bar{\phi}_{n_e}^{B} e^{-S[\bar{\phi}_{n_e}^{B}]} \int [\mathcal{D}\bar{\phi}_{n_e}|_{\Gamma_A}]\, e^{-S[\bar{\phi}_{n_e}]} \prod_a \int [\mathcal{D}\bar{\phi}_{n_e}|_{\Gamma_a}]\, e^{-S[\bar{\phi}_{n_e}]}\,, \end{aligned} \tag{3.25}$$

[3] There are additional non-universal factors $\propto n_e^{-\mathrm{L}(\Gamma_i)/2\epsilon}$, where $\mathrm{L}(\Gamma_i)$ is the length of Γ_i and ϵ a UV-cutoff, to the partition functions (3.25) and (3.26), arising from the Jacobian that results of the successive rotations applied to the fields, see [32, 33]. They only contribute to the area law and can thus be ignored.

where the last integrals indicate the sum over all possible values of the field at the entangling cuts [33, 34]. The $n_e/2$-th field is only free on $A = A_1 \cup A_2$ (it is not subject to Dirichlet boundary condition only at Γ_A) once we sum over the degrees of freedom along the cut Γ_A, such that

$$Z_{A_1\cup A_2} Z_B = \int_{\mathcal{B}} \mathcal{D}\bar{\phi}^{A_1}_{n_e/2}\, e^{-S[\bar{\phi}^{A_1}_{n_e/2}]} \int_{\mathcal{B}} \mathcal{D}\bar{\phi}^{A_2}_{n_e/2}\, e^{-S[\bar{\phi}^{A_2}_{n_e/2}]} \int_{\mathcal{B}} \mathcal{D}\bar{\phi}^{B}_{n_e/2}\, e^{-S[\bar{\phi}^{B}_{n_e/2}]} \int [\mathcal{D}\bar{\phi}_{n_e/2}|_{\Gamma_A}]\, e^{-S[\bar{\phi}_{n_e/2}]}\,. \tag{3.26}$$

Here the partition function over B is calculated with Dirichlet boundary conditions and the one over A with boundary conditions dictated by the geometry in question, as we will discuss in detail below. Hence, we can finally rewrite (3.21) as

$$\mathrm{Tr}\left(\rho_A^{T_2}\right)^{n_e} = \frac{(Z_{A_1} Z_{A_2} Z_B)^{n_e-2} Z_{A\cup B} Z_{A_1\cup A_2} Z_B}{Z_{A\cup B}^{n_e}}\,, \tag{3.27}$$

where the partition functions over A_1 and A_2 separately are also computed assuming Dirichlet boundary conditions. The resulting logarithmic negativity (1.3) is given by

$$\mathcal{E} = -\log\left(\frac{Z_{A_1} Z_{A_2}}{Z_{A_1\cup A_2}}\right). \tag{3.28}$$

As before, we expect this formal expression to be valid for $(d+1)$-dimensional Lifshitz theories with even exponent z on flat space and with some caveats on curved manifolds, such as $z \leq d$ for the sphere.

Notice that in analogy to the entanglement entropy [27, 32–34], the logarithmic negativity turns out to be a difference of free energies between the two subsystems involved and their union, confirming our expectation from section 2.4.4.

3.4 Adjacent submanifolds with winding

The basic procedure that we used in the previous section carries through to compact fields, that is fields with $\phi \sim \phi + 2\pi R_c$. However, as a consequence of the compact nature of ϕ, the boundary conditions (3.20) need only be satisfied modulo $2\pi R_c$. The periodic identification is taken into account in the standard way [51, 52], by writing each replicated field as a sum of a classical field and a fluctuation, $\phi = \phi^{\mathrm{cl}} + \varphi$. The classical field obeys the equations of motion and takes the value of the total field at the entangling cuts, including any winding contribution, while the fluctuation satisfies Dirichlet boundary conditions at all the cuts. This definition ensures that the action factorises as $S[\phi] = S[\phi^{\mathrm{cl}}] + S[\varphi]$, and we can rewrite our path integrals as

$$\int \mathcal{D}\phi_i\; e^{-S[\phi_i]} = \int \mathcal{D}\varphi_i\, e^{-S[\varphi_i]} \sum_{\phi_i^{\mathrm{cl}}} e^{-S[\phi_i^{\mathrm{cl}}]} \tag{3.29}$$

for each field $i = 1, \cdots, n_e$. The classical fields satisfy the boundary conditions

$$\phi_i^{\mathrm{cl}}|_{\Gamma_a} = \chi_a + 2\pi R_c\, \omega_i^a, \qquad \omega_i^a \in \mathbb{Z}\,, \tag{3.30}$$

instead of (3.20), where $a = 1, 2, A$ labels the cut Γ_a. The field $\phi_i^{\rm cl}$ is defined on the complete manifold. It is found by solving the equations of motion on each submanifold and stitching the resulting fields together across the cuts, subject to the above boundary conditions. Furthermore, depending on the global symmetries of the geometry, some of the winding modes ω_i^a may be redundant. This means that one needs to specify a geometry from the start, carefully identify the non-redundant winding modes, and only sum over these when performing the path integral manipulations of the last section. In the end, this procedure leads to a logarithmic negativity of the form

$$\mathcal{E} = -\log\left(\frac{Z_{A_1} Z_{A_2}}{Z_{A_1 \cup A_2}}\right) + \log W_{\mathcal{E}}(1)\,, \tag{3.31}$$

where $W_{\mathcal{E}}(n)$ is the contribution from the winding sector encoding the topological information that resides in the classical fields. We note that $W_{\mathcal{E}}$ is heavily dependent on the geometry as is illustrated below via explicit examples.

3.4.1 Spherical geometry

Let us consider the spherical configuration on the left in figure 6. There are only two cuts, Γ_A and Γ_2, but the previous formulae carry over if we simply ignore the trivial cut Γ_1. A priori, we have $2n_e$ winding numbers ω_i^a: one for each replica (labeled by $i = 1, \ldots, n_e$) at each cut (labeled by $a = \{2, A\}$). We also have three arbitrary functions, χ_2 defined along Γ_2 and χ_e, χ_o along Γ_A, which can be redefined so as to absorb one winding mode each. In what follows, we choose to eliminate the n_e-th mode at the cut Γ_2, and the $n_e/2$-th and n_e-th modes at Γ_A. In addition, the sphere admits a global shift symmetry, $S[\phi] = S[\phi + \text{const.}]$, which we can use to get rid of all the remaining winding modes at Γ_2. Since the global shift affects all cuts uniformly, the winding numbers at Γ_A get shifted to $\omega_i^A - \omega_i^2$, but we can, without loss of generality, relabel them as ω_i^A to avoid cluttering the notation. We thus end up with only $n_e - 2$ of the original $2n_e$ winding modes. The boundary conditions for the classical fields turn into

$$\mathcal{B}: \quad \begin{aligned} &\phi_i^{\rm cl}|_{\Gamma_2} = \chi_2\,, && i = 1, \ldots, n_e\,, \\ &\left.\begin{aligned} &\phi_k^{\rm cl}|_{\Gamma_A} = \chi_A^o + 2\pi R_c \omega_k^A\,, \\ &\phi_{n_e/2+k}^{\rm cl}|_{\Gamma_A} = \chi_A^e + 2\pi R_c \omega_{n_e/2+k}^A\,, \end{aligned}\right\} && k = 1, \ldots, n_e/2 - 1\,, \\ &\phi_{n_e/2}^{\rm cl}|_{\Gamma_A} = \chi_A^o\,, \\ &\phi_{n_e}^{\rm cl}|_{\Gamma_A} = \chi_A^e\,, \end{aligned} \tag{3.32}$$

while the fluctuations have Dirichlet boundary conditions at all cuts,

$$\varphi_i|_{\Gamma_a} = 0\,, \qquad i = 1, \cdots, n_e\,.$$

We proceed exactly as in section 3.3 and perform first a rotation $\tilde{U}_{n_e}$ of all the fields, followed by an additional U_2 rotation of the $n_e/2$-th and n_e-th fields. We obtain boundary conditions analogous to (3.24), except that now there is also a winding sector contribution

at Γ_A,

$$\bar{\mathcal{B}}: \quad \begin{aligned} &\bar{\phi}^{\rm cl}_{n_e}|_{\Gamma_2} = \sqrt{n_e}\,\chi_2\,, \\ &\left.\begin{aligned} \bar{\phi}^{\rm cl}_{j}|_{\Gamma_A} &= 2\pi R_c (U_{n_e/2})_{jk}\,\omega^A_k\,, \\ \bar{\phi}^{\rm cl}_{n_e/2+j}|_{\Gamma_A} &= 2\pi R_c (U_{n_e/2})_{jk}\,\omega^A_{n_e/2+k}\,, \end{aligned}\right\} \quad j,k = 1,\dots,n_e/2-1\,, \\ &\bar{\phi}^{\rm cl}_{n_e}|_{\Gamma_A} = \sqrt{\frac{n_e}{2}}\chi_+ + \frac{2\pi R_c}{\sqrt{n_e}}\sum_{i=1}^{n_e/2-1}\left(\omega^A_i + \omega^A_{i+n_e/2}\right), \\ &\bar{\phi}^{\rm cl}_{n_e/2}|_{\Gamma_A} = \sqrt{\frac{n_e}{2}}\chi_- + \frac{2\pi R_c}{\sqrt{n_e}}\sum_{i=1}^{n_e/2-1}\left(\omega^A_i - \omega^A_{i+n_e/2}\right), \end{aligned} \tag{3.33}$$

where $\chi_\pm = \frac{1}{\sqrt{2}}(\chi^o_A \pm \chi^e_A)$ and with the first $n_e - 1$ classical modes vanishing at Γ_2.

Just as in the non-compact case (see equations (3.25) and (3.26)) we can then use the n_e-th mode to reconstruct a full partition function on the sphere, while the $n_e/2$-th serves to reconstruct a partition function on $A = A_1 \cup A_2$ with Dirichlet boundary conditions at the boundary Γ_2. The remaining $n_e - 2$ fluctuating fields lead to Dirichlet partition functions on each submanifold, A_1, A_2 and B, and the classical modes yield pure winding sums. We thus arrive at the expression

$$\mathrm{Tr}\left(\rho_A^{T_2}\right)^{n_e} = \sqrt{n_e}\,\frac{(Z_{A_1}Z_{A_2}Z_B)^{n_e-2}Z_{A\cup B}Z_{A_1\cup A_2}Z_B}{Z^{n_e}_{A\cup B}}\,W_{\mathcal{E}}(n_e)\,, \tag{3.34}$$

with the winding sector given by

$$W_{\mathcal{E}}(n) = \sum_{\omega^A\in\mathbb{Z}^{n_e-2}} e^{-\sum_{i\neq n_e/2,n_e} S[\bar{\phi}^{\rm cl}_i]}\,. \tag{3.35}$$

$W_{\mathcal{E}}$ is constructed in terms of the $n_e - 2$ classical fields satisfying the conditions (3.33), which can be summarised as follows:

$$\begin{aligned} &\bar{\phi}^{\rm cl}_i|_{\Gamma_2} = 0\,, \qquad i = 1,\dots,n_e-1 \quad \text{with} \quad i \neq n_e/2\,, \\ &\left.\begin{aligned} \bar{\phi}^{\rm cl}_{j}|_{\Gamma_A} &= 2\pi R_c (M_{n_e/2-1})_{jk}\,\omega^A_k\,, \\ \bar{\phi}^{\rm cl}_{n_e/2+j}|_{\Gamma_A} &= 2\pi R_c (M_{n_e/2-1})_{jk}\,\omega^A_{n_e/2+k}\,, \end{aligned}\right\} \quad j,k = 1,\dots,n_e/2-1\,, \end{aligned} \tag{3.36}$$

where we have introduced a matrix M_{m-1} obtained by deleting the m-th row and column of U_m in (3.22), as was done in [33]. The factor $\sqrt{n_e}$ in (3.34) is essentially due to the global shift symmetry forcing all the classical fields at the entangling cut Γ_2 to be the same [33, 34]. Consequently, the n_e-th classical field gets its compactification radius amplified by $\sqrt{n_e}$, which in turn needs to be compensated for in the partition function. The factor of $\sqrt{n_e}$ does not contribute to the logarithmic negativity but is crucial for getting the correct entanglement entropy on hemispheres and tori [33, 34].

Thanks to the factorisation of the boundary conditions (3.36), the winding sector contribution (3.35) can be expressed as

$$W_{\mathcal{E}}(n_e) = \left(\sum_{\omega^A\in\mathbb{Z}^{n_e/2-1}} e^{-\sum_{j=1}^{n_e/2-1} S[\bar{\phi}^{\rm cl}_j]}\right)^2 = W(n_e/2)^2\,, \tag{3.37}$$

where each set of $n_e/2$-fields produces the winding sector $W(n_e/2)$ appearing in the entanglement entropy calculated in [33].

Classical solutions satisfying the boundary conditions (3.36) can be obtained via a conformal transformation which projects spherical caps to annuli [33]. With the annulus radial coordinate η given by $\eta = \tan(\theta/2)$, where θ is the polar angle in spherical coordinates, the classical solution reads

$$\phi^{\rm cl}(\eta) = \frac{\phi^{\rm cl}_{|\Gamma_A}}{\log\frac{\eta_A}{\eta_2}} \log\frac{\eta}{\eta_2}\,, \tag{3.38}$$

where $\eta_{A(2)} = \tan(\theta_{A(2)}/2)$ correspond to the positions of the entangling cuts $\Gamma_{A(2)}$ on the sphere.[4] The analytic continuation of $W(n)$ obtained in [33] is given by

$$W(n) = \sqrt{n}\, c^{-\frac{n-1}{2}} \int_{-\infty}^{\infty} \frac{dk}{\sqrt{\pi}} e^{-k^2} \left[\sum_{\omega\in\mathbb{Z}} \exp\left(-\frac{\pi}{c}\omega^2 - 2i\sqrt{\frac{\pi}{c}}k\omega\right)\right]^{n-1}, \tag{3.39}$$

where the constant c takes the value

$$c = \frac{8\pi^2 R_c^2 g}{\log(\eta_2/\eta_A)}.$$

Hence, from (3.34) and (3.37) we obtain for the logarithmic negativity

$$\mathcal{E} = -\log\left(\frac{Z_{A_1}Z_{A_2}}{Z_{A_1\cup A_2}}\right) + 2\log W(1/2)\,. \tag{3.40}$$

The partition functions in (3.40) can be computed via functional determinants and regularised by means of zeta-function techniques. For the regularised functional determinants we use the results of [33, 53, 54], reported in appendix C.1 below, where A_1 and $A_1 \cup A_2$ are spherical caps with Dirichlet conditions at the boundary, and A_2 is the "belt" region between two spherical caps (A_1 and B) with Dirichlet conditions at both boundaries. This yields

$$-\log\left(\frac{Z_{A_1}Z_{A_2}}{Z_{A_1\cup A_2}}\right) = \frac{1}{2}\log\log\frac{\eta_2}{\eta_A} - \frac{1}{2}\log\pi + \frac{1}{2}\sum_{m>0}\log\left(1-\left(\frac{\eta_A}{\eta_2}\right)^{2m}\right)^2, \tag{3.41}$$

while for the winding sector we have

$$2\log W(1/2) = \tag{3.42}$$
$$\log\sqrt{2\pi^2 g}R_c - \frac{1}{2}\log\log\frac{\eta_2}{\eta_A} + 2\log\int_{-\infty}^{\infty}\frac{dk}{\sqrt{\pi}}e^{-k^2}\left[\sum_{\omega\in\mathbb{Z}}\exp\left(-\frac{\pi}{c}\omega^2 - 2i\sqrt{\frac{\pi}{c}}k\omega\right)\right]^{-1/2}.$$

[4] Only classical fields with support in the region A_2 (see figure 6) are non-zero, and thus contribute to the winding sector [33].

Putting everything together, our explicit analytic expression for the logarithmic negativity is given by

$$\mathcal{E} = \log\sqrt{2\pi g}R_c + \frac{1}{2}\sum_{m>0}\log\left(1-\left(\frac{\eta_A}{\eta_2}\right)^{2m}\right)^2 + 2\log\int_{-\infty}^{\infty}\frac{dk}{\sqrt{\pi}}e^{-k^2}\left[\sum_{\omega\in\mathbb{Z}}\exp\left(-\frac{\pi}{c}\omega^2 - 2i\sqrt{\frac{\pi}{c}}k\omega\right)\right]^{-1/2}. \tag{3.43}$$

Let us consider the pure state regime, where $B \to \emptyset$. This corresponds to the limit $\eta_2 \gg \eta_A$, that is $c \ll 1$, and we obtain

$$\mathcal{E} = \log\sqrt{2\pi g}R_c - 2\left(\frac{\eta_A}{\eta_2}\right)^{\frac{1}{4\pi g R_c^2}} - \left(\frac{\eta_A}{\eta_2}\right)^2 + \dots, \tag{3.44}$$

since

$$2\log W(1/2) = \log\sqrt{2\pi^2 g}R_c - \frac{1}{2}\log\log\frac{\eta_2}{\eta_A} - 2\left(\frac{\eta_A}{\eta_2}\right)^{\frac{1}{4\pi g R_c^2}} + \cdots. \tag{3.45}$$

We expect to recover the 1/2-th Rényi entropy in that case, as discussed in section 3.1. Indeed, from [33, 34] one has for pure states

$$S_{A_1}^{(1/2)} = \log\sqrt{2\pi g}R_c\,,$$

which is in agreement with (3.44). We note, however, a curious difference in the dependence on the compactification radius between the Rényi entropy and the logarithmic negativity. On the one hand, in the pure state, the dependence of the Rényi entropy and entanglement entropy on the compactification radius R_c is due to a zero mode of the partition function on the sphere [33, 34]. On the other hand, the partition functions in (3.40) and (3.41) have no zero modes and therefore the same dependence in the logarithmic negativity $\mathcal{E}$ must arise from the winding sector.

3.4.2 Toroidal geometry

The toroidal geometry is shown in the right image of figure 6. We consider the torus to have area $L_1 \times L_2$ and to be cut along the L_1 direction. We denote the lengths of A_1, A_2, and B by ℓ_1, ℓ_2, and ℓ_B respectively. As before we partially trace over B first, and then we partially transpose over A_2. The first step is to understand how the boundary conditions (3.20) are modified by the presence of the winding modes. Each replicated field is split in classical and fluctuating fields, where the latter obey Dirichlet boundary conditions at the cuts. Hence, the only remaining task is understanding the boundary conditions obeyed by the classical fields $\phi^{\rm cl}$. In a torus the minimal choice we can do requires three cuts and thus a priori $3n_e$ winding numbers. From the discussion in section 3.3 we know that there are four cut functions: χ_1 (χ_2) for the cut Γ_1 (Γ_2) between A_1 (A_2) and B, and $\chi^{e/o}$ defined at the entangling cut Γ_A between A_1 and A_2. As in the spherical case, we redefine the χ functions at Γ_1, Γ_2 and Γ_A to absorb the n_e-th winding mode of each of the cuts, as well as the $n_e/2$-th winding mode in Γ_A. The torus admits a global shift symmetry

$\phi_i \to \phi_i + \text{const.}$, which we use it to get rid of all the $n_e - 1$ winding modes at the cut Γ_2 (the choice between Γ_1 and Γ_2 is completely equivalent). Relabelling the difference of winding modes, we end up with the following boundary conditions

$$\phi_i^{\text{cl}}|_{\Gamma_2} = \chi_2\,, \qquad i = 1, \dots, n_e\,, \tag{3.46a}$$

$$\phi_i^{\text{cl}}|_{\Gamma_1} = \begin{cases} \chi_1 + 2\pi R_c \omega_i^1\,, & i = 1, \dots, n_e - 1\,, \\ \chi_1\,, & i = n_e\,, \end{cases} \tag{3.46b}$$

$$\phi_i^{\text{cl}}|_{\Gamma_A} = \begin{cases} \chi_o + 2\pi R_c \omega_i^o\,, & i = 1, \dots, n_e/2 - 1\,, \\ \chi_o & i = n_e/2\,, \\ \chi_e + 2\pi R_c \omega_i^e\,, & i = 1, \dots, n_e/2 - 1\,, \\ \chi_e\,, & i = n_e/2\,, \end{cases} \tag{3.46c}$$

with $\omega_i^a \in \mathbb{Z}$. From the above conditions, it is clear that we have $2n_e - 3$ independent modes, which are not symmetrically distributed among the cuts: the two cuts Γ_1, Γ_A carry a different number of degrees of freedom, and thus of winding modes, which ultimately gives rise to a rather involved expression for the winding sector. As done previously, we rotate the classical fields with a $\tilde{U}_{n_e}$ rotation that acts separately on the first and second sets of $n_e/2$ fields, see equation (3.23), and obtain

$$\tilde{\phi}_i^{\text{cl}}|_{\Gamma_2} = \begin{cases} \sqrt{\frac{n_e}{2}}\chi_2 & i = n_e/2, n_e\,, \\ 0\,, & i = 1, \dots, n_e - 1, \quad \text{with} \quad i \neq n_e/2\,, \end{cases} \tag{3.47a}$$

$$\tilde{\phi}_i^{\text{cl}}|_{\Gamma_1} = \begin{cases} 2\pi R_c (M_{n_e/2-1})_{ij} \omega_j^1 - 2\pi R_c \sqrt{1 - \frac{2}{n_e}} \delta_{i, n_e/2-1} \omega_{n_e/2}^1\,, & i, j = 1, \dots, n_e/2 - 1\,, \\ \sqrt{\frac{n_e}{2}}\chi_1 + \frac{2\pi R_c}{\sqrt{n_e/2}} \sum_{k=1}^{n_e/2} \omega_k^1\,, & i = n_e/2\,, \end{cases} \tag{3.47b}$$

$$\tilde{\phi}_{i+n_e/2}^{\text{cl}}|_{\Gamma_1} = \begin{cases} 2\pi R_c (M_{n_e/2-1})_{ij} \omega_{j+n_e/2}^1\,, & i, j = 1, \dots, n_e/2 - 1\,, \\ \sqrt{\frac{n_e}{2}}\chi_1 + \sum_{k=1}^{n_e/2-1} \omega_{k+n_e/2}^1 & i = n_e\,, \end{cases}$$

$$\tilde{\phi}_i^{\text{cl}}|_{\Gamma_A} = \begin{cases} 2\pi R_c (M_{n_e/2-1})_{ij} \omega_j^o & i, j = 1, \dots, n_e/2 - 1\,, \\ \sqrt{\frac{n_e}{2}}\chi_o + \frac{2\pi R_c}{\sqrt{n_e/2}} \sum_{k=1}^{n_e/2-1} \omega_k^o\,, & i = n_e/2\,, \end{cases} \tag{3.47c}$$

$$\tilde{\phi}_{i+n_e/2}^{\text{cl}}|_{\Gamma_A} = \begin{cases} 2\pi R_c (M_{n_e/2-1})_{ij} \omega_j^e & i, j = 1, \dots, n_e/2 - 1\,, \\ \sqrt{\frac{n_e}{2}}\chi_e + \frac{2\pi R_c}{\sqrt{n_e/2}} \sum_{k=1}^{n_e/2-1} \omega_k^e\,, & i = n_e/2\,. \end{cases}$$

The "unusual" first line in (3.47b) is simply due to the explicit form of the matrix $U_{n_e/2}$. The winding mode $\omega_{n_e/2}^1$ is responsible for the coupling between the various frequencies, as

will become clear later. In order to simplify the notation, we define the following vectors

$$\begin{aligned} \mu^1 &:= (\omega^1_1,\dots,\omega^1_{n_e/2-1}), & \upsilon^1 &:= (\omega^1_{n_e/2+1},\dots,\omega^1_{n_e-1}),\\ \mu^A &:= (\omega^o_1,\dots,\omega^o_{n_e/2-1}), & \upsilon^A &:= (\omega^e_{n_e/2+1},\dots,\omega^e_{n_e-1}),\\ \gamma &:= \omega^1_{n_e/2}, & I &:= (1,\dots,1)\in\mathbb{Z}^{n_e/2-1}. \end{aligned} \tag{3.48}$$

Performing the last U_2 rotation on the fields labelled by n_e and $n_e/2$, we obtain

$$\bar\phi^{\rm cl}_i|_{\Gamma_2} = \begin{cases} 0, & i=1,\dots,n_e-1,\\ \sqrt{n_e}\chi_2, & i=n_e, \end{cases} \tag{3.49a}$$

$$\bar\phi^{\rm cl}_i|_{\Gamma_1} = \begin{cases} 2\pi R_c (M_{n_e/2-1})_{ij}\mu^1_j - 2\pi R_c\sqrt{1-\frac{2}{n_e}}\delta_{i,n_e/2-1}\gamma, & i,j=1,\dots,n_e/2-1,\\ \frac{2\pi R_c}{\sqrt{n_e}}\left(I\cdot\mu^1 - I\cdot\upsilon^1+\gamma\right), & i=n_e/2, \end{cases} \tag{3.49b}$$

$$\bar\phi^{\rm cl}_{i+n_e/2}|_{\Gamma_1} = \begin{cases} 2\pi R_c (M_{n_e/2-1})_{ij}\upsilon^1_j, & i,j=1,\dots,n_e/2-1,\\ \sqrt{n_e}\chi_1 + \frac{2\pi R_c}{\sqrt{n_e}} I\cdot\upsilon^1, & i=n_e, \end{cases}$$

$$\bar\phi^{\rm cl}_i|_{\Gamma_A} = \begin{cases} 2\pi R_c (M_{n_e/2-1})_{ij}\mu^A_j, & i,j=1,\dots,n_e/2-1,\\ \sqrt{\frac{n_e}{2}}\chi_- + \frac{2\pi R_c}{\sqrt{n_e}}\left(I\cdot\mu^A - I\cdot\upsilon^A\right), & i=n_e/2, \end{cases} \tag{3.49c}$$

$$\bar\phi^{\rm cl}_{i+n_e/2}|_{\Gamma_A} = \begin{cases} 2\pi R_c (M_{n_e/2-1})_{ij}\upsilon^A_j, & i,j=1,\dots,n_e/2-1,\\ \sqrt{\frac{n_e}{2}}\chi_+ + \frac{2\pi R_c}{\sqrt{n_e}}\left(I\cdot\mu^A + I\cdot\upsilon^A\right), & i=n_e, \end{cases}$$

where $I\cdot x := \sum_{i=1}^{n_e/2-1} x_i$ is the scalar product of $x\in\mathbb{Z}^{n_e/2-1}$ and I. Thus, the n_e-th field can be used to reconstruct the partition function over the whole manifold, while the $n_e/2$-th contributes to the partition function over the cylinder $A = A_1\cup A_2$. Hence, including the contributions from the fluctuating fields, our final expression is

$$\mathrm{Tr}\left(\rho_A^{T_{A_2}}\right)^{n_e} = \sqrt{n_e}\,\frac{(Z_{A_1}Z_{A_2})^{n_e-2}Z_{A_1\cup A_2}Z_B^{n_e-1}}{Z_{A\cup B}^{n_e-1}}\,W_{\mathcal{E}}(n_e), \tag{3.50}$$

where

$$W_{\mathcal{E}}(n_e) = \sum_{\substack{\mu\in\mathbb{Z}^{n_e-2}\\ \upsilon\in\mathbb{Z}^{n_e-2}\\ \gamma\in\mathbb{Z}}} e^{-\sum_{k=1}^{n_e-1} S[\bar\phi^{\rm cl}_i]}, \qquad \mu := (\mu^1,\mu^A), \quad \upsilon := (\upsilon^1,\upsilon^A), \tag{3.51}$$

and the classical fields satisfy the boundary conditions (3.49). Notice that in (3.51) the classical field $\bar\phi^{\rm cl}_{n_e/2}$ only sees two torus cuts, along Γ_1 and Γ_2. As for the spherical geometry, the factor $\sqrt{n_e}$ appears in (3.50) due to the different compactification radius for the n_e-th field. The logarithmic negativity (1.3) is then formally given by

$$\mathcal{E} = -\log\left(\frac{Z_{A_1}Z_{A_2}}{Z_{A_1\cup A_2}}\right) + \log W_{\mathcal{E}}(1). \tag{3.52}$$

The contribution from the fluctuating fields is straightforward to compute using the results reported in appendix C.2[5] and amounts to

$$\begin{aligned} -\log\left(\frac{Z_{A_1}Z_{A_2}}{Z_{A_1\cup A_2}}\right) &= \frac{1}{2}\log\left(\frac{\det\Delta_{A_1}\det\Delta_{A_2}}{\det\Delta_A}\right), \\ &= \frac{1}{2}\log\left(\frac{2u_1u_2}{u_{12}}|\tau|\right) + \log\left(\frac{|\eta(2u_1\tau)\eta(2u_2\tau)|}{|\eta(2u_{12}\tau)|}\right), \end{aligned} \tag{3.53}$$

where we used the aspect ratios

$$u_1 = \frac{\ell_1}{L_1}, \qquad u_2 = \frac{\ell_2}{L_1}, \qquad u_{12} = u_1 + u_2, \tag{3.54}$$

for the submanifolds A_1 and A_2, respectively. Notice that $u_1 + u_2 \neq 1$, since there is still the contribution from the B sector to the total lenght. This is even more pronounced in the winding function $W_{\mathcal{E}}$. Following appendix D, the expressions for $W_{\mathcal{E}}$ reads

$$\begin{aligned} &W_{\mathcal{E}}(n_e) \qquad\qquad (3.55)\\ &= \sum_{\mathbb{Z}^{2n_e-3}} \exp\left\{-\frac{g(2\pi R_c)^2}{|\tau|}\left[\mu^T\,\mathrm{T}\,\mu + \upsilon^T\,\mathrm{T}\,\upsilon + \left(1-\frac{2}{n}\right)\frac{1-u_2}{u_1(1-u_{12})}\left(\gamma - I\cdot\mu^1\right)^2\right.\right. \\ &\left.\left. + \frac{1}{n\,u_{12}(1-u_{12})}\left(\gamma - I\cdot\upsilon^1\right)^2 - \frac{4}{n\,u_1}\left(\gamma - I\cdot\mu^1\right)\left(\frac{1-u_2}{u_1(1-u_{12})}I\cdot\mu^1 - I\cdot\mu^A\right)\right]\right\}, \end{aligned}$$

where T is defined in (D.6). Collecting all the modes in a $(2n_e-3)$-vector, $\Omega = (\mu, \upsilon, \gamma)$, we can rewrite the above expression (3.55) as follows

$$W_{\mathcal{E}}(n_e) = \sum_{\Omega\in\mathbb{Z}^{2n_e-3}} \exp\left(-\frac{g(2\pi R_c)^2}{|\tau|}\Omega^T\,\mathcal{T}\,\Omega\right), \tag{3.56}$$

where $\mathcal{T}$ is reported in appendix D, equation (D.10). The matrix $\mathcal{T}$ is symmetric and positive definite, hence the sum (3.56) is convergent. Unfortunately, we were not able to find an analytic continuation of the winding sector (3.56), which means that we are not able to compute $\log W_{\mathcal{E}}(1)$ in (3.52).

4 Odd entropy

The odd entropy S_o introduced in [40] for a mixed state described by a density matrix ρ_A is defined as

$$S_o^{(n_o)}(\rho_A) = \frac{1}{1-n_o}\left(\mathrm{Tr}\left(\rho_A^{T_2}\right)^{n_o} - 1\right), \qquad S_o(\rho_A) = \lim_{n_o\to 1} S_o^{(n_o)}(\rho_A), \tag{4.1}$$

where n_o is an odd positive integer, and where, as before, we denote the union of A_1 and A_2 by A and indicate the partial transposition over A_2 by ^{T_2}. For pure states, the odd entropy reduces to the entanglement entropy [40], as per (3.12).

[5] Again, the functional determinants in the above expressions are regularised and calculated by means of zeta-function techniques.

In this section we compute S_o by means of the replica approach. We stress that, as for the logarithmic negativity, our calculation only gives us the universal terms. The computations are similar to those illustrated before, and mainly differ from them in the boundary conditions at the entangling cut between A_1 and A_2, as we explain below. First, we consider a spherical manifold in section 4.1, and then we analyse the case of a toroidal manifold, see section 4.2. On both geometries, we find the following formal expression for the odd entropy

$$S_o = -\log\left(\frac{Z_{A_1}Z_{A_2}Z_B}{Z_{A\cup B}}\right) - \frac{1}{2} - W'_{\rm OE}(1)\,, \tag{4.2}$$

where $W_{\rm OE}$ is the contribution from the corresponding winding sector.

4.1 Spherical geometry

Let us consider a spherical geometry. In the next section we discuss a geometrical configuration where the submanifolds A_1 and A_2 are disjoint, see figure 4, and in section 4.1.2 we treat the case of adjacent submanifolds as in figure 6.

4.1.1 Disjoint submanifolds

In the case of disjoints submanifolds and for an odd number of replicas, it is not difficult to realise that the gluing conditions force *all* the fields to agree at *both* entangling cuts. The situation is similar to the one depicted in figure 5. Using the same notation as in figure 5, we now have the following boundary conditions

$$\begin{aligned}
&\Gamma_1: \quad \phi_i^{A_1}|_{\Gamma_1} = \phi_j^{B}|_{\Gamma_1} = \chi_1\,, \qquad i,j = 1,\dots,n_o\,,\\
&\Gamma_2: \quad \phi_i^{A_2}|_{\Gamma_2} = \phi_j^{B}|_{\Gamma_2} = \chi_2\,, \qquad i,j = 1,\dots,n_o\,.
\end{aligned} \tag{4.3}$$

Separating the classical contributions from the fluctuating fields, and using the global shift symmetry to eliminate the frequency modes from the entangling cut Γ_2, we can write

$$\begin{aligned}
&\Gamma_1: \quad \phi_i^{\rm cl}|_{\Gamma_1} = \chi_1 + 2\pi R_c\omega_i\,, \qquad i = 1,\dots,n_o-1\,,\\
&\qquad\quad \phi_{n_o}^{\rm cl}|_{\Gamma_1} = \chi_1\,,\\
&\Gamma_2: \quad \phi_i^{\rm cl}|_{\Gamma_2} = \chi_2\,, \qquad i = 1,\dots,n_o\,.
\end{aligned} \tag{4.4}$$

At this point we can perform the usual rotation U_{n_o} and obtain

$$\begin{aligned}
&\Gamma_1: \quad \tilde\phi_i^{\rm cl}|_{\Gamma_1} = 2\pi R_c (M_{n_o-1})_{ij}\omega_j, \qquad i,j = 1,\dots,n_o-1\,,\\
&\qquad\quad \tilde\phi_{n_o}^{\rm cl}|_{\Gamma_1} = \sqrt{n_o}\chi_1 + \frac{2\pi R_c}{\sqrt{n_o}}\sum_{i=1}^{n_o-1}\omega_i\,,\\
&\Gamma_2: \quad \tilde\phi_i^{\rm cl}|_{\Gamma_2} = 0\,, \qquad i = 1,\dots,n_o-1\,,\\
&\qquad\quad \tilde\phi_{n_o}^{\rm cl}|_{\Gamma_2} = \sqrt{n_o}\chi_2\,.
\end{aligned} \tag{4.5}$$

The cassical field $\tilde\phi_{n_o}^{\rm cl}$ together with the fluctuating field φ_{n_o} can be used to reconstruct the whole partition function over the sphere. Notice that we do not need to perform any further rotation. The n_o-1 classical fields $\tilde\phi_i^{\rm cl}$ contribute to the winding sector $W_{\rm OE}(n_o)$

as before. The fluctuating fields obey Dirichlet conditions at the entangling cuts and give rise to the corresponding partition functions over the submanifolds. Hence, we can write

$$\mathrm{Tr}\left(\rho_A^{T_2}\right)^{n_o} = \sqrt{n_o}\left(\frac{Z_{A_1}Z_{A_2}Z_B}{Z_{A\cup B}}\right)^{n_o-1} W_{\mathrm{OE}}(n_o)\,. \tag{4.6}$$

In particular, the expression for the winding sector $W_{\mathrm{OE}}(n_o)$ is nothing but the function $W(n_o)$ given by (3.39), where c now reads

$$c = \frac{8\pi^2 g R_c^2}{\log\left(\eta_2/\eta_1\right)}\,.$$

As in section 3.4.1, η is the radial coordinate defined as $\eta = \tan\theta/2$, and the radii $\eta_{1(2)}$ correspond to the polar angles $\theta_{1(2)}$ where we place the cuts $\Gamma_{1(2)}$. The odd entropy (4.1) is then given by

$$\begin{aligned} S_o &= -\log\left(\frac{Z_{A_1}Z_{A_2}Z_B}{Z_{A\cup B}}\right) - \frac{1}{2} - W'(1) \\ &= \frac{1}{2}\log\frac{\det\Delta_{A_1}\det\Delta_{A_2}\det\Delta_B}{\det\Delta_{\mathrm{sphere}}} + \log\sqrt{4\pi g\mathcal{A}}R_c - \frac{1}{2} - W'(1)\,, \end{aligned} \tag{4.7}$$

which is nothing but the von Neumann entropy for two spherical caps A_1, A_2 computed in [33]. The term $\log\sqrt{4\pi g\mathcal{A}}R_c$ is the contribution from the zero mode in the partition function on the sphere with area $\mathcal{A}$ [33, 34]. The contribution from the regularised functional determinants (cf. appendix C.1) is

$$\begin{aligned} &\frac{1}{2}\log\frac{\det\Delta_{A_1}\det\Delta_{A_2}\det\Delta_B}{\det\Delta_{\mathrm{sphere}}} + \log\sqrt{4\pi g\mathcal{A}}R_c \\ &\quad= \frac{1}{2}\log\frac{(\det\Delta_{\mathrm{hemisphere}})^2}{\det\Delta_{\mathrm{sphere}}} + \frac{1}{2}\log\left(\frac{1}{\pi}\log\frac{\eta_2}{\eta_1}\prod_{m>0}\left(1-\left(\frac{\eta_1}{\eta_2}\right)^{2m}\right)^2\right) + \log\sqrt{4\pi g\mathcal{A}}R_c \\ &\quad= \log\sqrt{8\pi g}R_c + \frac{1}{2}\log\left(\frac{1}{\pi}\log\frac{\eta_2}{\eta_1}\prod_{m>0}\left(1-\left(\frac{\eta_1}{\eta_2}\right)^{2m}\right)^2\right), \end{aligned} \tag{4.8}$$

where we used that $\mathcal{A} = 4\pi$ for the unit sphere and the result (C.2). The contribution from the winding sector is [33]

$$-W'(1) = -\frac{1}{2} + \frac{1}{2}\log c - \int_{-\infty}^{\infty}\frac{dk}{\sqrt{\pi}}\,e^{-k^2}\log\left(\sum_{\omega\in\mathbb{Z}}\exp\left(-\frac{\pi}{c}\omega^2 - 2i\sqrt{\frac{\pi}{c}}k\omega\right)\right). \tag{4.9}$$

Finally, combining the two contributions, the odd entropy is given by

$$\begin{aligned} S_o = 2\left(\log\sqrt{8\pi g}R_c - \frac{1}{2}\right) + \log\prod_{m>0}\left(1-\left(\frac{\eta_1}{\eta_2}\right)^{2m}\right)^2 \\ - \int_{-\infty}^{\infty}\frac{dk}{\sqrt{\pi}}\,e^{-k^2}\log\left(\sum_{\omega\in\mathbb{Z}}\exp\left(-\frac{\pi}{c}\omega^2 - 2i\sqrt{\frac{\pi}{c}}k\omega\right)\right). \end{aligned} \tag{4.10}$$

Summarising, for disjoint submanifolds, here represented by two spherical caps A_1, A_2, the odd entropy is identical to the entanglement entropy of $A_1 \cup A_2$. For mixed states, one of the features of odd entropy is that it reduces to the corresponding von Neumann entropy if ρ_A is a product state [40]. We remind the reader that for disjoint submanifolds the logarithmic negativity vanishes, see sections 3.2 and 2.4.2. However, this is not a sufficient condition for a system to be unentangled. Hence, the results for the odd entropy and the logarithmic negativity are consistent.

4.1.2 Adjacent submanifolds

Let us now consider the case in which A_1 and A_2 are adjacent as in figure 6. Using figure 7 as a guiding example, but taking an odd number of replicas, we can easily convince ourselves that *all* the fields have to agree at the entangling cuts, indicated here as Γ_A, Γ_2. We can then repeat the discussion of the previous section almost identically, with the replacement $\Gamma_1 \to \Gamma_A$. It is thus clear that the odd entropy is given by (4.7), where now the parameter c in the function W is given by

$$c = \frac{8\pi^2 R_c^2 g}{\log\left(\eta_2/\eta_A\right)},$$

where $\eta_A = \tan\theta_A/2$ is the radial coordinate corresponding to the cut Γ_A.[6] Hence, the explicit expression of the odd entropy reads

$$\begin{aligned} S_o = 2\left(\log\sqrt{8\pi g}R_c - \frac{1}{2}\right) + \log\prod_{m>0}\left(1-\left(\frac{\eta_A}{\eta_2}\right)^{2m}\right)^2 \\ - \int_{-\infty}^{\infty}\frac{dk}{\sqrt{\pi}}\,e^{-k^2}\log\left(\sum_{\omega\in\mathbb{Z}}\exp\left(-\frac{\pi}{c}\omega^2 - 2i\sqrt{\frac{\pi}{c}}k\omega\right)\right). \end{aligned} \tag{4.11}$$

In the case of adjacent submanifolds, we can examine the pure state limit, as we have done for the logarithmic negativity. There are, however, some caveats. Looking at the expression (4.2), the divergences which we can expect are given by the interfaces between A_1 and A_2, and between A_2 and B [55], see also discussion in [33]. In the pure state limit, the odd entropy is expected to reduce to the von Neumann entropy of the corresponding pure state, which has a divergence controlled by the characteristic size of the entangling surface Γ_A between A_1 and A_2. Since we are only computing the universal terms, expression (4.2) also develops a divergent contribution related to the entangling surface Γ_2 between A_2 and B in the pure state limit. This means that in our approach only a "regulated" odd entropy, given by the difference of the odd entropy and an entanglement measure carrying a divergence at the entangling surface Γ_2, will correctly reduce to the entanglement entropy in the pure state limit. We choose the entanglement entropy $S_{\rm EE}(\rho_A)$ of the region A as regulator, since it carries the divergence that we want to subtract. In this case, $S_{\rm EE}(\rho_A)$ is the entanglement entropy of a spherical cap given by the union of A_1, A_2, that is [33, 34]

$$S_{\rm EE}(\rho_A) = \frac{1}{2}\log\left(\frac{\det\Delta_A\det\Delta_B}{\det_{A\cup B}}\right) + \log\left(\sqrt{4\pi g\mathcal{A}}R_c\right) - \frac{1}{2} = \log\left(\sqrt{8\pi g}R_c\right) - \frac{1}{2}. \tag{4.12}$$

[6] Notice that now the odd entropy is formally identical to the von Neumann entropy for the two spherical caps A_1 and B.

Hence, in the pure state limit, when $\eta_2 \gg \eta_A$, that is when $c \ll 1$, we have

$$\Delta S_o \equiv S_o - S_{\mathrm{EE}}(\rho_A) \approx \log \sqrt{8\pi g} R_c - \frac{1}{2} - 2\left(\frac{\eta_A}{\eta_2}\right)^{\frac{1}{4\pi g R_c^2}} - \left(\frac{\eta_A}{\eta_2}\right)^2 + \dots , \tag{4.13}$$

which correctly reproduces the pure state entanglement entropy result [33]. We have checked that using $S_{\mathrm{EE}}(\rho_A)$ as a regulator also provides a correct pure state limit in the case of cylindrical manifolds (in the non-compact case). There, the term removed by the entanglement entropy is actually divergent and ΔS_o correctly reduces to the finite universal term of the entanglement entropy for a pure state, cf. appendix E.

4.2 Toroidal geometry

Next, we consider the toroidal geometry depicted in figure 6. Let us proceed as in section 3.4.2 in order to understand the boundary conditions at each entangling cuts. When the replica index $n = n_o$ is odd, the boundary conditions at the cut Γ_A between A_1 and A_2 require *all* fields to be equal,[7] while the conditions at the cuts Γ_1 and Γ_2 remain unchanged. After separating each of the fields into a fluctuation φ_i satisfying Dirichlet boundary conditions at the cuts and a classical part ϕ_i^{cl}, the boundary conditions for the classical fields at the entangling cuts read

$$\begin{aligned} \phi_i^{\mathrm{cl}}|_{\Gamma_a} &= \chi_a + 2\pi\, R_c\, \omega_i^a + \phi_i^0 - \phi_{n_o}^0 \,, \qquad i = 1, \dots, n_o - 1 \,, \\ \phi_{n_o}^{\mathrm{cl}}|_{\Gamma_a} &= \chi_a \,, \end{aligned} \tag{4.14}$$

for $a = 1, 2, A$, where $\phi_i^0 - \phi_n^0$ are the zero modes. Note that we used our freedom to redefine the arbitrary cut functions χ_a to get rid of the n_o-th winding numbers and zero mode at all cuts, and relabelled $\omega_i^a - \omega_{n_o}^a$ to ω_i^a without loss of generality. We can choose $\phi_i^0 - \phi_{n_o}^0$ such that it removes the winding modes at the entangling cut Γ_2, the choice of Γ_2 here is completely equivalent to any other, since all the entangling cuts carry the same number of degrees of freedom. With this choice we obtain

$$\begin{aligned} \phi_i^{\mathrm{cl}}|_{\Gamma_a} &= \chi_a + 2\pi\, R_c \left(\omega_i^a - \omega_i^2\right), && a = 1, A \,, \quad i = 1, \dots, n_o - 1 \,, \\ \phi_{n_o}^{\mathrm{cl}}|_{\Gamma_a} &= \chi_a \,, && a = 1, A \,, \\ \phi_i^{\mathrm{cl}}|_{\Gamma_2} &= \chi_2 \,, && i = 1, \dots, n_o \,. \end{aligned} \tag{4.15}$$

We can then perform a U_{n_o} rotation, cf. (3.22), which gives us

$$\begin{aligned} \tilde{\phi}_i^{\mathrm{cl}}|_{\Gamma_a} &= 2\pi\, R_c\, (M_{n_o-1})_{ij}\, \omega_i^a, && a = 1, A \,, \quad i = 1, \dots, n_o - 1 \,, \\ \tilde{\phi}_{n_o}^{\mathrm{cl}}|_{\Gamma_a} &= \sqrt{n_o}\chi_a + \frac{2\pi\, R_c}{\sqrt{n_o}} \sum_{k=1}^{n_o-1} \omega_i^a \,, && a = 1, A \,, \\ \tilde{\phi}_i^{\mathrm{cl}}|_{\Gamma_2} &= 0 \,, && i = 1, \dots, n_o - 1 \,, \\ \tilde{\phi}_{n_o}^{\mathrm{cl}}|_{\Gamma_2} &= \sqrt{n_o}\, \chi_2 \,, \end{aligned} \tag{4.16}$$

[7] We remind the reader that for an even integer n_e the boundary conditions at Γ_A split the fields into two independent sets, cf. section 3.4.2.

where we, again, relabelled $\omega_i^a - \omega_i^2$ into ω_i^a without loss of generality. Notice that we have in total $2n_o - 2$ independent winding modes ω_i^a, which we can collect in a $\mathbb{Z}^{2n_o-2}$ vector as $\omega := (\omega^1, \omega^A)$. As usual, the n_o-th field can be used to reconstruct the partition function on the entire torus $Z_{A\cup B}$, and we obtain

$$\mathrm{Tr}\left(\rho_A^{T_2}\right)^{n_o} = \sqrt{n_o}\left(\frac{Z_{A_1}Z_{A_2}Z_B}{Z_{A\cup B}}\right)^{n_o-1} W_{\mathrm{OE}}(n_o)\,, \tag{4.17}$$

where $W_{\mathrm{OE}}(n_o)$ is again the contribution from the $2n_o - 2$ classical modes, now satisfying the boundary conditions (4.16), that is

$$W_{\mathrm{OE}}(n_o) = \sum_{\phi_i^{\mathrm{cl}}} e^{-\sum_i S[\phi_i^{\mathrm{cl}}]}\,. \tag{4.18}$$

Hence, the formal expression for the odd entropy (4.1) which follows from (4.17) is

$$S_o = -\log\left(\frac{Z_{A_1}Z_{A_2}Z_B}{Z_{A\cup B}}\right) - \frac{1}{2} - W'_{\mathrm{OE}}(1)\,. \tag{4.19}$$

The contribution from the fluctuating fields can be read straightforwardly from the results reported in appendix C.2, and we obtain

$$\begin{aligned} -\log\left(\frac{Z_{A_1}Z_{A_2}Z_B}{Z_{A\cup B}}\right) &= \frac{1}{2}\log\frac{\det\Delta_{\mathrm{cyl,A_1}}\det\Delta_{\mathrm{cyl,A_2}}\det\Delta_{\mathrm{cyl,B}}}{\det\Delta_{\mathrm{torus}}} + \frac{1}{2}\log 4\pi g R_c^2\mathcal{A} \\ &= \frac{1}{2}\log\left(8u_1u_2(1-u_{12})|\tau|^2\right) + \log\frac{\eta(2u_1\tau)\eta(2u_2\tau)\eta(2(1-u_{12})\tau)}{\eta^2(\tau)} \\ &\quad + \frac{1}{2}\log 4\pi g R_c^2\,, \end{aligned} \tag{4.20}$$

since $\mathcal{A} = L_1L_2$, and where the Dedekind η-function is defined in (C.4). The aspect ratios where defined in (3.54).

The explicit expression for the winding sector is calculated in appendix D.2, see equations (D.16) and (D.22), and reads

$$W_{\mathrm{OE}}(n_o) = n_o\left(\frac{|\tau|}{4\pi g R_c^2}\right)^{(n_o-1)}\left(u_1u_2(1-u_{12})\right)^{(n_o-1)/2}\Theta(\vec{0}\,|\,\mathrm{U})\,, \tag{4.21}$$

where $\Theta(\vec{0}\,|\mathrm{U})$ is a multi-dimensional theta function and U a positive definite matrix. Unfortunately, we have not found an analytic continuation to real n_o for the winding sector (4.21), hence we cannot compute the derivative of W_{OE} at $n_o = 1$.

5 Discussion

In this paper, we computed the logarithmic negativity for the quantum Lifshitz model — a prototype of non-relativistic field theories described by a free massless compact scalar with Lifshitz exponent $z = 2$ — in one and two spatial dimensions. To this end, we employed two different techniques: the correlator method for the $(1+1)$-dimensional QLM, where we assumed the scalar to be non-compact, and a replica method in $2+1$ dimensions.

In both cases, we first examined the QLM in its ground state and confirmed that the logarithmic negativity of a pure state reduces to the Rényi entropy with index 1/2, as generically expected in QFT [12]. We then investigated the QLM in a bipartite mixed state (A_1, A_2) obtained by tracing out the degrees of freedom of some subsystem (referred to as B throughout the paper) of the tripartite ground state. In particular, we studied the two cases where the subsystems A_1 and A_2 are either disjoint or adjacent. Both methods lead to the same general result: the logarithmic negativity vanishes for disjoint partitions regardless of the manifold, while it is given by a difference of free energies for adjacent subsystems.

A common feature we observed is the feasibility of analytic computations. As already mentioned, in one spatial dimension, the moments of the reduced density matrix and its partial transpose are obtained analytically, something that is not yet possible in $(1+1)$-dimensional CFT. Moreover, in the $(2+1)$-dimensional case, the computation of the logarithmic negativity simply reduces to a computation of partition functions for a free scalar relativistic theory, albeit on a non-trivial geometry. This is very different from what happens in CFTs, see e.g. [11, 12], and the feasibility of calculations in the QLM, in comparison with the conformal paradigm, is somehow surprising.

Another unexpected result is the fact that for disjoint submanifolds the QLM has a vanishing logarithmic negativity, similar to a topological theory, while for contiguous submanifolds the "CFT character" of the QLM dominates. We should stress here that the expression for the logarithmic negativity (2.35) in the (1+1)-dimensional QLM is suggestive of a relativistic field theory but on an infinite system (see discussion in section 2.4.4) and with an effective central charge given by $c_{\text{eff}} = z c_{\text{CFT}} = 2$, as proposed in [39].

To be more specific, the calculations in the real time formalism are carried out for a non-compact scalar on open and periodic chains. In the Euclidean formalism, the scalar is periodically identified (with the exception of section 3.3 which we use as a "warm-up exercise") and we take the spatial manifold to be either a 2-sphere or a 2-torus. For adjacent submanifolds on the sphere, we are able to analytically continue the winding sector contribution $W_{\mathcal{E}}$, but regrettably, we have not found a corresponding analytic continuation for $W_{\mathcal{E}}$ on the torus. The crucial difference between the two geometries, rendering one case completely solvable and the other not, is that only one entangling cut is "visible" to the winding sector on the sphere, while there are two "visible" cuts on the torus, see sections 3.4.1 and 3.4.2.

We also computed the odd entropy for the QLM on a 2-sphere and a 2-torus by means of the replica method. For the spherical case, regardless of whether the submanifolds are adjacent or disjoint, we always find a non-trivial result. Furthermore, the expressions for the odd entropy coincide with that of the entanglement entropy for two spherical caps, originally computed in [33]. This confirms the expectation that the odd entropy encodes both classical and quantum fluctuations [40]. For a toroidal manifold, we were not able to analytically continue the expression for the winding sector contribution to the odd entropy.

Interestingly, we notice that for non-compact fields the following relation holds:

$$S_o(\rho_A) - S_{\text{EE}}(\rho_A) = \mathcal{E}(\rho_A)\,, \tag{5.1}$$

where the odd entropy is given by keeping only the first term in (4.2), the entanglement entropy is formally given by (2.38) with $A = A_1 \cup A_2$, and the logarithmic negativity can be found in (3.28). For holographic CFTs, the quantity $S_o - S_{\rm EE}$ is conjectured [40] to be equal to the entanglement wedge cross-section (EWCS) in AdS spacetime, while it has been proposed[8] in [59, 60] that the logarithmic negativity $\mathcal{E}$ should to be dual to a backreacted EWCS. In particular, for simple subsystem configurations in $2d$ holographic CFTs, the backreacted EWCS picks up a factor of $3/2$ compared to that computed in pure AdS_3. We thus observe through (5.1) a clear difference between Lifshitz and conformal field theories. Let us also point out that (5.1) breaks down for compact fields — the relation being spoiled by the winding sector.

To our knowledge, our findings represent the first analytical results for the logarithmic negativity and the odd entropy in $2+1$ dimensions. Numerical studies for the logarithmic negativity in $3d$ CFTs were conducted in [44, 45]. This is one of the main remarkable properties of the QLM (and its higher-dimensional generalisations): it is a solvable theory for which one can perform controlled calculations in closed form, thus allowing us to extend analytical techniques beyond the $2d$ conformal framework, and also providing a benchmark for numerical investigations.

A substantial part of this work was focused on spherical and toroidal manifolds in $2+1$ dimensions. It would be interesting to consider other geometries, such as disks, and more general partitions. However, increasing the number of entangling cuts considerably increases the difficulty in performing analytic continuations. Indeed, the analytic continuation $n_e \to 1$ of the winding mode contributions remains an open problem (the same difficulties are present in $2d$ CFTs, see [11, 12]). The calculation of other entanglement measures for mixed states of relativistic and non-relativistic systems remains a relevant and challenging open problem.

Acknowledgments

We thank B. Chen, N. Jokela, K. Tamaoka, and especially D. Seminara and E. Tonni for valuable discussions and comments. VGMP would like to thank the Nordic Institute for Theoretical Physics (NORDITA), the University of Edinburgh, and the Galileo Galilei Institute for Theoretical Physics in Florence for the hospitality during the completion of this work. This research was supported in part by the Icelandic Research Fund under contracts 163419-053 and 195970-051, and by grants from the University of Iceland Research Fund. C.B. was supported in part by the National Natural Science Foundation of China (NSFC, Nos. 11335012, 11325522, 11735001), and by a Boya Postdoctoral Fellowship at Peking University.

[8] Another proposal for the holographic dual of entanglement negativity has been suggested in [56–58], and relates the logarithmic negativity in holographic CFTs to a certain combination of bulk minimal surfaces which reduces to the holographic mutual information.

A Invariance of the reduced density matrix under partial transposition for two disjoint intervals

In this appendix, we show that the reduced density matrix for two disjoint intervals in the $z = 2$ open chain is invariant under partial transposition. In the position representation, the ground state wave function reads

$$\Psi_0(\phi) \propto \exp\left(-\frac{1}{2}\phi^T W \phi\right), \tag{A.1}$$

and the associated density matrix is

$$\rho(\phi, \phi') \propto \exp\left(-\frac{1}{2}(\phi^T W \phi + \phi'^T W \phi')\right), \tag{A.2}$$

where $\phi^T = (\phi_1, \phi_2, \cdots)$, and $W \equiv K^{1/2}$ with the matrix K being a discrete version of the spatial biharmonic operator $\triangle^2 \equiv \partial_x^4$, see section 2.1.

For simplicity, we consider $A = A_1 \cup A_2$ to be a subsystem of the $z = 2$ open chain with A_1 and A_2 disjoint (of lengths ℓ_1 and ℓ_2, respectively) and each adjacent to one of the boundaries of the total system, although our reasoning carries through to general disjoint configurations. The reduced density matrix corresponding to A is obtained by integrating over the degrees of freedom in B. To perform the integration explicitly, we express $\phi = (\phi_{A_1}^T, \phi_B^T, \phi_{A_2}^T)^T$ in terms of oscillators belonging to each subsystems, and break W down into submatrices

$$W = \begin{pmatrix} W_{A_1} & V_1^T & V_A \\ V_1 & W_B & V_2 \\ V_A^T & V_2^T & W_{A_2} \end{pmatrix}. \tag{A.3}$$

It is then straightforward to obtain the reduced density matrix for the subsystem A as

$$\rho_A(\phi_A, \phi'_A) \propto \exp\left(-\frac{1}{2}\overline{\phi}_A^T \, \overline{W} \, \overline{\phi}_A\right), \tag{A.4}$$

where $\overline{\phi}_A = (\phi_{A_1}^T, \phi_{A_2}^T, \phi_{A_1}'^T, \phi_{A_2}'^T)^T$ and

$$\overline{W} = \begin{pmatrix} \overline{W}_{A_1} & \overline{V}_A & \overline{V}_{11} & \overline{V}_{12} \\ \overline{V}_A^T & \overline{W}_{A_2} & \overline{V}_{12}^T & \overline{V}_{22} \\ \overline{V}_{11} & \overline{V}_{12} & \overline{W}_{A_1} & \overline{V}_A \\ \overline{V}_{12}^T & \overline{V}_{22} & \overline{V}_A^T & \overline{W}_{A_2} \end{pmatrix}, \qquad \begin{aligned} &\overline{W}_{A_a} = W_{A_a} + \overline{V}_{aa}\,, \\ &\overline{V}_{ab} = -\frac{1}{4} V_a^T W_B^{-1} V_b\,, \quad a, b = \{1, 2\}\,, \\ &\overline{V}_A = V_A + \overline{V}_{12}\,. \end{aligned} \tag{A.5}$$

Invariance under partial transposition of the reduced density matrix, that is $\rho_A^{T_a} = \rho_A$, is equivalent to the condition $V_A = \mathbf{0}_{\ell_1 \times \ell_2}$. We have checked[9] that this condition always holds for two disjoint intervals in the critical $z = 2$ open chain, thus implying the invariance of ρ_A under partial transposition.

[9] The matrix W is nothing else than (twice) the two-point function given explicitly in (2.19), where one can readily check that V_A is a zero matrix.

B Spectrum of $C_A^{T_2}$ for two adjacent intervals

Open system. For two adjacent intervals of arbitrary lengths and relative position in the total system (say, A_1 is at a distance d_l from the left boundary), there are at most four eigenvalues of $C_A^{T_2}$ distinct from 1/2. They are the (positive) roots of the quartic equation $a\lambda^8 + b\lambda^6 + c\lambda^4 + d\lambda^2 + e = 0$ where

$$a = 256(L+1)\,, \tag{B.1}$$

$$b = -64\big((L-2d_l)(5\ell_1+\ell_2+6d_l+4) - (\ell_1+\ell_2)^2 - 4(\ell_1^2-1) + 2d_l(3d_l+4)\big)\,, \tag{B.2}$$

$$\begin{aligned} c = 16\big(&6 - 7\ell_1^2 - 2\ell_1(1+2\ell_1)\ell_2 - (3+4\ell_1)\ell_2^2 - 5d_l^2(1+\ell_1+\ell_2)\,,\\ &+ L(6+7\ell_1+3\ell_2+4\ell_1\ell_2) - d_l(9\ell_1+\ell_2+5(\ell_1+\ell_2)^2 - 5L(1+\ell_1+\ell_2))\big)\,, \end{aligned} \tag{B.3}$$

$$\begin{aligned} d = 4\big(&3\ell_1^2 - 4 + 2\ell_1(1+2\ell_1)\ell_2 + (3+4\ell_1)\ell_2^2 + 2d_l^2(2+\ell_1+\ell_2+2\ell_1\ell_2)\,,\\ &- 2d_l(L-\ell_1-\ell_2)(2+\ell_1+\ell_2+2\ell_1\ell_2) - L(4+3\ell_1+3\ell_2+4\ell_1\ell_2)\big)\,, \end{aligned} \tag{B.4}$$

$$e = (d_l+1)(\ell_1+\ell_2+1)(L-\ell_1-\ell_2-d_l+1)\,. \tag{B.5}$$

These roots are real and positive. Among them, only one is smaller than 1/2. It is given by

$$\lambda^2 = -\frac{b}{4a} - S - \frac{1}{2}\sqrt{\frac{p}{S} - 2q - 4S^2}\,, \tag{B.6}$$

where

$$p = \frac{b^3 - 4abc + 8a^2d}{8a^3}\,, \qquad q = \frac{8ac - 3b^2}{8a^2}\,, \quad S = \sqrt{(\Delta_0\cos\big(\phi/3\big) - ap)/(6a)}\,, \tag{B.7}$$

$$\Delta_0 = \sqrt{c^2 - 3bd + 12ae}\,, \qquad \phi = \arccos\Big(\frac{\Delta_1}{2\Delta_0^3}\Big)\,, \tag{B.8}$$

$$\Delta_1 = 2c^3 - 9bcd + 27b^2e + 27ad^2 - 72ace\,. \tag{B.9}$$

This eigenvalue λ may also be expressed with radicals, but its form is far too cumbersome to be displayed here. Now, considering the continuum regime, we find that λ does not actually depend on L nor d_l, i.e.

$$\lambda \overset{\text{cont.}}{\longrightarrow} \sqrt{\frac{\ell_1+\ell_2}{16\ell_1\ell_2}}\,. \tag{B.10}$$

This may indeed be checked numerically.

Periodic system. For the general case, with arbitrary $\ell_1 + \ell_2 < L$, the eigenvalues of $C_A^{T_2}$ in the critical limit ($m \to 0$, $mL \ll 1$) are

$$\text{Spectrum}(C_A^{T_2}) = \left\{\lambda_1, \lambda_2, \lambda_3, \sqrt{\frac{3}{2m^2L}}, \frac{1}{2}, \cdots, \frac{1}{2}\right\}\,, \tag{B.11}$$

where $\lambda_{1,2,3}$ are the roots of the cubic equation $a\lambda^6 - b\lambda^4 + c\lambda^2 - d = 0$ with

$$a = 384L\,, \tag{B.12}$$

$$b = 16\big(5(L-\ell_1-\ell_2+1)(\ell_1+\ell_2+1) + 8\ell_1\ell_2 + 4\big)\,, \tag{B.13}$$

$$c = 8\big((L-\ell_1-\ell_2+1)(\ell_1+\ell_2+2\ell_1\ell_2+2) + \ell_1+\ell_2+1\big)\,, \tag{B.14}$$

$$d = (L-\ell_1-\ell_2+1)(\ell_1+\ell_2+1)\,. \tag{B.15}$$

Only one eigenvalue in the spectrum of $C_A^{T_2}$, among $\lambda_{1,2,3}$, is smaller than $1/2$ and in the continuum limit it reads $\lambda^2 = (\ell_1 + \ell_2)/(16\ell_1\ell_2)$. Thus, similarly to the open chain, λ does not depend on the size of the total system.

C Functional determinants and reciprocal formulae

C.1 Spherical manifolds

Here we list the results for the various regularised functional determinants computed by means of zeta-function regularisation techniques in [53, 54, 61], and relevant for the spherical case discussed in section 3.4. In the following, whenever the manifold has a boundary, Dirichlet boundary conditions are assumed.

$$\begin{aligned}
&\frac{1}{2}\log\det\Delta_{\text{spherical cap}} = \frac{1}{2}\log\det\Delta_{\text{hemisphere}} - \frac{1}{3}\cos\theta - \frac{1}{6}\log\tan\frac{\theta}{2}\,,\\
&\frac{1}{2}\log\det\Delta_{\text{between spherical caps}} = \frac{1}{2}\log\det\Delta_{\text{annulus}} + \frac{1}{3}\left(\cos\theta_{\text{in}} - \cos\theta_{\text{fin}}\right)\,,\\
&\det\Delta_{\text{annulus}} = \frac{1}{\pi}\,\mu^{1/3}\,\log\frac{1}{\mu}\prod_{m>0}(1-\mu^{2m})^2\,, \qquad \mu = \frac{\eta_{\text{int}}}{\eta_{\text{out}}}\,.
\end{aligned} \tag{C.1}$$

The angles $\theta_{\text{in}}, \theta_{\text{fin}}$ are the smaller and larger angles respectively, starting from the North pole, which delimit the spherical surface between two spherical caps. The radii $\eta_{\text{int}}, \eta_{\text{out}}$ are the internal and external radii respectively of the annulus. The radial coordinate η and the polar angle θ are related by a stereographic projection, that is

$$\eta = \tan\frac{\theta}{2}\,.$$

Finally, the functional determinants for the Laplacian on the sphere and hemisphere are

$$\begin{aligned}
&\det\Delta_{\text{hemisphere}} = \frac{e^{\frac{1}{4}-2\left(\frac{1}{12}-\log(A)\right)}}{\sqrt{2\pi}}\,,\\
&\det\Delta_{\text{sphere}} = e^{\frac{1}{2}-4\left(\frac{1}{12}-\log(A)\right)}\,,\\
&\frac{1}{2}\log\frac{(\det\Delta_{\text{hemisphere}})^2}{\det\Delta_{\text{sphere}}} = \frac{1}{2}\log\frac{1}{2\pi}\,,
\end{aligned} \tag{C.2}$$

where A is the Glaisher constant.

C.2 Toroidal manifolds

Here we report the results for the regularised functional determinants of the Laplacian operator on a cylinder and a torus [51, 52], see also [34] and references therein for higher-dimensional generalisations. Consider a two-dimensional torus with area $L_1 \times L_2$. The functional determinant of the Laplacian on the torus is

$$\log\det\Delta_{\text{torus}} = \log\Big(L_1^2\,\eta^4(\tau)\Big)\,, \qquad \tau = i\frac{L_1}{L_2}\,, \tag{C.3}$$

where the Dedekind η-function is defined as follows

$$\eta(\tau) := q^{1/24}\prod_{n=1}^{\infty}(1-q^n)\,, \qquad q := e^{2i\pi\tau}\,. \tag{C.4}$$

Notice that the partition function on the torus is given by

$$Z_{\text{torus}} = 2\pi R_c\sqrt{\frac{g\mathcal{A}}{\pi}}\det{}^{-\frac{1}{2}}\Delta_{\text{torus}}\,, \tag{C.5}$$

due to the presence of a zero mode, with $\mathcal{A} = L_1L_2$ the area of the torus.

The functional determinant of the Laplacian operator on a cylinder of length L, that is $[0,L]\times S^1_{L_2}$, with Dirichlet boundary conditions, is

$$\log\det\Delta_{\text{cylinder}} = \log\Big(2\alpha|\tau|\eta^2(2\alpha\tau)\Big)\,, \qquad \alpha = \frac{L}{L_1}\,,\quad \tau = i\frac{L_1}{L_2}\,. \tag{C.6}$$

C.3 Reciprocal formulae

The reciprocal formula for the theta function is

$$\sum_{\omega\in\mathbb{Z}}\exp\left(-\frac{\pi}{c}\omega^2 - 2i\sqrt{\frac{\pi}{c}}k\omega\right) = \sqrt{c}\,e^{-k^2}\sum_{\omega\in\mathbb{Z}}\exp\Big(-\pi c\omega^2 + 2\sqrt{\pi c}\,k\omega\Big)\,. \tag{C.7}$$

The reciprocal formula for the multi-dimensional theta function [62] is

$$\sum_{\vec{m}\in\mathbb{Z}^n}\exp\Big(-\pi\,\vec{m}^T A\vec{m} + 2i\pi\,\vec{m}\cdot\vec{z}\Big) = \det A^{-\frac{1}{2}}\sum_{\vec{p}\in\mathbb{Z}^n}\exp\Big(-\pi(\vec{p}+\vec{z})^T A^{-1}(\vec{p}+\vec{z})\Big)\,. \tag{C.8}$$

D Winding sector for the 2-torus

In this section we illustrate in some detail the computation of the winding sectors $W_{\mathcal{E}}$ and W_{OE} for the torus, see equations (3.51) and (4.18). In order to construct the factor $\sum_{k=1}^{n_e-1}S[\bar{\phi}_i^{\text{cl}}]$ appearing in $W_{\mathcal{E}}$ and W_{OE}, we need to find the classical solutions $\bar{\phi}_i^{\text{cl}}$ which satisfy the corresponding boundary conditions, that is (3.49) and (4.16), respectively. Due to our surgery procedure, the classical fields do not depend on the direction along the cuts [33, 34], and we only have to solve the equations of motion on an interval. We remind the reader that a generic solution to the Laplace boundary value problem on the interval $[a,b]$, that is

$$\partial_x\partial^x f(x) = 0\,, \qquad f(a) = f_a\,, \qquad f(b) = f_b\,, \qquad x\in[a,b]\,,$$

is given by

$$f(x) = \frac{f_b - f_a}{b-a}x + \frac{f_a b - f_b a}{b-a}\,.$$

In the winding sectors $W_{\mathcal{E}}$ and W_{OE}, the only non-trivial term entering is $\partial_x f\partial_x f$, and it brings down the factor $\left(\frac{f_b-f_a}{b-a}\right)^2$.

D.1 Winding sector $W_{\mathcal{E}}$

In this section, we illustrate the computation of the winding sector $W_{\mathcal{E}}$ which appears in the logarithmic negativity for a toroidal manifold (3.51). The classical fields $\bar{\phi}_i^{\rm cl}$ for $i = 1, \dots, n_e - 1$ and $i \neq n_e/2$ have support on the torus of area $L_1 \times L_2$ divided into three parts A_1, A_2, and B along L_1 of lengths ℓ_1, ℓ_2, and ℓ_B, respectively, as seen in the right picture of figure 6. The classical field $\bar{\phi}^{\rm cl}_{n_e/2}$ has support on the same torus but cut into two cylinders $A_1 \cup A_2$ and B. Hence, we have

$$\begin{aligned}\sum_{k=1}^{n_e-1} S[\bar{\phi}_k^{\rm cl}] &= -g \sum_{\substack{k=1\\ k\neq n_e/2}}^{n_e-1} \int \mathrm{d}^2 x\, \partial_x \bar{\phi}_k^{\rm cl}\, \partial_x \bar{\phi}_k^{\rm cl} - g \int \mathrm{d}^2 x\, \partial_x \bar{\phi}^{\rm cl}_{n_e/2}\, \partial_x \bar{\phi}^{\rm cl}_{n_e/2}\,, \\ &= -gL_2 \sum_{\substack{k=1\\ k\neq n_e/2}}^{n_e-1} \left(\frac{1}{\ell_1} \left(\bar{\phi}_k^{\rm cl}|_{\Gamma_A} - \bar{\phi}_k^{\rm cl}|_{\Gamma_1} \right)^2 + \frac{1}{\ell_2} \left(\bar{\phi}_k^{\rm cl}|_{\Gamma_A} - \bar{\phi}_k^{\rm cl}|_{\Gamma_2} \right)^2 + \frac{1}{\ell_B} \left(\bar{\phi}_k^{\rm cl}|_{\Gamma_1} - \bar{\phi}_k^{\rm cl}|_{\Gamma_2} \right)^2 \right) \\ &\quad - gL_2 \left(\frac{1}{\ell_1 + \ell_2} + \frac{1}{\ell_B} \right) \left(\bar{\phi}^{\rm cl}_{n_e/2}|_{\Gamma_2} - \bar{\phi}^{\rm cl}_{n_e/2}|_{\Gamma_1} \right)^2 . \end{aligned} \tag{D.1}$$

Using the boundary conditions (3.49) it is easy to compute the above expression. We only need to notice that for $i, j = 1, \dots, n_e/2 - 1$

$$\begin{aligned}\left((M_{n_e/2-1})_{ij} x_j - \sqrt{1 - \frac{2}{n_e}}\, \delta_{i,n_e/2-1}\, \gamma \right)^2 &= x^T M^T_{n_e/2-1} M_{n_e/2-1} x - \frac{4}{n_e} \gamma\, I \cdot x - \left(1 - \frac{2}{n_e} \right) \gamma^2 , \\ &= x^T T_{n_e/2-1}\, x - \frac{4}{n_e} \gamma\, I \cdot x - \left(1 - \frac{2}{n_e} \right) \gamma^2 , \end{aligned} \tag{D.2}$$

since $M^T_{n_e/2-1} M_{n_e/2-1} =: T_{n_e/2-1}$ [33], and $I = (1 \dots, 1) \in \mathbb{Z}^{n_e/2-1}$. The matrix T_{m-1} appeared already in [33, 34], and it is given by

$$T_{m-1} := M^T_{m-1} M_{m-1} = \begin{bmatrix} 1 - \frac{1}{m} & -\frac{1}{m} & \dots & -\frac{1}{m} \\ -\frac{1}{m} & 1 - \frac{1}{m} & \dots & -\frac{1}{m} \\ \vdots & & & \\ -\frac{1}{m} & -\frac{1}{m} & \dots & 1 - \frac{1}{m} \end{bmatrix} . \tag{D.3}$$

The specific coefficients in the expression (D.2) are simply due to the explicit form of the matrix $M_{n_e/2-1}$, which is obtained by deleting the $n_e/2$-th row and column from $U_{n_e/2}$, given in (3.22). Hence, a straightforward computation gives the expression (D.5), where we have collected the modes as

$$\mu := (\mu^1, \mu^A) , \qquad \upsilon := (\upsilon^1, \upsilon^A) ,$$

and used the aspect ratios

$$u_1 = \frac{\ell_1}{L_1} , \qquad u_2 = \frac{\ell_2}{L_1} , \qquad u_B = \frac{\ell_B}{L_1} = 1 - u_1 - u_2 \equiv 1 - u_{12} . \tag{D.4}$$

Thus, we obtain the following expression for $W_{\mathcal{E}}$

$$W_{\mathcal{E}}(n_e) \tag{D.5}$$
$$= \sum_{\mathbb{Z}^{2n_e-3}} \exp\left\{-\frac{g(2\pi R_c)^2}{|\tau|}\left[\mu^T\,\mathrm{T}\,\mu+\upsilon^T\,\mathrm{T}\,\upsilon+\left(1-\frac{2}{n}\right)\frac{1-u_2}{u_1(1-u_{12})}\left(\gamma-I\cdot\mu^1\right)^2\right.\right.$$
$$\left.\left.+\frac{1}{n\,u_{12}(1-u_{12})}\left(\gamma-I\cdot\upsilon^1\right)^2-\frac{4}{n\,u_1}\left(\gamma-I\cdot\mu^1\right)\left(\frac{1-u_2}{u_1(1-u_{12})}I\cdot\mu^1-I\cdot\mu^A\right)\right]\right\},$$

where the $2n_e-2\times 2n_e-2$ matrix T is given by

$$\mathrm{T}=\frac{1}{u_1}\begin{bmatrix}\frac{1-u_2}{1-u_{12}}\,T_{n_e/2-1} & -T_{n_e/2-1}\\ -T_{n_e/2-1} & \frac{u_{12}}{u_2}\,T_{n_e/2-1}\end{bmatrix}, \tag{D.6}$$

and $T_{n_e/2-1}$ has been defined above, see (D.3). The second term in the first line of $W_{\mathcal{E}}$ (D.5) sources a coupling between the two sets of frequencies μ^1 and υ^1 (corresponding to the odd and even labelled fields originally), and it is responsible for the non-factorisation of the winding sector in the toroidal case. Indeed, the cut Γ_1 carries only one degree of freedom, represented by the cut function χ_1, and thus n_e-1 winding modes, and it does not see the factorisation into two sets of $n_e/2-1$ modes which is present at the cut Γ_A due to the partial transposition. We can shift the mode γ as

$$\gamma\to\gamma-I\cdot\mu^1\,, \tag{D.7}$$

since we are summing over all integers, and we obtain

$$W_{\mathcal{E}}(n_e) \tag{D.8}$$
$$= \sum_{\mathbb{Z}^{2n_e-3}} \exp\left\{-\frac{g(2\pi R_c)^2}{|\tau|}\left[\mu^T\,\mathrm{T}\,\mu+\upsilon^T\,\mathrm{T}\,\upsilon+\left(1-\frac{2}{n}\right)\frac{1-u_2}{u_1(1-u_{12})}\left(\gamma-I\cdot\mu^1\right)^2\right.\right.$$
$$\left.\left.+\frac{1}{n\,u_{12}(1-u_{12})}\left(\gamma-I\cdot\upsilon^1\right)^2-\frac{4}{n\,u_1}\left(\gamma-I\cdot\mu^1\right)\left(\frac{1-u_2}{1-u_{12}}I\cdot\mu^1-I\cdot\mu^A\right)\right]\right\}.$$

It is useful to rewrite $W_{\mathcal{E}}$ as a multi-dimensional theta function. Defining $\Omega\in\mathbb{Z}^{2n_e-3}$ as $\Omega=(\mu,\upsilon,\gamma)$, (D.8) can be written as

$$W_{\mathcal{E}}(n_e)=\sum_{\Omega\in\mathbb{Z}^{2n_e-3}}\exp\left(-\frac{g(2\pi R_c)^2}{|\tau|}\Omega^T\,\mathcal{T}\,\Omega\right), \tag{D.9}$$

where the matrix $\mathcal{T}$ is given by

$$\mathcal{T} = \left[\begin{array}{ccc|c} A_{n_e-2\times n_e-2} & \mathbf{0}_{n_e-2\times n_e-2} & -\frac{1-u_2}{u_1(1-u_{12})} I_{n_e/2-1} \\ & & \hdashline \frac{2}{nu_1} I_{n_e/2-1} \\ \hline \mathbf{0}_{n_e-2\times n_e-2} & B_{n_e-2\times n_e-2} & -\frac{1}{n(1-u_{12})u_{12}} I_{n_e/2-1} \\ & & \hdashline 0_{n_e/2-1} \\ \hline -\frac{1-u_2}{u_1(1-u_{12})} I^T_{n_e/2-1} \quad \frac{2}{nu_1} I^T_{n_e/2-1} & \frac{-1}{n(1-u_{12})u_{12}} I^T_{n_e/2-1} \quad \mathbf{0}^T_{n_e/2-1} & \frac{n-1}{n(1-u_{12})u_{12}} + \frac{(n-2)u_2}{nu_1u_{12}} \end{array}\right] \tag{D.10}$$

and the matrices A and B are defined as

$$A_{n_e-2\times n_e-2} = \begin{bmatrix} \frac{1-u_2}{u_1(1-u_{12})} T_{n_e/2-1} + (1+\frac{2}{n}) \frac{1-u_2}{u_1(1-u_{12})} \mathcal{I}_{n_e/2-1} & -\frac{1}{u_1} T_{n_e/2-1} - \frac{2}{nu_1} \mathcal{I}_{n_e/2-1} \\ -\frac{1}{u_1} T_{n_e/2-1} - \frac{2}{nu_1} \mathcal{I}_{n_e/2-1} & (\frac{1}{u_1} + \frac{1}{u_2}) T_{n_e/2-1} \end{bmatrix},$$

$$B_{n_e-2\times n_e-2} = \begin{bmatrix} \frac{1-u_2}{u_1(1-u_{12})} T_{n_e/2-1} + \frac{1}{n(1-u_{12})u_{12}} \mathcal{I}_{n_e/2-1} & -\frac{1}{u_1} T_{n_e/2-1} \\ -\frac{1}{u_1} T_{n_e/2-1} & (\frac{1}{u_1} + \frac{1}{u_2}) T_{n_e/2-1} \end{bmatrix}, \tag{D.11}$$

with $\mathcal{I}_m$ an $m \times m$ matrix with all entries equal to 1, that is

$$\mathcal{I}_m = \begin{bmatrix} 1 & 1 & \dots & 1 \\ 1 & 1 & \dots & 1 \\ \vdots & \vdots & \ddots & \vdots \\ 1 & 1 & \dots & 1 \end{bmatrix}. \tag{D.12}$$

D.2 Winding sector W_{OE}

Here, we report the calculation of the winding sector W_{OE} (4.18) which appears in the study of the odd entropy for a toroidal manifold. The classical fields $\tilde{\phi}^{\mathrm{cl}}$ are defined on the whole torus $L_1 \times L_2$, with entangling cuts Γ_1, Γ_2, and Γ_A specified by the boundary conditions (4.16). Hence, we can write

$$\begin{aligned} \sum_{k=1}^{n_o-1} S[\tilde{\phi}^{\mathrm{cl}}_k] &= -g \sum_{k}^{n_o-1} \int \mathrm{d}^2 x \, \partial_x \tilde{\phi}^{\mathrm{cl}}_k \, \partial_x \tilde{\phi}^{\mathrm{cl}}_k \\ &= -gL_2 \sum_{k=1}^{n_e-1} \left(\frac{1}{\ell_1} \left(\tilde{\phi}^{\mathrm{cl}}_k|_{\Gamma_A} - \tilde{\phi}^{\mathrm{cl}}_k|_{\Gamma_1} \right)^2 + \frac{1}{\ell_2} \left(\tilde{\phi}^{\mathrm{cl}}_k|_{\Gamma_A} - \tilde{\phi}^{\mathrm{cl}}_k|_{\Gamma_2} \right)^2 + \frac{1}{\ell_B} \left(\tilde{\phi}^{\mathrm{cl}}_k|_{\Gamma_1} - \tilde{\phi}^{\mathrm{cl}}_k|_{\Gamma_2} \right)^2 \right) \\ &= -gL_2 (2\pi R_c)^2 \left(\left(\frac{1}{\ell_1} + \frac{1}{\ell_2} \right) \nu_A^T T_{n_o-1} \nu_A + \left(\frac{1}{\ell_1} + \frac{1}{\ell_B} \right) \nu_1^T T_{n_o-1} \nu_1 - \frac{2}{\ell_1} \nu_1^T T_{n_o-1} \nu_A \right), \end{aligned} \tag{D.13}$$

where in the last line we used the boundary conditions (4.16). Defining the vector $\nu = (\nu_1, \nu_A) \in \mathbb{Z}^{2n_o-2}$, and the $2n_o - 2 \times 2n_o - 2$ matrix T_{OE} as

$$\mathrm{T}_{\mathrm{OE}} = \begin{pmatrix} \left(\frac{1-u_2}{1-u_{12}} \right) T_{n_o-1} & -T_{n_o-1} \\ -T_{n_o-1} & \left(1 + \frac{u_1}{u_2} \right) T_{n_o-1} \end{pmatrix}, \tag{D.14}$$

where the aspect ratios were defined in (D.4), we can rewrite (D.13) as

$$\sum_{k=1}^{n_o-1} S[\tilde{\phi}_k^{\rm cl}] = -g\frac{(2\pi R_c)^2}{|\tau| u_1}\nu^T \, \mathrm{T}_{\rm OE}\, \nu \,. \tag{D.15}$$

Thus, the explicit expression for the winding sector reads

$$W_{\rm OE}(n_o) = \sum_{\phi_i^{\rm cl}} e^{-\sum_i S[\phi_i^{\rm cl}]} = \sum_{\vec{\nu}\in\mathbb{Z}^{2n_o-2}} \exp\left\{-\pi\,\frac{4\pi\, g\, R_c^2}{|\tau| u_1}\,\vec{\nu}^T\,\mathrm{T}_{\rm OE}\,\vec{\nu}\right\}. \tag{D.16}$$

The matrix $\mathrm{T}_{\rm OE}$ is positive definite in the physical region where the aspect ratios u_1, u_2, u_B are positive and constrained to satisfy $u_1+u_2+u_B=1$, $u_{1,2,B}<1$. This guarantees the convergence of the series, indeed the sum in (D.16) is nothing but a multi-dimensional theta function. We can use the reciprocal formula for the multi-dimensional θ function, cf. (C.8), and write $W_{\rm OE}(n_o)$ as

$$W_{\rm OE}(n_o) = \frac{\left(\frac{4\pi g R_c^2}{|\tau| u_1}\right)^{-(n_o-1)}}{\det T_{n_o-1}} \left(\frac{u_1}{u_2(1-u_{12})}\right)^{-(n_o-1)/2} \sum_{\vec{\mu}\in\mathbb{Z}^{2n_o-2}} \exp\left\{-\pi\,\frac{|\tau|(1-u_{12})u_2}{4\pi g\, R_c^2}\,\vec{\mu}^T\,\hat{\mathrm{T}}^{-1}\,\vec{\mu}\right\}, \tag{D.17}$$

where the inverse matrix is

$$\hat{\mathrm{T}}^{-1} = \begin{pmatrix} \left(1+\frac{u_1}{u_2}\right) T_{n_o-1}^{-1} & T_{n_o-1}^{-1} \\ T_{n_o-1}^{-1} & \left(\frac{1-u_2}{1-u_{12}}\right) T_{n_o-1}^{-1} \end{pmatrix}. \tag{D.18}$$

The determinant of T_{n_o-1} is simply $1/n_o$ [33], hence we can write

$$W_{\rm OE}(n_o) = n_o \left(\frac{|\tau|}{4\pi g R_c^2}\right)^{(n_o-1)} \big(u_1 u_2 (1-u_{12})\big)^{(n_o-1)/2} \sum_{\vec{\mu}\in\mathbb{Z}^{2n_o-2}} \exp\left\{-\pi\,\frac{|\tau|(1-u_{12})u_2}{4\pi g\, R_c^2}\,\vec{\mu}^T\,\hat{\mathrm{T}}^{-1}\,\vec{\mu}\right\}. \tag{D.19}$$

The eigenvalues of $\hat{\mathrm{T}}^{-1}$ are straightforward to compute, and we find

$$\{n_o\,\lambda_+\,, n_o\,\lambda_-\,, \underbrace{\lambda_+\,,\ldots,\lambda_+}_{n_o-2}\,, \underbrace{\lambda_-\,,\ldots,\lambda_-}_{n_o-2}\}\,, \tag{D.20}$$

with

$$\lambda_\pm = 1 + \frac{u_1}{2u_2}\frac{1-u_1}{1-u_{12}} \pm \sqrt{1+\frac{u_1^2}{4}\left(\frac{1}{1-u_{12}}-\frac{1}{u_2}\right)^2}\,.$$

Using the multi-dimensional theta function we can write the winding sector as

$$W_{\rm OE}(n_o) = n_o \left(\frac{|\tau|}{4\pi g R_c^2}\right)^{(n_o-1)} \big(u_1 u_2 (1-u_{12})\big)^{(n_o-1)/2}\, \Theta(\vec{0}\,|\,\mathrm{U})\,, \tag{D.21}$$

where Θ and U are given by

$$\Theta(\vec{0}\,|\,\mathrm{U}) = \sum_{\vec{\mu}\in\mathbb{Z}^{2n_o-2}} e^{-\pi\,\vec{\mu}^{\,T}\,\mathrm{U}\,\vec{\mu}}\,, \tag{D.22}$$

$$\mathrm{U} = \frac{|\tau|(1-u_{12})u_2}{4\pi g\,R_c^2} R^T \begin{pmatrix} n_o\,\lambda_+ & & & & & \\ & n_o\,\lambda_+ & & & & \\ & & \lambda_+ & & & \\ & & & \ddots & & \\ & & & & \lambda_- & \end{pmatrix} R\,,$$

and where R is a unitary matrix.

E Pure state limit for the odd entropy

In this section we illustrate another example for the pure state limit of the odd entropy. Since we do not have an analytical continuation for the winding sector W_{OE} of the torus, we can only consider the pure state limit for non-compact fields. This is equivalent to considering only the contribution from the partition functions. The partition function for non-compact fields on the complete torus is divergent due to the zero mode, for this reason we will place the theory on a cylinder with Dirichlet boundary conditions at its endpoints. The contribution to the odd entropy from the fluctuations is essentially given by the expression (4.20), which now reads

$$\begin{aligned} -\log\left(\frac{Z_{A_1}Z_{A_2}Z_B}{Z_{A\cup B}}\right) &= \frac{1}{2}\log\frac{\det\Delta_{\mathrm{cyl,A_1}}\det\Delta_{\mathrm{cyl,A_2}}\det\Delta_{\mathrm{cyl,B}}}{\det\Delta_{\mathrm{cyl}}} \\ &= \frac{1}{2}\log\Big(4u_1u_2(1-u_{12})|\tau|^2\Big) + \log\left|\frac{\eta(2u_1\tau)\eta(2u_2\tau)\eta(2(1-u_{12})\tau)}{\eta(2\tau)}\right|, \end{aligned} \tag{E.1}$$

where in the last step we used the results (C.6) collected in appendix C.2. In the limit $u_B = 1-u_{12} = \varepsilon \to 0$, the above expression becomes

$$-\log\left(\frac{Z_{A_1}Z_{A_2}Z_B}{Z_{A\cup B}}\right) \approx \frac{1}{2}\log\big(2|\tau|u_1(1-u_1)\big) + \log\left|\frac{\eta(2u_1\tau)\eta(2(1-u_1)\tau)}{\eta(2\tau)}\right| - \frac{\pi}{24\varepsilon|\tau|} + \dots\,. \tag{E.2}$$

As explained in the main body, see discussions around (4.13), we need to consider a "regulated" odd entropy, where the contributions from the entangling surface at Γ_2 are correctly subtracted. Our choice is to use the entanglement entropy for the corresponding density matrix ρ_A. Concretely, it means that we subtract the universal term of the entanglement entropy of a bipartite cylinder, whose expression was initially obtained in [32, 33] (here we only need the non-compact contribution):

$$S_{\mathrm{EE}}(\rho_A) = \frac{1}{2}\log\big(2u(1-u)|\tau|\big) + \log\left|\frac{\eta(2u\tau)\eta(2(1-u)\tau)}{\eta(2\tau)}\right|, \tag{E.3}$$

where here $u = u_1+u_2$. When $u_B \to 0$ (i.e. $u_1+u_2 \to 1$), the above expression becomes

$$S_{\mathrm{EE}}(\rho_A) \approx -\frac{\pi}{24\varepsilon|\tau|}\,. \tag{E.4}$$

Hence, in the limit $u_B \to 0$, the "regulated" odd entropy is

$$\Delta S_o \approx \frac{1}{2}\log\left(2|\tau|u_1(1-u_1)\right) + \log\left|\frac{\eta(2u_1\tau)\eta(2(1-u_1)\tau)}{\eta(2\tau)}\right| . \tag{E.5}$$

This is the universal part of the entanglement entropy for a system on a bipartite cylinder, as expected [40].

References

[1] M.B. Plenio and S. Virmani, *An introduction to entanglement measures*, *Quant. Inf. Comput.* **7** (2007) 1 [quant-ph/0504163] [INSPIRE].

[2] L. Amico, R. Fazio, A. Osterloh and V. Vedral, *Entanglement in many-body systems*, *Rev. Mod. Phys.* **80** (2008) 517 [quant-ph/0703044] [INSPIRE].

[3] R. Horodecki, P. Horodecki, M. Horodecki and K. Horodecki, *Quantum entanglement*, *Rev. Mod. Phys.* **81** (2009) 865 [quant-ph/0702225] [INSPIRE].

[4] C.H. Bennett, H.J. Bernstein, S. Popescu and B. Schumacher, *Concentrating partial entanglement by local operations*, *Phys. Rev. A* **53** (1996) 2046 [quant-ph/9511030] [INSPIRE].

[5] C.H. Bennett, D.P. DiVincenzo, J.A. Smolin and W.K. Wootters, *Mixed state entanglement and quantum error correction*, *Phys. Rev. A* **54** (1996) 3824 [quant-ph/9604024] [INSPIRE].

[6] J. Eisert and M.B. Plenio, *A comparison of entanglement measures*, *J. Mod. Opt.* **46** (1999) 145 [quant-ph/9807034] [INSPIRE].

[7] G. Vidal and R.F. Werner, *Computable measure of entanglement*, *Phys. Rev. A* **65** (2002) 032314 [quant-ph/0102117] [INSPIRE].

[8] A. Peres, *Separability criterion for density matrices*, *Phys. Rev. Lett.* **77** (1996) 1413 [quant-ph/9604005] [INSPIRE].

[9] M. Horodecki, P. Horodecki and R. Horodecki, *On the necessary and sufficient conditions for separability of mixed quantum states*, *Phys. Lett. A* **223** (1996) 1 [quant-ph/9605038] [INSPIRE].

[10] M.B. Plenio, *Logarithmic Negativity: A Full Entanglement Monotone That is not Convex*, *Phys. Rev. Lett.* **95** (2005) 090503 [quant-ph/0505071] [INSPIRE].

[11] P. Calabrese, J. Cardy and E. Tonni, *Entanglement negativity in quantum field theory*, *Phys. Rev. Lett.* **109** (2012) 130502 [arXiv:1206.3092] [INSPIRE].

[12] P. Calabrese, J. Cardy and E. Tonni, *Entanglement negativity in extended systems: a field theoretical approach*, *J. Stat. Mech.* **2013** (2013) P02008.

[13] P. Calabrese, L. Tagliacozzo and E. Tonni, *Entanglement negativity in the critical Ising chain*, *J. Stat. Mech.* **1305** (2013) P05002 [arXiv:1302.1113] [INSPIRE].

[14] C. De Nobili, A. Coser and E. Tonni, *Entanglement entropy and negativity of disjoint intervals in CFT: Some numerical extrapolations*, *J. Stat. Mech.* **1506** (2015) P06021 [arXiv:1501.04311] [INSPIRE].

[15] A. Coser, E. Tonni and P. Calabrese, *Towards the entanglement negativity of two disjoint intervals for a one dimensional free fermion*, *J. Stat. Mech.* **1603** (2016) 033116 [arXiv:1508.00811] [INSPIRE].

[16] H. Shapourian, K. Shiozaki and S. Ryu, *Partial time-reversal transformation and entanglement negativity in fermionic systems*, *Phys. Rev. B* **95** (2017) 165101 [arXiv:1611.07536] [INSPIRE].

[17] P. Calabrese, J. Cardy and E. Tonni, *Finite temperature entanglement negativity in conformal field theory*, *J. Phys. A* **48** (2015) 015006 [arXiv:1408.3043] [INSPIRE].

[18] H. Shapourian and S. Ryu, *Finite-temperature entanglement negativity of free fermions*, *J. Stat. Mech.* **1904** (2019) 043106 [arXiv:1807.09808] [INSPIRE].

[19] A. Coser, E. Tonni and P. Calabrese, *Entanglement negativity after a global quantum quench*, *J. Stat. Mech.* **1412** (2014) P12017 [arXiv:1410.0900] [INSPIRE].

[20] M. Hoogeveen and B. Doyon, *Entanglement negativity and entropy in non-equilibrium conformal field theory*, *Nucl. Phys. B* **898** (2015) 78 [arXiv:1412.7568] [INSPIRE].

[21] X. Wen, P.-Y. Chang and S. Ryu, *Entanglement negativity after a local quantum quench in conformal field theories*, *Phys. Rev. B* **92** (2015) 075109 [arXiv:1501.00568] [INSPIRE].

[22] X. Wen, S. Matsuura and S. Ryu, *Edge theory approach to topological entanglement entropy, mutual information and entanglement negativity in Chern-Simons theories*, *Phys. Rev. B* **93** (2016) 245140 [arXiv:1603.08534] [INSPIRE].

[23] X. Wen, P.-Y. Chang and S. Ryu, *Topological entanglement negativity in Chern-Simons theories*, *JHEP* **09** (2016) 012 [arXiv:1606.04118] [INSPIRE].

[24] E. Ardonne, P. Fendley and E. Fradkin, *Topological order and conformal quantum critical points*, *Annals Phys.* **310** (2004) 493 [cond-mat/0311466] [INSPIRE].

[25] D.S. Rokhsar and S.A. Kivelson, *Superconductivity and the Quantum Hard-Core Dimer Gas*, *Phys. Rev. Lett.* **61** (1988) 2376 [INSPIRE].

[26] V. Keranen, W. Sybesma, P. Szepietowski and L. Thorlacius, *Correlation functions in theories with Lifshitz scaling*, *JHEP* **05** (2017) 033 [arXiv:1611.09371] [INSPIRE].

[27] E. Fradkin and J.E. Moore, *Entanglement entropy of 2D conformal quantum critical points: hearing the shape of a quantum drum*, *Phys. Rev. Lett.* **97** (2006) 050404 [cond-mat/0605683] [INSPIRE].

[28] J.-M. Stéphan, S. Furukawa, G. Misguich and V. Pasquier, *Shannon and entanglement entropies of one- and two-dimensional critical wave functions*, *Phys. Rev. B* **80** (2009) 184421.

[29] B. Hsu, M. Mulligan, E. Fradkin and E.-A. Kim, *Universal entanglement entropy in 2D conformal quantum critical points*, *Phys. Rev. B* **79** (2009) 115421 [arXiv:0812.0203] [INSPIRE].

[30] B. Hsu and E. Fradkin, *Universal Behavior of Entanglement in 2D Quantum Critical Dimer Models*, *J. Stat. Mech.* **1009** (2010) P09004 [arXiv:1006.1361] [INSPIRE].

[31] M. Oshikawa, *Boundary Conformal Field Theory and Entanglement Entropy in Two-Dimensional Quantum Lifshitz Critical Point*, arXiv:1007.3739 [INSPIRE].

[32] M.P. Zaletel, J.H. Bardarson and J.E. Moore, *Logarithmic terms in entanglement entropies of 2D quantum critical points and Shannon entropies of spin chains*, *Phys. Rev. Lett.* **107** (2011) 020402 [arXiv:1103.5452] [INSPIRE].

[33] T. Zhou, X. Chen, T. Faulkner and E. Fradkin, *Entanglement entropy and mutual information of circular entangling surfaces in the 2 + 1-dimensional quantum Lifshitz model*, *J. Stat. Mech.* **1609** (2016) 093101 [arXiv:1607.01771] [INSPIRE].

[34] J. Angel-Ramelli, V.G.M. Puletti and L. Thorlacius, *Entanglement Entropy in Generalised Quantum Lifshitz Models*, *JHEP* **08** (2019) 072 [arXiv:1906.08252] [INSPIRE].

[35] C. Berthiere and W. Witczak-Krempa, *Relating bulk to boundary entanglement*, *Phys. Rev. B* **100** (2019) 235112 [arXiv:1907.11249] [INSPIRE].

[36] K. Audenaert, J. Eisert, M.B. Plenio and R.F. Werner, *Entanglement Properties of the Harmonic Chain*, *Phys. Rev. A* **66** (2002) 042327 [quant-ph/0205025] [INSPIRE].

[37] I. Peschel, *Calculation of reduced density matrices from correlation functions*, *J. Phys. A* **36** (2003) L205 [cond-mat/0212631].

[38] X. Chen, E. Fradkin and W. Witczak-Krempa, *Quantum spin chains with multiple dynamics*, *Phys. Rev. B* **96** (2017) 180402 [arXiv:1706.02304] [INSPIRE].

[39] M.R. Mohammadi Mozaffar and A. Mollabashi, *Logarithmic Negativity in Lifshitz Harmonic Models*, *J. Stat. Mech.* **1805** (2018) 053113 [arXiv:1712.03731] [INSPIRE].

[40] K. Tamaoka, *Entanglement Wedge Cross Section from the Dual Density Matrix*, *Phys. Rev. Lett.* **122** (2019) 141601 [arXiv:1809.09109] [INSPIRE].

[41] C. Graham, R. Jenne, L.J. Mason and G.A.J. Sparling, *Conformally invariant powers of the laplacian, i: Existence*, *J. Lond. Math. Soc.* **s2-46** (1992) 557.

[42] H. Casini and M. Huerta, *Universal terms for the entanglement entropy in 2+1 dimensions*, *Nucl. Phys. B* **764** (2007) 183 [hep-th/0606256] [INSPIRE].

[43] H. Casini and M. Huerta, *Entanglement entropy in free quantum field theory*, *J. Phys. A* **42** (2009) 504007 [arXiv:0905.2562] [INSPIRE].

[44] V. Eisler and Z. Zimborás, *Entanglement negativity in two-dimensional free lattice models*, *Phys. Rev. B* **93** (2016) 115148.

[45] C. De Nobili, A. Coser and E. Tonni, *Entanglement negativity in a two dimensional harmonic lattice: Area law and corner contributions*, *J. Stat. Mech.* **1608** (2016) 083102 [arXiv:1604.02609] [INSPIRE].

[46] J. Helmes, L.E. Hayward Sierens, A. Chandran, W. Witczak-Krempa and R.G. Melko, *Universal corner entanglement of Dirac fermions and gapless bosons from the continuum to the lattice*, *Phys. Rev. B* **94** (2016) 125142 [arXiv:1606.03096] [INSPIRE].

[47] C. Berthiere, *Boundary-corner entanglement for free bosons*, *Phys. Rev. B* **99** (2019) 165113 [arXiv:1811.12875] [INSPIRE].

[48] M.R. Mohammadi Mozaffar and A. Mollabashi, *Entanglement in Lifshitz-type Quantum Field Theories*, *JHEP* **07** (2017) 120 [arXiv:1705.00483] [INSPIRE].

[49] X. Chen, E. Fradkin and W. Witczak-Krempa, *Gapless quantum spin chains: multiple dynamics and conformal wavefunctions*, *J. Phys. A* **50** (2017) 464002 [arXiv:1707.02317] [INSPIRE].

[50] L. Lami, A. Serafini and G. Adesso, *Gaussian entanglement revisited*, *New J. Phys.* **20** (2018) 023030 [arXiv:1612.05215].

[51] P.H. Ginsparg, *Applied conformal field theory*, in *Les Houches Summer School in Theoretical Physics: Fields, Strings, Critical Phenomena*, pp. 1–168, 1988 hep-th/9108028 [INSPIRE].

[52] P. Di Francesco, P. Mathieu and D. Senechal, *Conformal Field Theory*, Graduate Texts in Contemporary Physics, Springer-Verlag, New York U.S.A. (1997), [DOI] [INSPIRE].

[53] W.I. Weisberger, *Conformal Invariants for Determinants of Laplacians on Riemann Surfaces*, *Commun. Math. Phys.* **112** (1987) 633 [INSPIRE].

[54] J.S. Dowker, *Functional determinants on regions of the plane and sphere*, *Class. Quant. Grav.* **11** (1994) 557 [hep-th/9310128] [INSPIRE].

[55] J.L. Cardy and I. Peschel, *Finite Size Dependence of the Free Energy in Two-dimensional Critical Systems*, *Nucl. Phys. B* **300** (1988) 377 [INSPIRE].

[56] P. Chaturvedi, V. Malvimat and G. Sengupta, *Holographic Quantum Entanglement Negativity*, *JHEP* **05** (2018) 172 [arXiv:1609.06609] [INSPIRE].

[57] P. Jain, V. Malvimat, S. Mondal and G. Sengupta, *Holographic entanglement negativity conjecture for adjacent intervals in AdS_3/CFT_2*, *Phys. Lett. B* **793** (2019) 104 [arXiv:1707.08293] [INSPIRE].

[58] P. Jain, V. Malvimat, S. Mondal and G. Sengupta, *Holographic entanglement negativity for adjacent subsystems in AdS_{d+1}/CFT_d*, *Eur. Phys. J. Plus* **133** (2018) 300 [arXiv:1708.00612] [INSPIRE].

[59] J. Kudler-Flam and S. Ryu, *Entanglement negativity and minimal entanglement wedge cross sections in holographic theories*, *Phys. Rev. D* **99** (2019) 106014 [arXiv:1808.00446] [INSPIRE].

[60] Y. Kusuki, J. Kudler-Flam and S. Ryu, *Derivation of Holographic Negativity in AdS_3/CFT_2*, *Phys. Rev. Lett.* **123** (2019) 131603 [arXiv:1907.07824] [INSPIRE].

[61] J.S. Dowker and J.S. Apps, *Further functional determinants*, *Class. Quant. Grav.* **12** (1995) 1363 [hep-th/9502015] [INSPIRE].

[62] R. Bellman and R.S. Lehman, *The reciprocity formula for multidimensional theta functions*, *Proc. Am. Math. Soc.* **12** (1961) 954.

Paper III

Entanglement entropy of Excited States in the Quantum Lifshitz Model

Angel-Ramelli, J.

arXiv:2009.02283 [hep-th] (Currently under review at J. Stat. Mech.)

Note: The margins of the paper were trimmed to better fit the format of this thesis.

Entanglement Entropy of Excited States in the Quantum Lifshitz Model

J. Angel-Ramelli [1]

University of Iceland, Science Institute, Dunhaga 3, 107 Reykjavík, Iceland

Abstract

In this work we calculate the entanglement entropy of certain excited states of the quantum Lifshitz model. The quantum Lifshitz model is a $2+1$-dimensional bosonic quantum field theory with an anisotropic scaling symmetry between space and time that belongs to the universality class of the quantum dimer model and its generalizations. The states we consider are constructed by exciting the eigenmodes of the Laplace-Beltrami operator on the spatial manifold of the model. We perform a replica calculation and find that, whenever a simple assumption is satisfied, the bipartite entanglement entropy of any such excited state can be evaluated analytically. We show that the assumption is satisfied for all excited states on the rectangle and for almost all excited states on the sphere and provide explicit examples in both geometries. We find that the excited state entanglement entropy obeys an area law and is related to the entanglement entropy of the ground state by two universal constants. We observe a logarithmic dependence on the excitation number when all excitations are put onto the same eigenmode.

[1] jfa1@hi.is

Contents

1 Introduction

In recent years the study of entanglement has brought deep insights across numerous areas of physics such as quantum information, condensed matter physics, holography, quantum gravity, and quantum field theory (QFT). Amongst the many measures of entanglement the entanglement entropy is one of the oldest and most well-studied. For bipartite systems it is defined as follows. Let there be a quantum system on the manifold M with Hilbert space $\mathcal{H}$, and let us prepare a pure state of this system, for example the ground state, described by the density matrix ρ. Next, cut M into the two subsystems A and B and assume that the Hilbert space splits accordingly, that is $\mathcal{H} = \mathcal{H}_A \otimes \mathcal{H}_B$. The reduced density matrix on A is obtained by tracing out the degrees of freedom on B, that is $\rho_A = \mathrm{Tr}_B \rho$, and the entanglement entropy of the subsystem A in the state ρ is given by the von Neumann entropy of ρ_A

$$S[A] = -\mathrm{Tr}(\rho_A \log \rho_A). \tag{1}$$

The entanglement entropy is particularly well-suited for the study of entanglement in bipartite pure systems, where it effectively quantifies the amount of entanglement between the subsystems [1, 2].

In the context of condensed matter physics and quantum field theory the entanglement entropy has been shown to capture universal properties of critical systems, see for example [3–6]. The perhaps most famous example is that of $1+1$-dimensional conformal field theory (CFT), where the entanglement entropy has a leading logarithmic divergence

$$S[A] = \frac{c}{3} \log\left(\frac{L_A}{\varepsilon}\right), \tag{2}$$

with L_A the size of the subsystem A, c the central charge of the CFT [7–9], and ε a UV-cutoff. Here, the coefficient of the logarithmic divergence is universal, meaning it is independent of the regularization scheme used and constant within the universality class of the theory. One can thus adopt the point of view that the entanglement entropy is a machinery that extracts universal features from critical theories. However, this machinery is arduous to operate, as entanglement entropy calculations are generally hard, and thus analytic results are scarce. It is not surprising that most results for the entanglement entropy have arisen in the context of CFT (and in particular in 2-dimensional CFT), where powerful methods are available, and for simple states such as the ground state, see [3, 10, 11]. For ground state one expects the entanglement entropy to obey an area law [12, 13]. Concretely, for a d-dimensional CFT in its ground state one expects the entanglement entropy to have a leading UV-divergence

$$S[A] = c_{d-2} \frac{\mathrm{Area}(\partial A)}{\varepsilon^{d-2}} + \cdots + c_1 \log \frac{L_A}{\varepsilon} + c_0 + \mathcal{O}(\varepsilon), \tag{3}$$

where ∂A is the $d-2$-dimensional boundary of A and c_{d-2} is a non-universal coefficient, and L_A a characteristic length associated to ∂A. In even dimensions universal information is found in the coefficient of the logarithmic divergence term, whereas in odd dimensions, where the logarithmic divergence is absent, it is found in the constant sub-leading correction. In the

ground-state, the entanglement between A and its complement is thus dominated by short-range correlations across the boundary ∂A, as opposed to (2) where the logarithm indicates that long-range correlations dominate.

While not as widely studied, the entanglement entropy of excited states has also received some attention over the years. A particularly interesting result is that the entanglement entropy of a pure state picked at random from the Hilbert space will generically obey a volume and not an area law [5, 14–16]. The area law behavior of the ground state is consequently quite special within the Hilbert space. Notably, the dominance of extensive states implies that highly excited states are expected to obey volume laws. Another early study of excited states was performed in [17, 18], where it was found that for free scalars on a lattice the first excited states of the theory as well as a certain form of coherent state both still obeyed area laws. It was, in fact, argued by [19] that low lying excitations in a wide class of theories including many gapped Hamiltonian obey area laws with at most logarithmic corrections. It was further argued by [20, 21] that excitations of CFTs obtained by acting with a primary field on the vacuum continued to obey an area law, albeit with a universal correction with respect to the ground state entanglement determined by the conformal weights of the primary field. As this universal correction was derived from correlation functions of primary fields, one may say that the entanglement entropy of (at least certain) low-lying excitations of a CFT encodes information on the correlation functions of primary fields. A similar study was performed for finite quasiparticle excitations in a certain limit of a wide class of free theories, where it was again found that these excited states obey area laws with corrections to the ground state entanglement related to the correlation functions of the quasiparticle states [22, 23]. This analysis was extended by the same authors in [24, 25] to include the treatment of another measure of entanglement, the logarithmic negativity, and they further provided a fairly general proof in the case of a massive free boson showing that the previous results are valid in any dimension and for any entanglement surgery. Thus for a wide range of theories and low excited states, the excited state entanglement entropy has been observed to take the form

$$S_{ES} = S_{GS} + \beta_{ES}, \tag{4}$$

with $S_{ES}[A]$ and $S_{GS}[A]$ the entanglement entropies of the excited and ground states respectively, and β_{ES} a constant depending on the excited state and derived from certain correlation functions in the underlying theory. Apart from QFTs, some powerful calculations of the excited state entanglement entropy properties of spin chains have been performed, see for example [21, 26–28]. In particular, it has been observed that generally two types of excited states can be found in the Hilbert space. Excited states showing the same logarithmic behavior typical of the ground states of critical models, see (2), and excited states that exhibit extensive behavior.

In this paper we will perform analytic entanglement calculations for excited states of the quantum Lifshitz model (QLM). The QLM is a 2+1-dimensional QFT with a scaling symmetry that is anisotropic between time and space and characterized by a so-called dynamical critical exponent z. It was introduced in [29] at $z = 2$, where it describes the continuum limit of the quantum dimer model [30] and some of its interacting generalizations [31–35]. More

importantly for our purposes, the QLM has proven to offer a very fruitful playground for entanglement calculations, partly due to its close connections to CFT. In fact, the ground state of the QLM can be expressed in terms of the action of a free 2-dimensional CFT and is thus invariant under spatial conformal transformations [29]. Similarly, its equal-time correlation functions can be expressed in terms of correlation functions in that same CFT [36]. The ground state entanglement entropy of the QLM and its higher dimensional generalizations [36,37] have been extensively studied [38–44]. For the standard $2+1$-dimensional QLM at $z=2$, it has been found to be [38,39]

$$S[A] = c_1 \frac{L_A}{\varepsilon} + \frac{c}{6}\Delta\chi \log \frac{L_A}{\varepsilon} + \gamma_{QCP} + \cdots \tag{5}$$

with L_A the length of the boundary ∂A and c_1 a non-universal constant. The coefficient of the logarithm is universal and consists of the central charge c of the CFT whose action describes the ground state of the QLM and of the change in Euler characteristic $\Delta\chi$ due to the surgery. Furthermore, when $\Delta\chi = 0$ the sub-leading constant term γ_{QCP}, where QCP stands for quantum critical point, is also universal [39] and depends on the geometry and topology of the manifolds involved [37, 40, 42–44]. The entanglement of certain mixed states of the QLM has also been studied analytically [45].

There have been, to our best knowledge, only two works that deal with the excited state entanglement of the QLM. In [46] the entanglement entropy of a local excitation constructed by acting with a vertex and a time evolution operator on the ground state of the QLM is analyzed. The excess entanglement entropy after some time t is found to be related to correlation functions of certain operators on the full and sub-systems with Dirichlet boundary conditions. Finally, in [47] the authors put the QLM on a compact spatial manifold, and construct states by exciting the eigenmodes of the corresponding Laplacian. Restricting to the case of a single excitation, they show that the trace of the n-th power of the reduced density matrix of such a state (whose limit $n \to 1$ by the replica approach gives the entanglement entropy) can be expressed in terms of correlation functions on a certain n-sheeted geometry resulting from a replica calculation. By deriving a form of Wick's theorem on this geometry, the authors then proceed to evaluate these correlation functions and provide expressions for them in terms of quantities related to the Green's functions on the full and sub-systems which they dub entanglement propagator amplitudes (EPA's). A numerical analysis then provides evidence of the universality of these quantities. However, an analytic continuation in n remains elusive in the paper, and thus the authors can only provide expressions for the Rényi entropies and a conjecture for the entanglement entropy in the particular case when the two submanifolds resulting from the bipartition of M are equal.

To summarize, we find that the entanglement entropy of any finitely excited state $S_{ES}[A]$ of the QLM is related to its ground state entanglement entropy $S_{GS}[A]$ by

$$S_{ES}[A] = \alpha S_{GS}[A] + \beta, \tag{6}$$

where evidence points to the universality of the constants α and β. In the singly excited state and for m excitations in a single mode of the halved M geometry, we further find $\alpha = 1$,

in agreement with the expectation (4). In all other cases we provide analytic expressions for both constants. This implies that the entanglement of this class of finitely excited states of the QLM obeys an area law. When all excitations are put into the same mode, we observe a logarithmic dependence on the excitation number m. This simple dependence allows us to consider the highly excited limit, which, contrary to standard expectation, continues to obey an area law. This indicates that the state might be a quantum scar. Recently, there has been a lot of interests in these type of states [48, 49], as they exhibit a surprising form of ergodicity breaking and bear some importance to the eigenstate thermalization hypothesis. In particular such states have been observed for quantum dimer models [50, 51], which belong to the same universality class as the QLM.

The present work is closely related to [47]. In section 2 we review the basic properties of the QLM as well as the construction of its ground and excited states à la [47] (that is excitations that correspond to the eigenmodes of the Laplacian on the spatial manifold). In section 3 we concentrate on the special case considered in [47], where a single quantum of energy is put into a particular mode. We show that introducing a certain condition for the classical fields the complexity of the problem can be sufficiently reduced such that the previously tricky analytic continuation becomes straight forward, and an explicit expression for the entanglement entropy can be written down. We then show that our assumption is satisfied by all modes on the sphere and rectangle and analyze the entanglement entropy corresponding to the excitation of different modes on both geometries. In section 4, we generalize the previous calculation to encompass any excited state by making a slightly stronger assumption than before, and manage to find a closed expression for the entanglement entropy in terms of some complicated tensors of correlation functions. We then show that our assumption is again satisfied for all modes on the rectangle and for almost all modes on the sphere and provide explicit examples when a single mode is excited a finite amount of times. In this case we find that for a wide range of modes the entanglement entropy behaves like the logarithm of the excitation number. In both the singly and general excited state we confirm that the entanglement entropy can be expressed in terms of EPA's, although we define them slightly differently and refer to them as transformed propagators. We calculate these quantities by a spectral approach and find them in agreement with [47], providing further evidence for their universality.

2 The quantum Lifshitz model and its excited states

The quantum Lifshitz model (QLM) is the $(2+1)$ dimensional quantum field theory defined on the spatial manifold M by the Hamiltonian [29]

$$H = \frac{1}{2}\int_M \mathrm{d}^2x \left(\pi^2 + g^2(\Delta\phi)^2\right), \tag{7}$$

where $\phi \sim \phi + 2\pi R$ a compactified scalar field with compactification radius R, $\pi = -i\frac{\delta}{\delta\phi}$ its conjugate momentum, Δ the Laplace-Beltrami operator on M, and g a free parameter. For the particular value $g = \frac{1}{8\pi}$ the QLM describes the correlations of the Rokhsar-Kievelson

quantum dimer model on a square lattice. For simplicity, we will mostly refer to the Laplace-Beltrami operator as the Laplacian on M. Let us analyze the ground and excited states of this theory.

Ground state. In order to find the ground state of the theory we define the operators $A(x)$ and $A^\dagger(x)$

$$A(x) := \frac{1}{\sqrt{2}}\left[i\pi(x) + g\Delta\phi(x)\right], \qquad A^\dagger(x) := \frac{1}{\sqrt{2}}\left[-i\pi(x) + g\Delta\phi(x)\right]. \tag{8}$$

From the commutation relation $[\phi(x), \pi(y)] = i\delta(x-y)$, one can see that $A(x)$ and $A^\dagger(x)$ obey the commutation relation $[A(x), A^\dagger(y)] = g(-\Delta)\delta(x-y)$ and can be interpreted as annihilation and creation operators in position space. We note that g has to be greater than zero, since otherwise the roles of A and $A^\dagger$ are reversed and $A^\dagger$ becomes the annihilation operator. The Hamiltonian can be written in terms of A and $A^\dagger$ as

$$H = \int_M \mathrm{d}^2x\ A^\dagger(x)A(x), \tag{9}$$

where we, without loss of generality, subtracted the UV-divergent vacuum energy, thereby setting the energy of the ground state to zero. As the Hamiltonian (9) is positive semi-definite, the ground state $|\Psi_0\rangle$ of the theory is found by solving $A(x)|\Psi_0\rangle = 0$. The solution to this functional differential equation is given

$$|\Psi_0\rangle = \frac{1}{\sqrt{Z_M}}\int \mathcal{D}\phi\ e^{-\frac{1}{2}S[\phi]}|\phi\rangle, \qquad S[\phi] = g\int_M \mathrm{d}^2x\ \phi(-\Delta)\phi, \tag{10}$$

where we defined the partition function $Z_M := \int \mathcal{D}\phi\ e^{-S[\phi]}$. Note that the above definition coincides with the one given in [29] after an integration by parts.

Excited states. Let us concentrate on the case of a compact spatial manifold M, so that the spectrum of the Laplacian is discrete. Following [47], we can construct excited states of the QLM by exciting the eigenmodes of the Laplacian. Let $L_\lambda(x)$ be the eigenfunction to the eigenvalue λ of $(-\Delta)$, that is

$$-\Delta L_\lambda(x) = \lambda L_\lambda(x), \tag{11}$$

due to our sign convention, we note that $\lambda \geq 0$. If M has a boundary, we choose Dirichlet boundary conditions. For $\lambda \neq 0$ we can project the creation operator onto the the λ eigenfunction and define

$$A^\dagger_\lambda := \frac{1}{\sqrt{g\lambda}}\int_M \mathrm{d}^2x\ L_\lambda(x)A^\dagger(x), \qquad A_\lambda := \frac{1}{\sqrt{g\lambda}}\int_M \mathrm{d}^2x\ L_\lambda(x)A(x). \tag{12}$$

From the commutation relations for $A(x)$, we immediately get the correct commutation relations for a harmonic oscillator for each mode

$$[A_\lambda, A^\dagger_\mu] = \delta_{\lambda\mu}, \quad [A^\dagger_\lambda, A^\dagger_\mu] = [A_\lambda, A_\mu] = 0, \tag{13}$$

$$[H, A^\dagger_\lambda] = g\lambda\, A^\dagger_\lambda, \tag{14}$$

allowing for interpretation of $A_\lambda^\dagger$ and A_λ as the creation and annihilation operators for excitations of the λ-mode. The Hamiltonian decomposes into the different modes

$$H = \sum_{\lambda \neq 0} g\lambda \, A_\lambda^\dagger A_\lambda, \tag{15}$$

with $g\lambda$ the energy of a single excitation and $A_\lambda^\dagger A_\lambda$ counts the number of excitations in the λ-mode[2]. We can construct the general excited state by selecting a finite set of non-zero modes $\{\lambda_1, \ldots, \lambda_\nu\}$ and applying the respective creation operators to the ground state a finite amount of times $\{m_{\lambda_1}, \ldots, m_{\lambda_\nu}\}$. The general excited state is then labeled by that set of numbers and, taking into account proper normalization, given by

$$\left|(m_{\lambda_1}, \ldots, m_{\lambda_r}, \ldots, m_{\lambda_\nu})\right\rangle = \frac{\left(A_{\lambda_1}^\dagger\right)^{m_{\lambda_1}}}{\sqrt{m_{\lambda_1}!}} \cdots \frac{\left(A_{\lambda_r}^\dagger\right)^{m_{\lambda_r}}}{\sqrt{m_{\lambda_r}!}} \cdots \frac{\left(A_{\lambda_\nu}^\dagger\right)^{m_{\lambda_\nu}}}{\sqrt{m_{\lambda_\nu}!}} |\psi_0\rangle \tag{16}$$

$$= \frac{1}{\sqrt{Z_M}} \int \mathcal{D}\phi \left[\prod_{r=1}^{\nu} \frac{1}{\sqrt{2^{m_{\lambda_r}} m_{\lambda_r}!}} H_{m_{\lambda_r}}\left(\frac{\phi^{\lambda_r}}{\sqrt{2}}\right) \right] e^{-\frac{1}{2}S[\phi]} |\phi\rangle, \tag{17}$$

where $H_m(x)$ is a Hermite polynomial

$$H_m(x) = m! \sum_{k=0}^{\lfloor \frac{m}{2} \rfloor} \frac{(-1)^k (2x)^{m-2k}}{k!(m-2k)!}, \tag{18}$$

and where ϕ_r^λ is defined, similarly to (12), as the projection of the scalar onto the λ-eigenmode

$$\phi^\lambda = \sqrt{2g\lambda} \int_M \mathrm{d}^2x \; L_\lambda(x)\phi(x) \tag{19}$$

with the prefactor $\sqrt{2g\lambda}$ chosen with foresight to simplify later calculations.

3 A warm up exercise: Entanglement entropy of the singly excited state

Our final goal is to calculate the bipartite entanglement entropy of the general excited state. Considering that the corresponding calculation is quite involved, it is instructive to first consider the much simpler case of the singly excited. Furthermore, due to its simpler nature, the calculation of the entanglement entropy can be performed under more general assumptions in this case. This problem was first considered by [47], where the authors calculated the

[2] Before continuing, a comment on the zero-mode is in order. If the Laplacian has an eigenvalue $\lambda = 0$, we have to alter the definition (12) for that eigenvalue. A consistent choice is $A_0^\dagger = \int_M L_0(x) A^\dagger(x)$, where $L_0(x)$ is the zero mode. A priori, the expansion of the Hamiltonian then should also contain a term $A_0^\dagger A_0$, however one can check that the operator $A_0^\dagger A_0$ annihilates any state created by acting with either $A_0^\dagger$ or $A_\lambda^\dagger$ on the vacuum, and can thus be omitted from the Hamiltonian. From a different perspective, one can check that $[A_0, A_0^\dagger] = 0$ and thus A_0 and $A_0^\dagger$ cannot be considered ladder operators. Hence we cannot excite the 0-mode by $A_0^\dagger$ and whenever we write λ for an eigenvalue it is implied that $\lambda \neq 0$.

Rényi entropy of a singly excited state by replica approach and provided a conjecture for the entanglement entropy in the special case when the manifold is cut into equal parts. By following a similar procedure in the beginning, yet introducing a simple assumption on the classical fields, we achieve a simplification of the combinatorics of the problem that renders the problem of the analytic continuation straightforward, and thus allows us to find the entanglement entropy exactly. Our findings differ from those in [47], but agree with them to leading order in certain quantities. We discuss this at the end of section 3.1.

Let us consider the state with one single excitation in the λ-mode

$$|\psi_\lambda\rangle := |(m_\lambda = 1)\rangle = \frac{1}{\sqrt{Z_M}} \int \mathcal{D}\phi \; \phi^\lambda e^{-\frac{1}{2}S[\phi]} \, |\phi\rangle \,, \tag{20}$$

where we used the fact that $H_1(x) = 2x$. The action is given in equation (10), and after partial integration we choose to rewrite it as

$$S[\phi] = g \int_M \mathrm{d}^2x \; (\nabla\phi)^2. \tag{21}$$

The density matrix of the singly excited state can then be written as

$$\rho := |\psi_\lambda\rangle \langle\psi_\lambda| = \frac{1}{Z_M} \int \mathcal{D}\phi\mathcal{D}\phi' \; \phi^\lambda \phi'^\lambda e^{-\frac{1}{2}S[\phi]-\frac{1}{2}S[\phi']} \, |\phi\rangle \langle\phi'|. \tag{22}$$

We calculate the entanglement entropy by means of the replica method as developed by [9,52]. The ground state entanglement entropy of the QLM has been studied in detail by these methods, see [37,38,43,44]. Our application of the replica method follows [37,44] closely. Let us consider the bipartite geometry obtained by dividing M into the submanifolds A and B, and denote by Γ the entanglement cut that separates them. We will later consider two specific geometries: a sphere cut at the equator into its two hemispheres and a rectangle cut into two smaller rectangles.

Let us further assume that under the surgery described above the Hilbert space on M splits as $\mathcal{H} = \mathcal{H}_A \otimes \mathcal{H}_B$. For a state in $\mathcal{H}$ we consequently get the splitting $|\phi\rangle = |\phi_A\rangle \otimes |\phi_B\rangle$, where $|\phi_X\rangle \in \mathcal{H}_X$, and $X = A, B$ respectively. The field $\phi(x)$ splits as $\phi(x) = \phi_A(x) + \phi_B(x)$ for $x \in A \cup B$, where

$$\phi_A(x) = \begin{cases} \phi(x), & x \in A \\ 0, & x \in B \end{cases} \,, \tag{23}$$

and analogously for B. Whenever we index a field by a submanifold it can be assumed that it only has support there. At the boundary between A and B we have the continuity condition

$$\phi|_\Gamma = \phi_A|_\Gamma = \phi_B|_\Gamma. \tag{24}$$

One can easily see that the action splits as $S[\phi] = S_A[\phi_A] + S_B[\phi_B]$, where

$$S_X[\phi_X] := g \int_X \mathrm{d}^2x \; (\nabla\phi_X)^2, \quad X = A, B \tag{25}$$

and similarly $\phi^\lambda = \phi^\lambda_A + \phi^\lambda_B$, where

$$\phi^\lambda_X := \sqrt{2g\lambda} \int_X \mathrm{d}^2x \; L_\lambda(x)\phi_X(x), \quad X = A, B. \tag{26}$$

3.1 Replica method calculation

Let $\rho_A = \mathrm{Tr}_B\,\rho$ be the reduced density matrix obtained by tracing out the degrees of freedom on B. The gist of the replica method lies in noting that the Von Neumann entropy of the subsystem A can be rewritten as the limit

$$S[A] = -\,\mathrm{Tr}(\rho_A \log \rho_A) = -\lim_{n\to 1} \partial_n \,\mathrm{Tr}\,\rho_A^n, \tag{27}$$

as long as one is able to find an analytic continuation in n for $\mathrm{Tr}\,\rho_A^n$. In the following we construct the trace of the n-th power of the reduced density matrix of the singly excited state (22), and find that – under a certain assumption satisfied by all modes in the geometries that we consider – the analytic continuation is easily found.

After splitting the Hilbert space into $\mathcal{H}_A$ and $\mathcal{H}_B$, the density matrix takes the form

$$\rho_i = \frac{1}{Z_M}\int \mathcal{D}\phi_{A,i}\mathcal{D}\phi_{B,i}\mathcal{D}\phi'_{A,i}\mathcal{D}\phi'_{B,i}\ (\phi^{\lambda}_{A,i}+\phi^{\lambda}_{B,i})(\phi'^{\lambda}_{A,i}+\phi'^{\lambda}_{B,i})\times \\ e^{-\frac{1}{2}S_A[\phi_{A,i}]-\frac{1}{2}S_B[\phi_{B,i}]-\frac{1}{2}S_A[\phi'_{A,i}]-\frac{1}{2}S_B[\phi'_{B,i}]}|\phi_{A,i}\rangle\otimes|\phi_{B,i}\rangle\langle\phi'_{A,i}|\otimes\langle\phi'_{B,i}|, \tag{28}$$

where we introduced the replica index $i = 1,\ldots,n$ which serves as an accounting device to distinguish the copies of the reduced density matrix. We note here that all fields in (28) are integrated over so the replica index doesn't have a physical significance. As discussed in detail in [37] and depicted in figure 1, one finds three types of gluing conditions for the fields. These arise when we resolve the bras and kets of $\mathrm{Tr}\,\rho_A^n$ into δ-functions and then

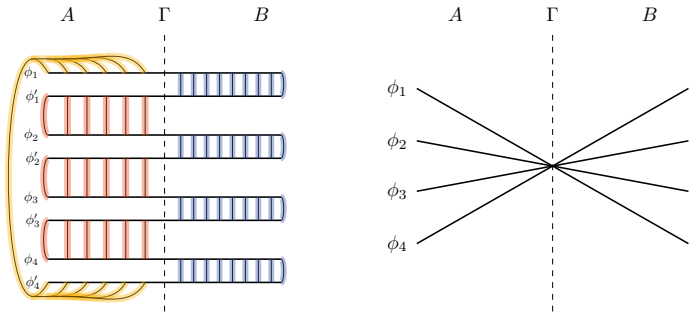

(a) Gluing conditions (b) Resulting configuration

Figure 1: The gluing conditions arising from the calculation of $\mathrm{Tr}\rho_A^n$ and the geometry that results are depicted. The blue lines represent the gluing conditions due to the partial tracing on the B-side of each replica needed to calculate the reduced density matrix ρ_A. The red lines represent the gluing conditions resulting from the multiplication of the replicated reduced density matrices. The yellow lines represent the gluing conditions from the final total trace.

integrate over them. The first gluing condition comes from the calculation of the reduced density matrix $\rho_A = \mathrm{Tr}_B\,\rho$ and tells us to glue the primed and unprimed B fields of the

same replica, that is $\phi_{B,i} = \phi'_{B,i}$ for $i = 1, \dots, n$. The second gluing condition is the result of the multiplication between adjacent replicas of the reduced density matrix $\rho_{A,i}\rho_{A,i+1}$ for $i = 1, \dots, n-1$ and, together with the third gluing condition resulting from the total trace $\operatorname{Tr}\rho_A^n$, tells us to cyclically glue adjacent primed and unprimed A fields, so $\phi'_{A,i} = \phi_{A,i+1}$ for $i = 1, \dots, n$ and with $n+1 \sim 1$. The fact that the gluing conditions on the A side are "shifted" with respect to the B side together with the continuity condition (24) forces *all* the fields to agree at the cut Γ. We denote this boundary condition by $\mathcal{B}$

$$\mathcal{B}: \quad \phi_{A,i}|_\Gamma(x) = \phi_{B,j}|_\Gamma(x) = \mathrm{cut}(x) \quad \forall i,j = 1, \dots, n, \tag{29}$$

where $\mathrm{cut}(x)$ is a function of the coordinates at the entanglement cut Γ. After enforcing the gluing conditions, the trace of the product of reduced density matrices takes the form

$$\operatorname{Tr}\rho_A^n = \frac{1}{(Z_M)^n} \int_{\mathcal{B}} \left[\prod_{i=1}^n \mathcal{D}\phi_{A,i}\mathcal{D}\phi_{B,i}\right] \times \left[\prod_{i=1}^n (\phi^\lambda_{A,i} + \phi^\lambda_{B,i})(\phi^\lambda_{A,i+1} + \phi^\lambda_{B,i})\right] \; e^{-\sum_{i=1}^n (S_A[\phi_{A,i}] + S_B[\phi_{B,i}])}. \tag{30}$$

Since the fields are compactified $\phi \sim \phi + 2\pi R$, the boundary conditions (29) only have to be respected modulo $2\pi R$. A standard way of accounting for this in the calculations, is to split the fields into classical parts and fluctuations, see [53, 54]. We write for each field

$$\phi_{X,i} = \phi^{\mathrm{cl}}_{X,i} + \varphi_{X,i}, \quad i = 1, \dots, n. \tag{31}$$

From the fluctuations φ we only demand that they satisfy Dirichlet boundary conditions

$$\varphi_{A,i}|_\Gamma = \varphi_{B,i}|_\Gamma = 0, \quad i = 1, \dots, n, \tag{32}$$

while the classical fields ϕ^{cl} obey the equations of motion

$$\Delta\phi^{\mathrm{cl}}_{A,i} = \Delta\phi^{\mathrm{cl}}_{B,i} = 0, \quad i = 1, \dots, n, \tag{33}$$

and account for the value of the total field ϕ at the boundary as well as for its compact behavior. It is not hard to check that the action decouples as

$$S[\phi_{A,i}] = S[\phi^{\mathrm{cl}}_{A,i}] + S[\varphi_{A,i}]. \tag{34}$$

Finally, we can rewrite the boundary conditions for the classical fields resulting from (29) as

$$\phi^{\mathrm{cl}}_{A,i}|_\Gamma(x) = \phi^{\mathrm{cl}}_{B,i}|_\Gamma(x) = \mathrm{cut}(x) + 2\pi R\omega_i, \quad i = 1, \dots n-1 \tag{35}$$

$$\phi^{\mathrm{cl}}_{A,n}|_\Gamma(x) = \phi^{\mathrm{cl}}_{B,n}|_\Gamma(x) = \mathrm{cut}(x), \tag{36}$$

where ω_i are integers called the winding numbers that reflect the compactness of ϕ^{cl}. Here we used the fact that the cut functions are arbitrary to absorb the n-th winding number[3]. It

[3] We redefine $\mathrm{cut} \mapsto \mathrm{cut} - 2\pi R\omega_n$ for all n. This effectively shifts the other winding numbers $\omega_i \mapsto \omega_i - \omega_n$ for $i = 1, \dots, n-1$. Since the winding numbers are just arbitrary integers, we can ignore the shift and rename the shifted winding numbers ω_i.

is worth noting at this point that the exact treatment of the winding numbers depends a lot on the geometry, see [44] for several examples. The geometries that we will later consider, that is the sphere and the rectangle, in principle would allow for simplifications at this point. However, in order to keep the discussion somewhat more general, we decide to, for the moment, keep the boundary conditions as given above. Furthermore, we note that the zero modes on A and B with the above boundary conditions are in general not trivially related to the zero mode on the complete manifold which doesn't know anything about the cut Γ. In particular, this means that they are a priori not orthogonal to the eigenmodes of the Laplacian on M, so $(\phi_A^{\mathrm{cl}})^\lambda + (\phi_B^{\mathrm{cl}})^\lambda \neq 0$. We will concentrate on situations where this equation *does* hold, as it leads to a significant simplification of the combinatorics. Thus, let us assume that the following is true

$$(\phi_A^{\mathrm{cl}})^\lambda + (\phi_B^{\mathrm{cl}})^\lambda = 0. \tag{37}$$

We will later see that this is in fact justified in the geometries we consider. Defining the field ϕ^{cl} obtained by stitching together together ϕ_A^{cl} and ϕ_B^{cl}, that is

$$\phi^{\mathrm{cl}}(x) := \begin{cases} \phi_A^{\mathrm{cl}}(x), & x \in A \\ \phi_B^{\mathrm{cl}}(x), & x \in B, \end{cases} \tag{38}$$

we can express the assumption (37) in the simpler form $(\phi^{\mathrm{cl}})^\lambda = 0$. We will later see that this condition is satisfied for all the eigenmodes of the Laplacian on both the sphere and rectangle. As defined above, ϕ^{cl} is well defined and continuous at Γ, since ϕ_A^{cl} and ϕ_B^{cl} satisfy the same boundary conditions there. In general, however, ϕ^{cl} is not smooth at the cut. We note here that in the derivation of the generalized Wick's theorem of [47] this assumption is also implicitly made[4]. However, since the authors only consider the rectangular case the assumption is justified.

At this step, the boundary conditions given in (29) can be recast as

$$\mathcal{B}: \quad \begin{aligned} &\phi_i^{\mathrm{cl}}|_\Gamma(x) = \mathrm{cut}(x) + 2\pi R\omega_i, && i = 1, \dots n-1 \\ &\phi_n^{\mathrm{cl}}|_\Gamma(x) = \mathrm{cut}(x) \\ &\varphi_{A,i}|_\Gamma = \varphi_{B,i}|_\Gamma = 0, && i = 1, \dots, n. \end{aligned} \tag{39}$$

Next, we perform the unitary transformation U_n from [43, 44] on the classical fields. This rotation shifts the dependence on the cut function to the boundary condition for the n-th field, while turning the boundary conditions of the remaining fields into pure winding

[4] Before eq. (A.11) in the reference, the field C_a is defined by stitching together solutions 0-modes of the Laplacian on the A and B sides of the manifold with non-trivial boundary conditions in between. Thus, the resulting function is in general *not* a harmonic function over M, and the terms denoted Har in (A.11) only vanish when integrated against eigenfunctions of the Laplacian on M iff our assumption (37) is fulfilled.

numbers. Explicitly, we define

$$U_n := \begin{bmatrix} \frac{1}{\sqrt{2}} & -\frac{1}{\sqrt{2}} & 0 & & \dots \\ \frac{1}{\sqrt{6}} & \frac{1}{\sqrt{6}} & -\frac{2}{\sqrt{6}} & 0 & \dots \\ \vdots & & & & \\ \frac{1}{\sqrt{n(n-1)}} & \frac{1}{\sqrt{n(n-1)}} & \dots & \dots & -\sqrt{1-\frac{1}{n}} \\ \frac{1}{\sqrt{n}} & \frac{1}{\sqrt{n}} & \dots & \dots & \frac{1}{\sqrt{n}} \end{bmatrix} \tag{40}$$

and rotate the classical fields as

$$\phi_i^{\mathrm{cl}} \mapsto \bar{\phi}_i^{\mathrm{cl}} := (U_n \phi^{\mathrm{cl}})_i. \tag{41}$$

This results in the altered boundary condition $\mathcal{B}'$

$$\mathcal{B}' : \begin{array}{ll} \bar{\phi}_i^{\mathrm{cl}}|_\Gamma(x) = 2\pi R \bar{\omega}_i, & i = 1, \dots n-1 \\ \bar{\phi}_n^{\mathrm{cl}}|_\Gamma(x) = \sqrt{n}\mathrm{cut}(x) + \frac{2\pi R}{\sqrt{n}} \sum_{i=1}^{n-1} \omega_i, & \\ \varphi_{A,i}|_\Gamma = \varphi_{B,i}|_\Gamma = 0, & i = 1, \dots, n, \end{array} \tag{42}$$

where $\bar{\omega}_i = (M_{n-1})_{ij}\omega_j$ and M_{n-1} is the minor matrix resulting from deleting the n-th row and column of U_n. Notice that after the rotation the compactification radius of the n-th field becomes $\sqrt{n}R$.

Finally, we can rewrite equation (30) for $\mathrm{Tr}\,\rho_A^n$ in terms of the classical fields and fluctuations as

$$\mathrm{Tr}\,\rho_A^n = \frac{1}{(Z_M)^n} W(n) \int_{\mathcal{B}'} \left[\prod_{i=1}^n \mathcal{D}\varphi_{A,i}\mathcal{D}\varphi_{B,i}\right] \mathcal{D}\bar{\phi}_n^{\mathrm{cl}} \times \left(\prod_{i=1}^n (\varphi_{A,i}^\lambda + \varphi_{B,i}^\lambda)(\varphi_{A,i+1}^\lambda + \varphi_{B,i}^\lambda)\right) e^{-S[\bar{\phi}_n^{\mathrm{cl}}] - \sum_{i=1}^n (S[\varphi_{A,i}] + S[\varphi_{B,i}])}, \tag{43}$$

where we used the definition (26) as well as the assumption (37) which together imply

$$\bar{\phi}_{A,i}^\lambda + \bar{\phi}_{B,i}^\lambda = \varphi_{A,i}^\lambda + \varphi_{B,i}^\lambda \tag{44}$$

and allow us to get rid of the classical fields with matching replica indices outside of the exponential. The remaining classical fields in the product, i.e. those coming from $\bar{\phi}_{A,i+1}^\lambda + \bar{\phi}_{B,i}^\lambda$, don't necessarily vanish by assumption (37). However, they don't contribute to the sum as they always appear multiplied by an odd number of fluctuations. When the path integrals are evaluated, these terms turn into correlation functions, and the correlation functions of an odd number of fluctuations vanish. We can thus safely discard all classical fields outside of the exponential. We further omitted an $n^{-\frac{\varepsilon}{2L}}$ factor coming from a change of path integral measure, with ε a UV cut-off and L the length of the entangling cut Γ, as it only contributes to a non-universal area law term, see [43, 44] for more details. Furthermore, we separated the

contributions from the classical part of the first $n-1$ fields into the so-called winding sector

$$W(n) := \prod_{i=1}^{n-1} \int \mathcal{D}\bar{\phi}^{\mathrm{cl}}_{A,i} \mathcal{D}\bar{\phi}^{\mathrm{cl}}_{B,i}\; e^{-S[\bar{\phi}^{\mathrm{cl}}_{A,i}]-S[\bar{\phi}^{\mathrm{cl}}_{B,i}]}$$
$$= \prod_{i=1}^{n-1} \int \mathcal{D}\bar{\phi}^{\mathrm{cl}}_{i}\; e^{-S[\bar{\phi}^{\mathrm{cl}}_{i}]} = \sum_{\omega \in \mathbb{Z}^{n-1}} e^{-\sum_{i=1}^{n-1} S[\bar{\phi}^{\mathrm{cl}}_{i}]}. \tag{45}$$

For clarity, let us make some comments. The assumption (37) is formulated for each unrotated replica. However, since U_n is an invertible matrix it is clear that $(\vec{\phi^{\mathrm{cl}}})^\lambda = \vec{0}$ iff $(U_n\vec{\phi^{\mathrm{cl}}})^\lambda = \vec{0}$ for $\vec{\phi^{\mathrm{cl}}} = (\phi_1^{\mathrm{cl}}, \dots, \phi_n^{\mathrm{cl}})$ and $(\vec{\phi^{\mathrm{cl}}})^\lambda = ((\phi_1^{\mathrm{cl}})^\lambda, \dots, (\phi_n^{\mathrm{cl}})^\lambda)$. Furthermore, after our path integral manipulations the n-th replica becomes a free field on the complete manifold, such that ϕ_n^{cl} turns into the 0-mode on M. Thus for the n-th rotated field our assumption will always be satisfied after restitching, and we only need to check the other fields[5]. In appendix A we show that, by performing some path integral manipulations, (43) can be brought into the form

$$\mathrm{Tr}(\rho_A^n) = \frac{1}{(Z_M)^n} W(n) \Bigg[\left(\int_{A_D} \mathcal{D}\varphi_A\; (\varphi_A^\lambda)^2 e^{-S[\varphi_A]} \right)^{n-1} \int \mathcal{D}\bar{\phi}\; \bar{\phi}^\lambda \bar{\phi}_A^\lambda e^{-S[\bar{\phi}]} +$$
$$+ \left(\int_{B_D} \mathcal{D}\varphi_B\; (\varphi_B^\lambda)^2 e^{-S[\varphi_B]} \right)^{n-1} \int \mathcal{D}\bar{\phi}\; \bar{\phi}^\lambda \bar{\phi}_B^\lambda e^{-S[\bar{\phi}]} \Bigg], \tag{46}$$

where the subscripts A_D and B_D indicate that those path integrals are performed on either A or B with Dirichlet boundary conditions. By linearity and using the definition (26), we can rewrite the path integrals on $X = A, B$ as

$$\int_{X_D} \mathcal{D}\varphi_X\; (\varphi_X^\lambda)^2 e^{-S[\varphi_X]} = 2g\lambda \int_X \mathrm{d}^2x\, \mathrm{d}^2x'\; L_\lambda(x) L_\lambda(x') \int_{X_D} \mathcal{D}\varphi_X\; \varphi_X(x)\varphi_X(x') e^{-S[\varphi_X]} \tag{47}$$
$$= Z_X\; \lambda \int_X \mathrm{d}^2x\, \mathrm{d}^2x'\; L_\lambda(x) L_\lambda(x') G_X(x,x'), \tag{48}$$

where Z_X is the partition function and $G_X(x,x')$ the Green's function corresponding to the Laplacian on X[6], both with Dirichlet boundary conditions at Γ. Similarly, we can write the following for the path integrals on the full manifold

$$\int \mathcal{D}\bar{\phi}\; \bar{\phi}^\lambda \bar{\phi}_A^\lambda e^{-S[\bar{\phi}]} = 2g\lambda \int_M \mathrm{d}^2x \int_A \mathrm{d}^2x' L_\lambda(x) L_\lambda(x') \int \mathcal{D}\bar{\phi}\; \bar{\phi}(x)\bar{\phi}(x') e^{-S[\bar{\phi}]}$$
$$= Z_M\; \lambda \int_M \mathrm{d}^2x \int_A \mathrm{d}^2x' L_\lambda(x) L_\lambda(x') G_M(x,x') \tag{49}$$

[5] Alternatively, we could have assumed (37) for only the first $n-1$ rotated fields from the beginning. This alters the form of (43) but also results in (46) after some manipulations.

[6] Note that the factor of $2g$ cancels, as the two point function actually gives the Green's function corresponding to $2g\Delta$ which is $\frac{1}{2g}G$ with G the Green's function of Δ.

with $G_M(x,x')$ the corresponding Green's function. Let us define the following transformed Green's functions

$$\begin{aligned} G^\lambda_{X,M} &:= \lambda \int_M \mathrm{d}^2x \int_X \mathrm{d}^2x' L_\lambda(x) L_\lambda(x') G_M(x,x'), \quad X = A, B \\ G^\lambda_X &:= \lambda \int_X \mathrm{d}^2x\, \mathrm{d}^2x'\; L_\lambda(x) L_\lambda(x') G_X(x,x'), \quad X = A, B, M. \end{aligned} \tag{50}$$

We emphasize here that $G_M(x,x')$, $G_A(x,x')$, and $G_B(x,x')$ are different objects, each calculated on their corresponding manifold with Dirichlet boundary conditions. In appendix B we take a closer look at these transformed propagators and use spectral methods to calculate them in some geometries. In particular we find that

$$G^\lambda_M = 1 \tag{51}$$

is always true. In [47], quantities of this form were dubbed "Entanglement Propagator Amplitudes" (EPA's) and some explicit results about them were given. In appendix C we show exactly how the EPA's are related to the transformed propagators and find our results in agreement with [47]. With all this, we can finally write

$$\begin{aligned} \mathrm{Tr}(\rho_A^n) &= \left(\frac{Z_{A_D} Z_{B_D}}{Z_M}\right)^{n-1} W(n) \left[\left(G^\lambda_A\right)^{n-1} G^\lambda_{A,M} + \left(G^\lambda_B\right)^{n-1} G^\lambda_{B,M}\right] \\ &= \mathrm{Tr}\left(\rho^n_{\mathrm{GS},A}\right) \left[\left(G^\lambda_A\right)^{n-1} G^\lambda_{A,M} + \left(G^\lambda_B\right)^{n-1} G^\lambda_{B,M}\right], \end{aligned} \tag{52}$$

where ρ_{GS} is the ground state density matrix, see [43, 44], meaning that the ground state Rényi entropy $S^{(n)}_{GS}[A]$ factors from the excited state Rényi entropies $S^{(n)}_\lambda[A]$

$$\begin{aligned} S^{(n)}_\lambda[A] &:= \frac{1}{1-n} \log(\mathrm{Tr}\rho^n_A) \\ &= S^{(n)}_{GS}[A] + \frac{1}{1-n} \log\left[\left(G^\lambda_A\right)^{n-1} G^\lambda_{A,M} + \left(G^\lambda_B\right)^{n-1} G^\lambda_{B,M}\right] \end{aligned} \tag{53}$$

In [47] an expression for the Rényi entropies of the first excited state was also obtained. Our result, however, differs from theirs. In the rectangular case, we will see that $G^\lambda_X = G^\lambda_{X,M} - d^X_\lambda$ for $X = A, B$. There, our result agrees with [47] to leading order in d^A_λ and d^B_λ. As a consequence, our results also disagree with their conjecture for $\mathrm{Tr}(\rho^n_A)/\mathrm{Tr}(\rho^n_{GS,A})$ and the resulting entanglement entropy (see eqs. (27) and (75) in [47]).

The structure of (52) offers a simple interpretation. In the above manipulations we effectively separated the A and B sides of the first $n-1$ replicas, while connecting the sides of the n-th replica into one complete copy over the whole manifold. The $n-1$-factors of G^λ_X encode the free propagation on either the A or B side of the first $n-1$ copies. The $G^\lambda_{A(B),M}$ factor, on the other hand, represents free propagation from either A or B to any point on M for the n-th copy. Meanwhile topological effects are factored into the winding sector and the partition functions which give rise to the ground state density matrix. Apart from the winding sector, n only appears in (52) as a power. Thus, if an analytic continuation for $W(n)$

is known, it is trivial to analytically continue the rest of the expression. The entanglement entropy of the state with a single excitation in the λ mode is thus

$$S_\lambda[A] = -\lim_{n\to 1}\partial_n \operatorname{Tr}(\rho_A^n) \tag{54}$$

$$= S_{GS}[A] - \log\Big(G_A^\lambda\Big)G_{A,M}^\lambda - \log\Big(G_B^\lambda\Big)G_{B,M}^\lambda \tag{55}$$

where we used that $G_{A,M}^\lambda + G_{B,M}^\lambda = G_M^\lambda = 1$ and where $S_{GS}[A]$ is the entanglement entropy of the ground state

$$S_{GS}[A] = -\lim_{n\to 1}\partial_n \operatorname{Tr}\Big(\rho_{GS,A}^n\Big). \tag{56}$$

Given the ground state entanglement entropy, the calculation of the entanglement entropy of the singly excited state reduces to the calculation of the transformed Green's functions (50). Let us consider some explicit cases.

3.2 Spherical geometry

Let $M = S^2$ be the unit sphere and divide it into two hemispheres $A = B = H^2$ at the equator. The ground state entanglement entropy of a hemisphere is [44]

$$S_{GS}[H^2] = \log\Big(\sqrt{8\pi g R}\Big) - \frac{1}{2}. \tag{57}$$

The eigenmodes of the Laplacian on the sphere are the spherical harmonics

$$L_\lambda(x) \equiv L_{\ell,m}(x) = Y_\ell^m(x), \tag{58}$$

where $x = (\theta, \phi)$ is a point on S^2, ℓ a non-negative integer, and $m = -\ell, \dots, \ell$. The eigenvalues of $-\Delta_{S^2}$ are $\lambda = \ell(\ell+1)$ and have a degeneracy of $2\ell+1$. As can be seen above, whenever we use λ as an index, we actually mean the two numbers (ℓ, m) that uniquely identify a mode. The eigenmodes on the hemisphere with Dirichlet boundary conditions at the equator are, up to normalization, the spherical harmonics such that $\ell + m$ is odd. The properly normalized modes on A and B are then

$$L_\lambda^{H^2}(x) = \sqrt{2}Y_\ell^m(x), \quad m + \ell = \text{odd}. \tag{59}$$

The first $n-1$ rotated classical fields on the hemisphere with boundary conditions (42) is constant and given by

$$\bar{\phi}_i^{\text{cl}} = 2\pi R\bar{\omega}_i. \tag{60}$$

Since the 0-mode $L_0 = 1/(4\pi)$ of the Laplacian on the full sphere is also constant $\bar{\phi}_i^{\text{cl}}$ is proportional to L_0, and thus orthogonal to the other eigenmodes. Therefore, our assumption (37) is fulfilled in this situation. In appendix B.1 we calculate all the transformed propagators in this geometry and find that

$$G_{A,M}^\lambda = G_{B,M}^\lambda = \frac{1}{2} \tag{61}$$

$$G_A^\lambda = G_B^\lambda = \frac{1}{2}\Sigma_\lambda \tag{62}$$

where Σ_λ is given by

$$\Sigma_\lambda = \begin{cases} \Sigma^{\mathrm{e}}_\lambda, & \ell_\lambda + m_\lambda = \text{even} \\ 1, & \ell_\lambda + m_\lambda = \text{odd}, \end{cases} \tag{63}$$

and $\Sigma^{\mathrm{e}}_\lambda$ is complicated expression involving an infinite sum and an integral over associated Legendre polynomials. It is given explicitly in (142) and can be easily evaluated numerically by truncating the sum at a sufficiently large number[7]. We note that $\Sigma_{\ell,-m} = \Sigma_{\ell,m}$ for all modes. The striking difference between the modes with $\ell + m$ even and odd is due to the fact that those with $\ell + m$ odd are orthogonal to the eigenmodes on the hemisphere while the others are not. Using (55) and (57) we can finally write the entanglement entropy as

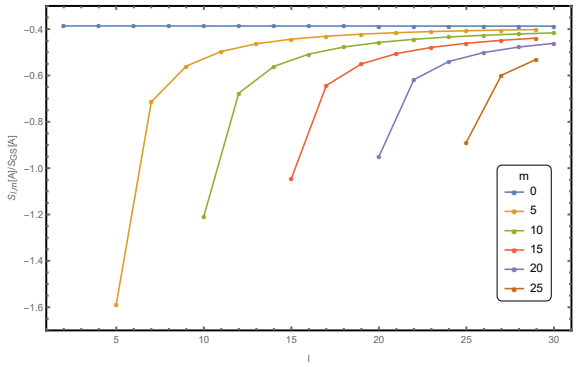

Figure 2: The value of the entanglement entropy $S_{\ell,m}[A]$ in units of the ground state entanglement entropy at the RK-point, i.e. $g = \frac{1}{8\pi}$, and for $R = 1$ plotted for ℓ up to 30 and a selection of values of m such that $\ell + m$ is even.

$$S_\lambda[A] = S_{GS}[A] - \log\left(G^\lambda_A\right) \tag{64}$$

$$= \log\left(\sqrt{2\pi g} R \Sigma_\lambda\right) - \frac{1}{2} \tag{65}$$

Note that the entanglement entropy of all singly excited modes with $\ell + m$ odd is the same. The behavior of the entanglement entropy for modes with $\ell + m$ even is depicted in Figure 2. We observe that the entanglement entropy for modes with $m = 0$ is the same for all ℓ. In fact, a numerical evaluation of Σ_λ seems to indicate that $\Sigma_{\ell,m} \approx 1$. Consequently, the entanglement entropy is the same for *all* modes with $m = 0$. Furthermore, we see that for fixed m the entanglement entropy of the modes with $\ell + m$ even and $m \neq 0$ approaches this value with growing ℓ. Thus, we conclude that

$$S_{\ell,m}[A] \approx S_{GS}[A] + \log 2 \tag{66}$$

is valid for all modes with $\ell + m$ odd, all modes with $m = 0$, and for all modes in the limit $\ell \gg 1$. In the case $\ell + m$ odd the equation is exact.

[7]This number must be larger than ℓ_λ as the summand has a peak there that has to be included.

3.3 Rectangular Geometry

Next, let $M = [0, L_x] \times [0, L_y]$ be a rectangle and cut it at $x = \ell_x$ into the two smaller rectangles $A = [0, \ell_x] \times [0, L_y]$ and $B = [\ell_x, L_x] \times [0, L_y]$. We impose Dirichlet boundary conditions $\phi|_{\partial M} = 0$. If we go through the replica method calculation, we see that the classical part of the field, after rotation, obeys the boundary conditions (42) at the cut. One can check that the only solution to the equation of motion $\Delta\phi_i^{\mathrm{cl}} = 0$ for $i = 1, \ldots, n-1$ with boundary conditions (42) at the cut and Dirichlet boundary conditions on the other boundaries is the trivial one $\phi_i^{\mathrm{cl}}(x, y) = 0$, which, in turn, is only a solution if the winding numbers vanish. Thus, there cannot be a winding sector for this geometry. The assumption (37) is then trivially satisfied for the first $n-1$ fields, since they all vanish.

The eigenmodes of the Laplacian on M with Dirichlet boundary conditions are given by

$$L_\lambda(x) \equiv L_{k_x,k_y}(x, y) = \frac{2}{\sqrt{L_x L_y}} \sin\left(\frac{\pi k_x}{L_x} x\right) \sin\left(\frac{\pi k_y}{L_y} y\right) \tag{67}$$

with eigenvalues

$$\lambda_{k_x,k_y} = \left(\frac{\pi}{L_x} k_x\right)^2 + \left(\frac{\pi}{L_y} k_y\right)^2, \quad k_x, k_y \in \mathbb{N}^+. \tag{68}$$

In appendix D we calculate the ζ-regularized determinant of the Laplacian on the rectangle M and find

$$\det \Delta = \frac{1}{\sqrt{2L_y}} \eta\left(i \frac{L_x}{L_y}\right), \tag{69}$$

where η is the Dedekind η-function. This coincides with the expression cited in [47] and calculated by lattice-regularization methods in [55] up to non-universal terms, and terms that diverge upon taking the continuum limit. We further note that due to the modular properties of the η-function this expression is invariant under the exchange of L_x and L_y. The eigenmodes and determinants on the submanifolds A and B are obtained by inserting ℓ_x and $L_x - \ell_x$ respectively instead of L_x into the above expressions. Writing the partition functions as $-\log Z_X = \frac{1}{2} \log \det \Delta_X$ for $X = M, A, B$, we can use the determinant (69) to express the ground state entanglement entropy on the rectangle as

$$S_{GS}[A] = \frac{1}{2} \log \left(\frac{\eta\left(i \frac{\ell_x}{L_y}\right) \eta\left(i \frac{L_x - \ell_x}{L_y}\right)}{\sqrt{2L_y}\, \eta\left(i \frac{L_x}{L_y}\right)} \right). \tag{70}$$

In appendix B.2 we show that the first transformed Green's functions on the rectangle are

$$G^\lambda_{A,M} = \frac{\ell_x}{L_x} - \frac{1}{2\pi k_x} \sin\left(2\pi k_x \frac{\ell_x}{L_x}\right) \tag{71}$$

$$G^\lambda_{B,M} = \left(1 - \frac{\ell_x}{L_x}\right) + \frac{1}{2\pi k_x} \sin\left(2\pi k_x \frac{\ell_x}{L_x}\right). \tag{72}$$

and the remaining are given by

$$G_A^\lambda = G_{A,M}^\lambda - \frac{1}{L_x}\frac{2\left(\frac{\pi}{L_y}k_y\right)\coth\left(\pi k_y\frac{\ell_x}{L_y}\right)\sin\left(\pi k_x\frac{\ell_x}{L_x}\right)^2 - \left(\frac{\pi}{L_x}k_x\right)\sin\left(2\pi k_x\frac{\ell_x}{L_x}\right)}{\left(\frac{\pi}{L_x}k_x\right)^2+\left(\frac{\pi}{L_y}k_y\right)^2} \tag{73}$$

$$G_B^\lambda = G_{B,M}^\lambda - \frac{1}{L_x}\frac{2\left(\frac{\pi}{L_y}k_y\right)\coth\left(\pi k_y\frac{L_x-\ell_x}{L_y}\right)\sin\left(\pi k_x\frac{\ell_x}{L_x}\right)^2 + \left(\frac{\pi}{L_x}k_x\right)\sin\left(2\pi k_x\frac{\ell_x}{L_x}\right)}{\left(\frac{\pi}{L_x}k_x\right)^2+\left(\frac{\pi}{L_y}k_y\right)^2}. \tag{74}$$

As shown in appendix C our result for the transformed propagators agrees with the approximation found in [47].

Finally, we find the entanglement entropy for the rectangle cut at ℓ_x by inserting the transformed propagators and ground state entanglement entropy into equation (55). In figure 3 we show how the entropy depends on the surgery for a selection of modes. We observe that for constant k_x the entanglement entropy is minimal at $k_x = k_y$ and becomes maximal as $k_y \to \infty$. As was the case for the sphere, there are two kinds of modes for a given surgery.

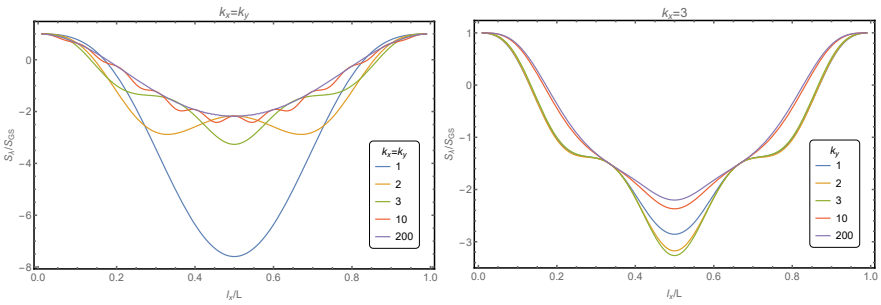

Figure 3: S_λ as a function of ℓ_x for a selection of modes and for $L_x = L_y$.

Modes that are at the same time eigenmodes of the complete manifold and the submanifolds (up to normalization), and modes that aren't. In the rectangular geometry the first kind of modes are determined by the condition that

$$k_x\frac{\ell_x}{L_x} = m, \quad m \in \mathbb{N}, \tag{75}$$

which can only be satisfied whenever ℓ_x/L_x is a rational number. For example, when the rectangle is halved by the surgery, that is $\ell_x = L_x/2$, all modes with even k_x belong to the first category and those with k_x odd to the second. The entanglement entropy is constant for all the modes satisfying condition (75) and given by

$$S_\lambda[A] = S_{GS}[A] - \log\left[\left(\frac{\ell_x}{L_x}\right)^{\frac{\ell_x}{L_x}}\left(1-\frac{\ell_x}{L_x}\right)^{1-\frac{\ell_x}{L_x}}\right]. \tag{76}$$

The eigenmodes that do not satisfy the condition have an intricate functional dependence on the k_x and k_y. However, it isn't hard to see from the dependence on k_x of the transformed

propagators, that for large k_x they converge to the value (76). Whenever condition (75) cannot be satisfied, that is when ℓ_x/L_x is not a rational number, there are no modes of the first kind and the entanglement entropy has a non-trivial dependence on the k_x and k_y for all modes. Nonetheless, equation (76) is also valid here for $k_x \gg 1$. When the rectangle is halved we can write

$$S_{k_x,k_y}[A] \approx S_{GS}[A] + \log 2 \tag{77}$$

for modes with k_x even and for all modes in the limit $k_x \gg 1$. In the former case the equation is exact. This result is analogous to that for the halved sphere (66).

4 General excited states

We are now ready to turn our attention to general excitations. From (16) we can directly write the corresponding density matrix as

$$\begin{aligned}\rho_i &= \left|(m_{\lambda_1},\dots,m_{\lambda_r},\dots,m_{\lambda_\nu})\right\rangle\left\langle(m_{\lambda_1},\dots,m_{\lambda_r},\dots,m_{\lambda_\nu})\right| \\ &= \frac{1}{Z_M}\int \mathcal{D}\phi_i\mathcal{D}\phi_i' \left(\prod_{r=1}^{\nu}\frac{1}{2^{m_{\lambda_r}}m_{\lambda_r}!}H_{m_{\lambda_r}}\left(\frac{\phi_i^{\lambda_r}}{\sqrt{2}}\right)H_{m_{\lambda_r}}\left(\frac{\phi_i'^{\lambda_r}}{\sqrt{2}}\right)\right) e^{-\frac{1}{2}S[\phi_i]-\frac{1}{2}S[\phi_i']}|\phi_i\rangle\langle\phi_i'|,\end{aligned} \tag{78}$$

where we also introduced a replica index. From our discussion about the singly excited state, we know that, in broad terms, computing $\operatorname{Tr}\rho_A^n$ amounts to writing down the product of density matrices, separating the fields into fields with support on the respective submanifolds as $\phi = \phi_A + \phi_B$, and enforcing the gluing conditions $\phi'_{A,i} = \phi_{A,i+1}$ and $\phi'_{B,i} = \phi_{B,i}$ for $i = 1,\dots,n$ with $n+1 \sim 1$, that result in the set of boundary conditions (29) on the path integrals. Since the details of the calculation are exactly the same as for the singly excited state we omit them and immediately write down

$$\begin{aligned}\operatorname{Tr}\left(\prod_{i=1}^{n}\rho_{A,i}\right) = \left(\prod_{r=1}^{\nu}\frac{1}{2^{m_{\lambda_r}}m_{\lambda_r}!}\right)^n \frac{1}{Z_M^n}\int_{\mathcal{B}}\left[\prod_{i=1}^{n}\mathcal{D}\phi_{A,i}\mathcal{D}\phi_{B,i}\right] e^{-\sum_{i=1}^{n}(S_{A,i}+S_{B,i})}\times \\ \prod_{i=1}^{n}\prod_{r=1}^{\nu}H_{m_{\lambda_r}}\left(\frac{1}{\sqrt{2}}\left(\phi_{A,i}^{\lambda_r}+\phi_{B,i}^{\lambda_r}\right)\right)H_{m_{\lambda_r}}\left(\frac{1}{\sqrt{2}}\left(\phi_{A,i+1}^{\lambda_r}+\phi_{B,i}^{\lambda_r}\right)\right).\end{aligned} \tag{79}$$

One can compare this expression with equation (30) for the singly excited state. As the expression stands, the fields on A and B are still tied together within the Hermite polynomials. We factor them by an identity of Hermite polynomials which we apply on the polynomials with shifted replica indices for $i = 1,\dots,n$ as

$$H_{m_r}\left(\frac{1}{\sqrt{2}}\left(\phi_{A,i+1}^{\lambda_r}+\phi_{B,i}^{\lambda_r}\right)\right) = \frac{1}{2^{\frac{m_r}{2}}}\sum_{k'_{r,i}=0}^{m_r}\binom{m_r}{k'_{r,i}}H_{k'_{r,i}}(\phi_{A,i+1}^{\lambda_r})H_{m_r-k'_{r,i}}(\phi_{B,i}^{\lambda_r}), \tag{80}$$

on the polynomials with matching replica indices for $i = 1,\dots,n-1$

$$H_{m_r}\left(\frac{1}{\sqrt{2}}\left(\phi_{A,i}^{\lambda_r}+\phi_{B,i}^{\lambda_r}\right)\right) = \frac{1}{2^{\frac{m_r}{2}}}\sum_{k_{r,i}=0}^{m_r}\binom{m_r}{k_{r,i}}H_{m_r-k_{r,i}}(\phi_{A,i}^{\lambda_r})H_{k_{r,i}}(\phi_{B,i}^{\lambda_r}), \tag{81}$$

where, with some foresight, we don't apply factorization to the n-th copy, as the A and B parts of the n-th field will be reunited into a free field on M. Also note that from now on we write m_r instead of m_{λ_r} to declutter the notation. Since we are applying the factorization above to each of the Hermite polynomials separately, and they are each labelled by a replica and an r index, there is no way around introducing the, at first overwhelming, amount of indices $k_{r,i}$ and $k'_{r,i}$ for $i = 1, \dots, n$ and $r = 1, \dots, \nu$.

After factoring the polynomials we can continue as in section 3. We first separate the fields into classical parts and fluctuations and then rotate the classical fields. For the singly excited state it was sufficient to demand the assumption (37) to be fulfilled in order to make the calculation tractable. Now, since the fields all appear inside Hermite polynomials, the calculations in appendix A don't apply, and we must make a new assumption. We demand that the first $n-1$ rotated fields satisfy

$$(\bar{\phi}^{\mathrm{cl}}_{A,i})^{\lambda} = (\bar{\phi}^{\mathrm{cl}}_{B,i})^{\lambda} = 0, \quad i = 1, \dots, n-1. \tag{82}$$

Note that this assumption is stricter than (37), demanding that the integrals on the A and B sides of the manifold vanish separately. We don't require anything from the n-th classical field and stitch it back together with the fluctuation to form a complete free field on M. As for the singly excited state, the assumption ensures that we don't have to consider correlation functions of the classical fields, which adds a difficult layer of complexity to calculations. While assumption (82) might seem rather restrictive for general geometries, we will see that it is satisfied by almost all modes on the halved-sphere and by all modes on the rectangle.

Apart from the stronger assumption on the classical fields, there is no difference in the method from the singly excited case and the details go through in an analogous way. With these considerations and some rearranging of the terms we can rewrite (79) as

$$\begin{aligned}
\mathrm{Tr}\left(\prod_{i=1}^{n}\rho_{A,i}\right) = \frac{1}{Z_M^n}W(n)\sum_{K_1}\sum_{K'_1}\cdots\sum_{K_\nu}\sum_{K'_\nu}\Bigg[\\
\prod_{i=1}^{n-1}\left(\int_{A_D}\mathcal{D}\varphi_{A,i}\left[\prod_{r=1}^{\nu}\frac{1}{2^{m_r}}\sqrt{\frac{1}{m_r!}\binom{m_r}{k_{r,i}}\binom{m_r}{k'_{r,i-1}}}H_{m_r-k_{r,i}}\left(\varphi^{\lambda_r}_{A,i}\right)H_{k'_{r,i-1}}\left(\varphi^{\lambda_r}_{A,i}\right)\right]e^{-S[\varphi_{A,i}]}\right) \\
\prod_{i=1}^{n-1}\left(\int_{B_D}\mathcal{D}\varphi_{B,i}\left[\prod_{r=1}^{\nu}\frac{1}{2^{m_r}}\sqrt{\frac{1}{m_r!}\binom{m_r}{k_{r,i}}\binom{m_r}{k'_{r,i}}}H_{k_{r,i}}\left(\varphi^{\lambda_r}_{B,i}\right)H_{m_r-k'_{r,i}}\left(\varphi^{\lambda_r}_{B,i}\right)\right]e^{-S[\varphi_{B,i}]}\right) \\
\int\mathcal{D}\bar{\phi}_n\left[\prod_{r=1}^{\nu}\frac{1}{2^{\frac{3m_r}{2}}m_r!}\sqrt{\binom{m_r}{k'_{r,n}}\binom{m_r}{k'_{r,n-1}}}H_{m_r}\left(\frac{1}{\sqrt{2}}\bar{\phi}_n{}^{\lambda_r}\right)H_{k'_{r,n}}\left(\bar{\phi}^{\lambda_r}_{A,n}\right)H_{m_r-k'_{r,n-1}}\left(\bar{\phi}^{\lambda_r}_{B,n}\right)\right]e^{-S[\bar{\phi}]}\Bigg]
\end{aligned} \tag{83}$$

where $\sum_{K_r} \equiv \sum_{k_{r,1}=0}^{m_r}\cdots\sum_{k_{r,n-1}=0}^{m_r}$ and $\sum_{K'_r} \equiv \sum_{k'_{r,1}=0}^{m_r}\cdots\sum_{k'_{r,n}=0}^{m_r}$. Note that for the first $n-1$ replicas there are always two Hermite polynomials for each replica at each side A and B which result from splitting the two Hermite polynomials in (79). For the n-th replica we only split one of the Hermite polynomials in (79), thus we see only three in the resulting

expression: the unsplit Hermite polynomial of a full field, and the two factors of the one we split. Although at first glance the resulting situation seems quite desperate, there are a couple of simplifications we can make. First of all, we note that all the replica indices for the fields are now dummy indices, and that the path integral expressions are just correlation functions. For example the path integral over A is just

$$\begin{aligned}\int_{A_D}\mathcal{D}\varphi_A\ &\left[\prod_{r=1}^{\nu}\frac{1}{2^{m_r}}\sqrt{\frac{1}{m_r!}\binom{m_r}{k_{r,i}}\binom{m_r}{k'_{r,i-1}}}H_{m_r-k_{r,i}}\left(\varphi_A^{\lambda_r}\right)H_{k'_{r,i-1}}\left(\varphi_A^{\lambda_r}\right)\right]e^{-S[\varphi_A]}\\ &= Z_A\left(\prod_{r=1}^{\nu}\frac{1}{2^{m_r}}\sqrt{\frac{1}{m_r!}\binom{m_r}{k_{r,i}}\binom{m_r}{k'_{r,i-1}}}\right)\left\langle\prod_{r=1}^{\nu}H_{m_r-k_{r,i}}\left(\varphi_A^{\lambda_r}\right)H_{k'_{r,i-1}}\left(\varphi_A^{\lambda_r}\right)\right\rangle_{A_D},\end{aligned}\tag{84}$$

and similarly for the path integrals over B and M. We further note that the quantity above is labelled by the 2ν indices $k_{r,i}$ and $k'_{r,i-1}$ with the replica index constant. Hence, we package them into rank 2ν tensors by defining

$$\mathcal{A}^{k'_1,\ldots,k'_\nu}_{k_1,\ldots,k_\nu} := \left(\prod_{r=1}^{\nu}\frac{1}{2^{m_r}}\sqrt{\frac{1}{m_r!}\binom{m_r}{k_r}\binom{m_r}{k'_r}}\right)\left\langle\prod_{r=1}^{\nu}H_{m_r-k_r}\left(\varphi_A^{\lambda_r}\right)H_{k'_r}\left(\varphi_A^{\lambda_r}\right)\right\rangle_{A_D}\tag{85}$$

$$\mathcal{B}^{k'_1,\ldots,k'_\nu}_{k_1,\ldots,k_\nu} := \left(\prod_{r=1}^{\nu}\frac{1}{2^{m_r}}\sqrt{\frac{1}{m_r!}\binom{m_r}{k_r}\binom{m_r}{k'_r}}\right)\left\langle\prod_{r=1}^{\nu}H_{m_r-k_r}\left(\varphi_B^{\lambda_r}\right)H_{k'_r}\left(\varphi_B^{\lambda_r}\right)\right\rangle_{B_D}\tag{86}$$

$$\mathcal{M}^{k'_1,\ldots,k'_\nu}_{k_1,\ldots,k_\nu} := \left(\prod_{r=1}^{\nu}\frac{1}{2^{\frac{3m_r}{2}}m_r!}\sqrt{\binom{m_r}{k_r}\binom{m_r}{k'_r}}\right)\left\langle\prod_{r=1}^{\nu}H_{m_r}\left(\frac{1}{\sqrt{2}}\bar{\phi}^{\lambda_r}\right)H_{k'_r}\left(\bar{\phi}_A^{\lambda_r}\right)H_{m_r-k_r}\left(\bar{\phi}_B^{\lambda_r}\right)\right\rangle_M\tag{87}$$

where the k_r and k'_r indices run from 0 to m_r. Using the Einstein summation convention we can define multiplication and a trace operation for these tensors in the standard way

$$(\mathcal{A}\mathcal{B})^{k'_1,\ldots,k'_\nu}_{k_1,\ldots,k_\nu} := \mathcal{A}^{k'_1,\ldots,k'_\nu}_{j_1,\ldots,j_\nu}\mathcal{B}^{j_1,\ldots,j_\nu}_{k_1,\ldots,k_\nu},\tag{88}$$

$$\operatorname{Tr}\mathcal{A} := \mathcal{A}^{k_1,\ldots,k_\nu}_{k_1,\ldots,k_\nu}.\tag{89}$$

These definitions take care of the index structure of (90), which can then be simply written as

$$\begin{aligned}\operatorname{Tr}(\rho_A^n) &= \left(\frac{Z_AZ_B}{Z_M}\right)^{n-1}W(n)\operatorname{Tr}\left[(\mathcal{A}\mathcal{B})^{n-1}\mathcal{M}\right]\\ &= \operatorname{Tr}\left(\rho^n_{\mathrm{GS},A}\right)\operatorname{Tr}\left[(\mathcal{A}\mathcal{B})^{n-1}\mathcal{M}\right].\end{aligned}\tag{90}$$

In order to find an analytic continuation in n for this expression, we first note that the tensors above can all be written as square matrices A^i_j with $i,j=1,\ldots,\prod_{r=1}^{\nu}(m_r+1)$ such that matrix multiplication and the standard trace correspond to the operations on the tensors defined in (88)[8]. As a matrix, the tensor $\mathcal{A}\mathcal{B}$ is invertible which provides a sufficient condition

[8]This is satisfied if we, for example, define A^i_j by the map

$$\mathcal{A}^{k'_1,\ldots,k'_\nu}_{k_1,\ldots,k_\nu}\mapsto A^{k'_1+\sum_{r=2}^{\nu}(m_{r-1}+1+k'_r)}_{k_1+\sum_{r=2}^{\nu}(m_{r-1}+1+k_r)}\tag{91}$$

for the existence of its matrix logarithm. Later, we will see that at least in the special case where all the excitations are on the same mode, the matrix $\mathcal{AB}$ is in fact diagonal and with real eigenvalues, making the matrix logarithm unique and well-defined. For now, we are satisfied knowing it exists as it provides us with the desired analytic continuation. We can next differentiate and take the limit $n \to 1$ to find

$$S_{m_{\lambda_1},\ldots,m_{\lambda_\nu}}[A] = S_{GS}[A]\,\mathrm{Tr}(\mathcal{M}) + \mathrm{Tr}\big(\log(\mathcal{AB})\mathcal{M}\big). \tag{92}$$

It is not hard to check that this agrees with the entanglement entropy of the singly excited state (55). The trace of $\mathcal{M}$ in the first term, is easy to evaluate using the identity of Hermite polynomials (81) and gives

$$\mathrm{Tr}(\mathcal{M}) \equiv \mathcal{M}^{k_1,\ldots,k_\nu}_{k_1,\ldots,k_\nu} = \left(\prod_{r=1}^{\nu} \frac{1}{2^{m_r} m_r!}\right) \left\langle \prod_{r=1}^{\nu} H_{m_r}\left(\frac{1}{\sqrt{2}}\bar{\phi}^{\lambda_r}\right) H_{m_r}\left(\frac{1}{\sqrt{2}}\bar{\phi}^{\lambda_r}\right)\right\rangle_M . \tag{93}$$

As was the case for the singly excited state, the coefficient of the ground state entanglement entropy encodes information about correlation functions on the complete manifold. The second term, also as before, includes information about the correlation functions in the submanifolds as well as correlation functions that communicate between them. Using our expression for $\mathrm{Tr}\rho_A^n$ (90) it is also straight forward to write down an explicit form for the Rényi entropies

$$S^{(n)}_{m_{\lambda_1},\ldots,m_{\lambda_\nu}}[A] = S^{(n)}_{GS}[A] + \frac{1}{1-n}\log\left(\mathrm{Tr}\Big[(\mathcal{AB})^{n-1}\mathcal{M}\Big]\right), \tag{94}$$

where we observe, as for the singly excited state, that the ground state Rényi entropy factors from the excited state. While it is quite nice that an analytic expression can be written down for the entropy of an arbitrarily excited state, its form is quite involved. In the next section we will consider an interesting subcase, and see how the result behaves in some specific geometries.

4.1 An interesting subcase: only one mode is excited

The density matrix corresponding to the state with m excitations in the λ-mode is follows directly from (16) with $\nu = 1$

$$\rho = \big|(m_\lambda)\big\rangle\big\langle(m_\lambda)\big| \tag{95}$$

$$= \frac{1}{Z_M}\frac{1}{2^{m_\lambda} m_\lambda!}\int \mathcal{D}\phi\mathcal{D}\phi'\; H_{m_\lambda}\left(\frac{\phi^\lambda}{\sqrt{2}}\right) H_{m_\lambda}\left(\frac{\phi'^\lambda}{\sqrt{2}}\right) e^{-\frac{1}{2}S[\phi]-\frac{1}{2}S[\phi']}|\phi_i\rangle\langle\phi_i'| \tag{96}$$

The replica calculation goes through as described in the previous section, leading to tensors (85) that are square $(m+1)$-dimensional matrices with elements

$$\mathcal{A}^{k'}_{k} = \frac{1}{2^m}\sqrt{\frac{1}{m!}\binom{m}{k}\binom{m}{k'}}\left\langle H_{m-k}\left(\varphi^\lambda_A\right) H_{k'}\left(\varphi^\lambda_A\right)\right\rangle_A, \tag{97}$$

$$\mathcal{B}^{k'}_{k} = \frac{1}{2^m}\sqrt{\frac{1}{m!}\binom{m}{k}\binom{m}{k'}}\left\langle H_{m-k}\left(\varphi^\lambda_B\right) H_{k'}\left(\varphi^\lambda_B\right)\right\rangle_B, \tag{98}$$

$$\mathcal{M}^{k'}_{k} = \frac{1}{2^{\frac{3m}{2}}m!}\sqrt{\binom{m}{k}\binom{m}{k'}}\left\langle H_{m}\left(\frac{1}{\sqrt{2}}\bar{\phi}^\lambda\right) H_{k}\left(\bar{\phi}^\lambda_A\right) H_{m-k'}\left(\bar{\phi}^\lambda_B\right)\right\rangle_M. \tag{99}$$

The correlation functions in the tensors are straight-forward to calculate. In appendix E we use the definition of Hermite polynomials and the linearity of the correlation functions to express the matrix elements above as sums of simple correlation functions of transformed fields. These can then be evaluated by Wick's theorem and simplified by considering that the Green's functions appearing in the expansion are all integrated against the same eigenfunctions of the Laplacian, turning the space variables into dummy integration variables. Thus, all Green's functions in Wick's expansion that are integrated over the same domain, are the same. For example, we have

$$\begin{aligned}\left\langle (\varphi^\lambda_X)^\beta\right\rangle_X &= \delta_{\beta,\text{even}}(\#\text{ of full Wick contractions})(G^\lambda_X)^{\frac{\beta}{2}}\\ &= \delta_{\beta,\text{even}}(\beta-1)!!(G^\lambda_X)^{\frac{\beta}{2}},\end{aligned} \tag{100}$$

which together with (18) is used to express the tensors $\mathcal{A}$ and $\mathcal{B}$ as polynomials in G^λ_A and G^λ_B. Explicitly, we have

$$\mathcal{A}^{k'}_{k} = F^m_{k,k'}\left(G^\lambda_A\right), \qquad \mathcal{B}^{k'}_{k} = F^m_{k,k'}\left(G^\lambda_B\right), \tag{101}$$

where F is a polynomial given in equation (178) of appendix E. We note that $F^m_{k,k'} \propto \delta_{m-k+k',\text{even}}$. The evaluation of the correlation functions in $\mathcal{M}$ is combinatorically more involved, as three different projections of the field appear in it. This means that there are three distinct transformed Green's functions appearing in Wick's expansion. We find it convenient to work with the following partial projections

$$G^\lambda_{X,Y} := \lambda\int_X \mathrm{d}^2x\int_Y \mathrm{d}^2x' L_\lambda(x)L_\lambda(x')G_M(x,x'), \tag{102}$$

where $X,Y = A,B$. Since $G^\lambda_{A,B} = G^\lambda_{B,A}$ these are three distinct objects. By definition, they are related to the transformed Green's functions we dealt with before, see (50), by

$$G^\lambda_{X,M} = G^\lambda_{A,B} + G^\lambda_{X,X}, \quad X = A,B \tag{103}$$

$$G^\lambda_M = G^\lambda_{A,A} + 2G^\lambda_{A,B} + G^\lambda_{B,B}. \tag{104}$$

As for $\mathcal{A}$ and $\mathcal{B}$, the correlation functions in $\mathcal{M}$ can be expressed as polynomials in the three transformed Green's functions by linearity of the correlation functions, identities of Hermite polynomials, and some combinatorics. The result is

$$\mathcal{M}^{k'}_{k} = T^m_{k,k'}\left(G^\lambda_{A,B}, G^\lambda_{A,A}, G^\lambda_{B,B}\right), \tag{105}$$

where T is a polynomial in three variables defined in equation (184) of appendix E. Note that for a fixed surgery and eigenmode $G^{\lambda}_{A,B}$, $G^{\lambda}_{A,A}$, and $G^{\lambda}_{B,B}$ are just real numbers. Furthermore, we note that $T^{m}_{k,k'} \propto \delta_{k+k',\text{even}}$.

In the following sections we will apply this to the same geometries we studied when considering singly excited states in section 3. We will concentrate on the modes that are simultaneously eigenmodes on the manifold and submanifolds, and observe the effect that adding excitations to them has on the entanglement entropy.

4.2 Spherical geometry

Let us start by considering again the geometry of section 3.2, that is the sphere M cut at the equator into the hemispheres A and B. The first thing we need to do, is identify the modes for which the assumption (82), that is $(\bar{\phi}^{\text{cl}}_{A_i})^{\lambda} = (\bar{\phi}^{\text{cl}}_{B,i})^{\lambda} = 0$ for $i = 1, \dots, n-1$, is satisfied. As the classical field is constant, the condition is satisfied iff

$$\int_A \mathrm{d}^2x \; Y^m_\ell(x) = \int_B \mathrm{d}^2x \; Y^m_\ell(x) = 0, \tag{106}$$

where Y^m_ℓ is a spherical harmonic. The spherical harmonics are proportional to $e^{im\varphi}$, and φ is integrated from 0 to 2π, so the condition is automatically satisfied for all spherical harmonics with $m \neq 0$. It isn't hard to see that, by the properties of Legendre polynomials, the remaining integrals vanish iff ℓ is even. Thus our results from section 4 are valid for all eigenmodes of the Laplacian on the sphere *except* those with $m = 0$ *and* ℓ odd.

During our analysis of the singly excited state, we observed that the transformed propagators, and thus the entanglement entropy, where highly dependent on whether the eigenmode on the complete manifold was also a eigenmode on the submanifold. In particular, all modes that were simultaneous eigenmodes on the manifold and submanifold had the same entanglement entropy. On the halved-sphere geometry these modes are characterized by having $\ell + m$ odd, and, as before, all of them have the same entanglement entropy. The calculations of the relevant transformed propagators are found in appendix B.1, they are given by

$$\ell + m = \text{odd and } m \neq 0 \qquad \Longrightarrow \qquad \begin{cases} G^{\lambda}_{A} = G^{\lambda}_{B} = \frac{1}{2} \\ G^{\lambda}_{A,A} = G^{\lambda}_{B,B} = 1/4 + \sigma_\lambda \\ G^{\lambda}_{A,B} = 1/4 - \sigma_\lambda \end{cases} \tag{107}$$

where we exclude the modes with $m = 0$ to fulfill the assumption on the classical fields, and σ_λ is defined in (133). We will see that the entanglement entropy is independent of σ_λ, so its exact value is irrelevant for our purposes. As we discussed for the singly excited state, the above expressions are also approximately valid for high angular momentum modes, that is modes in the limit $\ell \gg 1$. We can thus use the polynomial expressions (101) and (105) of the tensors appearing in the entanglement entropy for the state with m_λ excitations in one of the allowed modes by

$$\mathcal{A}^{k'}_{k} = \mathcal{B}^{k'}_{k} = F^{m}_{k,k'}\left(\frac{1}{2}\right), \qquad \mathcal{M}^{k'}_{k} = T^{m}_{k,k'}\left(\frac{1}{4} - \sigma_\lambda, \frac{1}{4} + \sigma_\lambda, \frac{1}{4} + \sigma_\lambda\right), \tag{108}$$

with $k, k' = 0, \ldots, m_\lambda$. One can check, that for these values the product matrix $\mathcal{AB}$ is diagonal and has the following simple form in terms of binomial coefficients

$$\mathcal{AB} = \frac{1}{2^m}\text{diag}\left[\binom{m}{0}, \ldots, \binom{m}{k}, \ldots, \binom{m}{m}\right]. \tag{109}$$

The matrix M has lower triangular form and shares the same diagonal elements as $\mathcal{AB}$, such that $\text{Tr}(\mathcal{M}) = 1$. In particular, this shows that σ_λ does not affect the entanglement entropy. Using the ground state entanglement entropy for this configuration, see (57), as well as our general result for the excited state entanglement entropy (92), we can write the entanglement entropy for m_λ quanta of energy in an eigenmode with $\ell + m$ odd and $m \neq 0$ in the halved-sphere geometry as

$$\begin{aligned} S_{m_\lambda}[H^2] &= S_{GS}[H^2]\,\text{Tr}(\mathcal{M}) + \text{Tr}\big(\log(\mathcal{AB})\mathcal{M}\big) \\ &= \log\Big(\sqrt{8\pi g}R\Big) - \frac{1}{2} + \sum_{k=0}^{m}\frac{1}{2^m}\binom{m}{k}\log\left(\frac{1}{2^m}\binom{m}{k}\right). \end{aligned} \tag{110}$$

The equation above is also valid as an approximation for all modes with $\ell + m$ even in the limit of high angular momentum $\ell \gg 1$. In figure 4 the value of the entanglement entropy is shown for different excitation levels. As can be seen in the right image of the figure, a

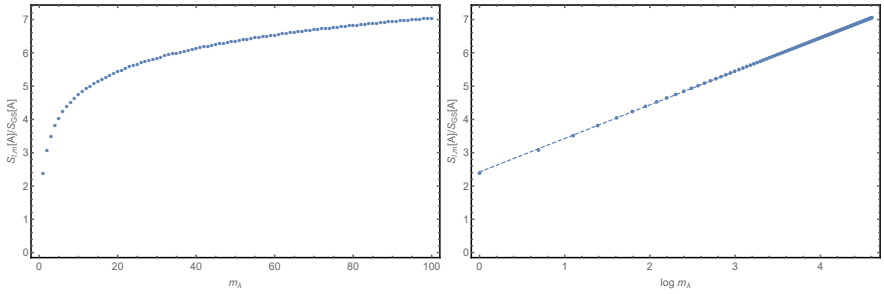

Figure 4: In the first image S_{m_λ} is plotted as a function of the number of excitations m_λ for any mode satisfying $\ell + m =$odd and $m \neq 0$. We evaluate it at the RK-point $g = \frac{1}{8\pi}$ and for $R = 1$. The second image is a log-linear plot of the same data, the dashed line represents the linear fit $y = 1.008x + 2.421$ with an R^2 value above 0.999.

logarithmic behavior in m dominates. We can thus provide the following approximation for the entanglement entropy

$$S_{m_\lambda}[H^2] \approx S_{GS}[H^2] - a_1 \log m_\lambda - a_2 \tag{111}$$

with $a_1 \approx 0.504$ and $a_2 \approx 0.711$. In particular, we learn that for highly excited states, that is for $m_\lambda \gg 1$, the entanglement entropy for this type of modes develops a logarithmic divergence in m_λ.

4.3 Rectangular geometry

Let us turn again to the rectangular geometry of section 3.3, with M a rectangle of side lengths L_x and L_y cut at ℓ_x into the two smaller rectangles A and B. As was the case for the single excitation, the vanishing of the classical part of the field ensures that our assumption (82) is trivially satisfied for all modes.

The transformed propagators needed to write down the explicit expression for the entanglement entropy for a general surgery are calculated in appendix B.2. As far as we know, there are no simple closed forms to be written down in this case, as both the transform Green's function and the entanglement entropy have an intricate functional dependence on the surgery parameter ℓ_x. We thus refrain from repeating what general formulas we have stated up to now, and concentrate on a specific surgery.

Let us choose the halved rectangle geometry, that is $\ell_x = L_x/2$. Here, for k_x even, the eigenmodes on the complete rectangle are also eigenmodes on A and B, and from the expressions for the propagators given in B.2, we get

$$k_x \text{ even} \qquad \Longrightarrow \qquad \begin{cases} G^\lambda_A = G^\lambda_B = \frac{1}{2} \\ G^\lambda_{A,A} = G^\lambda_{B,B} = 1/4 + \sigma_\lambda \\ G^\lambda_{A,B} = 1/4 - \sigma_\lambda. \end{cases} \tag{112}$$

From our discussion about the single excitation, we know the above equations to be approximately true for all modes with high wave number perpendicular to the entanglement cut, that is $k_x \gg 1$. From the point of view of the tensors, the situation here is exactly the same as on the halved sphere[9], and the entanglement entropy only differs in the contribution from the ground state entanglement entropy which is now given by (70). Thus, for even k_x the excited state entanglement entropy with m_λ quanta of energy in the mode labeled by k_x and k_y is given by

$$S_{m_\lambda}[H^2] = \frac{1}{2}\log\left(\frac{\eta\left(\frac{i}{2}\frac{L_x}{L_y}\right)^2}{\sqrt{2L_y}\eta\left(i\frac{L_x}{L_y}\right)}\right) + \sum_{k=0}^{m}\frac{1}{2^m}\binom{m}{k}\log\left(\frac{1}{2^m}\binom{m}{k}\right). \tag{113}$$

We note that we don't expect the contribution from the excited state to the entanglement entropy to be independent on the geometry in general. Here, this is a feature of the type of modes that we chose and also of the surgery. We do, however, expect the excited states corresponding to eigenmodes that are simultaneously eigenmodes on the full and halved submanifold to have an entanglement entropy of the above form for any similar "halved" geometry (for example halved cylinders or tori). In figure 5 we show the dependence of S_{m_λ} on m_λ. As expected, we see the same type of logarithmic behavior as for the sphere. In particular, equation (111) is also valid here for all modes with k_x even or $k_x \gg 1$, and replacing the ground state entanglement entropy corresponding to the sphere by that corresponding to the rectangle.

[9]Note that the value of σ_λ on the rectangle a priori differs from that on the sphere. This is however not relevant, as σ_λ doesn't contribute to the entanglement entropy.

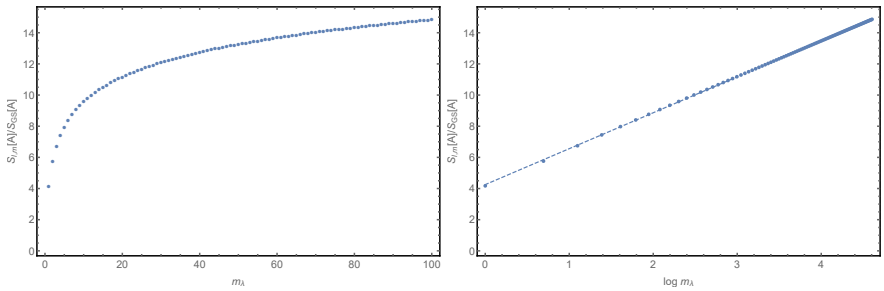

Figure 5: In the first image S_{m_λ} is plotted as a function of the number of excitations m_λ for any mode satisfying k_x even in the halved rectangle geometry with $L_x = L_y$. The second image is a log-linear plot of the same data. The dashed line represents the linear fit $y = 2.306x + 4.252$ with an R^2 value above 0.999.

5 Discussion

We calculated the entanglement entropy of the states of the QLM obtained by exciting the eigenmodes of the Laplace-Beltrami on a compact spatial manifold. These are natural states for the model, as the ground state is given in terms of a conformal action determined by that same operator. Assuming that certain integrals of the classical fields vanish, see (37) and (82), which can be interpreted as its partial projections onto the excited eigenmodes, we show that the replica calculation becomes tractable for even the most general excited state. This allows us to provide the elusive analytic continuations needed to find the entanglement entropy, which we do separately for the singly excited state – where the assumption on the classical fields is a little less stringent – and for the general case.

We find that the ground state Rényi entropy factors from the excited state Rényi entropy in agreement with [47], and further confirm that these can be written down in terms of the EPA's from [47], although we write them slightly differently and refer to them as transformed propagators. We further find that, though the leading terms in the Rényi entropies of the singly excited states agree to those in [47], the other terms do not. We believe the differences to origin in the derivation of the generalized Wick's theorem by [47], although at the time of writing we have been unable to locate their root. In the general case, we find that the entanglement entropy is again written in terms of transformed propagators, though here they are packaged inside complicated tensors. We calculate the transformed propagators by spectral methods and provide explicit formulae in both the spherical and rectangular geometry. In the latter our results are in agreement with the expressions found in [47] which adds to the evidence given by [47] for the universality of the objects.

An interesting observation about these transformed propagators is that they distinguish between two classes of modes. The first class are modes that are, up to normalization, simultaneously eigenmodes on the full manifold and the submanifold. In the spherical geometry, for example, this condition is satisfied by the spherical harmonics with $\ell + m$ odd, which

are both eigenfunctions of the Laplacian on the sphere and on the hemisphere with Dirichlet boundary conditions. The transformed propagators are the same for all of these modes. In particular, this implies that the entanglement entropy is constant within this class of modes. The second class of modes are those, for which the above condition is not satisfied. There we find a non-trivial dependence of the transformed propagators on the chosen mode, and thus also a dependence of the entanglement entropy on the modes. Looking back at equation (92), we see that the excited state entanglement entropy is related to the ground state entanglement entropy by two universal constants. Notably, this implies that the excited state entanglement entropy still obeys an area law. Keeping in mind that the two universal constants are derived from correlation functions on the different subsystems, our findings are similar to those in [20–23, 46], where excited states are constructed that obey area laws with corrections with respect to the ground state entanglement determined by certain correlation functions of the underlying theories. For the halved sphere and rectangle we observe that when m quanta of energy are put into one mode, the entanglement entropy behaves logarithmically in m, that is $S_m \sim \log m$. For a highly excited state, we thus observe a logarithmic divergence in the excitation number, instead of the extensive behavior one would generically expect.

Our results and calculation can be applied to any bipartite compact geometry on which the spectrum of the Laplace-Beltrami operator on both the full manifold and the submanifolds is known. A generalization to higher dimensional geometries as in [37] and any even critical exponent z should also be relatively straight forward. The key element here being the replacement of the Laplace-Beltrami operator by the higher dimensional conformal generalization of one of its powers (for example a GJMS operator in the spherical case), whose eigenmodes would be excited. Up to some subtleties that are treated in [37], we expect our replica calculation to hold up also in these cases. While not as straight forward, a generalization to non-compact geometries would also be desirable. Even in that case, we would still expect our results to hold up for any excited state that can be written in the form (16). We would further like to find ways to relax our assumptions on the classical fields. As was already noted in [47] the combinatorics of the problem become prohibitively difficult in the most general case. However a slight relaxation of our assumptions – such as demanding the assumption (37) for all excited states instead of only the singly excited ones – should be possible at least in some situations. Finally, a deeper exploration of the highly excited states of the model is desireable. In particular, we would like to better understand whether the area law behavior that we observe in the highly excited state with all excitations in one mode is in fact connected to a quantum scar, and, if this is the case, if this is a property of only that type of states. This also indicates that an analysis of the eigenstate thermalization hypothesis in the QLM might provide interesting results.

6 Acknowledgements

First of all I would like to thank Valentina Giangreco M. Puletti for her help and patience during this project. I also thank Watse Sybesma, Lukas Schneiderbauer, and Lárus Thorlacius for their valuable comments on the manuscript, as well as Erik Tonni for his comments on

an early version of the project, and Daniel E. Parker for his comments and in particular for pointing out the possible connection to quantum scars. I would also like to thank Clément Berthiere for providing me with an excellent template for figure 1. Finally, I thank our research group at the University of Iceland for enduring more than one presentation on the topic with keen interest, and providing some helpful comments along the way. This research was supported in part by the Icelandic Research Fund under contract 163419-053, and by grants from the University of Iceland Research Fund.

A Rewriting $\operatorname{Tr}\rho_A^n$

In this appendix we perform the path integral manipulations needed to get from (43) to (46). We start with the following factor that appears in (43)

$$I := \int_{\mathcal{B}'} \left[\prod_{i=1}^{n} \mathcal{D}\varphi_{A,i}\mathcal{D}\varphi_{B,i}\right] \mathcal{D}\bar{\phi}_n^{\mathrm{cl}} \times \left(\prod_{i=1}^{n} (\varphi_{A,i}^{\lambda} + \varphi_{B,i}^{\lambda})(\varphi_{A,i+1}^{\lambda} + \varphi_{B,i}^{\lambda})\right) e^{-S[\bar{\phi}_n^{\mathrm{cl}}] - \sum_{i=1}^{n}(S[\varphi_{A,i}]+S[\varphi_{B,i}])}. \quad (114)$$

Let us take a closer look at the product of fields in the path integral. Keeping in mind the calculations of [37, 44], we want to separate the n-th field from the rest, and find out which terms survive the integration. Remembering that our assumption (37) implies $\phi_n^{\lambda} = \varphi_{A,n}^{\lambda} + \varphi_{B,n}^{\lambda}$ the product can be written as

$$\left(\prod_{i=1}^{n-1} (\varphi_{A,i}^{\lambda} + \varphi_{B,i}^{\lambda})(\varphi_{A,i+1}^{\lambda} + \varphi_{B,i}^{\lambda})\right) (\varphi_{A,1}^{\lambda} + \varphi_{B,n}^{\lambda})\phi_n^{\lambda} = \left(\prod_{i=1}^{n-1} (\varphi_{A,i}^{\lambda})^2 \varphi_{A,n}^{\lambda}\phi_n^{\lambda}\right) + \left(\prod_{i=1}^{n-1} (\varphi_{B,i}^{\lambda})^2 \varphi_{B,n}^{\lambda}\phi_n^{\lambda}\right) + (\text{at least one field appears alone}). \quad (115)$$

When we perform the path integrals only the leading terms survive, since the other terms will contain something proportional to at least one one-point function of the fluctuations or the full field, which vanish. We can also glue the integration of the n-th field back together by

$$\int_{\mathcal{B}'} \mathcal{D}\bar{\phi}_n^{\mathrm{cl}} \mathcal{D}\varphi_{A,n}\mathcal{D}\varphi_{B,n}\, (\cdots) = \int \mathcal{D}\bar{\phi}_n\, (\cdots), \quad (116)$$

to form an integral over a free field on the complete manifold (see [38, 43, 44]). This then leads us to

$$I = \left(\prod_{i=1}^{n-1} \int_{A_D} \mathcal{D}\varphi_{A,i}\, (\varphi_{A,i}^{\lambda})^2 e^{-S[\varphi_{A,i}]}\right) \int \mathcal{D}\bar{\phi}_n\, \bar{\phi}_n^{\lambda}\bar{\phi}_{A,n}^{\lambda} e^{-S[\bar{\phi}_n]} + \left(\prod_{i=1}^{n-1} \int_{B_D} \mathcal{D}\varphi_{B,i}\, (\varphi_{B,i}^{\lambda})^2 e^{-S[\varphi_{B,i}]}\right) \int \mathcal{D}\bar{\phi}_n\, \bar{\phi}_n^{\lambda}\bar{\phi}_{B,n}^{\lambda} e^{-S[\bar{\phi}_n]}, \quad (117)$$

where A_D and B_D remind us that those path integrals are taken over A and B respectively and with Dirichlet boundary conditions, and where we also used the fact that

$$\begin{aligned}
&\int \mathcal{D}\bar{\phi}_n \ \bar{\phi}_n^\lambda \bar{\phi}_{A,n}^\lambda e^{-S[\bar{\phi}_n]} \\
&= \int \mathcal{D}\varphi_{A,n}\mathcal{D}\varphi_{B,n}\mathcal{D}\bar{\phi}_n^{\mathrm{cl}} \left[(\phi_{A,n}^{\mathrm{cl}})^\lambda + \varphi_{A,n}^\lambda\right] \left[\varphi_{A,n}^\lambda + \varphi_{B,n}^\lambda\right] e^{-S[\bar{\phi}_n^{\mathrm{cl}}]-S[\varphi_{A,n}]-S[\varphi_{B,n}]} \\
&= \int \mathcal{D}\bar{\phi}_n \ \bar{\phi}_n^\lambda \varphi_{A,n}^\lambda e^{-S[\bar{\phi}_n]} + \\
&\qquad \underbrace{\int \mathcal{D}\varphi_{A,n}\mathcal{D}\varphi_{B,n}\mathcal{D}\bar{\phi}_n^{\mathrm{cl}} (\phi_{A,n}^{\mathrm{cl}})^\lambda \left[\varphi_{A,n}^\lambda + \varphi_{B,n}^\lambda\right] e^{-S[\bar{\phi}_n^{\mathrm{cl}}]-S[\varphi_{A,n}]-S[\varphi_{B,n}]}}_{=0} \\
&= \int \mathcal{D}\bar{\phi}_n \ \bar{\phi}_n^\lambda \varphi_{A,n}^\lambda e^{-S[\bar{\phi}_n]}. \qquad (118)
\end{aligned}$$

In the second to last line the term vanishes because it is proportional to a one-point function of the fluctuations on either A or B. If we furthermore notice that all the fields in the path integrals are dummy fields that are integrated over, we can get rid of the replica indices and write

$$\begin{aligned}
I = \left(\int_{A_D} \mathcal{D}\varphi_A \ (\varphi_A^\lambda)^2 e^{-S[\varphi_A]}\right)^{n-1} \int \mathcal{D}\bar{\phi} \ \bar{\phi}^\lambda \bar{\phi}_A^\lambda e^{-S[\bar{\phi}]} + \\
+ \left(\int_{B_D} \mathcal{D}\varphi_B \ (\varphi_B^\lambda)^2 e^{-S[\varphi_B]}\right)^{n-1} \int \mathcal{D}\bar{\phi} \ \bar{\phi}^\lambda \bar{\phi}_B^\lambda e^{-S[\bar{\phi}]}, \qquad (119)
\end{aligned}$$

which is precisely the factor that appears in (46).

B Transformed Green's functions

We calculate the transformed Green's functions $G_{X,M}^\lambda$ and G_X^λ by means of their eigenvalue expansions as well as the orthogonality and completeness of the eigenmodes of the Laplacian. We denote the eigenmodes of the Laplacian on M by $L_\lambda(x)$, and on $X = A, B$ as $L_\alpha^X(x)$, where we always take Dirichlet boundary conditions. In order to avoid confusion, we index eigenmodes and eigenvalues on M by λ and μ, and eigenmodes and eigenvalues on A and B by α and β. The Green's function $G_M(x, x')$ has an eigenvalue expansion of the form

$$G_M(x, x') = \sum_\lambda \frac{L_\lambda(x) L_\lambda(x')}{\lambda}, \qquad (120)$$

where the sum runs over the complete set of eigenmodes of the Laplacian on M, and similarly we have the eigenvalue expansion on $X = A, B$

$$G_X(x, x') = \sum_\alpha \frac{L_\alpha^X(x) L_\alpha^X(x')}{\alpha}, \qquad (121)$$

where the sum now runs over the complete set of eigenmodes of the Laplacian on either A or B. Let us take a look at the different transformed Green's functions in (50). The integral in

G_M^λ is easily evaluated by the orthonormality of the eigenfunctions leading to

$$G_M^\lambda = \lambda \sum_\mu \frac{1}{\mu} \left(\int_M \mathrm{d}^2x \; L_\lambda(x) L_\mu(x) \right)^2 = \lambda \sum_\mu \frac{\delta_{\lambda\mu}}{\mu} = 1. \tag{122}$$

We can proceed with $G_{X,M}^\lambda$ in a similar fashion and write

$$\begin{aligned} G_{X,M}^\lambda &= \lambda \int_M \mathrm{d}^2x \int_X \mathrm{d}^2x' L_\lambda(x) L_\lambda(x') G_M(x,x') \\ &= \lambda \int_M \mathrm{d}^2x \int_X \mathrm{d}^2x' L_\lambda(x) L_\lambda(x') \sum_\mu \frac{L_\mu(x) L_\mu(x')}{\mu} \\ &= \lambda \int_X \mathrm{d}^2x' L_\lambda(x') \sum_\mu \frac{L_\mu(x')}{\mu} \int_M \mathrm{d}^2x L_\lambda(x) L_\mu(x) \\ &= \lambda \int_X \mathrm{d}^2x' L_\lambda(x') \sum_\mu \frac{L_\mu(x')}{\mu} \delta_{\lambda\mu} \\ &= \int_X \mathrm{d}^2x' (L_\lambda(x'))^2. \end{aligned} \tag{123}$$

Using the expansion (121) we can rewrite G_X^λ as

$$\begin{aligned} G_X^\lambda &= \lambda \int_X \mathrm{d}^2x \, \mathrm{d}^2x' L_\lambda(x) L_\lambda(x') G_X(x,x') \\ &= \lambda \int_X \mathrm{d}^2x \, \mathrm{d}^2x' L_\lambda(x) L_\lambda(x') \sum_\beta \frac{L_\beta^X(x) L_\beta^X(x')}{\beta} \\ &= \lambda \sum_\beta \frac{1}{\beta} \left(\int_X \mathrm{d}^2x \; L_\lambda(x) L_\beta^X(x) \right)^2. \end{aligned} \tag{124}$$

Let us take a look at the specific situation, where the eigenmodes α on the submanifold are simultaneously eigenmodes on the full manifold (i.e. $\exists\lambda$ s.t. $\alpha = \lambda$). In other words, this is the case where some of the eigenmodes on M coincide, up to normalization, with the eigenmodes on A and B. Here, we have a notion of orthogonality between $L_\lambda(x)$ and $L_\alpha^X(x)$. In particular we can write $c_\alpha^X L_\alpha^X(x) = L_\alpha(x)$, where c_α^X accounts for the different normalization of the eigenmodes. For this type of mode we can, for example, evaluate the following integral exactly

$$\int_X \mathrm{d}^2x \; L_\alpha(x) L_\beta(x) = \delta_{\alpha\beta} \left(c_\alpha^X \right)^2, \tag{125}$$

allowing us to evaluate (123)

$$G_{X,M}^\alpha = (c_\alpha^X)^2. \tag{126}$$

We can also continue the calculation in (124) and write

$$G_X^\alpha = \alpha \sum_\beta \frac{(c_\beta^X)^2}{\beta} \left(\int_X \mathrm{d}^2x \; L_\alpha^X(x) L_\beta^X(x) \right)^2 = (c_\alpha^X)^2, \tag{127}$$

Finally, we can rewrite $G^{\lambda}_{A,B}$ using the same techniques

$$\begin{aligned} G^{\alpha}_{A,B} &= \alpha \int_A \mathrm{d}^2x \int_B \mathrm{d}^2x' L_\alpha(x) L_\alpha(x') G_M(x,x') \\ &= \alpha \int_A \mathrm{d}^2x \int_B \mathrm{d}^2x' L_\alpha(x) L_\alpha(x') \sum_\mu \frac{L_\mu(x) L_\mu(x')}{\mu} \\ &= \alpha \sum_\mu \frac{1}{\mu} \left(\int_A \mathrm{d}^2x \; L_\alpha(x) L_\mu(x) \right) \left(\int_B \mathrm{d}^2x \; L_\alpha(x) L_\mu(x) \right) \\ &= \left(c^A_\alpha \right)^2 \left(c^B_\alpha \right)^2 + \sigma^{A,B}_\alpha, \end{aligned} \tag{128}$$

where $\sigma^{A,B}_\alpha$ is defined as

$$\sigma^{A,B}_\alpha := \alpha \sum_{\mu \in S} \frac{1}{\mu} \left(\int_A \mathrm{d}^2x \; L_\alpha(x) L_\mu(x) \right) \left(\int_B \mathrm{d}^2x \; L_\alpha(x) L_\mu(x) \right). \tag{129}$$

Here, S is the set of eigenmodes on M that are *not* eigenmodes on A and B. Similarly for $X = A, B$

$$G^{\alpha}_{X,X} = \left(c^X_\alpha \right)^4 + \sigma^{X,X}_\alpha \tag{130}$$

with

$$\sigma^{X,X}_\alpha := \alpha \sum_{\mu \in S} \frac{1}{\mu} \left(\int_X \mathrm{d}^2x \; L_\alpha(x) L_\mu(x) \right)^2. \tag{131}$$

Note that

$$\begin{aligned} \int_A \mathrm{d}^2x \; L_\alpha(x) L_\mu(x) &= \int_M \mathrm{d}^2x \; L_\alpha(x) L_\mu(x) - \int_B \mathrm{d}^2x \; L_\alpha(x) L_\mu(x) \\ &= - \int_B \mathrm{d}^2x \; L_\alpha(x) L_\mu(x), \end{aligned} \tag{132}$$

where in the second line we used the fact that the integral over M is proportional to $\delta_{\alpha\mu}$, but $\mu \neq \alpha$ since we are only summing over modes μ that are not eigenmodes on A and B. In particular, we can define

$$\sigma_\alpha := \sigma^{A,A}_\alpha = \sigma^{B,B}_\alpha = -\sigma^{A,B}_\alpha. \tag{133}$$

Next we discuss the calculation of the transformed Green's functions for specific geometries.

B.1 Spheres and hemispheres

Let us consider the situation when a sphere $M = S^2$ is cut into the northern hemisphere $A = H^2_N$ and the southern hemisphere $B = H^2_S$ along the equator. The relevant eigenfunctions are then $L^{S^2}_{\ell,m}(x) = Y^m_l(x)$ on the sphere and $L^{H^2}_{\ell,m}(x) = \sqrt{2} Y^m_\ell(x)$ with $m + \ell$ odd on the hemispheres with Dirichlet boundary conditions. Thus the eigenmodes on the hemisphere are also eigenmodes of the sphere, and in our notation $\lambda = (\ell, m)$ and $\alpha = (\ell, m)$ with $\ell + m$ odd. We note that in this case $c^{H^2}_\alpha = \frac{1}{\sqrt{2}}$. Using equations (122), (126), (127), (128), (130), and

(133) we find

$$\ell + m = \text{odd} \qquad \Longrightarrow \qquad \begin{cases} G^{\alpha}_{M} = 1 \\ G^{\alpha}_{A,M} = G^{\alpha}_{B,M} = G^{\alpha}_{A} = G^{\alpha}_{B} = \frac{1}{2} \\ G^{\alpha}_{A,A} = G^{\alpha}_{B,B} = 1/4 + \sigma_{\alpha} \\ G^{\alpha}_{A,B} = 1/4 - \sigma_{\alpha} \end{cases} \tag{134}$$

Let us take a look at the other modes, that is those with $\ell + m$ even. We remind the reader that the spherical harmonics transform as $Y_l^m(\pi - \theta, \phi) = (-1)^{l+m} Y_l^m(\theta, \phi)$ under reflection over the equatorial plane. In particular this implies that

$$\int_A \mathrm{d}^2x \ (L_\lambda(x))^2 = \int_B \mathrm{d}^2x \ (L_\lambda(x))^2 = \frac{1}{2}\int_M \mathrm{d}^2x \ (L_\lambda(x))^2 = \frac{1}{2} \tag{135}$$

and thus from equation (123) we see that $G^{\lambda}_{A,M} = G^{\lambda}_{B,M} = \frac{1}{2}$ is actually true for all modes. Furthermore it isn't hard to see from the reflection properties and normalization that and that $G^{\lambda}_{X,X} = G^{\lambda}_{X}/2$ and $G^{\lambda}_{A,B} = -G^{\lambda}_{X}/2$. Thus finding G^{λ}_{X} provides us with the remaining propagators. The transformed propagators G^{λ}_{X} are given by

$$\begin{aligned} G^{\lambda}_{X} &= \lambda \sum_{\alpha} \frac{1}{\alpha} \left(\int_X \mathrm{d}^2x \ L_\lambda(x) L^X_\alpha(x) \right)^2 \\ &= 2 \ \ell_\lambda(\ell_\lambda + 1) \sum_{\substack{\ell_\mu, m_\mu \\ \ell_\mu + m_\mu = \text{odd}}} \frac{1}{\ell_\mu(\ell_\mu + 1)} \left(\int_X \mathrm{d}^2x \ Y^{m_\lambda}_{\ell_\lambda}(x) \left(Y^{m_\mu}_{\ell_\mu}(x) \right)^* \right)^2, \end{aligned} \tag{136}$$

where $\ell_\lambda + m_\lambda =$even. Using the definition of the spherical harmonics

$$Y^m_\ell(\theta, \phi) = N(\ell, m) e^{im\phi} P^m_\ell(\cos(\theta)), \tag{137}$$

where N is the normalization

$$N(\ell, m) = \sqrt{\frac{2\ell + 1}{4\pi} \frac{(\ell - m)!}{(\ell + m)!}}, \tag{138}$$

and $P^m_\ell(x)$ are associated Legendre polynomials, we can evaluate part of the integral and write

$$\begin{aligned} \int_A \mathrm{d}^2x \ Y^{m_\lambda}_{\ell_\lambda}(x) \left(Y^{m_\mu}_{\ell_\mu}(x) \right)^* = -\int_B \mathrm{d}^2x \ Y^{m_\lambda}_{\ell_\lambda}(x) \left(Y^{m_\mu}_{\ell_\mu}(x) \right)^* = \\ 2\pi \delta_{m_\lambda, m_\mu} N(\ell_\lambda, m_\lambda) N(\ell_\mu, m_\lambda) \int_0^1 \mathrm{d}x \ P^{m_\lambda}_{\ell_\lambda}(x) P^{m_\lambda}_{\ell_\mu}(x). \end{aligned} \tag{139}$$

Unfortunately, to our best knowledge, there is no simple closed form for the integral over the associated Legendre polynomials. We can however write the transformed propagator as

$$G^{\lambda}_{A} = G^{\lambda}_{B} = \frac{1}{2}\Sigma_\lambda, \tag{140}$$

with

$$\Sigma_\lambda = \begin{cases} \Sigma^{\mathrm{e}}_\lambda, & \ell_\lambda + m_\lambda = \text{even} \\ 1, & \ell_\lambda + m_\lambda = \text{odd}, \end{cases} \tag{141}$$

and where for $\ell_\lambda + m_\lambda = \text{even}$ we defined

$$\Sigma^e_\lambda \equiv \Sigma^e_{\ell_\lambda, m\lambda} := (2\ell_\lambda + 1)\ell_\lambda(\ell_\lambda + 1)\times \\ \frac{(\ell_\lambda - m_\lambda)!}{(\ell_\lambda + m_\lambda)!} \sum_{\substack{\ell_\mu \geq m_\lambda \\ \ell_\mu + m_\lambda = \text{odd}}}^{\infty} \frac{(2\ell_\mu + 1)}{\ell_\mu(\ell_\mu + 1)} \frac{(\ell_\mu - m_\lambda)!}{(\ell_\mu + m_\lambda)!} \left(\int_0^1 \mathrm{d}x \; P^{m_\lambda}_{\ell_\lambda}(x) P^{m_\lambda}_{\ell_\mu}(x) \right)^2. \tag{142}$$

Note that we used the fact that $P^{m_\lambda}_{\ell_\mu} = 0$ for $\ell_\mu < m_\lambda$ to alter the starting point of the sum. We also note that the conditions that $m_\lambda + \ell_\mu$ be odd is equivalent to demanding that ℓ_μ be odd whenever ℓ_λ is even and vice-versa. We further note that $\Sigma^e_{\ell,-m} = \Sigma^e_{\ell,m}$, due to the transformation behavior of associated Legendre polynomials when $m \mapsto -m$:

$$P^{-m}_\ell(x) = (-1)^m \frac{(\ell - m)!}{(\ell + m)!} P^m_\ell(x). \tag{143}$$

The value of Σ_λ can be determined numerically from this expression by truncating the sum at some sufficiently large value and performing a numerical integration at each step. We note that the sum converges for all desired values.

B.2 Rectangles

We now consider the case described in 3.3, that is $M = [0, L_x] \times [0, L_y]$, $A = [0, \ell_x] \times [0, L_y]$, and $B = [\ell_x, L_x] \times [0, L_y]$. As before, $G^\lambda_M = 1$. We start with $G^\lambda_{X,M}$

$$G^\lambda_{X,M} = \int_X \mathrm{d}^2x' (L_\lambda(x'))^2. \tag{144}$$

Using (67) for the eigenmodes, the integral can be easily evaluated and gives

$$G^\lambda_{A,M} = \frac{\ell_x}{L_x} - \frac{1}{2\pi k_x} \sin\left(2\pi k_x \frac{\ell_x}{L_x}\right), \tag{145}$$

$$G^\lambda_{B,M} = \left(1 - \frac{\ell_x}{L_x}\right) + \frac{1}{2\pi k_x} \sin\left(2\pi k_x \frac{\ell_x}{L_x}\right). \tag{146}$$

Now we can tackle G^λ_X. We take, as before, L_λ to be eigenfunctions on M and L^X_α eigenfunctions on $X = A, B$, and start by considering G^λ_A. In order to calculate

$$G^\lambda_A = \lambda \sum_\alpha \frac{1}{\alpha} \left(\int_A \mathrm{d}^2x \; L_\lambda(x) L^A_\alpha(x) \right)^2, \tag{147}$$

we first need to evaluate the integral. Due to the surgery we perform on M the eigenmodes on M and A have the same y dependence. In particular, this means that the y integral only

contributes a δ-function and we can write

$$\begin{aligned}\int_A \mathrm{d}^2x\ L_\lambda(x)L^A_\alpha(x) &\equiv \int_A \mathrm{d}^2x\ L_{k_x,k_y}(x)L^A_{n_x,n_y}(x)\\ &= \frac{2}{\sqrt{\ell_x L_x}}\delta_{k_y,n_y}\int_0^{\ell_x}\mathrm{d}x\sin\left(\pi k_x\frac{x}{L_x}\right)\sin\left(\pi n_x\frac{x}{\ell_x}\right)\\ &= \frac{2}{\sqrt{\ell_x L_x}}(-1)^{n_x}\sin\left(\pi k_x\frac{\ell_x}{L_x}\right)\frac{\frac{\pi}{\ell_x}n_x}{\left(\frac{\pi}{\ell_x}n_x\right)^2-\left(\frac{\pi}{L_x}k_x\right)^2}.\end{aligned} \tag{148}$$

With this integral we can conclude the evaluation of G^λ_A

$$\begin{aligned}G^\lambda_A = \frac{4}{\ell_x L_x}&\left(\left(\frac{\pi}{L_x}k_x\right)^2+\left(\frac{\pi}{L_y}k_y\right)^2\right)\sin\left(\pi k_x\frac{\ell_x}{L_x}\right)^2\times\\ &\sum_{n_x=1}^{\infty}\frac{1}{\left(\frac{\pi}{\ell_x}n_x\right)^2+\left(\frac{\pi}{L_y}k_y\right)^2}\frac{\left(\frac{\pi}{\ell_x}n_x\right)^2}{\left(\left(\frac{\pi}{\ell_x}n_x\right)^2-\left(\frac{\pi}{L_x}k_x\right)^2\right)^2}\\ = \frac{\ell_x}{L_x}&-\frac{1}{2\pi k_x}\sin\left(2\pi k_x\frac{\ell_x}{L_x}\right)-d^A_\lambda,\end{aligned} \tag{149}$$

where we defined

$$d^A_\lambda := \frac{1}{L_x}\frac{2\left(\frac{\pi}{L_y}k_y\right)\coth\left(\pi k_y\frac{\ell_x}{L_y}\right)\sin\left(\pi k_x\frac{\ell_x}{L_x}\right)^2-\left(\frac{\pi}{L_x}k_x\right)\sin\left(2\pi k_x\frac{\ell_x}{L_x}\right)}{\left(\frac{\pi}{L_x}k_x\right)^2+\left(\frac{\pi}{L_y}k_y\right)^2}. \tag{150}$$

We can proceed similarly with G^λ_B and get

$$G^\lambda_B = \left(1-\frac{\ell_x}{L_x}\right)+\frac{1}{2\pi k_x}\sin\left(2\pi k_x\frac{\ell_x}{L_x}\right)-d^B_\lambda, \tag{151}$$

with

$$d^B_\lambda := \frac{1}{L_x}\frac{2\left(\frac{\pi}{L_y}k_y\right)\coth\left(\pi k_y\frac{L_x-\ell_x}{L_y}\right)\sin\left(\pi k_x\frac{\ell_x}{L_x}\right)^2+\left(\frac{\pi}{L_x}k_x\right)\sin\left(2\pi k_x\frac{\ell_x}{L_x}\right)}{\left(\frac{\pi}{L_x}k_x\right)^2+\left(\frac{\pi}{L_y}k_y\right)^2}. \tag{152}$$

C EPA's and transformed Green's functions on the rectangle

In [47] quantities dubbed Entanglement Propagator Amplitudes (EPA's) are introduced. These are closely related to our transformed propagators. In fact, the first two EPA's are, up to a different normalization, just G^λ_A and G^λ_B

$$\alpha = G^\lambda_A \tag{153}$$

$$\beta = G^\lambda_B. \tag{154}$$

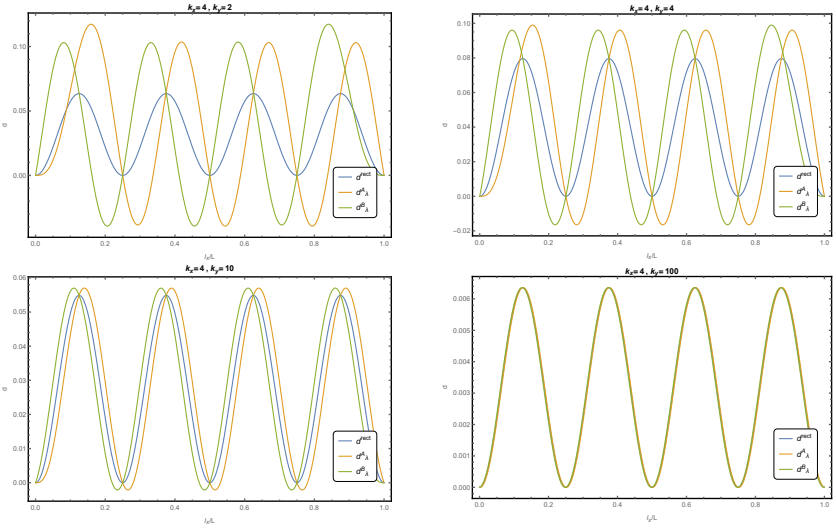

Figure 6: The quantity d^{rect} calculated by [47] is compared to our exact results d_λ^A and d_λ^B for constant $k_x = 4$ and $k_y = 2, 4, 10, 100$. The approximation used to calculate d^{rect} is only valid at large k_y, there it agrees with our result.

The remaining EPA can be expressed in terms of our quantities as

$$\gamma = G_M^\lambda - G_A^\lambda - G_B^\lambda = 1 - G_A^\lambda - G_B^\lambda. \tag{155}$$

As an example these quantities are calculated explicitly on a rectangle with side lengths L_x and L_y and an entanglement cut at ℓ_x, where the the eigenmodes of the Laplacian are labeled by the positive integers k_x and k_y and correspond to the Fourier modes on the rectangle. In [47] the following expression is given for the transformed propagators

$$G_A^\lambda = \frac{\ell_x}{L_x} - \frac{1}{2\pi k_x}\sin\left(2\pi k_x \frac{\ell_x}{L_x}\right) - d^{\text{rect}}, \tag{156}$$

$$G_B^\lambda = \left(1 - \frac{\ell_x}{L_x}\right) - \frac{1}{2\pi k_x}\sin\left(2\pi k_x \frac{\ell_x}{L_x}\right) - d^{\text{rect}}, \tag{157}$$

where the following approximation[10], valid for large k_y and $L_x = L_y$, is given for d^{rect}

$$d^{\text{rect}} \approx \frac{4}{\pi^3}\frac{2\pi k_y \int_0^{2\pi k_y}\frac{\sin t}{t}\,\mathrm{d}t - \pi k_y \int_0^{\pi k_y}\frac{\sin t}{t}\,\mathrm{d}t - (-1)^{k_y} + 1}{k_x^2 + k_y^2}\sin\left(\pi k_x \frac{\ell_x}{L_x}\right)^2. \tag{158}$$

In figure 6 we compare this result to our analytic results for d_λ^A and d_λ^B at $L_x = L_y$ from section B.2, see equations (150) and (152) in particular. We find the results in good agreement where the approximation for d^{rect} is valid.

[10] Note that in [47] there is a an extra factor of 2 in equation (72) with respect to their calculation of γ in appendix C.2 of the paper.

D Determinant of the Laplacian on a rectangle

In this section we calculate the zeta regularized determinant of the Laplacian on a rectangle. The determinant of the Laplacian can be written as

$$\det \Delta = e^{-\zeta_S'(0)}, \tag{159}$$

where ζ_S is the spectral ζ-function corresponding to the Laplacian. On the rectangle, where the eigenvalues of the Laplacian are

$$\lambda_{k_x,k_y} = \left(\frac{\pi}{L_x}k_x\right)^2 + \left(\frac{\pi}{L_y}k_y\right)^2, \quad k_x, k_y \in \mathbb{N}^+, \tag{160}$$

the spectral ζ-function takes the form

$$\zeta_S(s) = \sum_{k_x,k_y=1}^{\infty} \left(\left(\frac{\pi}{L_x}k_x\right)^2 + \left(\frac{\pi}{L_y}k_y\right)^2\right)^{-s}. \tag{161}$$

Our goal is thus to find an analytic continuation of this expression to $s = 0$ and calculate the value of its derivative at that point. Let us first recall some identities. The integral representation of the Γ function can be used to write

$$\ell^{-s} = \frac{1}{\Gamma(s)} \int_0^\infty \mathrm{d}t\ t^{s-1} e^{-\ell t}. \tag{162}$$

The Poisson summation formula is given by

$$\sum_{n=1}^{\infty} e^{-an^2} = -\frac{1}{2} + \frac{1}{2}\sqrt{\frac{\pi}{a}} + \sqrt{\frac{\pi}{a}} \sum_{n=1}^{\infty} e^{-\frac{n^2\pi^2}{a}}. \tag{163}$$

The Riemann ζ-function is defined as

$$\zeta(s) = \sum_{n=1}^{\infty} \frac{1}{n^s}, \tag{164}$$

and finally the integral representation of a modified Bessel function is

$$K_\nu(z) = \frac{1}{2} \int_0^\infty \mathrm{d}u\ e^{-\frac{z}{2}\left(u+\frac{1}{u}\right)} u^{\nu-1}. \tag{165}$$

We can now use these identities to perform some manipulations on the spectral ζ-function

$$\begin{aligned}
\zeta_S(s) &= \frac{1}{\Gamma(s)} \sum_{k_x,k_y=1}^{\infty} \int_0^\infty \mathrm{d}t\; t^{s-1} e^{-t\left(\left(\frac{\pi}{L_x}k_x\right)^2+\left(\frac{\pi}{L_y}k_y\right)^2\right)} \\
&= \frac{1}{\Gamma(s)} \sum_{k_y=1}^{\infty} \int_0^\infty \mathrm{d}t\; t^{s-1} e^{-t\left(\frac{\pi}{L_y}k_y\right)^2} \sum_{k_x=1}^{\infty} e^{-t\left(\frac{\pi}{L_x}k_x\right)^2} \\
&= \frac{1}{\Gamma(s)} \sum_{k_y=1}^{\infty} \int_0^\infty \mathrm{d}t\; t^{s-1} e^{-t\left(\frac{\pi}{L_y}k_y\right)^2} \left(-\frac{1}{2} + \frac{L_x}{2\sqrt{\pi}} t^{-\frac{1}{2}} + \frac{L_x}{\sqrt{\pi}} t^{-\frac{1}{2}} \sum_{k_x=1}^{\infty} e^{-\frac{k_x^2 L_x^2}{t}}\right) \\
&= -\frac{1}{2} \sum_{k_y=1}^{\infty} \left(\frac{\pi}{L_y}k_y\right)^{-2s} + \frac{L_x}{2\sqrt{\pi}} \frac{\Gamma(s-\frac{1}{2})}{\Gamma(s)} \sum_{k_y=1}^{\infty} \left(\frac{\pi}{L_y}k_y\right)^{-2s+1} + \\
&\qquad \frac{2L_x^{s+\frac{1}{2}}}{\Gamma(s)\sqrt{\pi}} \sum_{k_x,k_y=1}^{\infty} \left(\frac{L_y k_x}{\pi k_y}\right)^{s-\frac{1}{2}} K_{s-\frac{1}{2}}\left(2\pi \frac{L_x}{L_y} k_x k_y\right) \\
&= -\frac{1}{2}\left(\frac{L_y}{\pi}\right)^{2s} \zeta(2s) + \frac{L_x}{2\sqrt{\pi}} \frac{\Gamma(s-\frac{1}{2})}{\Gamma(s)} \left(\frac{L_y}{\pi}\right)^{2s-1} \zeta(2s-1) + \\
&\qquad \frac{2L_x^{s+\frac{1}{2}}}{\Gamma(s)\sqrt{\pi}} \sum_{k_x,k_y=1}^{\infty} \left(\frac{L_y k_x}{\pi k_y}\right)^{s-\frac{1}{2}} K_{s-\frac{1}{2}}\left(2\pi \frac{L_x}{L_y} k_x k_y\right). \qquad (166)
\end{aligned}$$

The derivative at $s = 0$ of the first term is straight forward to calculate for the first term

$$-\frac{d}{ds}\frac{1}{2}\left(\frac{L_y}{\pi}\right)^{2s} \zeta(2s)|_{s=0} = \frac{1}{2}\log(2L_y). \qquad (167)$$

In order to evaluate the derivatives at $s = 0$ of the remaining two terms we need consider the following asymptotic behavior of the Γ- function. For ε close to zero

$$\frac{1}{\Gamma(\varepsilon)} = \varepsilon + \ldots, \qquad (168)$$

$$\frac{d}{ds}\frac{1}{\Gamma(s)}|_{s=\varepsilon} = 1 + \ldots. \qquad (169)$$

Since all other parts of the expressions are regular around $s = 0$, this means that the only terms that survive are those where the the derivative hits the Γ-function. We can thus write for the second term in the spectral ζ-function

$$\frac{d}{ds}\frac{L_x}{2\sqrt{\pi}} \frac{\Gamma(s-\frac{1}{2})}{\Gamma(s)} \left(\frac{L_y}{\pi}\right)^{2s-1} \zeta(2s-1)\Big|_{s=0} = \frac{\sqrt{\pi}}{2}\frac{L_x}{L_y}\Gamma(-\frac{1}{2})\zeta(-1) = \frac{\pi}{12}\frac{L_x}{L_y} \qquad (170)$$

and similarly for the third

$$\begin{aligned}
&\frac{d}{ds}\frac{2L_x^{s+\frac{1}{2}}}{\Gamma(s)\sqrt{\pi}} \sum_{k_x,k_y=1}^{\infty} \left(\frac{L_y k_x}{\pi k_y}\right)^{s-\frac{1}{2}} K_{s-\frac{1}{2}}\left(2\pi \frac{L_x}{L_y} k_x k_y\right)\Big|_{s=0} = \\
&\qquad 2\sqrt{\frac{L_x}{L_y}} \sum_{k_x,k_y=1}^{\infty} \sqrt{\frac{k_y}{k_x}} K_{-\frac{1}{2}}\left(2\pi \frac{L_x}{L_y} k_x k_y\right). \qquad (171)
\end{aligned}$$

Using the explicit form of $K_{-\frac{1}{2}}$ we can further simplify this to

$$2\sqrt{\frac{L_x}{L_y}}\sum_{k_x,k_y=1}^{\infty}\sqrt{\frac{k_y}{k_x}}K_{-\frac{1}{2}}\left(2\pi\frac{L_x}{L_y}k_xk_y\right)=\sum_{k_x,k_y=1}^{\infty}\frac{1}{k_x}e^{-2\pi\frac{L_x}{L_y}k_xk_y}$$
$$=-\frac{\pi}{12}\frac{L_x}{L_y}-\log\left(\eta\left(i\frac{L_x}{L_y}\right)\right), \tag{172}$$

where η is the Dedekind η-function. Putting everything together, we see that the derivative of the spectral ζ-function at zero is

$$\zeta_S'(0)=\frac{1}{2}\log(2L_y)-\log\left(\eta\left(i\frac{L_x}{L_y}\right)\right) \tag{173}$$

and the determinant of the Laplacian on the rectangle is

$$\det\Delta=\frac{1}{\sqrt{2L_y}}\eta\left(i\frac{L_x}{L_y}\right). \tag{174}$$

We note that due to the behavior of the Dedekind η-function under modular transformations the expression above is invariant under the exchange of L_x and L_y.

E Correlation functions

In this appendix we evaluate the correlation functions needed in the calculation of the entanglement entropy of the state with m excitations in the λ mode, see section 4.1. As a starting point, we can easily see that for integer β and by linearity

$$\left\langle(\varphi_X^\lambda)^\beta\right\rangle_X=\delta_{\beta,\text{even}}(\#\text{ of full Wick contractions})(G_X^\lambda)^{\frac{\beta}{2}}$$
$$=\delta_{\beta,\text{even}}(\beta-1)!!(G_X^\lambda)^{\frac{\beta}{2}}, \tag{175}$$

where $X = A, B, M$ and $\delta_{\beta,\text{even}} := \delta_{\beta,2n}$ for some integer n. Using the definition of Hermite polynomials (18) and linearity we can rewrite the following correlation function as

$$\begin{aligned}
&\frac{1}{2^m}\sqrt{\frac{1}{m!}\binom{m}{k}\binom{m}{k'}}\left\langle H_{m-k}(\varphi_X^\lambda)H_{k'}(\varphi_X^\lambda)\right\rangle_X \\
&\quad= (m-k)!k'!\sqrt{\frac{1}{m!}\binom{m}{k}\binom{m}{k'}}\times \\
&\qquad\sum_{\ell=0}^{\lfloor\frac{m-k}{2}\rfloor}\sum_{\ell'=0}^{\lfloor\frac{k'}{2}\rfloor}\frac{(-1)^{\ell+\ell'}2^{k'-k-2(\ell+\ell')}}{\ell!\ell'!(m-k-2\ell)!(k'-2\ell')!}\left\langle(\varphi_X^\lambda)^{m-k+k'-2(\ell+\ell')}\right\rangle_X \\
&\quad= \delta_{m-k+k',\text{even}}(m-k)!k'!\sqrt{\frac{1}{m!}\binom{m}{k}\binom{m}{k'}}\times \\
&\qquad\sum_{\ell=0}^{\lfloor\frac{m-k}{2}\rfloor}\sum_{\ell'=0}^{\lfloor\frac{k'}{2}\rfloor}\frac{(-1)^{\ell+\ell'}2^{k'-k-2(\ell+\ell')}(m-k+k'-2(\ell+\ell')-1)!!}{\ell!\ell'!(m-k-2\ell)!(k'-2\ell')!}\left(G_X^\lambda\right)^{\frac{m-k+k'-2(\ell+\ell')}{2}} \\
&\quad= \delta_{m-k+k',\text{even}}\sum_{\ell=0}^{\lfloor\frac{m-k}{2}\rfloor}\sum_{\ell'=0}^{\lfloor\frac{k'}{2}\rfloor}f^m_{k,k'}(\ell,\ell')\left(G_X^\lambda\right)^{\frac{m-k+k'-2(\ell+\ell')}{2}},
\end{aligned} \tag{176}$$

where we included the prefactor that appears in front of the correlation functions that make up the tensors $\mathcal{A}$ and $\mathcal{B}$ in (97) and (98), and in the last line we defined

$$f^m_{k,k';\ell,\ell'} := \frac{(-1)^{\ell+\ell'}}{2^{k-k'+2(\ell+\ell')}}\sqrt{\frac{1}{m!}\binom{m}{k}\binom{m}{k'}}\frac{(m-k)!k'!(m-k+k'-2(\ell+\ell')-1)!!}{\ell!\ell'!(m-k-2\ell)!(k'-2\ell')!}. \tag{177}$$

If we define the following polynomial

$$F^m_{k,k'}(z) := \delta_{m-k+k',\text{even}}\sum_{\ell=0}^{\lfloor\frac{m-k}{2}\rfloor}\sum_{\ell'=0}^{\lfloor\frac{k'}{2}\rfloor}f^m_{k,k';\ell,\ell'}z^{\frac{m-k+k'-2(\ell+\ell')}{2}} \tag{178}$$

then we can simply write

$$\frac{1}{2^m}\sqrt{\frac{1}{m!}\binom{m}{k}\binom{m}{k'}}\left\langle H_{m-k}(\varphi_X^\lambda)H_{k'}(\varphi_X^\lambda)\right\rangle_X = F^m_{k,k'}(G_X^\lambda). \tag{179}$$

Next, we want to evaluate the correlation on M appearing in the tensor $\mathcal{M}$ in equation (99). Reminding ourselves that $\bar{\phi}^\lambda = \bar{\phi}^\lambda_A + \bar{\phi}^\lambda_B$ and using the identity of Hermite polynomials (81)

we can rewrite the correlation function as

$$\begin{aligned}
&\frac{1}{2^{\frac{3m}{2}}m!}\sqrt{\binom{m}{k}\binom{m}{k'}}\left\langle H_m\left(\frac{1}{\sqrt{2}}\bar{\phi}^\lambda\right)H_k\left(\bar{\phi}_A^\lambda\right)H_{m-k'}\left(\bar{\phi}_B^\lambda\right)\right\rangle_M \\
&\quad=\frac{1}{2^{2m}m!}\sqrt{\binom{m}{k}\binom{m}{k'}}\sum_{n=0}^{m}\binom{m}{n}\left\langle H_k\left(\bar{\phi}_A^\lambda\right)H_{m-n}\left(\bar{\phi}_A^\lambda\right)H_n\left(\bar{\phi}_B^\lambda\right)H_{m-k'}\left(\bar{\phi}_B^\lambda\right)\right\rangle_M \\
&\quad=\frac{1}{2^{2m}}\sqrt{\binom{m}{k}\binom{m}{k'}}\sum_{n=0}^{m}k!(m-k')!\times \\
&\qquad\sum_{r=0}^{\lfloor\frac{k}{2}\rfloor}\sum_{r'=0}^{\lfloor\frac{m-n}{2}\rfloor}\sum_{\ell=0}^{\lfloor\frac{n}{2}\rfloor}\sum_{\ell'=0}^{\lfloor\frac{m-k'}{2}\rfloor}\frac{(-1)^{r+r'+\ell+\ell'}2^{2m+k-k'-2(r+r'+\ell+\ell')}}{r!r'!\ell!\ell'!(k-2r)!(m-n-2r')!(n-2\ell)!(m-k'-2\ell')!}\times \\
&\qquad\qquad\left\langle\left(\bar{\phi}_A^\lambda\right)^{m+k-n-2(r+r')}\left(\bar{\phi}_B^\lambda\right)^{m+n-k'-2(\ell+\ell')}\right\rangle_M
\end{aligned}\tag{180}$$

where we used the definition of Hermite polynomials in the last line. We will take care of the prefactors later, for now it is enough to see that the expression above is just a sum of correlation functions of the form $\langle A^\alpha B^\beta\rangle_M$, where we use the short-hand notation $A\equiv\bar{\phi}_A^\lambda$ and $B\equiv\bar{\phi}_B^\lambda$. When we apply Wick's theorem to this type of correlation function, three distinct types of transformed two-point functions appear: $\langle AB\rangle_M=G_{A,B}^\lambda$, and $\langle X^2\rangle_M=G_{X,X}^\lambda$ with $X=A,B$. Since we know from before what correlation functions of the form $\langle X^\alpha\rangle_M$ look like, we can evaluate $\langle A^\alpha B^\beta\rangle_M$ by successively taking mixed contractions creating an expansion of the form

$$\left\langle A^\alpha B^\beta\right\rangle=a_0\left\langle A^\alpha\right\rangle\left\langle B^\beta\right\rangle+a_1\left\langle AB\right\rangle\left\langle A^{\alpha-1}\right\rangle\left\langle B^{\beta-1}\right\rangle+a_2\left\langle AB\right\rangle^2\left\langle A^{\alpha-2}\right\rangle\left\langle B^{\beta-2}\right\rangle+\ldots,\tag{181}$$

where a_ρ is a combinatorial factor counting the ways to select ρ pairs AB out of $A^\alpha B^\beta$ given by

$$a_\rho=\frac{1}{\rho!}\frac{\alpha!}{(\alpha-\rho)!}\frac{\beta!}{(\beta-\rho)!}.\tag{182}$$

As a consistency check it isn't hard to see that this combinatorial factor leads to the expected amount of full Wick contractions: $(\alpha+\beta-1)!!$. Using equation (175) one can then evaluate the remaining correlation functions and write

$$\begin{aligned}
\left\langle A^\alpha B^\beta\right\rangle=&\sum_{\rho=0}^{\min(\alpha,\beta)}\delta_{\alpha-\rho,\text{even}}\delta_{\beta-\rho,\text{even}}\times \\
&\frac{1}{\rho!}\frac{\alpha!}{(\alpha-\rho)!!}\frac{\beta!}{(\beta-\rho)!!}\left(G_{A,B}^\lambda\right)^\rho\left(G_{A,A}^\lambda\right)^{(\alpha-\rho)/2}\left(G_{B,B}^\lambda\right)^{(\beta-\rho)/2},
\end{aligned}\tag{183}$$

where we used the fact that $n!/(n-1)!! = n!!$. Let us thus define the following polynomial in three variables

$$T^m_{k,k'}(x,y,z) := \delta_{k+k',\text{even}} \sqrt{\binom{m}{k}\binom{m}{k'}} \sum_{n=0}^{m} k!(m-k')! \times \sum_{r=0}^{\lfloor \frac{k}{2} \rfloor} \sum_{r'=0}^{\lfloor \frac{m-n}{2} \rfloor} \sum_{\ell=0}^{\lfloor \frac{n}{2} \rfloor} \sum_{\ell'=0}^{\lfloor \frac{m-k'}{2} \rfloor} \frac{(-1)^{r+r'+\ell+\ell'} 2^{k-k'-2(r+r'+\ell+\ell')}}{r!r'!\ell!\ell'!(k-2r)!(m-n-2r')!(n-2\ell)!(m-k'-2\ell')!} \times \sum_{\rho=0}^{\min(m+k-n-2(r+r'), m+n-k'-2(\ell+\ell'))} \delta_{m+k-n-\rho,\text{even}} \frac{1}{\rho!} \frac{(m+k-n-2(r+r'))!}{(m+k-n-2(r+r')-\rho)!!} \times \frac{(m+n-k'-2(\ell+\ell'))!}{(m+n-k'-2(\ell+\ell')-\rho)!!} x^{\rho} y^{(m+k-n-2(r+r')-\rho)/2} z^{(m+n-k'-2(\ell+\ell')-\rho)/2} \quad (184)$$

where we simplified the δ-functions as $\delta_{m+k-n-\rho,\text{even}}\delta_{m+n-k'-\rho,\text{even}} = \delta_{m+k-n-\rho,\text{even}}\delta_{k+k',\text{even}}$. In the end, we can write for the correlation function

$$\frac{1}{2^{\frac{3m}{2}} m!} \sqrt{\binom{m}{k}\binom{m}{k'}} \left\langle H_m\left(\frac{1}{\sqrt{2}}\bar{\phi}^{\lambda}\right) H_k\left(\bar{\phi}^{\lambda}_A\right) H_{m-k'}\left(\bar{\phi}^{\lambda}_B\right) \right\rangle_M = T^m_{k,k'}(G^{\lambda}_{A,B}, G^{\lambda}_{A,A}, G^{\lambda}_{B,B}). \quad (185)$$

Note that for a fixed surgery and eigenmode $G^{\lambda}_{A,B}$, $G^{\lambda}_{A,A}$, and $G^{\lambda}_{B,B}$ are just real numbers.

References

[1] C. H. Bennett, D. P. DiVincenzo, J. A. Smolin, and W. K. Wootters, "Mixed-state entanglement and quantum error correction," *Phys. Rev. A* **54** (Nov, 1996) 3824–3851. https://link.aps.org/doi/10.1103/PhysRevA.54.3824.

[2] M. B. Plenio and S. Virmani, "An Introduction to entanglement measures," *Quant. Inf. Comput.* **7** (2007) 1–51, arXiv:quant-ph/0504163. https://arxiv.org/abs/quant-ph/0504163.

[3] P. Calabrese and J. L. Cardy, "Entanglement entropy and quantum field theory: A non-technical introduction," *Int. J. Quant. Inf.* **4** (2006) 429, arXiv:quant-ph/0505193 [quant-ph]. https://arxiv.org/abs/quant-ph/0505193. Workshop on Quantum Entanglement in Physical and Information Sciences Pisa, Italy, December 14-18, 2004.

[4] L. Amico, R. Fazio, A. Osterloh, and V. Vedral, "Entanglement in many-body systems," *Rev. Mod. Phys.* **80** (May, 2008) 517–576. https://link.aps.org/doi/10.1103/RevModPhys.80.517.

[5] J. Eisert, M. Cramer, and M. B. Plenio, "Area laws for the entanglement entropy - a review," *Rev. Mod. Phys.* **82** (2010) 277–306, arXiv:0808.3773 [quant-ph]. https://arxiv.org/abs/0808.3773.

[6] N. Laflorencie, "Quantum entanglement in condensed matter systems," *Physics Reports* **646** (2016) 1 – 59. http://www.sciencedirect.com/science/article/pii/S0370157316301582. Quantum entanglement in condensed matter systems.

[7] C. Callan and F. Wilczek, "On geometric entropy," *Physics Letters B* **333** no. 1, (1994) 55 – 61. http://www.sciencedirect.com/science/article/pii/0370269394910073.

[8] C. Holzhey, F. Larsen, and F. Wilczek, "Geometric and renormalized entropy in conformal field theory," *Nuclear Physics B* **424** no. 3, (1994) 443 – 467. http://www.sciencedirect.com/science/article/pii/0550321394904022.

[9] P. Calabrese and J. Cardy, "Entanglement entropy and quantum field theory," *J. Stat. Mech.* (2004) . https://arxiv.org/abs/hep-th/0405152.

[10] T. Nishioka, S. Ryu, and T. Takayanagi, "Holographic entanglement entropy: an overview," *Journal of Physics A: Mathematical and Theoretical* **42** no. 50, (Dec, 2009) 504008. https://doi.org/10.1088%2F1751-8113%2F42%2F50%2F504008.

[11] M. Rangamani and T. Takayanagi, "Holographic entanglement entropy," *Lecture Notes in Physics* **931** (2017) . https://arxiv.org/abs/1609.01287.

[12] M. Srednicki, "Entropy and area," *Phys. Rev. Lett.* **71** (Aug, 1993) 666–669. https://link.aps.org/doi/10.1103/PhysRevLett.71.666.

[13] M. Hastings, "An area law for one-dimensional quantum systems," *J. Stat. Mech.* **0708** (2007) P08024, arXiv:0705.2024 [quant-ph].

[14] D. N. Page, "Average entropy of a subsystem," *Phys. Rev. Lett.* **71** (Aug, 1993) 1291–1294. https://link.aps.org/doi/10.1103/PhysRevLett.71.1291.

[15] S. K. Foong and S. Kanno, "Proof of page's conjecture on the average entropy of a subsystem," *Phys. Rev. Lett.* **72** (Feb, 1994) 1148–1151. https://link.aps.org/doi/10.1103/PhysRevLett.72.1148.

[16] S. Sen, "Average entropy of a quantum subsystem," *Phys. Rev. Lett.* **77** (Jul, 1996) 1–3. https://link.aps.org/doi/10.1103/PhysRevLett.77.1.

[17] M. Ahmadi, S. Das, and S. Shankaranarayanan, "Is entanglement entropy proportional to area?," *Canadian Journal of Physics* **84** no. 6-7, (2006) 493–499, https://doi.org/10.1139/p06-002. https://doi.org/10.1139/p06-002.

[18] S. Das and S. Shankaranarayanan, "How robust is the entanglement entropy-area relation?," *Phys. Rev. D* **73** (Jun, 2006) 121701. https://link.aps.org/doi/10.1103/PhysRevD.73.121701.

[19] L. Masanes, "Area law for the entropy of low-energy states," *Phys. Rev. A* **80** (Nov, 2009) 052104. https://link.aps.org/doi/10.1103/PhysRevA.80.052104.

[20] F. C. Alcaraz, M. I. Berganza, and G. Sierra, "Entanglement of low-energy excitations in conformal field theory," *Phys. Rev. Lett.* **106** (May, 2011) 201601. https://link.aps.org/doi/10.1103/PhysRevLett.106.201601.

[21] M. I. Berganza, F. C. Alcaraz, and G. Sierra, "Entanglement of excited states in critical spin chains," *Journal of Statistical Mechanics: Theory and Experiment* **2012** no. 01, (Jan, 2012) P01016. https://doi.org/10.1088%2F1742-5468%2F2012%2F01%2Fp01016.

[22] O. A. Castro-Alvaredo, C. De Fazio, B. Doyon, and I. M. Szécsényi, "Entanglement content of quasiparticle excitations," *Phys. Rev. Lett.* **121** (Oct, 2018) 170602. https://link.aps.org/doi/10.1103/PhysRevLett.121.170602.

[23] O. A. Castro-Alvaredo, C. De Fazio, B. Doyon, and I. M. Szécsényi, "Entanglement content of quantum particle excitations. part i. free field theory," *Journal of High Energy Physics* **2018** no. 10, (Oct, 2018) 39. https://doi.org/10.1007/JHEP10(2018)039.

[24] O. A. Castro-Alvaredo, C. De Fazio, B. Doyon, and I. M. Szécsényi, "Entanglement content of quantum particle excitations. part ii. disconnected regions and logarithmic negativity," *Journal of High Energy Physics* **2019** no. 11, (Nov, 2019) 58. https://doi.org/10.1007/JHEP11(2019)058.

[25] O. A. Castro-Alvaredo, C. De Fazio, B. Doyon, and I. M. Szécsényi, "Entanglement content of quantum particle excitations. part iii. graph partition functions," *Journal of Mathematical Physics* **60** no. 8, (2019) 082301. https://doi.org/10.1063/1.5098892.

[26] F. C. Alcaraz and M. S. Sarandy, "Finite-size corrections to entanglement in quantum critical systems," *Phys. Rev. A* **78** (Sep, 2008) 032319. https://link.aps.org/doi/10.1103/PhysRevA.78.032319.

[27] V. Alba, M. Fagotti, and P. Calabrese, "Entanglement entropy of excited states," *Journal of Statistical Mechanics: Theory and Experiment* **2009** no. 10, (Oct, 2009) P10020. https://doi.org/10.1088%2F1742-5468%2F2009%2F10%2Fp10020.

[28] J. Mölter, T. Barthel, U. Schollwöck, and V. Alba, "Bound states and entanglement in the excited states of quantum spin chains," *Journal of Statistical Mechanics: Theory and Experiment* **2014** no. 10, (Oct, 2014) P10029. https://doi.org/10.1088%2F1742-5468%2F2014%2F10%2Fp10029.

[29] E. Ardonne, P. Fendley, and E. Fradkin, "Topological order and conformal quantum critical points," *Annals of Physics* **310** no. 2, (Apr, 2004) 493551. http://dx.doi.org/10.1016/j.aop.2004.01.004.

[30] D. S. Rokhsar and S. A. Kivelson, "Superconductivity and the quantum hard-core dimer gas," *Phys. Rev. Lett.* **61** (Nov, 1988) 2376–2379. https://link.aps.org/doi/10.1103/PhysRevLett.61.2376.

[31] C. L. Henley, "Relaxation time for a dimer covering with height representation," *Journal of Statistical Physics* **89** no. 3, (Nov, 1997) 483–507. https://doi.org/10.1007/BF02765532.

[32] R. Moessner, S. L. Sondhi, and E. Fradkin, "Short-ranged resonating valence bond physics, quantum dimer models, and ising gauge theories," *Phys. Rev. B* **65** (Dec, 2001) 024504. https://link.aps.org/doi/10.1103/PhysRevB.65.024504.

[33] C. Castelnovo, C. Chamon, C. Mudry, and P. Pujol, "From quantum mechanics to classical statistical physics: Generalized rokhsarkivelson hamiltonians and the stochastic matrix form decomposition," *Annals of Physics* **318** no. 2, (2005) 316 – 344. http://www.sciencedirect.com/science/article/pii/S0003491605000096.

[34] M. Freedman, C. Nayak, and K. Shtengel, "Extended hubbard model with ring exchange: A route to a non-abelian topological phase," *Phys. Rev. Lett.* **94** (Feb, 2005) 066401. https://link.aps.org/doi/10.1103/PhysRevLett.94.066401.

[35] P. Fendley, "Topological order from quantum loops and nets," *Annals of Physics* **323** no. 12, (2008) 3113 – 3136. http://www.sciencedirect.com/science/article/pii/S0003491608000614.

[36] V. Keränen, W. Sybesma, P. Szepietowski, and L. Thorlacius, "Correlation functions in theories with lifshitz scaling," *Journal of High Energy Physics* **2017** no. 5, (May, 2017) 33. https://doi.org/10.1007/JHEP05(2017)033.

[37] J. Angel-Ramelli, V. G. M. Puletti, and L. Thorlacius, "Entanglement entropy in generalised quantum lifshitz models," *Journal of High Energy Physics* **2019** no. 8, (Aug, 2019) 72. https://doi.org/10.1007/JHEP08(2019)072.

[38] E. Fradkin and J. E. Moore, "Entanglement entropy of 2d conformal quantum critical points: Hearing the shape of a quantum drum," *Phys. Rev. Lett.* **97** (Aug, 2006) 050404. https://link.aps.org/doi/10.1103/PhysRevLett.97.050404.

[39] B. Hsu, M. Mulligan, E. Fradkin, and E.-A. Kim, "Universal entanglement entropy in two-dimensional conformal quantum critical points," *Phys. Rev. B* **79** (Mar, 2009) 115421. https://link.aps.org/doi/10.1103/PhysRevB.79.115421.

[40] B. Hsu and E. Fradkin, "Universal behavior of entanglement in 2d quantum critical dimer models," *Journal of Statistical Mechanics: Theory and Experiment* **2010** no. 09, (Sep, 2010) P09004. https://doi.org/10.1088%2F1742-5468%2F2010%2F09%2Fp09004.

[41] J.-M. Stéphan, S. Furukawa, G. Misguich, and V. Pasquier, "Shannon and entanglement entropies of one- and two-dimensional critical wave functions," *Phys. Rev. B* **80** (Nov, 2009) 184421. https://link.aps.org/doi/10.1103/PhysRevB.80.184421.

[42] M. Oshikawa, "Boundary conformal field theory and entanglement entropy in two-dimensional quantum lifshitz critical point," arXiv:1007.3739 [cond-mat.stat-mech].

[43] M. P. Zaletel, J. H. Bardarson, and J. E. Moore, "Logarithmic terms in entanglement entropies of 2d quantum critical points and shannon entropies of spin chains," *Phys. Rev. Lett.* **107** (2011) 020402, arXiv:1103.5452 [cond-mat.str-el]. https://arxiv.org/abs/1103.5452.

[44] T. Zhou, X. Chen, T. Faulkner, and E. Fradkin, "Entanglement entropy and mutual information of circular entangling surfaces in 2 + 1-dimensional quantum lifshitz model," *J. Stat. Mech. 2016(9):093101, 2016* (2016) . https://arxiv.org/abs/1607.01771.

[45] J. Angel-Ramelli, C. Berthiere, V. G. M. Puletti, and L. Thorlacius, "Logarithmic Negativity in Quantum Lifshitz Theories," arXiv:2002.05713 [hep-th].

[46] T. Zhou, "Entanglement entropy of local operators in quantum lifshitz theory," *Journal of Statistical Mechanics: Theory and Experiment* **2016** no. 9, (Sep, 2016) 093106. https://doi.org/10.1088%2F1742-5468%2F2016%2F09%2F093106.

[47] D. E. Parker, R. Vasseur, and J. E. Moore, "Entanglement entropy in excited states of the quantum lifshitz model," *Journal of Physics A: Mathematical and Theoretical* **50** no. 25, (May, 2017) 254003. https://doi.org/10.1088%2F1751-8121%2Faa70b3.

[48] H. Bernien, S. Schwartz, A. Keesling, H. Levine, A. Omran, H. Pichler, S. Choi, A. S. Zibrov, M. Endres, M. Greiner, V. Vuletić, and M. D. Lukin, "Probing many-body dynamics on a 51-atom quantum simulator," *Nature* **551** no. 7682, (Nov, 2017) 579–584. https://doi.org/10.1038/nature24622.

[49] C. J. Turner, A. A. Michailidis, D. A. Abanin, M. Serbyn, and Z. Papić, "Weak ergodicity breaking from quantum many-body scars," *Nature Physics* **14** no. 7, (Jul, 2018) 745–749. https://doi.org/10.1038/s41567-018-0137-5.

[50] Z. Lan and S. Powell, "Eigenstate thermalization hypothesis in quantum dimer models," *Phys. Rev. B* **96** (Sep, 2017) 115140. https://link.aps.org/doi/10.1103/PhysRevB.96.115140.

[51] J. Wildeboer, A. Seidel, N. S. Srivatsa, A. E. B. Nielsen, and O. Erten, "Topological quantum many-body scars in quantum dimer models on the kagome lattice," 2020.

[52] P. Calabrese and J. Cardy, "Entanglement entropy and conformal field theory," *Journal of Physics A: Mathematical and Theoretical* **42** no. 50, (Dec, 2009) 504005. https://doi.org/10.1088%2F1751-8113%2F42%2F50%2F504005.

[53] P. H. Ginsparg, "Applied conformal field theory," in *Les Houches Summer School in Theoretical Physics: Fields, Strings, Critical Phenomena Les Houches, France, June*

28-August 5, 1988, pp. 1–168. 1988. arXiv:hep-th/9108028 [hep-th]. https://arxiv.org/abs/hep-th/9108028.

[54] P. Di Francesco, P. Mathieu, and D. Senechal, *Conformal Field Theory*. Graduate Texts in Contemporary Physics. Springer-Verlag, New York, 1997. http://www-spires.fnal.gov/spires/find/books/www?cl=QC174.52.C66D5::1997.

[55] B. Duplantier and F. David, "Exact partition functions and correlation functions of multiple hamiltonian walks on the manhattan lattice," *Journal of Statistical Physics* **51** no. 3, (May, 1988) 327–434. https://doi.org/10.1007/BF01028464.